Environmental
Studies
Research
Funds

114 Beaufort Sea Extreme Waves Study

Canada

March 1992

The Environmental Studies Research Funds are financed from special levies on the oil and gas industry and are administered by the National Energy Board for the Minister of Energy, Mines and Resources, and for the Minister of Indian Affairs and Northern Development.

The Environmental Studies Research Funds and any person acting on their behalf assume no liability arising from the use of the information contained in this document. The opinions expressed are those of the authors and do not necessarily reflect those of the Environmental Studies Research Funds agencies. The use of trade names or identification of specific products does not constitute an endorsement or recommendation for use.

Environmental Studies Research Funds

Report No. 114

March, 1992

BEAUFORT SEA EXTREME WAVES STUDY

By: Bassem M. Eid and Vince J. Cardone

MacLaren Plansearch (1991) Limited
Suite 200, Park Lane Terraces
5657 Spring Garden Road
Halifax, Nova Scotia
B3J 3R4
CANADA

Oceanweather Inc.
Suite One
5 River Road
Cos Cob, Connecticut
06807
U.S.A.

Scientifc Advisor: V.R. Swail

The correct citation for this report is:

Eid, B.M. and V.J. Cardone. 1992. Beaufort Sea extreme waves study. Environmental Studies Research Funds, Report Series No. 114. Calgary, Alberta, 143 p. + Appendices.

Published under the auspices of
the Environmental Studies
Research Funds
ISBN 0-921652-13-5
© 1992 - MacLaren Plansearch (1991) Limited

TABLE OF CONTENTS

TABLE OF CONTENTS (cont'd)

TABLE OF CONTENTS (cont'd)

LIST OF TABLES

LIST OF FIGURES

ACKNOWLEDGEMENT

This study was carried out by MacLaren Plansearch (1991) Limited (MPL), Halifax, Nova Scotia, in association with Oceanweather Inc., (OWI), Cos Cob, Connecticut and D. F. Dickins and Associates, Vancouver, British Columbia. MPL provided the literature review, data base assembly, storm classification and storm selection, review of methodologies, model hindcast verifications, extremal analysis and report preparation. OWI was responsible for wave model development and storms hindcast; Dickins and Associates provided ice edge for the storm events considered in this study.

The study was initiated and funded by Environmental Studies Research Funds (ESRF). Additional funding was provided by COGLA under DSS contract #KM169-0-8160 for hindcasting additional 15 storms. The Scientific Authority for this study was Mr. Val Swail, Atmospheric Environment Services (AES), Environment Canada. The Study Review Committee consisted of Mr. Val Swail, Dr. Ken Sato, National Energy Board, Mr. Brian Wright, Gulf Canada Resources Limited, and Mr. Tom Agnew, AES.

EXECUTIVE SUMMARY

The objective of this study was to develop new and definitive estimates of the extreme wave climate in the Canadian Beaufort Sea, with emphasis on offshore exploration areas in deep and shallow water. A hindcast approach was adopted, which includes: (1) assembly of comprehensive data base of archived historical meteorological, waves, and ice cover data; (2) identification and ranking of historical storm occurrences during the potential open-water season, over as long an historical period as allowed by the data, and selection of a top-ranked severe wave generating storm population (30 storms) for hindcasting; (3) adaptation and validation of accurate numerical hindcasting procedures to specify time histories of surface wind fields, wave fields and directional spectra in each hindcast storm; (4) hindcast production of the selected storms; and (5) statistical analysis of hindcast extremes at a selected number of model grid points. The ODGP spectral ocean wave model, as adapted recently to shallow water and a variable ice edge, was used for the wave hindcasts. Wind fields were calculated from the sea surface pressure fields using proven marine planetary boundary layer model.

The Beaufort Sea presents a number of special problems: (1) the relative scarcity of historical meteorological and seastate data; and (2) the highly variable and complex nature of sea-ice cover, which exert a significant control over the wave field. The presence of sea ice also complicates the storm selection process, hindcast processes, and extremal analysis methods. In order to account for the variability and uncertainty of extremes associated with ice edge effects, four different ice edges were used for each storm: actual ice edge and climatological ice edges for three probability levels (98%, 50% and 30% occurrences). The results are presented for individual and combined ice edge scenarios.

Comparison of the present results with other previous studies indicated that this study produced extreme values which are at the lower end of the wide range of extremes provided by previous studies.

RÉSUMÉ

L'objectif de la présente étude consistait à mettre au point de nouvelles et définitives estimations du régime extrême des vagues dans la partie canadienne de la mer de Beaufort avec emphase sur les régions d'exploration au large en eau profonde et peu profonde. Une approche de prévision à postériori englobant les composantes suivantes a été adoptée : 1) assemblage d'une base de données exhaustive de données historiques archivées sur la météorologie, les vagues et la couverture glacielle; 2) l'identification et le classement des tempêtes historiques survenues pendant la saison possible d'eau libre pour une période d'aussi longue durée que le permettaient les données et la sélection d'une population (30 tempêtes) de tempêtes de premier rang ayant soulevé les plus grosses vagues pour la prévision à postériori; 3) la modification et la validation de procédures précises de prévision à postériori permettant de spécifier des historiques temporels de champs de vent en surface; 4) la production à postériori des tempêtes choisies; et 5) l'analyse statistique des conditions extrêmes prévues à postériori en un certain nombre de points choisis du quadrillage du modèle. Le modèle spectral de vagues océaniques ODGP, tel que récemment modifié pour l'application à des eaux peu profondes et à une lisière des glaces variable a été utilisé pour la prévision à postériori des vagues. Les champs de vent ont été calculés d'après les champs de pression à la surface de la mer au moyen de l'éprouvé modèle marin de la couche limite planétaire.

La mer de Beaufort pose un certain nombre de problèmes spéciaux : 1) les données historiques sur la météorologie et l'état de la mer y sont relativement rares; 2) la couverture de glace de mer y est de nature très variable et complexe, ce qui y détermine de manière importante le champ de vagues. La présence de glace de mer complique également le processus de sélection des tempêtes, les processus de prévision à postériori et les méthodes d'analyse des conditions extrêmes. Afin de tenir compte de la variabilité et de l'incertitude associées aux effets de la lisière des glaces, quatre lisières des glaces différentes ont été utilisées pour chaque tempête; la lisière réelle des glaces et des lisières des glaces climatologiques associées à trois niveaux de probabilité (98 %, 50 % et 30 %). Les résultats sont présentés pour des scénarios individuels et combinés de lisières des glaces.

La comparaison des présents résultats à ceux d'études antérieures indique que les valeurs extrêmes obtenues dans le cadre de la présente étude se situent à la partie inférieure de la plage étendue de valeurs extrêmes obtenues lors d'autres études.

1.0 INTRODUCTION

The objective of this study was to produce, via hindcasting, a climatology for extreme storm waves in the Beaufort Sea, to be used as a reference for design considerations of offshore structures. Phase I, of this study was aimed at reviewing previous environmental studies for the Beaufort region, and establishing an appropriate procedure to provide the design reference information, selecting an appropriate spectral wave model, selecting severe storms affecting the Canadian Beaufort Sea region, and evaluation of model hindcasts. Phase II of the study consisted of the final selection of the top severe storm population, hindcast production, extremal analysis, treatment of ice edge and presentation of final results.

Already at the outset, it was realized that considerable effort would be required in order to provide adequate overwater wind fields and specification of the effects of sea ice and shallow water. Compared to previous studies with similar objectives for other areas such as the Canadian East and West Coasts or the Gulf of St. Lawrence, the number of available marine observations of weather and sea state from ships and rigs in the Beaufort is relatively small. The selection and hindcast of the potential severe storms is further complicated by the existence of sea ice. Extra care must therefore be taken when determining the wind and ice fields.

Due to the special operating conditions in the Beaufort Sea, where drilling is mostly carried out on structures which differ from those used elsewhere, different considerations must be taken for establishing design criteria and critical conditions, and when selecting severe storm events for hindcasting. Some effort was therefore put into estimating which storms were likely to generate extreme currents for example, as these would likely increase the potential for erosion of artificial islands.

In the following sections, the results of a major literature review covering previous environmental and design studies for the Beaufort Sea are discussed, followed by a description of the data sources utilized, event selection methods and the resulting lists of storm events. A description of the wave hindcast model selected for this application

is also given in this report with hindcast verification results provided. The production hindcast of the top 30 storms is described and hindcast results presented. Finally extremal analysis techniques are described and final results are presented for different statistical ice edge conditions (eg. 30%, 50%, 98% and actual ice edge are considered).

1.1 STUDY AREA

The study area covers the Canadian Beaufort Sea region bounded by longitudes 162°W and 120°W, latitude 76°N and the shoreline to the south (Figure 1.1). This covers the maximum extent of open water expected to occur during a summer season. Figure 1.1 also shows the selected model domain and the wind hindcast model grid.

1.2 HISTORICAL PERIOD COVERED

Experience from studies in other areas shows that a 30 year data base provides a sufficient number of storm events for establishing design criteria for offshore structures. The period covered in this study was the summer seasons (15 June -15 November) of 1957-1988 (32 years). The quality and quantity of data from earlier periods is often insufficient, and much harder to verify.

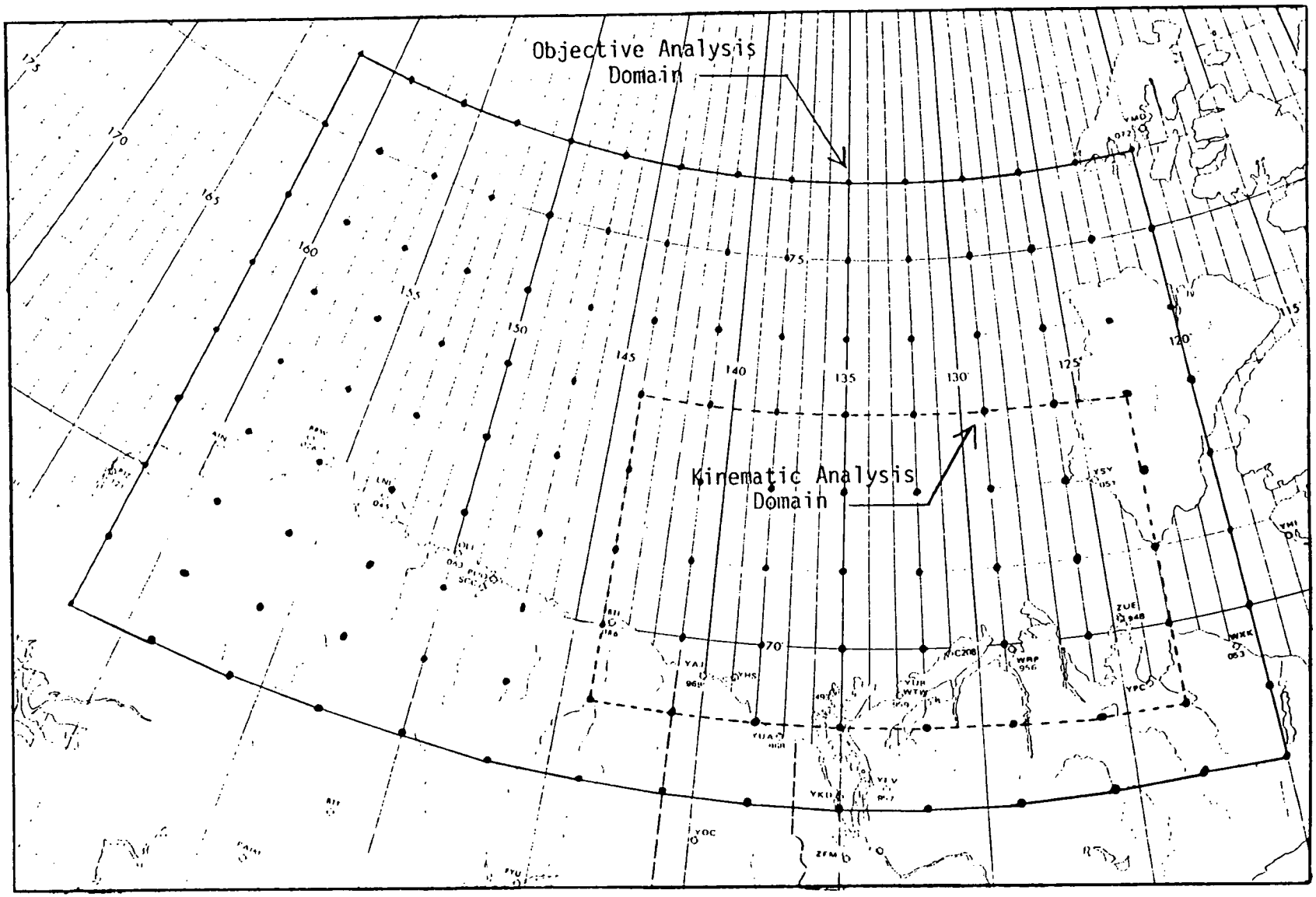

Figure 1.1 Study Area

2.0 LITERATURE REVIEW AND METHODOLOGY

2.1 REVIEW OF PREVIOUS STUDIES

It must be emphasized that the main objective of this study is to produce a climatology for extreme storm waves in the Beaufort Sea, to be used as a common reference guide for design consideration of offshore structures, artificial islands, and facilities. This is to be done by hindcasting the highest wave generating storms in the past several years (e.g. 30 years) with considerable attention paid to the specification of over water wind fields, the effect of the marginal ice zone (MIZ), and shallow water effect.

In addition, the study is to identify and select parameters that encompass the definition of "design storms", including wave height, period and direction, storm duration, and associated storm currents and erosion potential (i.e. the storm parameters which are critical for the design and operation of various offshore structures, artificial islands, pipelines, etc.). The hindcasting of the storm currents and erosion potential is beyond the scope of this study and should be considered in future investigation.

The approach we adopted here is based on a comprehensive hindcasting technique which is based on an extensive review of all marine data bases, careful selection of potential severe storms and the use of a well calibrated spectral ocean wave model. This approach is similar to that used in a recent East Coast Extreme Wind and Wave Hindcast Study by MacLaren Plansearch Limited and Oceanweather Inc., 1991 (see also Swail et al. 1989). However, additional complexity due to sparse data and ice effect must be addressed in the Beaufort Sea application.

A comprehensive literature review was carried out with the following objectives:

1. Provide an overview of previous environmental studies related to the Beaufort Sea, and review the state-of-the-art in estimating extreme values for offshore

structure design parameters.

2. Extract and compile a list of all Beaufort Sea storm events previously identified and studied.

3. Identify limitations of previous studies and devise a strategy to overcome them if possible.

4. Establish an appropriate methodology for conducting the present extreme waves study.

Several extreme wave studies have previously been carried out for the Beaufort Sea. As pointed out by Murray and Maes (1986), the studies provided a wide spread in the resulting estimates of extreme waves, for example the estimated 100 year return period extreme wave height varied from 4 m to 16 m. This may be attributed to the different approaches and data bases used in these various studies. Murray and Maes (1986) reviewed several studies of which two were given most attention, Hydrotechnology (1980) and Seaconsult (1981). Murray and Maes recommended several improvements to the methods they reviewed. These include using synoptic weather charts in combination with a kinematic analysis to specify wind fields varying in space and time, and using a hindcast model with improved resolution, both temporally and spatially. They pointed out that an improvement of the specified wind fields would provide the single most important contribution towards improving the extreme wave estimates. The Baird & Associates (1987) study to estimate the wave climate at Minuk-I-52, is an example. They used wind data from a few land stations, converted to over-water values through a transfer function, to derive wind-fields for the Beaufort. This did not account for spatial variations in the wind field, which in turn affects the spectral shape and directional distribution of the hindcast waves. Also, it is questionable whether or not land observations from one or a few selected

points are representative of offshore conditions, as considerable variability in coastal wind fields is found due to the orographic effect of Brook Mountain (Kozo and Robe, 1986).

Another common feature of the previous studies is the relatively limited consideration which was given to ice cover in deriving the wave climate. Although ice cover was included in model runs in recent hindcast studies, e.g. Baird & Associates (1987), sea ice cover variability was generally not included in the ensuing statistical analyses used to estimate extreme values, e.g. the 100 year extreme wave height. This could possibly have lead to substantial over- or underestimation of the extreme values which were determined.

As the emphasis for several of the previous studies has been on establishing design criteria for Sacrificial Beach Islands (SBI's), erosion has been of concern. Storm event duration, waves and currents as well as extreme currents were therefore also studied. The recent Seaconsult (1989) design storm study addressed these concerns. This study utilized more measured data than hindcast results. Storms were classified according to the shape of their normalized time history of significant wave height, peak period and current speed, which could help to determine what "type" of storm is likely to produce the most severe overall conditions. The Seaconsult study, however, did not proceed to examine if different storm types were related to different generating situations, such as wind field characteristics, ice cover, storm propagation direction and season. Such relationships might however, help to understand how extreme conditions occur.

The estimation of extreme current speeds, and the correlation between extreme winds, waves and currents has so far been somewhat limited by the relatively scarce amount of current data available. For the existing measurements, data quality is of concern, as pointed out by Buckley and Budgell (1988). Buckley and Budgell (1988) carried out hindcast studies of currents using a storm surge model. However, the results are more representative for low frequency type wind-related current events, rather than extreme storm values. We therefore find that both existing hindcast and measured

current data are mostly of limited value for extreme value estimations, and for use in combination with other parameters for determining design conditions for certain structures such as SBI's.

2.2 STORM PARAMETERS IDENTIFICATION

In order to identify events where environmental parameters are considered extreme and pose danger to a structure, the essential design parameters must be identified. These depend strongly on the type of structure under consideration. In the Beaufort Sea, SBI's have been widely used. In a number of the studies we reviewed, SBI's were used for determining design criteria.

Our review identified the following parameters to be most important:

- wind speed and direction
- waves (significant wave height, peak periods, and directionality);
- current speed and direction;
- duration of high values of the above parameters;
- measures of erosion, based on the above parameters;
- water level;
- ice cover; and
- joint probability distributions for the above mentioned quantities.

For an SBI, erosion is of primary concern. In this case, it seems that water level and current conditions are of significant importance, in addition to wave action. These factors may not have been considered sufficiently in the reviewed studies. The selection of storms which may produce serious erosion will be quite a different problem than selecting storms which produce the highest waves.

The derivation of extreme, or return period, values of design parameters depends on a reliable method for identification of storm events, and on which events are selected as the most severe. It would be desirable to determine a reduced number of parameters for ranking the storms according to severity. It therefore seems that the definition of an erosion index, as was done by Baird & Associates (1987), is a useful approach. This could be modified to account for other variables such as currents. The severity measure should be based on the energy available in a storm for carrying out erosion work, and the duration for which it is capable of carrying out this work.

However, in order to identify the most extreme storms in the above mentioned manner, the storms would all have to be hindcast, so that necessary wave information would be available. This would be time consuming and expensive.

Alternatively, an initial index for selecting potential severe storms can be estimated as:

$$S_W = \frac{1}{N}\sum_{i=1}^{N} U_j^2 \cdot F \cdot D$$

where N is the number of samples during the storm, U is the wind speed, F is the fetch for the wind direction corresponding to U_j, and D is the event duration. The inclusion of fetch and duration in this expression will indirectly give a measure of the expected wave and wind-driven current energy present in each storm. Having used this index to select a sufficient number of the most severe storms, a more detailed analysis can then be carried out, using the above mentioned (modified) erosion (or wave power) index to rank the storms according to severity.

The selection of the most severe wave-generating storms (combined with large currents and high erosion potential) is a very important and perhaps the most crucial step in such a process. Large effort, must therefore be spent in review all relevant data bases (e.g. marine observations, land station data, weather charts, buoy measurements) and previous studies.

In two previous studies, carried out by MPL and OWI for AES (MacLaren Plansearch Limited, 1987 and 1989), wind fields for a total of 24 summer storms in the Beaufort Sea were Hindcast. The selection criteria of these storms and hindcast methods were given by Agnew et al (1989). Two selection criteria were used:

1) Fourteen high wind producing storms were selected with highest severity index (which is defined by multiplying the maximum wind speed times storm duration above 30 knots).

2) Independently the 10 "high" wave producing storms were selected where wave measurements were available.

In the above selection no consideration was given to storm type, wind direction, ice conditions, or to a certain extent, storm duration.

The above storm selection procedure needs to be reexamined since the existing wind fields span a limited historical period, during which not all storm types have been sufficiently sampled, with the most severe storms possibly missed. At least 20 and possibly 30 years are needed to properly capture a sample of storm population in the entire potentially open water season. One of the approaches to the derivation of extremes assumes that the storm climatology and the ice-cover climatology are independent. Therefore, we are interested not only in storms which occurred in large open water conditions but those storms which might have occurred in maximum ice conditions, but within the calendar period in which open water conditions are possible (i.e. June - October).

If the storm climate and ice-cover climate are independent, the storm population needs to be selected irrespective of the actual ice-cover, but within the potential open-water season. The above hindcast storm set (which is referred to as AES set) is biased toward larger open ice years, since the selection criteria depended mainly upon MEDS buoy measured wave records. An unbiased storm selection should develop a production of several hindcast storms in 20-30 years, stratified into monthly or

perhaps biweekly periods between late June and late October, and refined to a target population of say 30 storms. There should be some overlap between this set and the AES set, but probably new wind fields need to be developed for about half of the storms to be hindcast. In addition, in the selection of the top severe events, considerations may be given to their potential extreme current generation, direction and storm duration.

2.3 SEA ICE COVER

Historical ice cover information for the Beaufort Sea is needed in this study in several forms. The approaches to the extremal analysis discussed below (Section 2.6) require not only ice cover actually associated with particular historical storms to be hindcast, but also a climatological description of the ice edge as a function of time in a potentially open season. The following sea-ice data sources were considered:

1) Records of composite sea-ice data for the Beaufort Sea which are held by the Ice Branch of AES, Ottawa. The period of data coverage is from 1959 to present in a form of hard copy of daily and weekly composite charts or digitized charts on 55 km grid.

2) The Canadian Climate Centre, AES, Downsview has complied a digital ice data base (1959 - 1986). This data set contains weekly information on ice concentration, extent, age/type, etc. This data base can be accessed through the CRISP System (Climate Research in Ice Statistics Program) at AES. It can provide various summaries and analysis of ice data , e.g. concentration frequencies, ice edge for given concentration, etc., and presents results in either tabulated or graphical form.

3) Digitized data set compiled by Walsh and Johnson (1979) where sea ice concentrations are available on a one degree grid. The data are available from the National Centre for Atmospheric Research (NCAR).

4) U.S. Navy and NOAA Joint Ice Centre (JIC), Suitland, MD, has archived maps of weekly synoptic analysis of sea ice cover. These maps have been digitized and made available on tape by the NOAA NCDC at a 1/4° latitude-longitude resolution for period 1972-1984.

5) Climatological Atlas of Brower et al (1977) which summarized about 20 years of ice data in terms of charts of mean, maximum and minimum sea ice extent and concentration in biweekly periods.

6) Marine climatological Atlas-Canadian Beaufort Sea, Agnew et al. (1987). It provides ice cover concentration summary, percent occurrences of any ice maps in a semi-monthly period and mean concentration where ice is present (98%, 90%, 70%, 50%, 30% and 10%).

2.4 STORM HINDCASTING

A spatially and temporally varying wind field is necessary to account for gradients and storm propagation across the Beaufort Sea. The best method of deriving acceptable wind fields is proven to be the application of objective analysis of weather charts in combination with a kinematic wind analysis. The method developed by Cardone et al (1980) and described by MacLaren Plansearch Ltd. (1987 and 1989) is proposed for this study.

A fully discrete spectral model of proven capability in shallow water as well as deep water is required for hindcasts. A spectral model also provides special advantages in the treatment of ice cover, since the effects of an irregular ice-edge as it affects the fetch lengths and widths, are automatically accounted for in such models. For this study, a special version of the ODGP (Ocean Data Gathering Program) spectral ocean wave model is used. The model incorporates a shallow water algorithm and a variable ice edge. The model is an extension of the deep water ODGP algorithm, which has provided skilful deep water hindcasts in a wide range of regimes, including the Beaufort, Chukchi and Bering Seas, and in the North Atlantic and Pacific Oceans

(Canadian Climate Centre, 1991; Eid and Cardone, 1987).

2.5 EXTREME VALUE ANALYSIS

Having selected and hindcast a given number of storms (e.g. 30 or more), an extreme value analysis may be carried out on either the wind and wave data, or on computed severity indices.

From the literature review, it seems that the most practical approach is to use a Peak Over Threshold (POT) model as described by Baird et al. (1987). Included in the analysis should be a test of goodness of fit of the selected distributions to the data. If a Gumbel distribution is found to be appropriate, the fitting method which according to theory should give the least bias is the Maximum Likelihood Estimate (MLE). The Method Of Moments (MOM) fitting method may also be used, as it is easier to implement, and gives reliable results. Different methods were examined in this study and the Gumbel distribution fitted to the Method of Moment is recommended.

2.6 JOINT PROBABILITIES OF ICE AND STORMS

None of the studies which were reviewed addressed the problem of joint occurrence of extreme winds, waves and ice coverage. In order to reliably assess 100 year return period waves, the variability of the ice cover should be included.

The difficulty in estimating extreme wave conditions, e.g. 100 year return values, in the Beaufort Sea is enhanced by the effects of the sea ice cover. The ice conditions affect the wave conditions, and to some extent, vice versa. When estimating extreme conditions are it therefore does not seem correct to assume that the ice and wave conditions are completely independent. Joint probability distributions are therefore not easy to determine, as these methods usually require the assumption that the processes under study are independent. Moreover, a possible larger scale (in time and

space) dependence of storm occurrence/genesis on other climate factors, which may also affect ice conditions, has not been determined. It is possible, for example, that higher temperatures in the region (due to global warming) would result in less ice, a higher frequency of storm occurrences, and that storms would generally be more severe. The combination of less ice and more severe storms would likely result in significantly higher waves. This has by no means been established though.

A commonly used method of estimating extreme wave conditions, is to extract a given number of the most severe storms (30-50) from a historical data base of weather conditions, generally covering a 30 year period. This procedure was carried out for the Beaufort Sea, where several hundred storms were identified, and ranked according to severity, in order to determine the most severe cases. As the available wave observations are very limited in this region, extreme wave conditions are estimated on the basis of hindcasts from a numerical model. In order to reduce costs, only the top 30 storms were hindcast. This procedure would, however, not provide a large enough sample to estimate the "true" extreme wave values, when taking reasonable variations in ice cover into consideration.

One method which has been proposed, is to hindcast storms several times, with different ice edges varied according to ice coverage statistics. For example 30 storms hindcast with 4 different ice edges, would then give wave fields for 120 storms, which could be analyzed for extreme values and return periods. However, it is difficult to assess how reliable these results are. The extreme value analysis procedures generally assume that the samples are independent. These storms will clearly not be, as groups of 4 will have the exact same driving forces, i.e. the wind fields.

An alternative approach is to use an empirical orthogonal functions technique as described below.

Two-dimensional fields, such as ice coverage, may be characterized by Empirical Orthogonal Functions (EOF's). A number of studies involving analysis of atmospheric pressure fields have been carried out in meteorology, using this technique. Similarly,

vector processes, such as ocean current, have been analyzed using EOF's.

Decomposing time series into EOF's is essentially a coordinate transformation, resulting in a set of functions with zero covariance. Each of the functions' amplitude time series will contain some fraction of the total variance of the original process. Usually, just a few of the largest functions will account for the major part of the variance (70-90%) of the parent process. Also, in many cases, each EOF can be related to a given underlying physical process. If this were the case for EOF's derived for the ice fields, we could likely relate one EOF to wind-driven ice coverage variability, and maybe a second function to ocean circulation controlled ice variability.

Joint probabilities of each EOF and wave heights could then be calculated, using multivariate normal and log-normal distributions. This method would necessarily be quite involved and requires greater level of efforts which is beyond the scope of this study. This should be addressed in future investigations.

In this study, the first approach is used, i.e. by hindcasting the selected severe storms with different ice edges, which includes actual ice edge, 30%, 50% and 98% occurrence of any ice. Extremal analysis is then applied to each group separately and for the entire population with different climatological ice edges. The results are then analyzed to study the sensitivity of the estimated values to different ice edges. This in turn provides the range of extreme values which may be expected.

3.0 DATA BASE ASSEMBLY

A comprehensive file of historical meteorological and sea state data was assembled for the selection of severe storms in the study area.

The data fall into the following categories:

1) archived surface weather charts;
2) weather observations from ships in transit;
3) weather observations from stationary offshore platforms and land stations; and
4) wave data from instruments, visual observations and numerical models.

The following sections describe the various source data bases which were used.

3.1 ATMOSPHERIC ENVIRONMENT SERVICE

The Hydrometeorology and Marine Division (CCAH) of the Canadian Climate Centre (CCC), AES, has collected and compiled a large number of marine data sets. In addition, several software packages are also available to access these data bases and analyze the data (e.g., MAST, LAST, DUST).

The following AES digital data bases were accessed using MAST/LAST systems:

a) COADS ship observations (1957-1988);
b) Drilling rigs (1974-1985);
c) Geostrophic Wind Climatology GWC (1957-1987);
d) Land stations data (1957-1988);
e) Digital pressure data (SPASM) (1958-1987); and
f) Ice data bases.

3.2 MARINE ENVIRONMENTAL DATA SERVICE

The Marine Environmental Data Services Branch (MEDS) of the Department of Fisheries and Oceans has been largely responsible for collection, retrieval, and analysis of data from the majority of wave measurement programs in Canadian waters since 1970. The bulk of MEDS wave data are from non-directional waverider buoys. A typical waverider observing program has a buoy located close to a nearby vessel, drilling platform, or land station where the signal is radioed and recorded on tape. The digital wave data base archived at MEDS can be accessed from remote terminals or data can be obtained on magnetic tapes.

3.3 THE BEAUFORT WEATHER OFFICE

During the 10 year period 1976-1985, the Atmospheric Environment Service operated the Beaufort Weather and Ice Office (BWIO or BWO) on contract to the offshore oil industry operating in the area. The office was operational in the summer seasons, lasting from June to November.

The BWO received weather and other available environmental observations (e.g. wave height, period) on a regular basis from drilling rigs and ships in the area, from ARGOS buoys when available and from aircraft, in addition to regular weather information through data links to other agencies (mainly AES-Edmonton). The office issued a variety of ice and weather reports. The reports used in this study were the annual reports providing seasonal summaries of time series and statistics for key parameters, lists of storm events, as well as a discussion of some of the major storm events in a given year. This information was used to identify storms for the Master Candidate List (MCL) and rank them according to severity.

3.4 LITERATURE

As described in Section 2, a number of storms were identified and documented in previous studies. Lists of storms were extracted from the following reports and

entered in the storm Master Candidate List (MCL):

- Murray & Maes (1986): Beaufort Sea Extreme Wave Studies Assessment - ESRF Study #023;
- Seaconsult (1986): An Extreme Value Analysis of Storm Wave Power at Minuk;
- Seaconsult (1989): Amauligak Development Studies 1988/89 - Design Storm Characteristics; Amauligak Region, Beaufort Sea;
- Baird & Associates (1986): Estimation of the Wave Climate at Minuk I-53 1960-1985;
- Buckley and Budgell (1988): Meteorologically Induced Currents in the Beaufort Sea;
- MacLaren Plansearch previous hindcast studies for AES (1988, 1989); and
- Manak, D.K. (1988) Climatic Study of Arctic Sea Ice Extent and Anomalies. CRG Rep. # 88-10.
- AES, Canadian Climate Centre report #87-2 (1987). Severe storms over the Canadian Western High Arctic, 1957-1983.

The Murray and Maes report provided an extensive review of two reports:

- Hydrotechnology (1980): Wave Hindcast Study, Beaufort Sea. Report for Gulf Canada; and
- Seaconsult (1981) A hindcast study of extreme water levels in the Beaufort Sea. Report for Esso Resources Canada Ltd.

Several other reports and publications were studied for further documentation of the storm of September 15-18, 1985.

3.5 ICE DATA

The Canadian Climate Centre of AES, Downsview, Ontario, has compiled digital ice data bases for the Canadian Arctic for the period 1959-86. This data set contains

weekly information on ice concentration and ice age/type on irregularly spaced grid points. This data base can be accessed through the CRISP (Climate Research in Ice Statistics Program) system at AES. CRISP can provide various summaries and analyses of ice data, such as ice concentration statistics, frequencies of each ice concentration by date, ice concentration for each year by date, different areas, etc. The results can be displayed in a form of contour maps using the CONAN and DUST packages.

Weekly Canadian ice charts for the study are from 1975 to 1989, June to October are also available to the project from Ice Central, Ottawa.

3.6 MICROFILM ARCHIVED WEATHER CHARTS

The National Climatic Data Centre (USA) archives a vast amount of world-wide weather data, records, and charts. The microfilm charts used in this study were the Northern Hemisphere Surface Charts covering the period May 1954 to October 1989.

These 6-hourly charts (00z, 06z, 12z, and 18z) are plotted and analyzed by The National Meteorological Centre (USA). The Final Analysis Charts are derived from all available land stations, buoys, ship reports, and rigs.

3.7 BWO ARCHIVED SURFACE ANALYSIS CHARTS

The Beaufort Weather Office archived surface analysis weather charts were used in the previous wind hindcast studies carried out by MPL/OWI for AES. The relevant charts for selected storms were obtained from BWO for use in the present study.

4.0 STORM CLASSIFICATION AND STORM SELECTION

4.1 INTRODUCTION

The single most important property of candidate storms in this study is the potential for generation of severe sea states somewhere within the study area. The process of identifying candidate storms is greatly complicated by the large size of the study area involved, unlike previous extreme wave climate studies, which generally considered specific sites. This is greatly complicated by the existence of the sea ice. Therefore, it was necessary to explore in this study many different possible indicators of storm occurrences and their severity.

Previous experience has shown that the most effective screening parameter is simply the maximum integrated wind speed (integration time 12 to 24 hours) in the fetch zone of wave generation directed toward the target site or area. Unfortunately, this parameter is not usually directly available as a screening parameter in archived meteorological data, except where continuous measured series are available from Ocean Station Vessels, e.g. in the North Atlantic. Therefore indirect estimates of storm wave generation potential derived from ship, coastal, or island wind observations, and surface pressure patterns must be used. Ultimately, some subjective assessments by meteorologists with specific experience in correlation of meteorological storm properties with wave generation must also be used in the ranking process, especially in the selection of the final most severe storms.

In a previous study, carried out for the Canadian East Coast, Canadian Climate Centre (1991) indirect estimates of storm wave generation potential were used to identify potentially severe storms. These included maximum sea-level pressure gradients, storm central pressure, and deepening rate. Szabo et al. (1989) were able to demonstrate objectively that the indirect procedures using parameters gleaned from operational Northern Hemisphere 6-hourly surface analysis correctly selected all storms which exceeded the effective wave height threshold of the extremal analysis at a given target point. That study also showed that the spatial structure of storms

was very important in the selection of extreme events for an area as opposed to a point location.

In the present study, sea-level pressure gradients and storm duration were found to be the two most important parameters. This was mainly due to the fact that severe conditions were not always linked to specific storm centres, which meant that storm centre pressures and deepening rates could not be quantified.

Storm frequency is relatively high for the study area. A target of 50 storms was set for a final list. During the process of storm list compilation, several hundred storms were identified. The task of reducing the list was carried out in several steps.

First, all assembled data sources and previous studies were utilized to develop a comprehensive list of candidate storms in the study area. This list was then reduced in several stages to a refined storm list, with the aid of both objective storm intensity ranking parameters and subjective ranking and intensity assessments.

In summary, the storm selection is accomplished in three main steps:

1) selection of candidate population of severe storms;
2) storm verification and cross-checking between data sources; and
3) storm ranking and final selection.

4.2 IDENTIFICATION OF POTENTIAL SEVERE STORMS

In addition to the storms compiled during the literature survey, the development of the initial coarse list of potentially severe wave-producing storms consisted of examining the data bases listed in Table 4.1. For each storm identified, the starting and ending dates/times, available maximum values of wind speed and wave height, maximum significant wave height, and duration of wind speed and wave heights above given thresholds, were extracted from the data records.

Data and storms were, for selection purposes, restricted to the ice free season - June 15th to November 15th. Following a major cross-referencing and consolidation task, an initial coarse list of storms was established, consisting of 1,058 storms or storm events. Through further cross-checking between data sources, data quality, combination of events, review of synoptic conditions, etc., this list was reduced to 511 events to provide the Master Candidate List (MCL) as shown in Appendix A (Table A.1). The MCL shows storm duration, peak wind and wave parameters and data sources utilized.

Table 4.1
Initial Storm Selection Criteria

Data Source	Coverage	Threshold	Number of Events
LAST Wind	1957-1988	Wind ≥ 25 kts	647
COADS Waves	1957-1988	Waves ≥ 1.5 m	245
COADS Wind	1957-1988	Wind ≥ 25 kts	346
RIG Waves	1976-1985	Waves ≥ 1.5 m	152
RIG Wind	1974-1985	Wind ≥ 25 kts	245
SPASM	1958-1987	Pressure ≤ 970 mb	73
MEDS	1975-1987	Waves ≥ 1.5 m	92
GWC	1957-1987	Wind ≥ 40 kts	143
Literature	-	As given in literature	220

4.3 REDUCTION OF THE MASTER CANDIDATE LIST

From the MCL (Master Candidate List), a subjective analysis using microfilm scan and examination of wind/wave peak values was made to eliminate some of the weaker storms and isolated events. In general, storms with a significant wave height less than 2.0 m were eliminated. As well, if there was only one wind or wave observation and a wind speed less than 30 knots, the storm was not included in the MCL. This cut-down also took into account wind and wave scenarios that would be producing

strong currents; that is, significant durations (24 hours or greater) of wind with an easterly or westerly component. Storms that contained high wind or wave values but short durations remained on the list, especially if they were quoted by numerous data sources. The latter were evaluated for storm duration, observed wind speed and wave height. Measured or observed values were also "weighted" higher than derived computations. Numerous events were also "lumped" together into single storm events. A "Semi-Final" storm list was then made up of 160 storms as shown in Appendix A, Table A.2. This selection process identified possible severe storms where wave generation may have been restricted due to ice conditions.

4.4 THRESHOLD ANALYSIS RANKING (TAR)

In recent hindcast studies carried out by Oceanweather, increased emphasis has been given to a method of objective ranking of historical storms based upon readily available properties of the surface pressure pattern of extratropical storms. In a study by Szabo et al.(1989), it was shown that there is a high correlation between certain storm properties and maximum H_S in a storm at a site, (see also Canadian Climate Centre, 1991).

These properties were:

1) minimum central pressure;
2) deepening rate;
3) maximum pressure gradient in the fetch zone of wave generation oriented such that waves generated therein affect the site of interest;
4) duration of maximum pressure gradient and a storm intensity parameter or a severity index made up of the product of the strength of the gradient and its duration; and
5) total pressure drop across the storm.

Given sufficient measured wave height data in storms, the correlations between measured wave height and the above parameters may be used to calibrate a ranking system in terms of parameter thresholds. This is simply done by defining for each

parameter a threshold value for which H_S exceeds a specified value in all observed or hindcast storms. The established thresholds then provide a basis for a scoring system which can be used for identifying and ranking storms. For example, if the properties of a candidate storm are such that the given thresholds for all the above 5 listed parameters are exceeded, then the storm is assigned a threshold analysis ranking (TAR) score of 5, on a scale of 0 to 5.

For the Beaufort, the above typical TAR scores could not be used in the same manner as for storms in the mid-latitudes. Minimum central pressure usually had no bearing on the gradient in the study area. At times, there were no individual central low pressure over the study area in storms analyzed. Strong gradients could be generated by a trough of low pressure over Alaska and high pressure north of the Beaufort. In other instances, with the study region being relatively small, gradients from storms as far way as the Gulf of Alaska which cover a vast area would spread their effects into the Beaufort Sea. Since there were no storm centres to pin-point, maximum deepening rate had no meaning. The storm gradient (difference in mb of the high pressure centre and low pressure centre affecting the study area) was not always uniform. A packing of isobars along the coastline existed independent of the storm gradient and also independent of any individual low or high pressure extremes. A storm "pattern" rather than the above individual parameters then became the deciding factor for extreme wave height and current generation. These patterns were comparable to those described by the Beaufort Weather Office. Patterns 1, 3 and 5 (see Figure 4.1) likely to produce the highest waves and strongest current with a westerly wind. Patterns 2 and 7 most likely to generate the highest wave and current with an easterly wind.

With these storm patterns in mind, a final storm list made up of 50 storms was selected out of the 160 semi-final storms with the following general thresholds:

Westerly Winds:	Pressure Gradient/2° Lat	with Duration of
	8 mb	≥48 hrs
	9	36
	10	24
	11	21
	≥12	18

Easterly Winds:	Pressure Gradient/2° Lat with Duration of	
	8 mb	≥60 hrs
	9	54
	10	48
	11	42
	≥12	36

The storms selected met these thresholds. When there were any storms that could not follow these guidelines, as in one storm with a strong north wind and high wave height, actual measured parameters from either MEDS or BWO reports were used in the selection or elimination process.

The final top 50 severe storms are listed in Table 4.2.

For further reduction of storms to the target population of about 30 events, additional careful analysis is required. This analysis may include among other things, the currents, erosion index, severity index, and sea ice conditions. In order to obtain sufficient population to present storm directionality, 30 storms may not be sufficient. In this case it is recommended to hindcast the entire 50 storms.

The final selection will also depend on the results of the model verification (Section 6.0) and review model response to different types of storms.

Again it must be mentioned here that the main objective of this study was to select the storm population which produce the highest waves to define the "design" wave parameters. Separately, we need to identify some number of current/erosion storms, which may or may not have large waves. This should be a subject of future

investigations. No doubt the selected storm population in the semi-final list of 160 storms would have captured those potential severe erosion storms.

Seventeen storms out of the above 50 were previously hindcast in MPL (1987) and (1989). Some of these storms required additional hindcast efforts to extend the storm duration to allow sufficient model spin-up, covering storm peak and allow the wave field to decay.

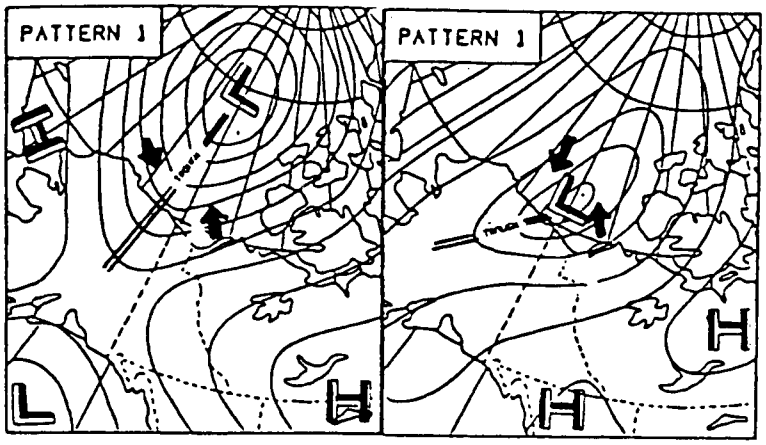

Pattern 1

Low or trough moves eastward across the Beaufort with or without a front(s) associated.

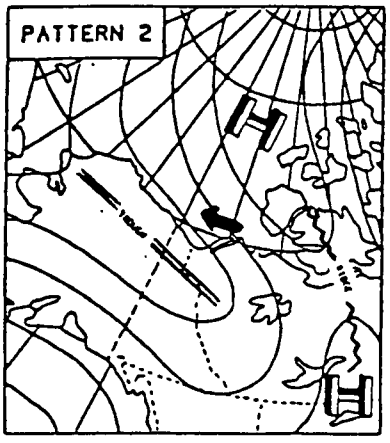

Pattern 2

Trough WNW to ESE across central or northern Alaska extending across the Yukon into the Mackenzie Valley. Ridge NW to SE across the eastern Beaufort, Amundsen Gulf or Banks Island. Often evolves into a pattern 3 or 4.

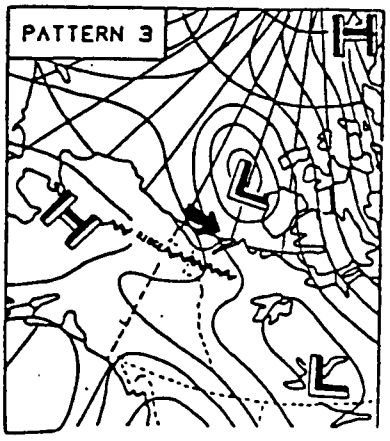

Pattern 3

Starts off as a pattern 2 or 7 (trough over Alaska). Trough moves offshore into the southern Beaufort. One or more low centres may develop in the trough. Trough and low(s) move northeastward as a ridge develops over Alaska.

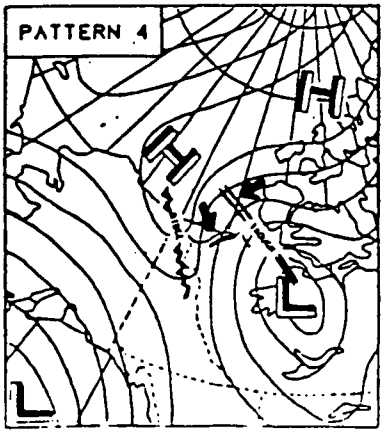

Pattern 4

Initially a deepening low over the Mackenzie Valley or the Great Arctic lakes. As the low develops and moves off, a trough extends into the Beaufort. A ridge develops across the north Alaska and north Yukon coasts and builds into the Mackenzie Valley.

Beaufort storm patterns.

Figure 4.1 Beaufort Weather Office Weather Patterns

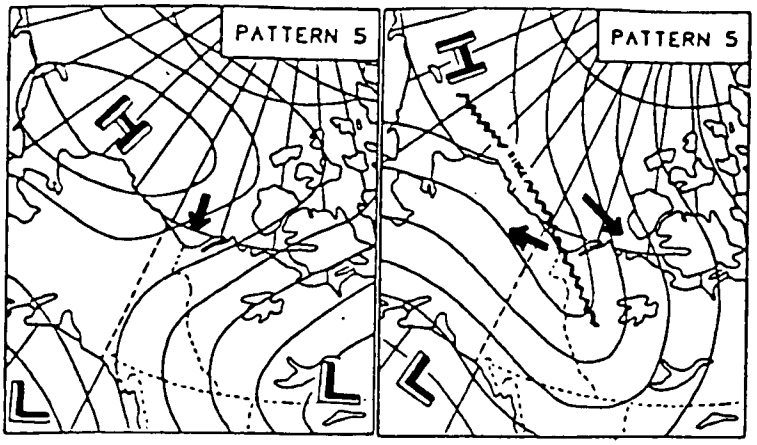

Pattern 5

Area of high pressure over the Beaufort or northern Mackenzie Valley.

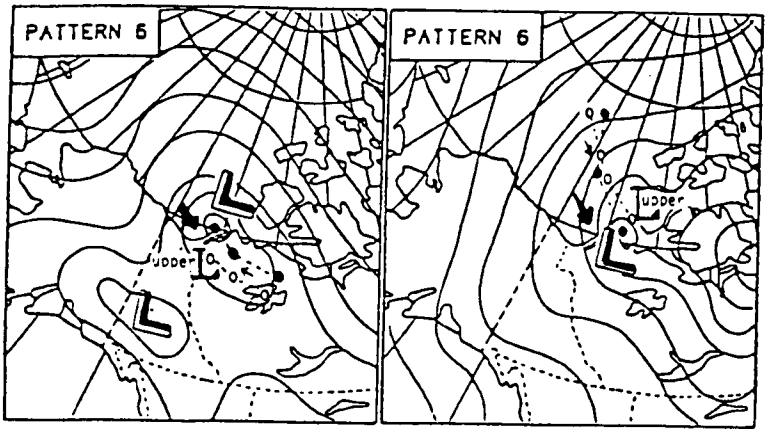

Pattern 6

Surface lows moving with upper cold lows.

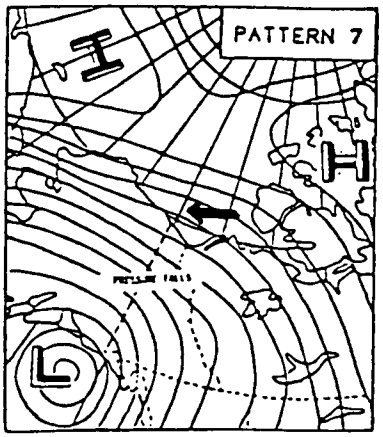

Pattern 7

A major Pacific storm moves toward southern Alaska. Overrunning warm air causes pressures to fall over Alaska and the Yukon. A strong cyclonic gradient eventually covers Alaska, Yukon, Mackenzie Valley and the southern Beaufort. Often evolves into a pattern 3

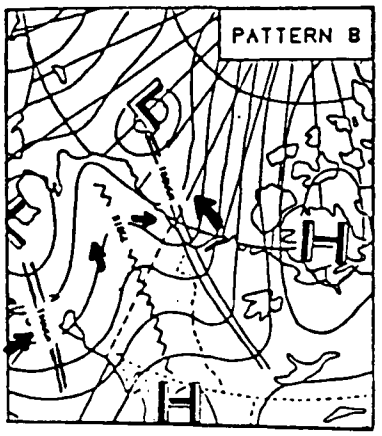

Pattern 8

Pacific disturbances migrate into the Bering Sea or Chukchi Sea. Associated troughs and ridges move northeastward across Alaska. Concurrently, a high pressure area usually lies over the western or central Arctic islands.

Figure 4.1 (cont'd)

Table 4.2 List of Top 50 Storms

FINAL-"50" Storm list for the Beaufort Sea

SOURCES:

A Severe storms over the Canadian Western High Arctic 1957-1983 Report #87-2
B Beaufort Weather Office Annual Summaries (1976-1985)
C Arctic Petroleum Operator's Association, 1983: Beaufort Sea Hindcast Study 1970-1982. APOA Study 203
D Seaconsult, 1986: An extreme value analysis of Storm Wave Power at Minuk.
E Baird & Associates, 1987: Estimation of the Wave Climate of Minuk I-53 1960-1985
F Buckley and Budgell, 1988:Meteorologically Induced Currents in the Beaufort Sea
G Sea Consult, 1989: Design Storm Characteristic, Amuligak Region, Beaufort Sea
H Maclaren Plansearch Database
I Seaconsult 1987: Wind and wave Hindcast for the storm of September 15 to 19, 1985
J Seaconsult 1986: Analysis of the ADGO Wave Measurements for the storm of September 15 to 18,1985
K Baird $ Associates, 1987: Estimation of the Wave Climate at Minuk I-53 during the storm of September 15 to 19,1985
L COADS.wave waves >= 1.5 m
M COADS.wind winds >= 25 kts
N LAST.wind winds >= 25 kts
P RIG.wave waves >= 1.5 m
R RIG.wind winds >= 25 kts
S SPASM central pressure <= 970 mb
T MPL HINDCAST
V MEDS

	START YYMMDDHH	END YYMMDDHH	Dur (hr)	Obs	Wind Spd (kts)	Wind Dir	Combined Hs (m)	Combined Tp (s)	Sea Dir	SEVERETY INDEX	Min Cent Pressure (mb)	Waverider Hs (m)	Waverider Tp (s)	Sources
* 86.	62072115	62072506	88	21	50.	290	4.0	5.0	080	4400				L,M
95.	62090311	62090715	100	34	56.	310	9.5	16.0	310	5600				L,M
97.	62090903	62091106	51	14	48.	250	8.0	6.0	230	2448				L,M
196.	70090218	70090716	118	37	45.	110	4.5	12.0	330	5310		3.6	8	C,L,M,N,V
198.	70091218	70091512	47	28	63.	240	5.6	7.0	284	2961	968.	2.5	6	A,C,L,N,N,T,V
*213.	71082112	71082412	72	5	26.	360	2.9	7.1		1872		2.9	7	C,N,V
270.	75080815	75081118	75	29	40.	280	4.7	10.0	310	3000		2.4	6	L,M,V
274.	75082606	75082814	56	29	45.	230	5.0	0.0	270	2520		2.2	6	D,L,M,N,V
282.	76081121	76081423	72	61	35.	050	4.3	6.2		2520		2.8	6	B,C,D,L,M,N,P,R,V
293.	76092814	76100208	90	166	32.	070	4.0	6.0	070	2880		1.9	7	L,M,P,R,V
302.	77082512	77090118	102	59	41.	320	3.4	6.9	290	4182		3.2	8	B,C,D,E,F,L,M,N,P,R,T,V
310.	77092100	77092214	38	60	42.	270	3.0	6.0	290	1596		2.9	7	D,N,P,R,V
313.	77100515	77101300	166	179	45.	130	3.5	5.0	120	7470		2.2	8	B,D,F,N,P,R,T,V
320.	78082218	78082618	104	54	40.	300	3.1	6.7		4160				C,E,N,R
321.	78090100	78090900	240	211	40.	090	2.7	6.0	037	9600		2.7	8	B,C,D,F,L,M,N,P,R,T,V
322.	78090906	78091412	126	54	38.	030	6.3	8.0	062	4788	969.0	1.9	7	L,M,R,S,V
325.	78091900	78092206	91	99	40.	070	7.5	12.0	098	3640		3.6	10	B,C,D,L,M,N,R,V
326.	78092800	78100303	99	98	45.	280	3.5	5.0		4455		2.4	9	M,N,R,T,V
327.	78100600	78101004	100	162	50	050	3.5	7.0		5000				B,F,M,N,R,T
333.	79091110	79091923	205	448	36.	070	4.0	6.0	090	7830		2.5	8	D,L,M,N,P,R,V

Table 4.2 (cont'd)

	START YYMMDDHH	END YYMMDDHH	Dur (hr)	Obs	Wind Spd (kts)	Wind Dir	Combined Sea Hs (m)	Combined Sea Tp (s)	Sea Dir	SEVERETY INDEX	Min Cent Pressure (mb)	Waverider Hs (m)	Waverider Tp (s)	Sources
334a.	79092900	79100806	246	339	42.	080	3.5	6.0		10332	965.2	2.4	7	B,C,D,E,F,L,M,N,P,R,S,T,V
335.	79100800	79101720	236	441	40.	110	4.5	6.0	080	9440		2.0	6	B,D,L,M,N,P,R,V
337.	79102112	79102606	114	122	45.	060	0.5	5.0	070	5130	953.9			M,N,R,S,T
350.	80082800	80090412	120	12	22.	280	3.3	8.0	240	2640		3.3	8	G,P,T,V
351.	80082900	80090503	171	117	40.	130	3.7	6.0	100	3960		1.9	6	B,N,P,R
366.	81080100	81081021	70	201	40	310	4.0	5.0	310	2800		2.7	7	B,D,E,F,L,M,N,P,R,T,V
369.	81081500	81081812	60	125	45.	290	6.0	5.0	290	2700		3.4	8	B,D,E,F,L,M,N,P,R,T,V
370.	81081900	81082700	167	212	35.	310	3.5	6.0	080	5845	967.3	2.3	7	C,D,E,L,M,N,P,R,S,V
371.	81082818	81090212	124	299	45.	240	4.0	8.0	270	5580		2.4	7	B,C,D,F,L,M,N,P,R,T,V
376.	81092700	81092912	275	710	36.	040	5.0	8.0	020	9900		2.8	8	B,C,D,E,F,M,N,P,R,T,V
378.	82071901	82072218	88	67	35.	350	3.0	6.3		3080		2.5	6	B,C,E,N,R
380.	82072614	82072912	70	111	50.	315	5.0	6.4		3500	1008	3.4	8	A,B,N,P,R,T,V
386.	82081912	82082318	93	121	38.	280	3.5	6.0		3534		2.8		B,D,E,M,N,P,R,V
391.	82091600	82091806	52	53	41.	230	3.0	5.0		2132		2.4	7	B,D,N,P,R,V
392.	82091900	82092321	117	268	41.	110	4.0	6.0	110	4797		3.3	8	B,D,F,L,M,N,P,R,T,V
395.	82100200	82100600	192	151	34.	290	3.0	3.0		6528	965.3			B,E,N,P,R,S
397.	82101717	82102312	253	147	54.	270	4.0	5.0		13662	967.3			B,F,N,P,R,S,T
415	83082917	83091200	295	179	45.	280	5.4	6.0	262	13275				B,D,L,M,N,P
436.	84071709	84072200	72	55	35.	250	2.0	5.0		2520		2.0	5	B,N,P,R
444.	84081006	84081418	99	88	36.	180	2.5	6.0	270	3564		2.2	6	D,H,N,P,R,V
446.	84082400	84082912	96	122	38.	360	2.5	5.0	280	3648		2.5	5	E,B,N,P,R
454.	84091800	84092412	110	143	38.	090	2.5	5.0	100	4180		2.5	5	B,L,M,N,P,R
456.	84092803	84100120	89	131	34.	110	4.0	5.0	350	3026		2.5	5	B,N,P,R
466.	85080506	85080917	77	66	32.	130	2.0	5.0		2464		2.0	5	B,R
473.	85090103	85090318	63	40	34.	110	3.5	5.0		2520		3.5	5	B,L,P,R
475.	85091221	85091906	153	312	50.	280	6.0	6.0	280	7650				B,E,F,I,J,K,L,M,N,P,R,T
483.	86082118	86082512	90	26	36.	320	5.1	9.0	331	3240		3.2	5	H,M,N
487.	86090706	86091712	246	32	32.	120	4.0	8.0	110	7872		3.0	9	H,L,M,N
*492.	87082400	87090106	102	68	46.	270	6.5	6.0	260	4692		3.5	9	L,M,N,V
507.	88080103	88080500	93	61	38.	310	4.3	8.0	288	3534		2.7		L,M,N

* COMBINES TWO EVENTS FROM THE MASTER CANDIDATE LIST (TOP160 STORMS)

4.5 ROLE OF THE ICE EDGE IN STORM EVENTS

A simple comparison was conducted to determine if a relationship exists between storms and ice edges. The actual storm ice edge was compared to the median ice edge to determine if it was offshore or inshore of the median edge position. Canadian ice charts prepared by Ice Forecasting Central, Atmospheric Environment Service, were used to determine the storm ice edge position. Ice charts were available for 45 of the 50 storms listed in Table 4.2. The median ice edge location was obtained from Markham's ice atlas (1980 and 1984) which summarizes ice charts from 1959 - 1980. Webster's ice atlas (1982) was used to double check and verify Markham's maps. The ice edges were surveyed along the whole length of the study area, from 130° to 160°. The ice edge was defined as 5/10 concentration as this concentration was presented by both Markham (1981) and Webster (1982).

The results of the comparison confirmed that a correlation exists between ice edge location and storm events. In general, the ice edge location during storms was offshore of the median position as shown in Table 4.3. 58% of the storm ice edges were offshore, 20% were not significantly different from the median position, and only 22% were classified as inshore of the median ice edge position. One potential explanation is that if wave heights were used as an initial criterion to select storms, then offshore ice edges will provide greater fetch than an inshore ice edge. A possible conclusion from the comparison is that an extreme storm would occur with an extreme offshore ice edge.

Several methods could be used to bring the ice edge location into the analysis of extreme storms. First, the actual ice edge during the storm could be used. For this purpose, the weekly ice charts from Ice Central Branch, AES can be used for 45 of the top 50 storms selected. The ice edge for the other 5 storms (earlier dates) can be obtained from other sources.

Table 4.3 Position of Ice Edges for the Top 50 Storms

Storm Number	Position	Storm Number	Position
213	M	371	O
270	M	376	O
274	I	378	O
282	M	380	O
293	O	386	O
302	O	391	O
310	O	392	O
313	O	395	O
320	I	397	M
321	O	415	I
322	O	436	I
323	O	444	M
326	O	446	I
327	O	454	M
333	O	456	M
334	O	466	I
335	O	473	I
337	M	475	M
350	I	483	O
351	I	487	M
366	O	492	O
369	O	507	O
370	O		

O Offshore The Median Ice Edge
M Median Ice Edge
I Inshore The Median Ice Edge

A second alternative would be to construct a set of storm ice edges to use as part of the probabilistic approach. Since the storm ice edges tend to be further offshore than the set of all ice edges, a set of storm ice edges would possess different characteristics. Ice edges for the top 160 storms could be used to provide a large enough set. Ice edges could then be selected at random and matched to various storms. It is felt that the ice edges should not be amalgamated and used to produce contours of percentage occurrence. This process smooths the gross irregularities of the ice edges.

What ice concentration should define the ice edge for storm purposes? The 7/10

concentration is defined as close pack ice composed of floes which are mostly in contact with each other. The 5/10 concentration falls in the category of open pack ice where the floes are just beginning to come in contact with each other, but generally are not in contact. Studies of the marginal ice zone and its effect on wave damping have found that 5/10 ice concentration will damp out all wave periods less than 10 seconds (Squire, 1983). This is for waves generated in open water moving into the pack ice. The 5/10 ice concentration is probably the best definition of the ice edge for the purposes of wave generation. At this concentration the ice cover is sufficient to prevent wave generation and to damp out short period waves. Nevertheless, this subject requires further research work to establish, not only the representative ice edge for modelling purposes, but also the wave generation inside the marginal ice zone (MIZ) and Wave propagation into the MIZ. This has recently been one of the objectives of the LIMEX (Labrador Ice Margin Experiments) projects.

4.6 STORM POPULATION CHARACTERISTICS

In an attempt to analyze the characteristics of the selected top severe storms (e.g. climatology, storm types, direction characteristics, and trends). The top 160 storms and the final top 50 events were distributed by year of occurrence (Figure 4.2 and 4.3) in order to examine the bias in selection, if any, trends, and any correlations with climate variabilities and anomalies. As shown in Figures 4.2. and 4.3 most of the storms were selected from the period 1970 to 1988 (e.g. 140 out of 160 were found in period 1970 to 1988 and 47 storms out of 50 are from the period 1970 to 1988). Earlier storms are not represented in proportion to their frequency of occurrence and therefor may not be included in the final selection for hindcast. The extremal analysis therefore may be based upon 20 years rather than 30 years as initially suggested.

As shown, the storm selection is bias towards more recent years. This is mainly due to the marine data coverage and data quality. The earlier storms are not detectable due to the poor meteorological charts, sparse observations, and poor quality data for early years.

BEAUFORT SEA STORMS
Histogram of Top 160 Storms

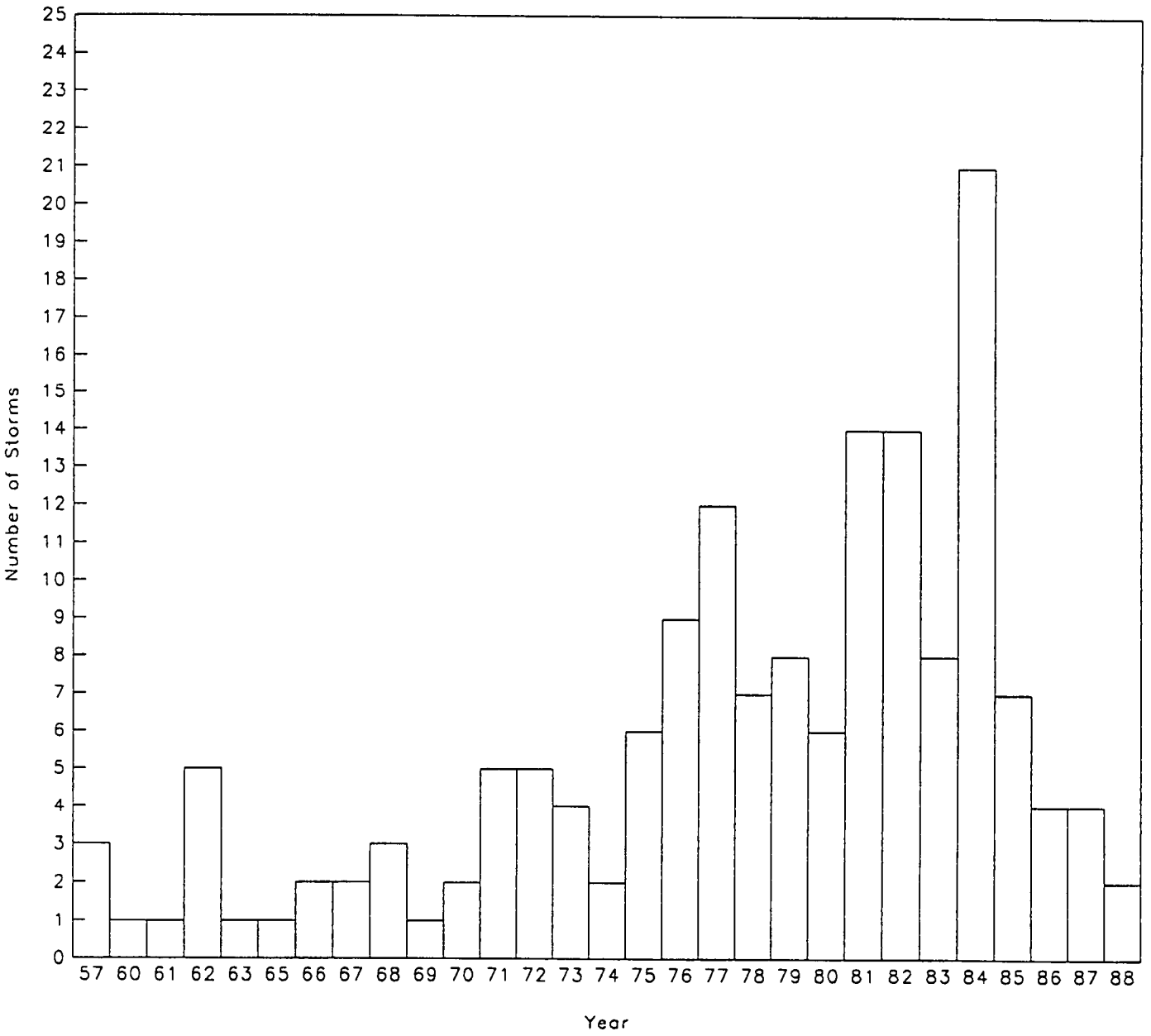

Figure 4.2

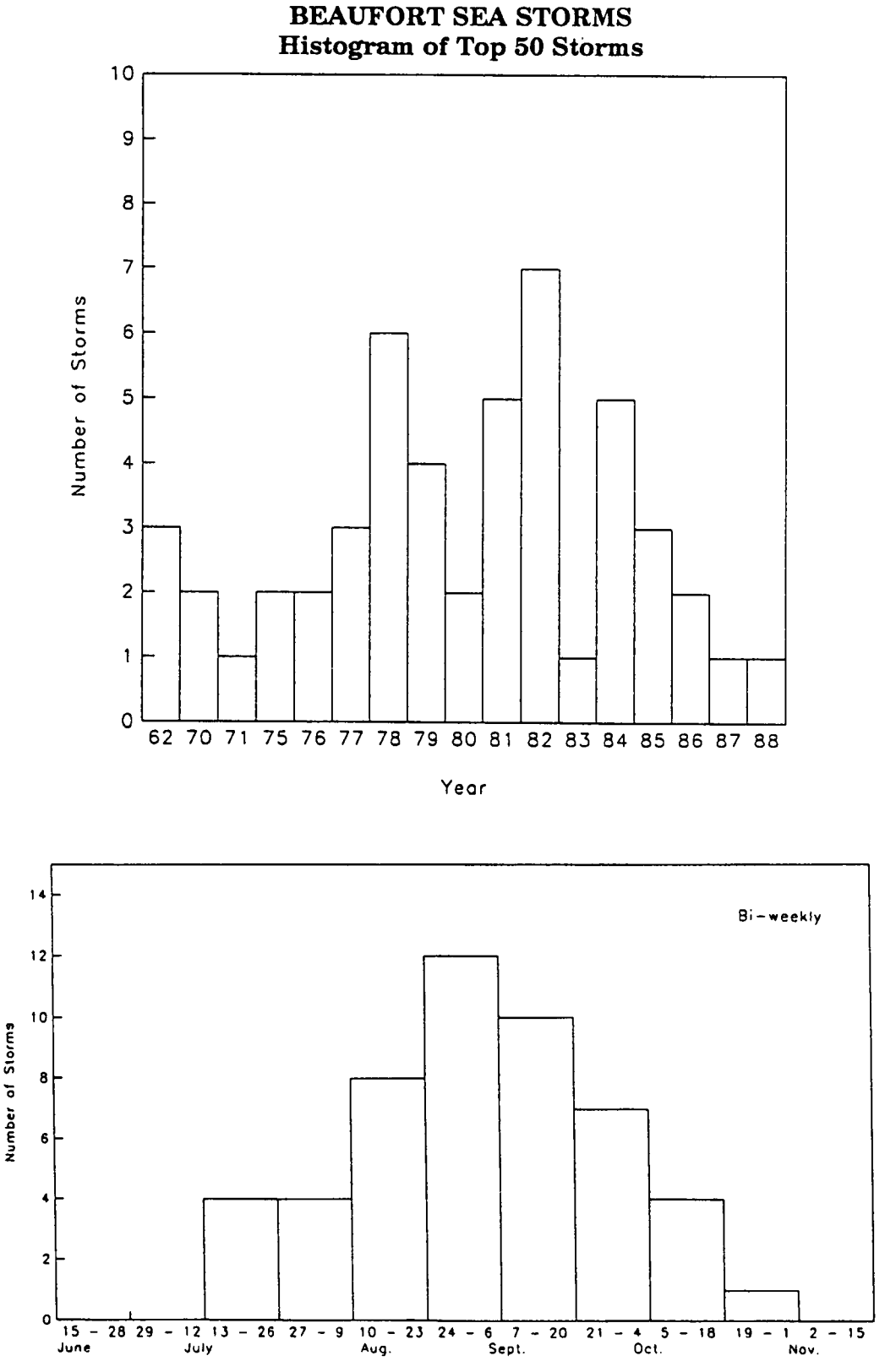
BEAUFORT SEA STORMS
Histogram of Top 50 Storms
Number of Storms
0
1
2
3
4
5
6
7
8
9
10
62 70 71 75 76 77 78 79 80 81 82 83 84 85 86 87 88
Year
Bi-weekly
Number of Storms
0
2
4
6
8
10
12
14
15 - 28 June
29 - 12 July
13 - 26
27 - 9
10 - 23 Aug.
24 - 6 Sept.
7 - 20
21 - 4 Oct.
5 - 18
19 - 1 Nov.
2 - 15

Figure 4.3

The variability in the distribution of storm population may be related to climate variability and sea ice anomalies. Manak (1988) studied the Arctic sea ice extent and anomalies for the period 1953 - 1984 and its correlation with climate variabilities. It was found that there is a 4 - 6 year cycle which he related to El-Nino, Southern Oscillation (ENSO) phenomenon or to natural interannual variability in Northern Pacific sea level pressure which may or may not be related to ENSO. A close look at Figures 4.2 and 4.3 shows a cycle of high number of storms in years with periodicity of about 4 - 6 years which may correspond to the above finding of Manak (1988), i.e. the variation in the ice edge. These speculations should be studied further in future work.

Of the storms to be hindcast from Table 4.2, wind fields are available (from previous AES study) only for 17 storms (smaller numbers of this may reach the final target population). The expansion of this population to say 30 storms should consider the directional distribution of storm types. As shown in Figure 4.4, the top 50 storms are distributed evenly over the three main directional sectors (i.e. W, N, and E) where as the 17 AES hindcast storms are more or less evenly divided between the westerly and easterly sectors. In the selection of the final storms, it is recommended that at least 10 storms are to be chosen from each directional sector (which also represent three different storm types).

Finally, a correlation between the storm severity index (SI) and the corresponding "observed peak significant wave height (H_s) is presented in Figure 4.5 (for the 160 and 50 top storm lists). As shown, a weak correlation between SI and H_s was found. The severity index would be a good indicator for current strength and erosion potential (as it includes both prime parameters, wind strength and storm duration). This weak correlation between SI and H_s indicates that the storms with large wave generation potential may not be a severe "erosion storms".

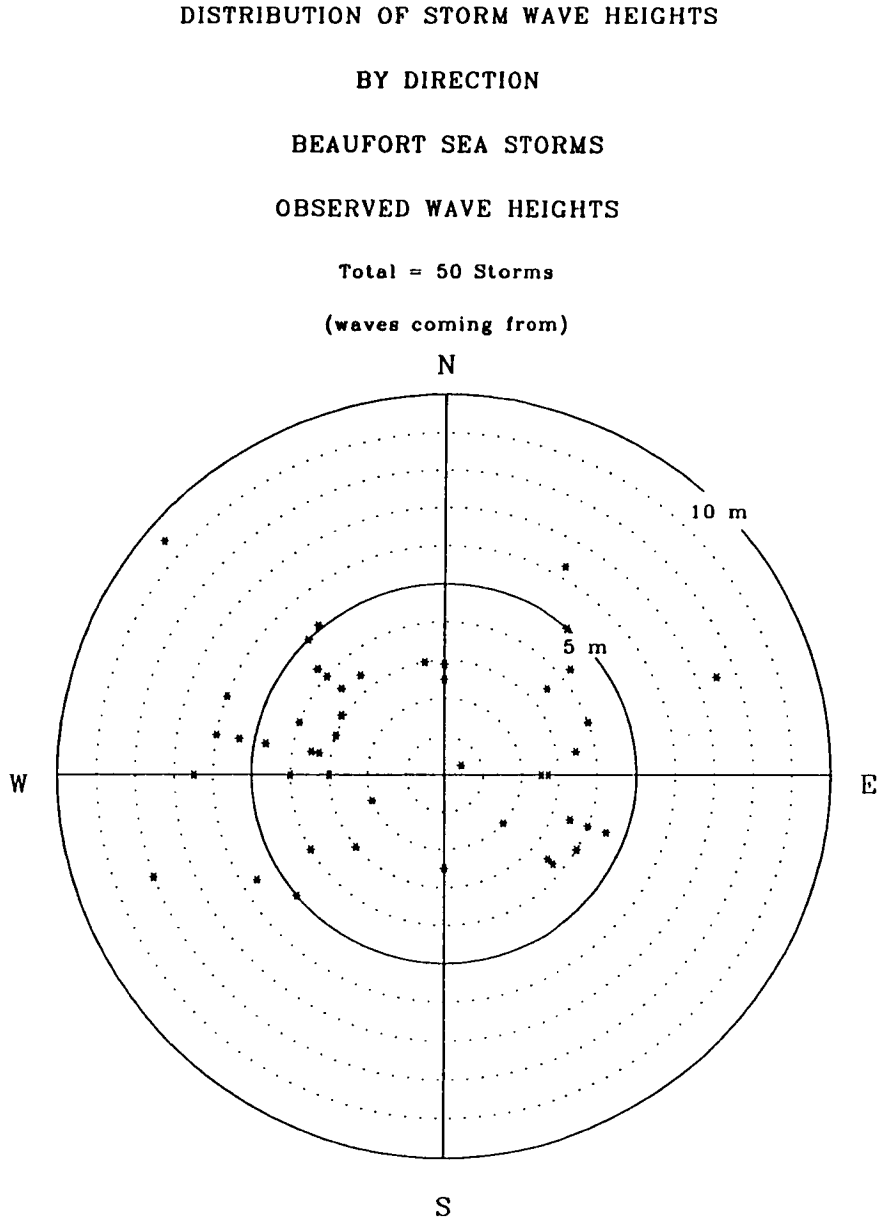

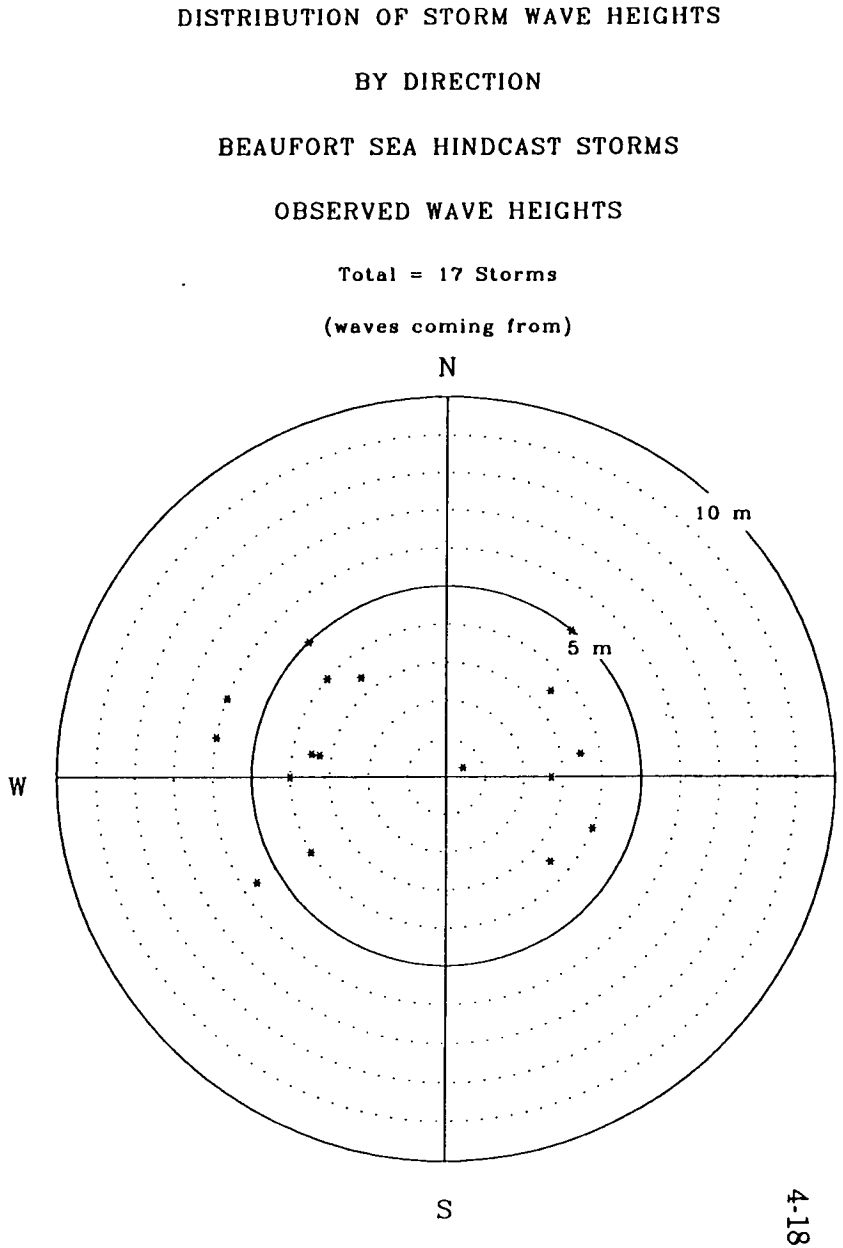

Figure 4.4 Distribution of Storm Wave Height by Direction

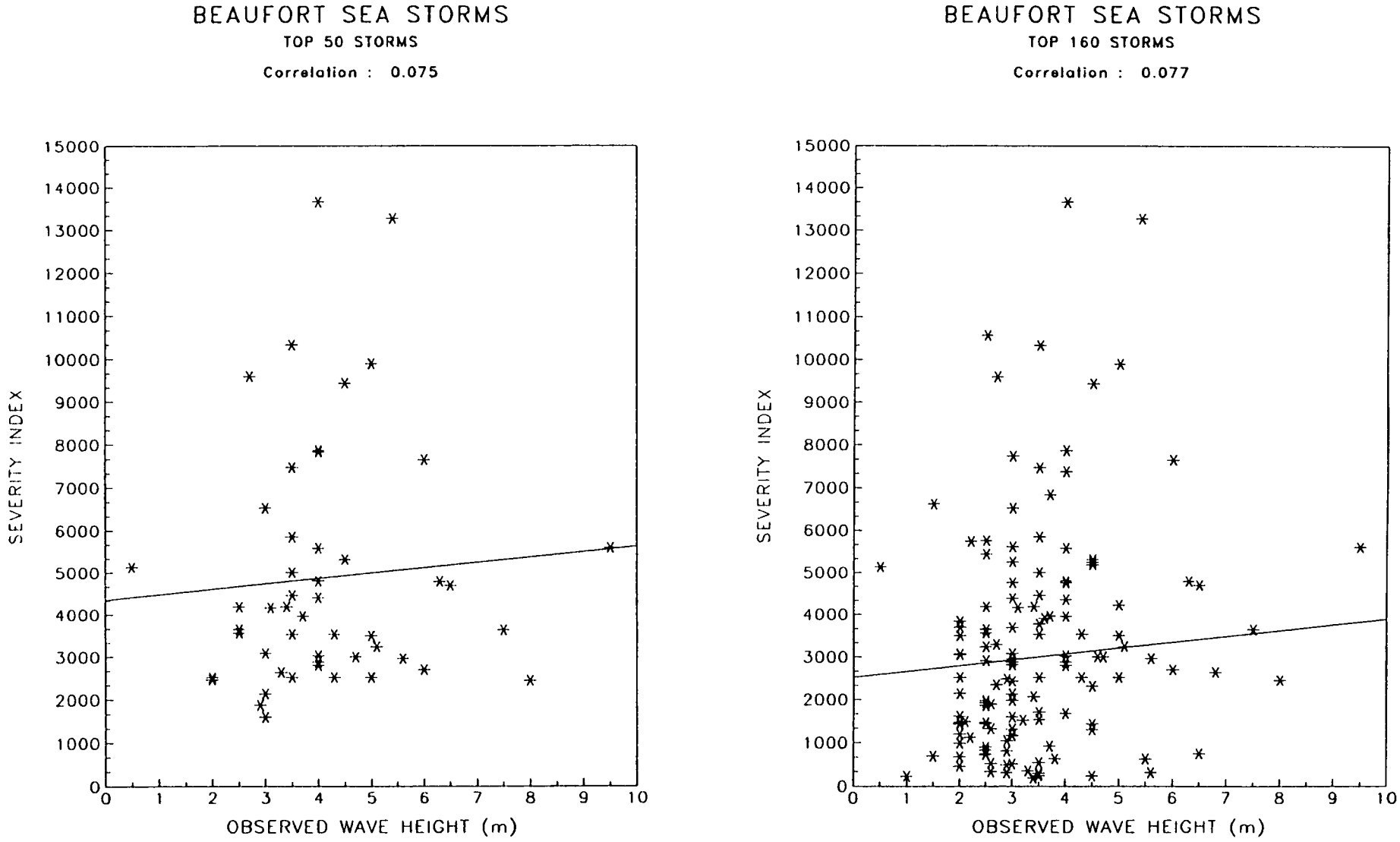

Figure 4.5 Correlation Between Storm Scatter Index and Wave Height

4.7 FINAL STORMS LIST

It is recommended that at least 30 storms be hindcast, drawn from the list of the 50-top events listed in Table 4.2. Of those event, 47 are from the period 1970-1989. Earlier storms are not represented in proportion to their frequency of occurrence and therefore should not be included. The extremal analysis therefore will be based upon 20-years. The reason that a longer historical period is not recommended is that earlier storms are not detectable owing to the poor meteorological charts for earlier years. In addition, even if such storms could be reliably detected, the attendant ice conditions would be poorly known.

Of the storms to be hindcast from Table 4.2, wind fields are available only for 17 storms from previous studies. The expansion to 30 storms must consider the rather broad directional distribution of storm types. Basically, the top-50 storms are distributed almost evenly over the three main sectors of considerations, i.e. northerly, easterly and westerly as shown in Figure 4.4. It is recommended that the final population should include at least 10 storms in each sector, therefore even more than 30 storms should be hindcast if possible.

The consideration of direction is believed to be important in this study since each class does not merely represent variability in direction of wave approach from storm to storm, but rather result from fundamentally different storm types, as classified for example by the BWO. The ultimate intensity to be attained by each class may be controlled by rather different meteorological processes and therefore the extreme distribution of say central pressure or maximum wind speed may vary from class to class, in turn providing rather different extreme wave distributions. It is well established by now that different storm classes should not be mixed in the extremal analysis. For example along the east coast of North America hurricanes and winter storms are treated separately. In the Beaufort, it should be at least considered that the different storm types may possess different extremal distributions.

Three further considerations support a larger storm population. First, since design

is affected not only by peak wave heights but by storm duration effects on erosion and currents, a wider range of storm types within each directional class is required to sample all relevant storm extremes. Second, the storm selection process is imperfect, and in view of the scarcity of historical meteorological data in the area, it is even more imperfect than is typical of studies of this type in other areas. Therefore it is necessary to hindcast more storms just to ensure that the true top-ranked historical storms of each class are included in the selected population. Finally, ice coverage affects each storm class differently. Easterly storms are the least affected by variability of ice cover from year to year, westerly storms somewhat more affected than easterly types, and northerly storms most affected as the fetch limitation in northerly storms is almost always limited directly by the ice field.

The list of final 30 storms was subjectively selected from the top 50 storms. The selection was based on a review of all available information i.e., microfilm of weather charts, observed/measured data, storm characteristics, wind conditions and storm intensity and direction, ice conditions, etc.

The top 30 storms are shown in Table 4.4. As shown, the top 30 storms consist of 15 previously hindcast storms and 15 new storms. The surface pressure analysis charts were obtained from AES for the new storms, from Beaufort weather office for the period 1976-1985, and from Arctic Weather Centre (AWC) for periods outside this period.

Since the extremes are to be derived following a hindcast approach, each part of that approach must be specified, including the specification of the storm population as described previously, the selection of reliable hindcast method, and the treatment of the ice effect both within the hindcast process and the extremal analysis. As part of the hindcast process it is important to provide the best possible specification of the ice cover and to explore the sensitivity to errors in the location and concentration of the ice field upwind the main fetch zone of wave generation in each particular storm. In the specification of the effective fetch limit imposed by ice cover, the 5/10th isoline was considered although there are indications that this may lead to somewhat conservative

sea state specification in fetch (ice) limited conditions. It would also be desirable to investigate the possible effect of relatively low concentrations of ice (less than 5/10th) on the definition of the effective upwind fetch, although such a research program appears to be beyond the scope of the present study.

Table 4.4 Final Top 30 Storms

		Storm Periods (YY MM DD HR)	
Number	**MCL I.D. Number**	**Start Date**	**End Date**
1	198	70 09 13 00	70 09 16 12
2	270	75 08 09 00	75 08 11 12
3	274	75 08 25 12	75 08 29 00
4	282	76 08 11 12	76 08 14 00
5	293	76 09 28 00	76 10 02 00
6	302	77 08 25 12	77 08 28 00
7	310	77 09 23 12	77 09 26 00
8	325	78 09 19 00	78 09 22 12
9	326	78 09 28 00	78 10 01 00
10	327	78 10 06 00	78 10 10 12
11	333	79 09 14 00	79 09 17 12
12	334a	79 09 29 12	79 10 06 18
13	335	79 10 08 12	79 10 11 12
14	350	80 08 28 12	80 09 04 00
15	366	81 08 01 00	81 08 04 12
16	369	81 08 16 00	81 08 19 00
17	371	81 08 30 00	81 09 03 00
18	376	81 09 27 00	81 09 29 00
19	380	82 07 26 00	82 08 02 00
20	386	82 08 19 12	82 08 22 12
21	391	82 09 16 00	82 09 18 00
22	392	82 09 20 00	82 09 23 00
23	405	82 10 19 00	82 10 27 00
24	446	84 08 25 00	84 08 28 00
25	456	84 09 29 00	84 10 02 12
26	475	85 09 16 00	85 09 19 00
27	483	86 08 22 00	86 08 24 00
28	487	86 09 08 00	86 09 10 00
29	492	87 08 28 00	87 09 02 12
30	507	88 08 02 00	88 08 05 06

5.0 THE WAVE HINDCAST MODEL

5.1 BACKGROUND

The wave hindcast model adapted for this study is a special version of the ODGP which includes shallow water formulation. This model is a so-called fully-discrete spectral wave model. That is, the wave spectrum is resolved in discrete frequency-direction bins, a grid of points is laid out to represent the basin of interest, and a solution is obtained based upon integration of the spectral energy balance equation, a process which successively simulates, at each model grid point, and for each time step, the physical processes of wave growth and dissipation (through the source terms of the energy balance) and wave propagation.

Three classes of spectral models are generally recognized. First-generation models (1G), such as the ODGP model (Cardone, Pierson, and Ward, 1976), are part of the family of fully-discrete spectral models originally proposed by Pierson, Tick, and Baer (1966). This type of model is characterized by a source-term formulation which does not include an explicit representation of conservative transfers of energy between spectral components, believed to be associated with resonant non-linear wave-wave interactions. Second-generation models (2G) were introduced to include at least a parametric representation of a wave-wave interaction source term, while third-generation (3G) models, only recently introduced, attempt to model the wave-wave interaction source term rigorously.

The formulation of the ODGP model has been described in detail in past studies, most recently in MacLaren Plansearch Limited (1985) and ESRF (Eid and Cardone 1987). The skill of the model has also been documented in numerous studies, including Reece and Cardone (1982), and more recently by Cardone and Greenwood (1987), wherein the characteristics of the model are compared to those of recent 2G and 3G models.

While a number of 2G models and the so-called 3G-WAM model (WAMDI Group, 1988) have been demonstrated in some applications to achieve hindcast skill

comparable to the ODGP 1G model, no clear superiority of these later formulations has been established. For example, the 2G model developed at Oceanweather for an international wave model comparison program (SWAMP, 1985), and known as the SAIL model (Greenwood, Cardone, and Lawson, 1985), has been calibrated against the same data used for the ODGP model, and validated against wave measurements in some of the same validation storms used in this study with good skill, but only in a deep water mode. The 3G-WAM was not considered for this study. It has been tested against three Gulf of Mexico hurricanes (WAMDI Group, 1988) and provides no greater skill in specification of peak wave height and period than provided by ODGP when driven by identical wind fields, yet 3G-WAM requires a factor of 5 or more computer time than ODGP. The 3G-WAM model was also applied in a deep water mode for those tests. The shallow water version of 3G-WAM has not been tested against tropical cyclone data.

5.2 GRID SYSTEM

Basically, the ODGP wave model was adapted in this problem on a very high resolution grid system covering the domain shown in Figure 5.1. The model has basically the following attributes:

grid domain:	69°-76° North latitude 120°-162° West longitude
grid spacing:	37.3 km nominal, 614 grid points
projection:	transverse mercator, assumed meridian at 141 degrees West
time step:	60 minutes (30 minutes grow, 60 minutes propagation, 30 minutes grow)
angular spectral resolution:	24 directions, 15 degree bandwidth
frequency spectral resolution:	15 frequencies, binned as given in Table 5.1

spectral growth algorithms:	ODGP2 (deep water); ODGPS (shallow water)
propagation:	interpolatory, deep water and shallow water, great circle effects and refraction and shoaling included.

Table 5.1

Band	Nominal Frequency	Bandwidth
1	14/360 Hz = .03889 Hz	1/180 Hz
2	16/360 = .04444	1/180
3	18/360 = .05000	1/180
4	20/360 = .05556	1/180
5	22/360 = .06111	1/180
6	24/360 = .06667	1/180
7	26/360 = .07222	1/180
8	29/360 = .08056	1/ 90
9	33/360 = .09167	1/ 90
10	37/360 = .10278	1/ 90
11	42/360 = .11667	1/ 60
12	48/360 = .13333	1/ 60
13	57/360 = .15833	1/ 30
14	75/360 = .20833	1/ 15
15	111/360 = .30833	2/ 15

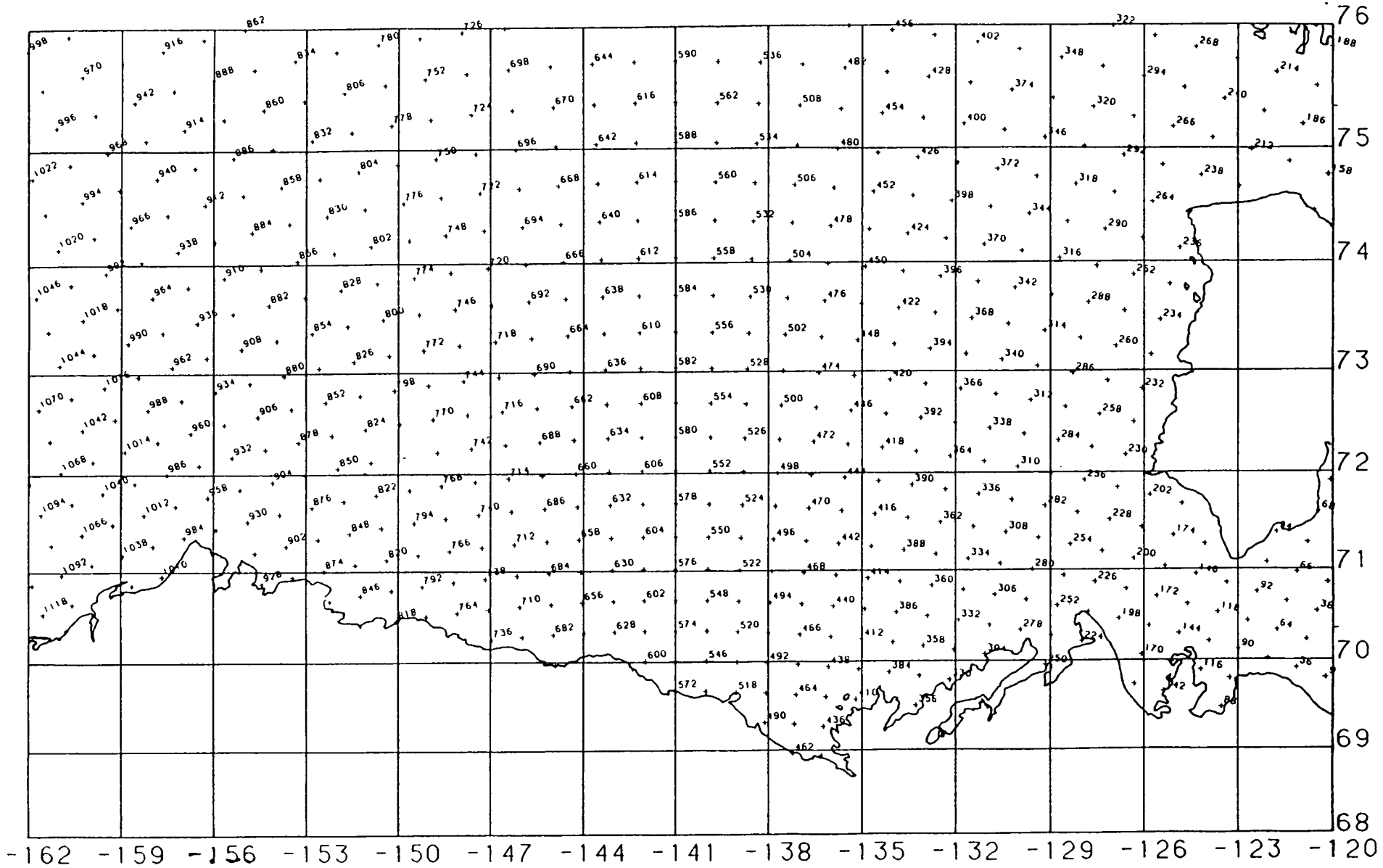

Figure 5.1 ODGP Model Grid for the Beaufort Sea

5.3 BASIC PROPAGATION SCHEME

The propagation scheme is basically interpolatory. Convergence of meridians (great circle effects) is modelled. This scheme, whose dispersion properties are described in detail by Greenwood, Cardone, and Lawson (1985), has been used with success by Oceanweather in its wave models set-up since the industry-sponsored Gulf of Alaska Pilot Study (GAPS), carried out in 1978. The scheme was first described by Greenwood and Cardone (1977).

5.4 DEEP-WATER SOURCE-TERM ALGORITHMS

The variants of the ODGP spectral/growth model were applied in this model, one for deepwater grid point, the second at shallow water grid points (points with water depth less than 200 m.)

The original ODGP algorithm was implemented in a wave model as a subroutine called CMPE24. While a few changes in the code and numerics of this subroutine have been effected since the original version was developed in the ODGP-Analysis Phase (ODGP-AP), the calibration of this spectral growth/dissipation algorithm and the quantitative behaviour of hindcasts of tropical and extratropical cyclones have not changed. The algorithm is described in most detail in the original ODGP-AP report (proprietary to ODGP-AP participants) and most recently in the pubic domain in MacLaren Plansearch Limited (1985).

A slightly modified version of the ODGP spectral/growth algorithm (ODGP2) was developed in 1983, and has been used operationally since then. The subroutine which implements the modified algorithm is called CMPE27. The changes affect only the behaviour of the high-frequency part of the wave spectrum, and were made in order to make the so-called saturation range of the spectrum more responsive to the stage of wave development. CMPE27 differs from CMPE24 in the following three particulars:

1. The integrated band (0.24167 hz to 3.0 hz) is not automatically saturated by the local wind, but is subject to grow, propagate, and dissipate.

2. The f^{-4} range in the representation of the high-frequency tail of saturated spectrum in the ODGP algorithm is not used, as an f^{-5} representation through out the tail is assumed.

3. Phillips "constant" is allowed to float as a function of sea state, specifically,

$$\alpha = 0.0081(E_{sat}/E)^{0.23}$$

where E is the non-dimensional total variance and E_{sat} is the fully-developed value of same.

5.5 SHALLOW-WATER PROPAGATION AND DEPTH GRID

The propagation scheme of the shallow-water model is analogous to that used in the deep-water model. In the construction of the table of propagation coefficients at each grid point and for each frequency and direction bin, a numerical shallow-water tracing program is used instead of the simple spherical trigonometric calculation of the ray path in the deep-water program. Effects of shoaling and refraction over an irregular bathymetry as resolved on the model grid are included.

The depth field was derived from the digital database produced at the U.S. National Geophysical Data Centre (NGDC), known as ETOPO5. That database is stored on one 6250 bpi magnetic tape and resolves the global topography/bathymetry on a 5 minute grid.

Depths are assigned to the wave model grid by simply averaging all ETOPO5 grid depths which lie within a grid box defined by each point. Since there are typically 12 or 16 ETOPO5 depths within a rectangle represented by each grid point, the binning effects considerable smoothing of the depth field, and no further smoothing was

applied. At a few points near shore, the depth was limited to a minimum depth of 7.5 m, to avoid computational problems with the ray-tracing routine.

The assignment of grid points to land or sea was made by digitizing the coastline off standard charts, plotting the digitized coastline together with the entire grid array, then manually reading off those points which lie on land. The grid was then replotted to check the assignments. After deletion of land points, the grid contains 614 active points. A facility is included in any given run to treat as land, grid point which lie within an ice field.

5.6 SHALLOW-WATER SOURCE TERMS

A shallow-water version of the ODGP spectral growth algorithm (CMPE24/ CMPE27) has been under development since 1984. The first significant test of the algorithm against field measurements was made during the Canadian Atlantic Storms Project (CASP), which was carried out on the Canadian Scotian Shelf in the period January - March 1986. The performance of the model hindcasts, which were carried out as part of a real-time analysis/ forecast system, exceeded that of the several other operational and research shallow-water models which also participated in the experiment (Eid and Cardone, 1987).

The modifications of the ODGP deep-water routine spectral/growth subroutine made to extend the model to shallow water are:

1) transformation of the fully-developed Pierson-Moskowitz spectrum to shallow water;
2) calculation of an explicit attenuation associated with bottom friction, which is modelled after the comprehensive treatment of Grant and Madsen (1982);
3) calculation of the exponential growth rate using the shallow-water celerity; and
4) adoption of wave-number scaling of the high-frequency saturation range

of the spectrum, with the equilibrium range coefficient, α, expressed as a function of the stage of wave development.

A somewhat more detailed description of these aspects of the model is given in Appendix B.

5.7 WIND FIELD SPECIFICATION

Wind fields are specified by the methodology described by Cardone et al. (1980) for marine winds, which combines winds calculated from pressure fields through a marine planetary boundary layer model (MPBL) with winds specified by kinematic analysis of direct wind observations. The kinematic analysis is applied on a small part of the whole analysis area, since, unlike mid-latitude oceanic regions in which ship reports are relatively numerous, in-situ reports in the Canadian Beaufort are available only near the coast and, in recent years, only in areas of offshore drilling. The model domain extends from 68°N to 76°N and 120°W to 162°W as shown in Figure 1.1. The grid size was chosen to be 1° latitude by 3° longitude.

The wind field analysis method used in the present study is described in detail in a number of previous publications, MacLaren Plansearch Limited (1987) and (1989), Agnew et al. (1989). Only a brief description is provided here.

The six-hourly synoptic surface analysis weather charts were obtained from the available sources. These include the Beaufort Weather Office (BWO), the Arctic Weather Centre (AWC), the Canadian Meteorological Centre (CMC) and the NOAA 6-hourly northern hemisphere surface analysis charts. In addition, marine observations and wind records from six coastal land stations were obtained from AES' archives (on magnetic tapes). These data were plotted on a base map for each storm and used for reanalysis of the pressure fields.

All charts were reanalysed using all available data (including microfilms). The previously hindcast wind fields (15 old storms) were reviewed and some cases were

revisited where the hindcast duration was extended to cover storm peaks and decay.

The gridded pressure fields derived from the above hand-drawn analysis charts were then used to provide the objective analysis wind fields using Cardone's marine planetary boundary layer (MPBL) model.

Over open water, or water with less than five-tenths ice cover, winds were calculated from the MPBL, which in general requires the following parameters at each grid point: sea level pressure gradient; horizontal air transport gradient (baroclinicity effect); air sea temperature difference (stratification effect). Air and sea temperature fields are not digitized in general, though if available the air-sea temperature difference may be specified at grid points. The horizontal air temperature gradient is specified from climatological data.

The MPBL provides unbiased and reasonably accurate surface winds over open water, when accurate inputs are specified, and acceleration terms are small. The atmospheric boundary layer over sea-ice is rather complicated, even for relatively small fractional covers (about four-tenths or more). The surface wind stress, and the near surface wind field, averaged over a region depends not only on the external conditions of the PBL, but also sensitivity on the details of the distribution and structure of the sea ice, the buoyancy flux associated with leads and polynas, and height of the shallow inversions often characterizing arctic boundary layers.

For the purpose of wave modelling, only MPBL winds were provided. The impact of errors on surface winds due to sea-ice is small and is limited to areas in the immediate vicinity of the ice edge.

The kinematic wind fields are by far the most accurate and least biased winds, primarily because the method allowed a thorough re-analysis of the evolution of the wind field. Kinematic analysis also allows the wind fields to represent effects not well modelled by pressure-wind transformation techniques, such as temporal variations in surface pressure gradients, and deformation in surface winds near the downstream

of coasts. However, the degree of accuracy of such analysis is primarily a function of available observations.

The transformation of wind speed measured at coastal stations by equivalent over-water speed was considered in the present study. The orographic effect of the Brooks Mountain Range on the coastal winds was also used in the kinematic analysis.

Kinematic analysis is a manual process that involves the following basic steps: (1) assembling and plotting all synoptic observations of wind speed and direction, and sea level pressure, from rigs, ships and land stations at 6-hourly intervals on a suitable base map projection for the storm event of usually 2-4 days duration; (2) identification and rejection of erroneous and unrepresentative observations to the extent possible; (3) construction of a continuity chart which defines the movements of storm centres, fronts and other significant features of the surface wind field; (4) construction of streamlines and isotachs; and (5) gridding of wind speed and direction by hand from the streamline/isotach fields.

For the purpose of wave modelling, the period over which wind fields must be specified in selected storm ranges between 2 and 4 days. The storm period may be considered to be composed of three phases: (1) a spinup period (24-48 hrs); (2) the period in which the major storm crosses the region and generates maximum sea states; and (3) the period from 12-24 hours after the occurrence of peak states, during which the wind field no longer plays a critical role in the hindcast but which should be modelled nevertheless so the hindcast wave series will include an adequate period of wave decay at the sites of interest.

The kinematic analysis domain extended from 69°N to 73°N and from 123°W to 144°W (Figure 1.1) which includes most ship/rig locations and represents the average to maximum open-water area in the Canadian Beaufort Sea.

Finally, a blend of the objective and kinematic analyses is carried out with the kinematic analysis reserved for the most critical parts of the wind field as mentioned

previously. In this manner, the method is rather a spatial blending of objective and kinematic analysis winds in lieu of local blending at a certain weighting factor. In this case, the kinematic winds replaced the winds derived from the pressure field in the interior of the kinematic domain and were blended with the pressure-derived winds along the boundaries of that domain (i.e., some smoothing was applied).

5.8 DESCRIPTION OF ICE EDGES FOR HINDCAST STORMS

Ice edges for the storms were mapped primarily from AES daily ice analysis charts.

The AES daily ice charts are prepared from four sources: reconnaissance, satellite images, ship observations, and shore reports. Each chart indicates the sources used and the date of the source data. Usually all four sources were available and within a day or two of the map date. In some cases either the reconnaissance or satellite data were unavailable, but the majority of the charts included all four sources. Daily ice charts were obtained for every third day of each storm period (e.g., for the storm of Sept 29-Oct 2 1984, ice charts for Sept 29 and Oct 1 were used).

Generally the 5 tenths ice edge was mapped for every third day of the storm period. There were a few exceptions to this rule. If the ice edge did not move appreciably during a storm duration (more than 30 n.mi.) and the wind was not blowing from the west, then ice edge with the most open water was chosen to represent the storm (i.e., Oct 1 1984 was used for the storm of Sept 29 to Oct 2 1984). Four storms were treated in this manner. For two other easterly storms, the AES weekly chart was used to map the ice edge. As AES ice charts, weekly or daily, were unavailable for the storm of Sept. 23 to 26 1970, the ice chart presented in Lindsay (1977) for Sept 12 was used.

The daily ice charts tended to cover the area from the west coast of Banks Island to Point Barrow, although in some cases they only extended slightly west of Barter Island. Weekly ice charts were used to fill in the ice edge for the remainder of the study area. Selecting the appropriate weekly chart and combining it with the daily

chart was a time-consuming process.

Edges of 3 tenths concentration were included on the ice edge map if the 3 tenths and 5 tenths ice edge differed by more than 60 n.mi. (Note: this rule was applied very conservatively, and generally differences of 30 n.mi. were mapped).

Table 5.2 provides a list of ice edge charts for the top 30 hindcast storms; their dates and number of charts for each storm are indicated. The ice charts are provided in Appendix C.

In addition, the digital ice data base at the Canadian Climate Centre, AES, Downsview was also accessed using the CRISP package. It proved ice concentration charts for the verifications storms as described in the next chapter. The ice edges obtained from this source were compared with those mapped from AES daily ice charts. Statistical ice charts, i.e. the percentage of occurrences of any ice, were obtained from "the marine climatological Atlas - Canadian Beaufort Sea" by Agnew, Spicer and Maxwell (1987). It presents semi-monthly charts provided in contour intervals of 98%, 90%, 70%, 50%, 30% and 10%. In the present study, three cases: 98%, 50%, 30% occurrences were used (see Appendix C).

Table 5.2

ICE EDGE CHARTS FOR TOP 30 STORMS

BEAUFORT SEA WAVE STUDY (15 OLD STORMS)

Storm No.	Period Start	Period End	No. of Charts	Ice Edge Chart Date
198	70091300	70091612	1	Sept. 12, 1970
302	77082512	77082800	2	August, 25 & 28, 1977
310	77092312	77092600	1	Sept. 30
326	78092800	78100100	1	Sept. 28 - Oct. 1, 1978
327	78100600	78101012	1	Oct. 9, 1978
334a	79092912	79100618	1	Oct. 4, 1978
350	80082812	80090400	2	Aug. 28 - Sept. 3, 1980
366	81080100	81080412	1	Aug. 4, 1981
369	81081600	81081900	1	Aug. 16, 1981
371	81083000	81090200	2	Aug. 30 - Sept. 2, 1981
376	81092700	81092900	1	Sept. 29, 1981
380	82072600	82080200	1	July 26, 1982
392	82092000	82092300	1	Sept. 20, 1982
405	82101900	82102700	2	Oct. 18 & 22, 1982
475	85091600	85091900	1	Sept. 16, 1985

Table 5.2 (cont'd)

BEAUFORT SEA WAVE STUDY (15 NEW STORMS)

Storm No.	Period Start	Period End	No. of Charts	Ice Edge Chart Date
270	75080900	75081112	2	Aug. 8 & 11, 1975
274	75082512	75082900	2	Aug. 22 & 29, 1975
282	76081112	76081400	2	Aug. 11 & 14, 1976
293	76092800	76100200	2	Sept. 25 & Oct. 1, 1978
325	78091900	78092212	1	Sept. 22, 1978
333	79091400	79091712	2	Sept. 14 & 17, 1979
335	79100812	79101112	1	Oct. 8, 1979
386	82081912	82082212	2	Aug. 19 & 22, 1982
391	82091600	82091800	2	Sept. 16 & 19, 1982
446	84082500	84082800	2	Aug. 24 & 28, 1984
456	84092900	84100212	1	Oct. 1, 1984
483	86082200	86082400	2	Aug. 22 & 25, 1986
487	86090800	86091000	1	Sept. 8 & 11, 1986
492	87082800	87090212	2	Aug. 28 & 31, 1987
507	88080200	88080506	2	Aug. 2 & 5, 1988

Additional Charts: October 6, 1977
August 8 and 11, 1986

6.0 HINDCAST VERIFICATION

This section provides the results of a preliminary verification of model hindcasts. For this purpose, five recent storms were selected from the Top 50 Storm List (Table 4.2). These particular verification storms were selected from those included in the previous wind field hindcast studies carried out by MacLaren Plansearch Limited and Oceanweather Inc. (1988 and 1989).

6.1 VERIFICATION CASES

The following five storms were selected from the final storm selection list for model verification.

	HINDCAST PERIOD		VERIFICATION PERIOD	
STORM #	START	END	START	END
1	770825-12	770828-00	770826-09	770828-00
2	780928-00	781001-00	780929-06	781001-00
3	810816-00	810819-00	810816-12	810818-00
4	810830-00	810903-00	810830-12	810903-00
5	820920-00	820923-00	820920-12	830922-00

The wind fields were hindcast in the previous study by MPL and OWI (1987, 89). These wind fields of the above storms were used directly in verification runs.

The ice edge used in each hindcast was determined using ice concentration charts from CRISP, a program which extracts data from the AES ice database. The ice edges used in the model were the 5/10 contours from the ice chart closest in time to the storm period. The following ice charts were used for the hindcasts:

August 23-24, 1977
September 26-27, 1978
August 18-19, 1981
September 1-2, 1981
September 21-22, 1982

Hand drawn ice edge charts were also produced to verify the above CRISP produced charts as described previously (see Appendix C). The final hindcast used the best presentation of ice edge from the above two sources.

6.2 WAVE VERIFICATION DATA

The amount of wave and wind measurements in the Beaufort Sea is limited to the amount of activity in the area. The verification storms were chosen during time periods when waverider buoy data were available. In addition to the waverider measurements, MANMAR (Manual Marine) observations from rigs were also available and were used to compare observed and modelled winds.

The locations of the observation on measurement sites are listed in Table 6.1, and shown in Figure 6.1.

Table 6.1 Locations of Waverider Buoys and Rigs

MEDS #	LAT (°N)	LONG (°W)	SITE/RIG	WATER DEPTH (M)	NEAREST GRID POINT	MODEL DEPTH (M)
1977						
190	70.1	133.6	GULF I	33.	358	36.02
191	70.1	136.4	GULPH II	43.	439	41.75
192	70.2	132.8	CANMAR I	34.	331	22.06
193	70.4	135.1	CANMAR II	64.	413	57.35
194	70.0	134.4	ISSERK	14.	384	10.09
	70.5	136.3	EXPLORER III	--	439	41.75
1978						
192	70.2	132.7	CANMAR I	31.	358	36.02
193	70.4	135.1	CANMAR II	57.	413	57.35
1981						
196	70.5	134.1	EXPLORER III	60.	386	42.78
201	70.1	134.4	EXPLORER II	27.	385	36.02
	70.2	135.1	EXPLORER I	--	412	39.47

1982						
196	70.4	136.5	EXPLORER III	58.	439	41.75
201	70.4	134.0	EXPLORER II	60.	386	42.78
204	69.8	136.0	TARSUIT ISLAND	21.	411	18.38
205	69.9	134.5	ITIYOK ISLAND	14.	384	10.09
206	70.0	131.2	MCINLEY BAY	8.	304	10.12
	70.6	134.2	IRKALUK	--	386	42.78
	70.7	134.0	EXPLORER IV	--	386	42.78

6.3 VERIFICATION PROCEDURES

The following evaluation methods were applied:

1. Time Series Plots of Hindcasts vs. Observations

   For each storm, time series of the hindcast wind speed and direction, significant wave height, peak period, and vector mean wave direction were plotted with the corresponding measured values at the selected evaluation sites. The time series can be found in Appendix D.

2. Statistical Comparison of Hindcasts vs. Observations

   A quantitative statistical analysis was carried out to provide an overall evaluation of the model predictions. The statistical parameters considered in this study are:

   Mean Error (Bias) $= \Sigma (X_1 - X_2)/NPTS$

   Mean Absolute Error $= \Sigma |X_1 - X_2|/NPTS$

   Root Mean Square Error (RMSE) $= [\Sigma(X_1 - X_2)^2/NPTS]$

   Scatter Index (%) $= (RMSE/AVE) \times 100$

   where X_1 is the hindcast value

   X_2 is the observed value

   AVE is the mean of observed values

   NPTS is the number of data pairs

These statistics were provided for each site for significant wave height and peak period. Table 6.2 presents the above evaluation results.

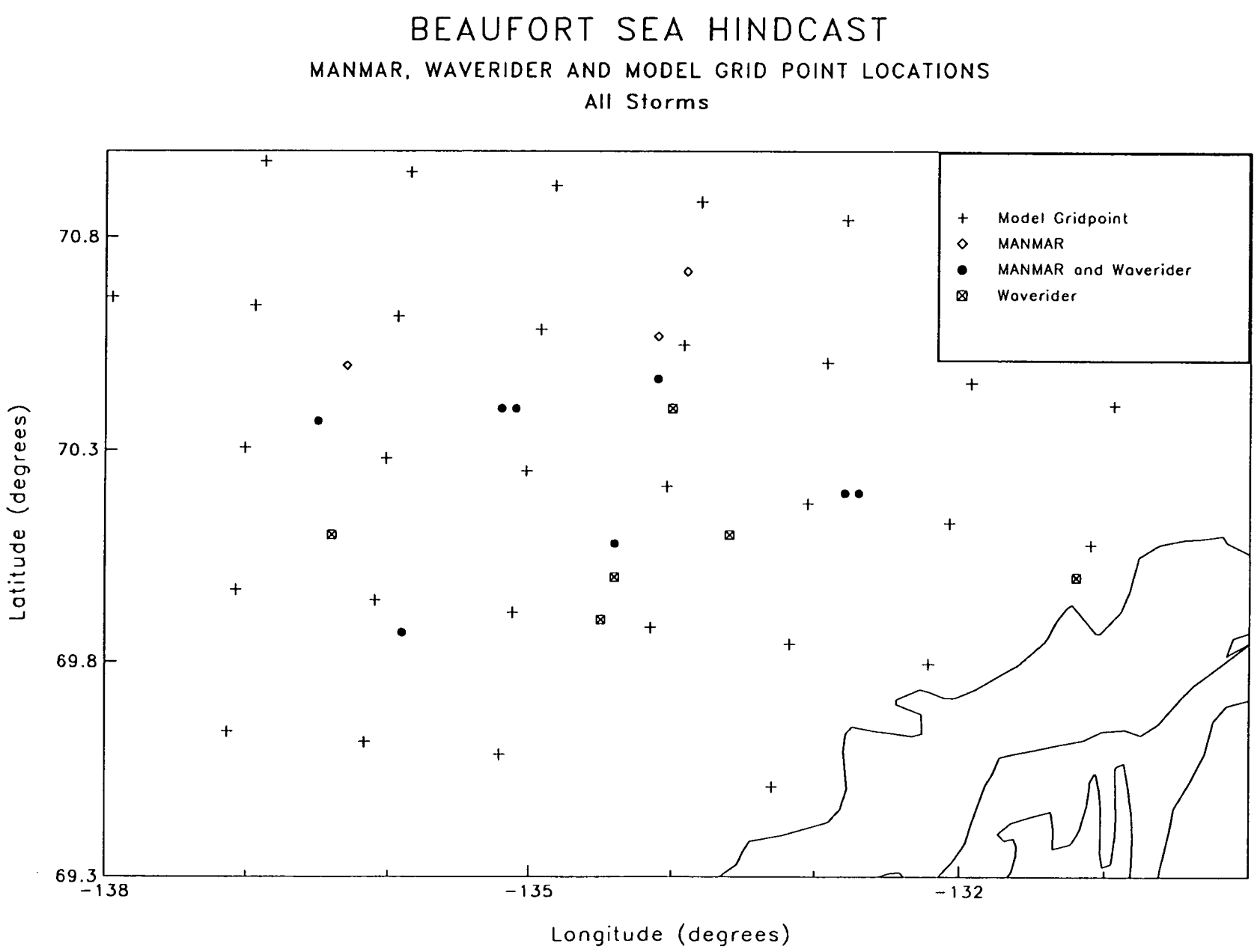

Figure 6.1 Beaufort Sea Verification Sites

3. Peak-to-Peak Comparisons

In Table 6.3, storm peak values of H_S and T_P are listed for measured data and model predictions. These values were then used to evaluate the storm peak parameters of the models.

4. Scatter Plots and Linear Regression Analysis

The correlation between measured and hindcast parameters was carried out using linear regression analysis. The scatter plots in Figures 6.2 and 6.3 show the correlation between measured and model values for both H_S and T_P.

Table 6.2
Hindcast Verification Statistics

Var	Storm Date	Num of Points	Average Obs	Standard Dev.	Average Model	Standard Dev	Mean Err	Absolute Mean Err	RMSE	Scatter Index	Corr Coef
HS	770825	63	1.38	0.65	1.43	0.54	0.05	0.26	0.34	24.64	0.856
	780928	28	1.76	0.17	2.13	0.16	0.37	0.42	0.46	26.29	-0.320
	810816	19	2.37	0.62	2.79	0.53	0.42	0.58	0.67	28.41	0.585
	820920	36	2.29	0.53	2.55	0.57	0.25	0.34	0.40	17.35	0.847
	OVERALL	146	1.81	0.70	2.02	0.74	0.21	0.35	0.44	24.06	0.861
	810830	33	1.64	0.49	3.04	0.45	1.40	1.40	1.48	90.54	0.492
TP	770825	63	7.10	1.05	5.08	1.34	-2.02	2.03	2.50	35.15	0.268
	780928	28	7.15	0.64	7.16	0.28	0.01	0.59	0.83	11.64	-0.549
	810816	19	6.75	0.85	7.26	1.09	0.51	1.30	1.50	22.16	-0.039
	820920	36	7.24	0.57	7.79	0.82	0.55	0.84	0.94	12.95	0.439
	OVERALL	146	7.10	0.87	6.43	1.59	-0.67	1.36	1.82	25.70	0.150
	810830	33	6.31	1.27	8.06	0.65	1.74	1.93	2.04	32.37	0.548

Table 6.3

Storms Peak-to-Peak Comparison Statistics

MEDS BUOY	WAVERIDER Hs (m)	WAVERIDER Tp (s)	ODGP grid point	ODGP Hs (m)	ODGP Tp (s)
Storm period - 770825:1200 to 770828:0000					
191	3.2	8.0	439	2.4	6.9
190	1.8	7.6	358	1.9	5.8
192	1.2	8.0	331	1.4	6.0
192	1.2	8.0	358	1.9	5.8
193	1.9	7.2	413	2.2	6.2
Storm period - 780929:0600 to 781001:0000					
192	1.8	7.2	331	2.2	7.4
192	1.8	7.2	358	2.4	7.6
193	1.9	8.0	413	2.4	7.3
Storm period - 810816:1200 to 810819:0000					
196	3.4	8.0	386	3.5	8.3
201	3.1	7.6	411	3.0	7.4
201	3.1	7.6	385	3.4	8.4
Storm period - 810830:1200 to 810903:0000					
196	2.4	7.2	386	3.6	8.6
196	2.4	7.2	412	3.3	8.4
196	2.4	7.2	413	3.5	8.6
201	1.5	4.6	385	3.4	8.5
Storm period - 820920:1200 to 820922:0000					
204	2.8	7.2	411	2.4	8.8
206	0.9	5.7	304	1.8	7.4
196	3.3	8.0	439	3.4	9.1
201	3.3	7.6	386	3.4	8.4
205	2.2	6.5	384	2.2	8.5

Peak to Peak Comparison -- All Storms Except 810830

Depths > 20 m

Var	Num of Points	Average Obs	Standard Dev.	Average Model	Standard Dev	Mean Err	Absolute Mean Err	RMSE	Scatter Index	Corr Coef
HS	11	2.58	0.64	2.52	0.76	-0.06	0.30	0.38	14.73	0.872
TP	11	7.44	1.08	7.67	0.33	0.24	1.00	1.15	15.51	0.013

Peak to Peak Comparison -- All Storms

HS	13	2.71	0.59	2.43	0.75	-0.28	0.40	0.55	20.23	0.778
TP	13	7.86	0.65	7.40	0.87	-0.46	0.82	1.26	16.08	-0.173

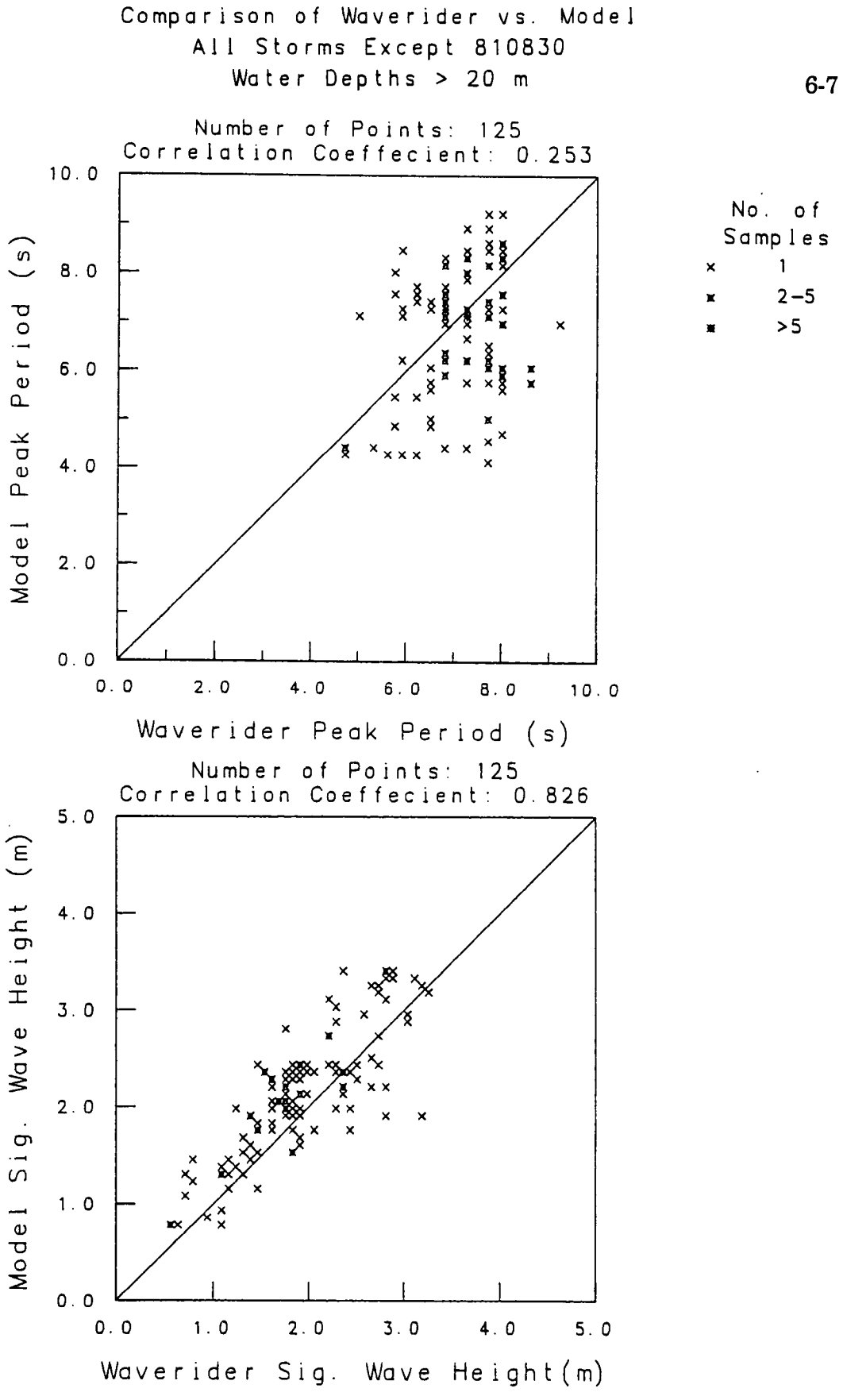

Figure 6.2 Scatter Diagrams of Measured vs. Hindcast Data

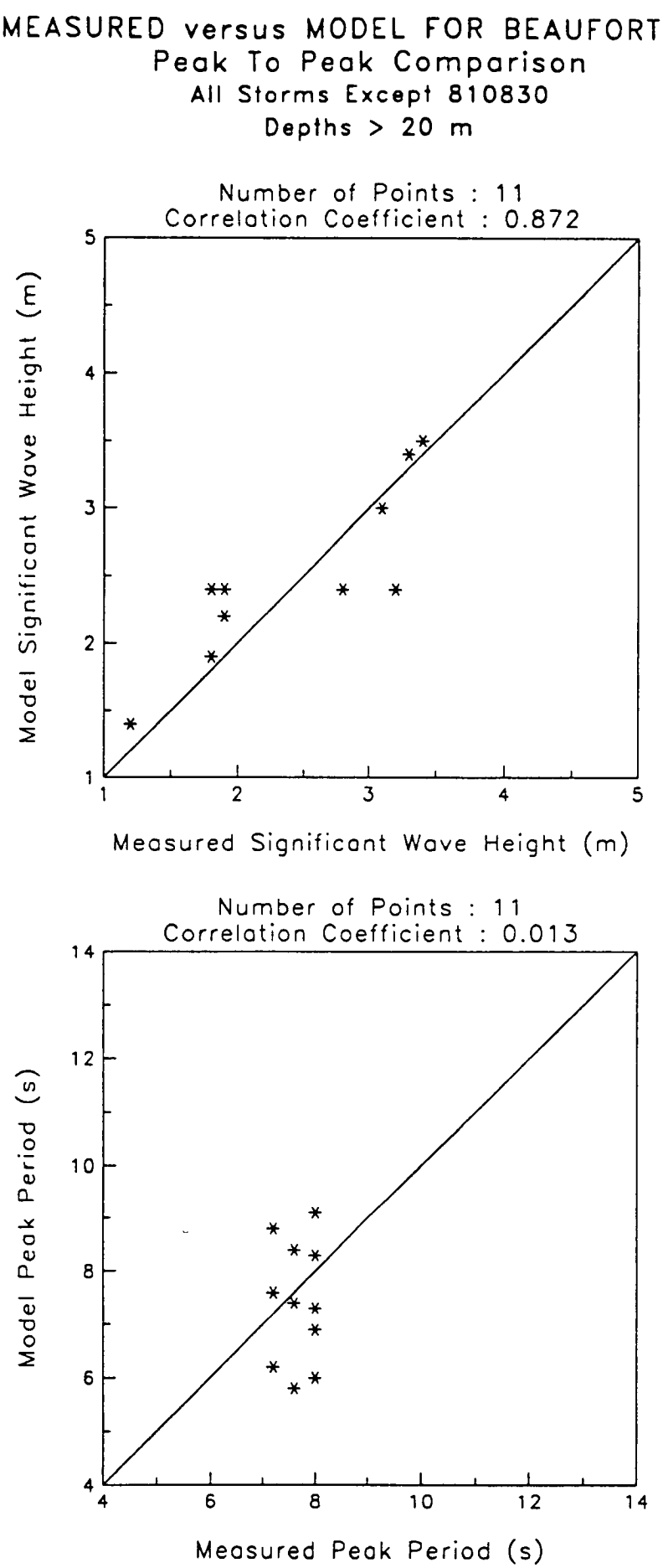

Figure 6.3 Scatter Diagrams of Peak-to-Peak Comparison

6.4 STORM-BY-STORM VERIFICATION RESULTS

Storm #1 - August 25 - 28, 1977

Synoptic Evolution: This storm most resembles pattern 4 (see Figure 4.1) of the Beaufort Weather Office storm patterns. Initially, a trough extends northwestward into the Canadian Beaufort with light northeasterly winds of 10-15 knots in the eastern part (see Explorer 1 wind comparison) and northerly winds of about 20 knots in the western part (see Explorer II wind comparison). Evidently, late on the 26th, a small scale low pressure system developed in the central part of the exploration areas, just east of Explorer III, which experienced wind speeds up to 40 knots for a brief time, followed by nearly calm winds early on the 27th. This low gradually fills, with little movement, during the 28th. The kinematic analyses, as originally derived, captured the larger scale features of the wind field evolution, but apparently did not fully resolve the small scale features near the developing mesoscale low centre on the 27th. The effect of this small scale system on the wave field is discussed below.

Ice Cover: According to the ice chart for this storm (Appendix C), the area between the shore and 73°N was almost completely ice-free, providing fetch lengths of at least 150 n. mi. upwind of the available measurement sites. The width of the transition zone between ice-free conditions and the solid ice-pack is rather narrow, and probably less than 30 n. mi. wide. Therefore, the "effective ice edge" offshore specified in the wave model as the locus of 5/10 coverage is probably a reasonable measure of the fetch restriction.

Hindcast Evaluation: At Kopanoar, the model appeared to spin-up in time to capture the peak in wave height which occurred early on the 27th, just as the observed wind speeds drop. Observed and hindcast wave heights vary little thereafter. At Ukalerk, in the eastern region, the wave heights were quite low and hindcast accurately. Peak period was hindcast to be 1-2 seconds lower than observed. Basically the same type of measured-hindcast differences characterize the comparison at WR-190. At WR 194, winds are not available and the measurement record is incomplete, but the indications

are that the hindcast wave height history is too high. WR-194 is in 14 m water depth, but the cause of the hindcast overspecification is more likely overspecification of wind speed, since this waverider is near the calm centre of the small scale low. WR-191, on the other hand is in the area west of WR-194 which probably experienced a wind speed history like that observed at Explorer III, as the measured peak late on the 26th is missing in the hindcast.

Summary: Hindcast-measured differences in this basically low intensity event appear to be dominated by the failure of the kinematic analysis to resolve a small scale cyclonic disturbance embedded in broad scale trough of low pressure extending over the central Canadian Beaufort. A reanalysis and regridding of the wind field at higher resolution could confirm this suspicion.

Storm #2 - September 28, 1978 - October 1, 1978

Synoptic Evolution: This case is a definite BOW Pattern 1 (eastward moving low). The centre of the parent low pressure system was located far north of the exploration areas, near 75°N, and the wind flow over the Canadian Beaufort was basically westerly at speeds of around 20 knots. The Brooks range induced some enhancement of this westerly flow as indicated by coastal observations in the western part of the area offshore Herschel Island. As the low moved eastward, wind directions gradually veered from westerly to northwesterly with little change in speed. Wind speed and direction are specified quite well for this hindcast, as shown in the comparisons at Kopanoar and Ukalerk.

Ice Cover: The ice charts for this event indicated that the ice-pack was moving southward during the period hindcast. The 5/10 contour was interpolated between positions indicated on two ice charts (September 28th and October 1st) straddling the time of peak wave conditions. The interpolated contour lies basically east-west along 72°N of the exploration areas, though on the U.S. side of the Beaufort, it lies closer to 71.5°N, with lower concentrations southward to the shore. On the Canadian side, the charts indicate less than 1/10 concentration south of the pack ice.

Hindcast Evaluation: Waverider measured wave histories were available to two sites, both in intermediate water depths (30-50 m). Both of these locations show similar storm responses, as wave heights built from near calm conditions early on the 28th to reach its maximum height of about 2 m 24 hours later, with little change thereafter during the period hindcast. The hindcast began about 18 hours later than the beginning of the observed buildup, and thereafter the hindcast could benefit from additional spin-up period. As a result of the late start, the hindcast peak wave heights lag the observed by about 12 hours, but eventually the storm peak is well specified at both sties. Peak period is also well specified.

Summary: Overall, winds and sea states are well specified at two widely separated measurement sites in this case. Since the ice-edge is well north of the site, and winds are basically westerly, ice-induced fetch restrictions play a minor role in this storm, and peak seas are basically limited by upwind shoreline geometry, wind speed and, to a very limited extent, storm duration.

Storm #3 - August 16, 1981 - August 19, 1981

Synoptic Evolution: This case fits a BWO Pattern type 3 as a low developed in the southern Canadian Beaufort Sea on August 16 in a pre-existing trough. As the low was undergoing initial development, surface winds in the drilling areas were light and shifting from southeast to westerly. As the low moved rapidly northeastward and intensified, the westerly to west-northwesterly winds over the drilling areas increased to about 30 knots early on the 17th, and then decreased steadily as the storm centre moved further away. Observed surface wind histories were available at three sites. There are relatively small but temporally coherent differences between observed and modelled winds, mainly a slight underspecification of the storm peaks early on the 17th by about 4 knots at Kopanoar and Koakoak, and nearly 10 knots at Issungnak, where a lull around midday the 17th is also missed.

Ice Cover: The ice distribution was more complicated in this case than in the preceding cases, especially to the west of the measurement sites, where the ice chart

indicated that a band of up to 7/10 coverage ice extended southeastward to the coast, from the main pack edge which lied along 72°N. For the adopted 5/10 contour (invariant with time through the hindcast), the implied fetch upwind of the measurement sites varied significantly for small changes in wind direction. Further adding to the complexity is the indication of ice cover of lesser concentrations located well south and east of the main pack.

Hindcast Evaluation: At Kopanoar, only MANMAR wave estimates were available, and these suggest that the storm peak was underspecified by about 1 m. However, just 20 n. mi. to the east at Koakoak, the waverider record confirms a fairly accurate hindcast. To the south at Issungnak, the wave hindcast also lies within about 0.5 m of the waverider record leading up to the storm peak, while differences between MANMAR and waverider wave height estimates are larger than 1 m at times. The peak period associated with peak sea states is rather well specified at both waverider sites.

Summary: At waverider measurement sites, the wave hindcast verifies well, while at the MANMAR site, differences are larger. However, at sites with both MANMAR and waverider histories, differences between the alternate "observed" wave series are often larger than the difference between measured and hindcast wave height histories.

Storm #4 - August 31, 1981 - September 3, 1981

Synoptic Evolution: This case most resembles BWO Pattern 5, as a quasi-stationary pattern of strong northwesterly flow covered the Canadian Beaufort between a large high pressure over the western Beaufort and a large low pressure system over Banks Island. Surface winds were observed at three sites and range within 20-30 knots. Modelled wind directions and speeds agree closely with the observed winds at all sites, the small differences attributable to anemometer level variations (precise heights are not known) and averaging interval limitations.

Ice-Cover: The ice chart analyses are similar to those of the previous case, except that the shoreward ice extension of 5/10 or greater ice shown west of the exploration areas in the previous case (two weeks earlier) has been analyzed as having diminished in concentration to less than 5/10. Therefore the ice edge adopted for the hindcast placed the 5/10 contour near 72°N along virtually the entire Beaufort Sea. However, there is undoubtedly some ice south of this contour of quite variable concentration, and in areas quite close and to the west (and upwind) of the measurement sites.

Hindcast Evaluation: A striking feature of the wave hindcast of this case at all measurement sites is the overprediction of wave height, and corresponding overspecification of peak period. At Kopanoar, only MANMAR observations are available, and while at Koakoak, the MANMAR and waverider determination agree closely, at Issungnak the alternate estimates disagree greatly. Indeed, at Issungnak, it is hard to reconcile the waverider peak wave height of about 1 m in view of the MANMAR estimates of about 4 m.

Summary: In view of the well defined and rather accurately specified wind field in this case, it is tempting to attribute the positive bias in the wave height hindcast to the assumption of unrestricted fetch to the west of the measurement sites. This would suggest that even low concentrations of ice can inhibit wave growth in fetch-limited conditions and that a more physically correct treatment of ice within a wave model, together with a precise specification of the ice field, is required. However, before this conclusion can be accepted, the rather large differences between the MANMAR and waverider wave estimates seen in this case should be investigated. This storm results were excluded from the overall error statistics shown in Tables 6.2 and 6.3.

Storm #5 - September 20, 1982 - September 22, 1982

Synoptic Evolution: This is a classic BWO Pattern 7 event, characterized by prolonged and fairly steady east to east-northeast flow. Winds were not specified with uniform

accuracy in all areas however. At Explorer I, in the southern part of the measurement array, observed wind speeds were 30-40 knots, while analyzed winds were closer to 25 knots. At Explorer II and IV, located well offshore, measured and modeled winds were in good agreement, with peak wind speeds of about 30 knots. To the west, at Explorer II, modeled wind speeds were a few knots larger than observed.

Ice Cover: The ice-pack edge was well defined for this case and the 5/10 contour was taken to lie in an east-west orientation along the north of 73°N. In this easterly regime, therefore, ice does not affect the upwind fetch at all.

Hindcast Evaluation: There is a measurement site well east of the main exploration area nearshore (WR-206). The wave hindcast is positively biased there, but since there are no wind measurement stations nearby to validate the modelled winds, it is not possible to identify the source of this hindcast error. Sea states are rather low, however, in this area for this type of storm. At WR-204 the hindcast verifies well, despite the apparent underspecification of wind speed. Possibly, the observed winds at nearby Explorer I are biased hight due to anemometer level or platform effects. Near Explorer II and IV, only MANMAR wave data are available, and definite evaluation is not advisable. However, at WR-205 in 14 m water depth, located just east of Explorer I, the sea state history is reproduced very well.

Summary: Differences between measured and hindcast wave histories are small. Sea states are specified well at most sites in this case.

6.5 OVERALL CONCLUSIONS

1. Where surface wind fields verify well against measured wind data, and where the ice edge is sharply defined and well located, the wave hindcasts verify well against waverider measurements, with scatter index in the order of 24% for H_s and 25% for T_p, and 0.44m and 2s RMSE for H_s and T_p, respectively. For peak-to-peak comparison, better error statistics were found (e.g. 0.38m RMS and 14.7% SI for H_s and 1.2s RMS and 15.5% SI for T_p).

2. Small scale features in the wind fields can induce significant percentage errors in peak sea states at least in storms of low-moderate intensity. In the most severe storms, small scale features should have less impact, though every attempt should be made to minimize wind errors in all storms hindcast.

3. Effect of partial ice cover may need to be accounted for in the wave hindcast process. This requires research into the effects of partial ice cover on the wave model source terms as well as on wave propagation, and very accurate determination of ice concentration in historical storms.

7.0 HINDCAST PRODUCTION

7.1 WIND FIELD HINDCAST

The wind fields for the final top 30 storms were specified using the techniques and procedures described previously. The wind fields for the "old" 15 storms which were previously hindcast for AES (Table 5.2) were reviewed, some cases needed to be extended to cover the entire storm duration and some cases needed further refinements. Wind fields were developed for the new 15 storms. The 6-hourly grided wind fields (given at 10 m above MSL) were then input to the ODGP Beaufort Sea wave model.

7.2 ICE EDGE SPECIFICATIONS

The ice edge specifications were prepared for input to the wave model as described previously (all ice edge charts used in this study are provided in Appendix C). As mentioned, two regimes were considered:

a) actual ice edge occurred during each storm; and
b) climatological ice edge (i.e. 98%, 50% and 30% occurrences of any ice).

The actual ice edge was produced from careful analysis of the AES daily and weekly ice charts whereas the climatological ice edge was obtained from the semi-monthly charts of Agnew et al. (1987). The appropriate ice edge was digitized for each case. It was assumed that the ice edge remained constant during each storm, i.e. only one ice edge was used for each storm. The required ice edges were digitized and used as input to the wave model.

7.3 WAVE HINDCAST PRODUCTION

The ODGP Beaufort Sea spectral wave model was executed for the top 30 storms with the four different ice edge scenarios as mentioned above (i.e. total 120 runs). The hindcast results (both wind and wave) were archived and delivered to AES on magnetic tapes. The archived data included all gridded wind fields, all wave fields

(H_s, T_p and vector mean direction) at all active (water) grid points. In addition detailed model hindcast results (i.e. wind speed, direction, wave height, period and direction, and directoral wave spectral variance (15 frequencies x 24 directions) were provided at a selected 51 grid points in the model domain.

These 51 grid points were selected in the dominant open water region of the Canadian Beaufort Sea extending for 120°W to 150°W and from 69°N to 72°N. It covers all offshore hydrocarbon exploration areas. Figure 7.1 shows the 51 grid points at which the hindcast data were archived and extremal analysis results were provided.

For each storm, the peak significant wave height and corresponding peak period, wave mean direction, wind speed and direction were compiled, and other parameters were computed (i.e. ratios of H_{max}/H_s and H_c/H_s) at each of the 51 points. The peak H_s was identified at each of the 51 grid points. This information was used in the extremal analysis as described in Chapter 8.0.

The peak significant wave height at each of the 51 grid point is given on a map of the study area for each storm as shown in Appendix E. As shown, the Minuk storm (September 16, 1985) was the most severe storm in the selected 30 cases. It produced a maximum significant wave height of 5.40 m at grid point #492 (approximately 70°N, 138°W) and about 5.0 m near the Minuk site. This storm was a subject of several studies by Esso Resources Canada Limited as it resulted in washing away the artificial island at the Minuk site. As shown in the next chapter, this storm would have a return period greater than 50 years. It should also be noted that the ice edge for this storm (Appendix C) was less than the median ice edge (i.e. smaller fetch), i.e. a larger wave height would have been produced if this storm was combined with a larger open water area. This is investigated further in the next chapter.

A summary of model hindcast results for each storm at a selected number of locations in the study area is presented in Table 7.1. It provides peak wind speed and direction, peak H_s and corresponding T_p, and wave direction for the four ice edge scenarios.

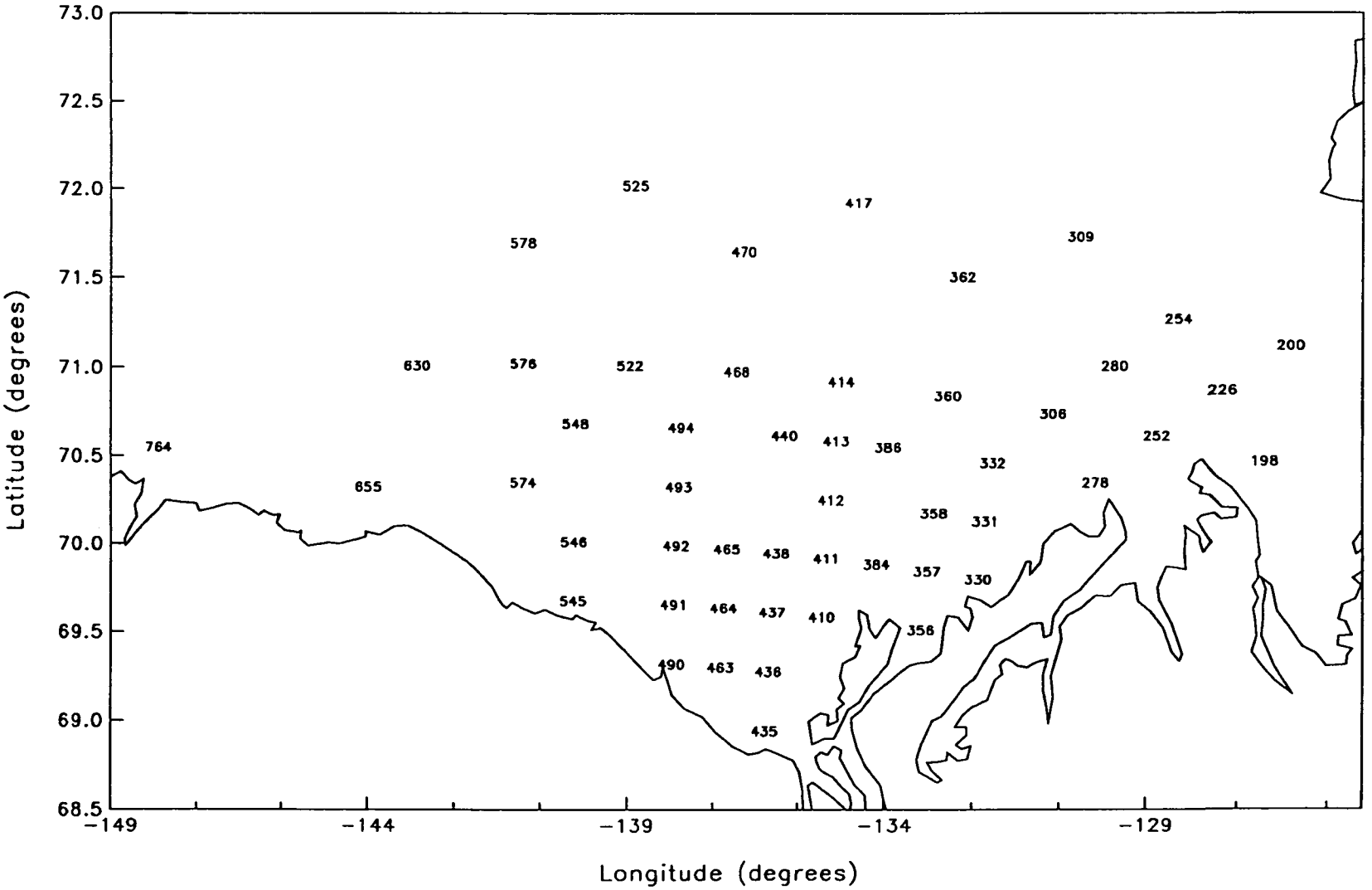

Figure 7.1 Selected 51 Grid Points At Which Model Hindcasts Were Archived

Table 7.1 Model Hindcast Results at Selected Locations

STORM PEAKS AT 360 AT 70.84N, 132.79W

STORM	WIND		REAL ICE EDGE			98% OCCUR EDGE			50% OCCUR EDGE			30% OCCUR EDG		
	SPD	DIR	HS	TP	VMD	HS	TP	VMD	HS	TP	VMD	HS	TP	VMD
1	18.9	309	4.5	9.2	97	4.9	9.7	124	4.1	8.7	90	---	---	---
2	14.9	270	3.4	8.2	89	3.9	8.8	98	2.9	7.1	57	---	---	---
3	17.2	270	3.5	8.2	43	4.8	9.5	100	3.8	8.6	84	---	---	---
4	16.3	24	---	---	---	3.4	8.1	218	2.6	7.2	226	---	---	---
5	15.4	77	3.3	8.1	259	3.3	8.1	259	3.3	8.0	261	---	---	---
6	7.7	331	1.5	6.0	149	1.5	6.0	149	1.3	4.3	218	---	---	---
7	13.4	230	2.9	7.6	55	2.9	7.6	55	2.9	7.6	54	---	---	---
8	17.4	87	3.7	8.2	266	3.7	8.2	266	3.7	8.2	267	---	---	---
9	9.2	314	2.2	7.1	112	2.3	7.2	121	2.1	7.1	107	---	---	---
10	15.4	48	3.2	8.0	244	3.6	8.3	238	2.8	7.3	253	---	---	---
11	15.9	98	3.0	7.2	271	3.0	7.2	270	3.0	7.2	273	---	---	---
12	13.9	70	3.2	8.1	255	3.2	8.1	254	2.9	7.7	265	---	---	---
13	16.1	99	3.3	7.4	276	3.3	7.5	275	3.1	7.3	280	---	---	---
14	14.8	267	3.7	8.6	94	4.2	9.2	101	3.3	8.1	88	---	---	---
15	16.2	320	3.2	7.4	144	3.5	8.1	147	2.4	6.2	133	---	---	---
16	14.7	302	3.6	8.3	120	3.8	9.0	122	2.8	7.1	108	---	---	---
17	15.7	310	3.3	7.7	128	4.2	9.5	132	3.0	7.3	102	---	---	---
18	16.0	42	3.8	8.4	226	3.8	8.4	225	3.5	8.1	232	---	---	---
19	20.9	310	4.4	9.2	124	4.6	9.3	121	---	---	---	---	---	---
20	16.6	290	4.0	8.6	110	4.4	9.3	112	3.5	8.1	102	---	---	---
21	13.4	320	3.2	8.1	127	3.3	8.1	128	3.1	7.7	46	---	---	---
22	15.6	88	3.4	8.2	263	3.4	8.2	263	3.4	8.2	264	---	---	---
23	18.2	281	3.7	8.2	86	5.2	10.2	100	---	---	---	---	---	---
24	18.3	336	---	---	---	4.4	8.6	160	3.5	7.2	161	---	---	---
25	12.1	81	---	---	---	2.2	5.9	263	2.1	5.9	268	---	---	---
26	21.4	281	---	---	---	6.2	10.9	106	5.4	10.4	93	---	---	---
27	15.0	327	2.3	5.9	130	3.9	8.9	143	2.9	7.0	135	---	---	---
28	15.7	138	3.0	7.1	308	3.0	7.1	308	3.0	7.1	309	---	---	---
29	15.6	301	3.9	9.3	122	4.3	9.8	128	3.3	8.1	95	---	---	---
30	17.9	319	3.7	8.1	122	4.4	9.2	134	2.8	7.1	115	---	---	---

SPD: Wind speed in (m/s)
DIR: Wind direction (coming from)
HS: Significant wave height in (m)
TP: Peak period in (s)
VMD: Wave vector mean direction (towards)

Table 7.1 (cont'd)

STORM PEAKS AT 437 AT 69.61N, 136.17W

STORM	WIND		REAL ICE EDGE			98% OCCUR EDGE			50% OCCUR EDGE			30% OCCUR EDG		
	SPD	DIR	HS	TP	VMD	HS	TP	VMD	HS	TP	VMD	HS	TP	VMD
1	22.4	294	3.8	9.3	119	4.0	9.5	121	3.6	9.3	122	3.2	8.1	113
2	17.7	282	2.8	8.1	112	3.1	8.5	117	2.8	8.1	112	---	---	---
3	18.2	273	2.8	8.1	101	3.5	9.6	113	3.1	8.5	106	2.8	8.1	101
4	15.1	30	2.1	7.2	203	2.4	8.2	203	2.2	7.4	203	2.0	7.1	204
5	11.6	20	2.1	8.4	193	2.1	8.5	192	2.0	8.4	198	---	---	---
6	12.3	308	2.5	8.3	137	2.5	8.3	137	2.2	7.2	135	1.8	5.8	132
7	12.4	244	1.7	5.8	78	1.7	5.8	78	1.7	5.8	78	1.6	4.6	72
8	17.9	74	2.5	8.5	236	2.5	8.5	236	2.5	8.5	236	2.3	8.2	238
9	14.9	308	2.8	8.3	131	2.8	8.3	132	2.7	8.2	129	2.3	7.0	124
10	15.8	47	2.4	8.2	216	2.5	8.4	212	---	---	---	---	---	---
11	13.6	90	1.7	8.1	247	1.7	8.1	247	1.7	8.1	247	1.6	7.1	249
12	19.0	90	2.4	8.2	247	2.4	8.2	247	2.3	8.0	251	---	---	---
13	16.9	92	1.9	7.1	259	1.9	7.1	259	---	---	---	---	---	---
14	14.4	272	2.5	8.4	109	2.7	9.3	112	2.2	7.1	105	1.9	5.7	100
15	14.5	337	2.3	7.2	160	2.5	8.0	159	1.9	5.8	160	1.8	5.6	158
16	13.1	297	2.4	8.0	130	2.5	8.4	130	2.2	7.1	124	1.9	5.7	119
17	12.5	313	2.1	7.3	147	2.5	8.6	144	2.0	7.1	141	1.7	5.7	136
18	15.1	16	2.7	8.4	198	2.7	8.6	189	2.7	8.3	199	2.3	7.1	202
19	19.8	310	3.5	9.3	134	3.7	9.4	134	2.8	7.1	131	---	---	---
20	17.7	290	3.0	8.2	121	3.2	9.1	123	2.9	8.1	117	2.5	7.0	115
21	15.3	316	2.7	8.2	135	2.8	8.2	135	2.5	7.5	130	2.0	5.9	125
22	10.4	41	1.8	9.2	216	1.8	9.2	216	1.8	9.2	216	1.5	4.4	258
23	20.4	273	---	---	---	4.0	10.3	112	---	---	---	---	---	---
24	18.0	324	2.7	7.1	148	3.1	8.3	151	3.0	8.1	150	2.7	7.1	150
25	16.5	111	1.8	4.3	279	1.8	4.3	278	1.8	4.3	278	---	---	---
26	22.1	286	4.4	10.6	118	4.7	10.7	121	4.4	10.5	117	3.6	8.7	109
27	18.1	320	3.1	8.3	138	3.5	9.3	142	3.1	8.2	139	2.6	7.1	138
28	11.1	296	2.0	7.7	122	2.0	7.7	122	1.9	7.2	121	1.6	5.6	118
29	16.6	300	3.2	9.1	135	3.3	9.3	136	2.8	8.1	130	2.4	7.0	128
30	16.1	314	2.9	8.3	136	3.0	8.4	138	2.5	7.1	128	2.2	6.0	124

Table 7.1 (cont'd)

STORM PEAKS AT 463 AT 69.30N, 137.20W

STORM	WIND		REAL ICE EDGE			98% OCCUR EDGE			50% OCCUR EDGE			30% OCCUR EDG		
	SPD	DIR	HS	TP	VMD	HS	TP	VMD	HS	TP	VMD	HS	TP	VMD
1	19.3	302	3.8	9.2	129	3.8	9.3	130	3.6	8.6	128	3.1	7.4	123
2	15.0	290	2.7	7.2	116	3.0	8.3	125	2.8	7.2	117	---	---	---
3	17.8	275	2.8	7.0	104	3.4	9.3	116	3.2	8.1	111	2.8	7.0	104
4	14.4	30	2.5	7.2	206	2.7	8.2	206	2.5	7.5	205	2.4	7.0	211
5	12.1	54	2.4	8.7	224	2.4	8.7	224	2.3	8.3	205	---	---	---
6	12.9	310	2.8	8.1	142	2.8	8.1	142	2.5	7.1	140	2.2	5.9	137
7	11.4	219	1.7	4.9	51	1.7	4.9	51	1.7	4.9	51	1.7	4.7	48
8	15.3	71	2.7	8.8	232	2.7	8.8	232	2.7	8.7	232	2.5	8.1	235
9	14.0	311	2.9	8.1	138	2.9	8.1	138	2.8	7.6	137	2.4	6.7	131
10	14.3	54	2.6	8.1	220	2.8	8.4	218	---	---	---	---	---	---
11	12.9	90	2.1	6.6	249	2.1	6.6	249	2.1	6.6	249	2.0	6.2	252
12	18.5	90	2.7	8.1	251	2.7	8.1	251	2.7	7.9	252	---	---	---
13	16.3	92	2.4	6.9	261	2.4	6.9	261	---	---	---	---	---	---
14	13.6	272	2.5	8.2	112	2.6	9.3	115	2.2	6.9	107	2.0	5.6	100
15	12.6	356	2.3	7.0	170	2.5	7.4	168	2.0	5.8	171	2.0	5.7	170
16	11.5	300	2.3	7.2	133	2.5	7.8	132	2.2	7.0	129	2.0	5.7	123
17	11.1	319	2.2	7.1	147	2.4	8.1	146	2.2	7.0	145	1.9	5.7	144
18	16.4	21	3.1	8.4	200	3.1	8.4	200	3.0	8.3	201	2.7	7.3	202
19	18.1	310	3.5	8.6	137	3.6	9.2	137	2.7	6.9	133	2.2	5.9	125
20	15.5	290	2.8	7.5	125	3.1	9.2	127	2.8	7.2	122	2.5	6.3	117
21	15.1	313	2.9	7.7	137	3.0	8.0	137	2.7	7.2	133	2.2	5.8	126
22	8.8	34	1.9	9.2	217	1.9	9.2	217	1.9	9.2	217	1.7	6.9	232
23	20.7	268	---	---	---	3.8	9.4	113	---	---	---	---	---	---
24	16.8	321	2.8	7.1	151	3.2	8.2	153	3.1	7.7	152	2.8	7.1	158
25	15.6	100	2.3	6.6	270	2.3	6.5	268	2.3	6.6	269	---	---	---
26	21.1	283	4.2	9.8	121	4.3	10.4	123	4.2	9.8	120	3.5	8.2	110
27	16.8	320	3.2	8.2	142	3.6	9.2	144	3.1	8.0	143	2.7	7.0	141
28	11.3	300	2.1	6.9	125	2.1	6.9	125	2.0	6.4	125	1.8	5.7	118
29	15.8	300	3.3	9.1	139	3.3	9.2	139	2.9	7.7	136	2.5	6.6	133
30	14.9	317	3.0	8.0	141	3.1	8.3	142	2.6	7.0	137	2.3	5.9	130

Table 7.1 (cont'd)

STORM PEAKS AT 492 AT 69.99N, 138.05W

STORM	WIND		REAL ICE EDGE			98% OCCUR EDGE			50% OCCUR EDGE			30% OCCUR EDG		
	SPD	DIR	HS	TP	VMD	HS	TP	VMD	HS	TP	VMD	HS	TP	VMD
1	19.5	310	4.6	9.4	129	4.7	9.5	130	4.2	8.4	123	2.5	7.1	115
2	17.4	290	3.2	7.2	105	3.8	9.1	115	3.2	7.3	105	---	---	---
3	19.8	275	2.7	6.9	20	4.6	9.9	110	3.8	8.1	101	2.7	6.9	20
4	14.1	40	2.7	7.2	225	3.2	8.1	226	2.8	7.4	225	2.3	7.0	235
5	14.9	70	3.5	8.8	244	3.5	8.8	244	3.4	8.5	244	---	---	---
6	14.9	320	3.4	8.2	148	3.4	8.2	148	2.9	7.1	164	1.9	5.7	135
7	13.6	240	2.3	5.9	67	2.3	5.9	67	2.3	5.9	67	1.8	5.7	32
8	16.0	70	3.9	9.1	246	3.9	9.2	245	3.9	9.1	246	3.2	8.1	253
9	19.2	310	3.6	7.6	135	3.7	7.7	136	3.5	7.3	131	2.3	6.6	120
10	17.5	50	3.6	8.1	255	4.0	9.1	232	3.7	8.2	251	---	---	---
11	14.9	90	3.1	8.0	258	3.1	8.0	258	3.1	8.0	258	2.6	7.0	266
12	19.5	90	3.9	8.2	259	3.9	8.2	258	3.8	8.2	261	---	---	---
13	18.0	90	3.6	8.0	268	3.6	8.0	268	2.6	7.3	258	---	---	---
14	14.9	280	3.2	8.2	106	3.5	9.5	109	2.7	6.9	97	1.9	5.7	33
15	12.0	0	2.0	5.8	182	2.7	7.5	171	1.9	5.7	177	1.4	4.4	180
16	12.4	299	2.7	7.1	129	3.1	8.2	132	2.5	6.0	116	1.6	5.5	108
17	10.9	319	2.2	6.3	151	3.0	9.0	144	2.2	6.3	148	1.5	5.5	150
18	15.9	30	3.9	9.1	214	4.0	9.1	214	3.7	8.6	217	2.6	7.2	223
19	19.0	310	4.0	8.4	135	4.3	9.1	136	---	---	---	---	---	---
20	17.9	290	3.1	7.2	117	3.9	8.8	120	3.2	7.2	112	2.1	6.0	105
21	14.4	320	3.3	8.1	139	3.4	8.2	140	2.9	7.2	132	1.9	5.7	43
22	10.4	57	2.9	9.2	239	2.9	9.2	239	2.9	8.9	245	2.3	6.9	270
23	24.6	270	---	---	---	5.3	9.6	107	---	---	---	---	---	---
24	16.9	320	2.1	6.3	178	3.6	7.8	156	3.2	7.2	152	2.2	6.3	179
25	18.0	110	3.4	7.3	283	3.5	7.4	282	3.4	7.4	282	---	---	---
26	23.1	285	5.4	10.3	113	5.7	10.6	117	5.3	10.3	112	3.0	8.1	94
27	16.9	320	3.5	8.0	137	4.3	9.3	146	3.3	7.2	138	2.1	5.8	137
28	15.3	120	2.7	6.0	288	2.7	6.0	288	2.7	6.0	288	2.5	6.0	295
29	16.9	300	4.1	9.1	138	4.2	9.3	138	3.2	7.2	138	2.0	5.7	138
30	15.4	320	3.3	8.0	142	3.7	8.4	142	2.7	6.1	126	---	---	---

Table 7.1 (cont'd)

STORM PEAKS AT 574 AT 70.35N, 141.00W

STORM	WIND		REAL ICE EDGE			98% OCCUR EDGE			50% OCCUR EDGE			30% OCCUR EDG		
	SPD	DIR	HS	TP	VMD	HS	TP	VMD	HS	TP	VMD	HS	TP	VMD
1	20.4	312	4.2	8.5	132	4.5	9.3	132	3.5	7.3	128	---	---	---
2	18.4	290	---	---	---	3.4	7.7	118	---	---	---	---	---	---
3	18.1	275	---	---	---	4.1	9.6	112	2.3	6.9	88	---	---	---
4	12.1	41	---	---	---	2.8	7.7	232	---	---	---	---	---	---
5	13.2	73	3.4	8.5	254	3.4	8.6	253	3.2	8.7	258	---	---	---
6	13.3	334	2.9	7.4	164	3.0	7.5	164	1.7	5.7	159	---	---	---
7	11.0	240	1.8	5.6	66	1.8	5.6	66	1.8	5.6	66	---	---	---
8	14.2	80	3.8	8.9	259	3.8	9.1	259	3.6	9.2	261	---	---	---
9	15.7	320	2.8	7.0	145	2.9	7.1	147	2.6	6.0	143	---	---	---
10	18.7	87	3.7	8.1	267	4.2	8.8	262	---	---	---	---	---	---
11	12.9	90	3.2	8.3	265	3.2	8.3	265	3.1	8.3	267	---	---	---
12	19.0	100	4.2	8.6	269	4.2	8.7	268	3.9	8.5	271	---	---	---
13	16.0	86	3.8	8.5	269	3.8	8.5	269	---	---	---	---	---	---
14	14.8	274	3.0	8.1	102	3.4	9.4	106	1.8	5.7	81	---	---	---
15	9.9	351	---	---	---	1.9	5.8	159	---	---	---	---	---	---
16	11.7	304	---	---	---	2.7	7.2	135	---	---	---	---	---	---
17	10.6	313	---	---	---	2.9	8.3	139	1.5	5.5	147	---	---	---
18	13.9	20	3.4	8.6	220	3.5	8.6	219	3.0	7.4	222	---	---	---
19	16.3	307	2.8	7.0	133	3.3	7.8	135	---	---	---	---	---	---
20	16.7	280	---	---	---	3.3	8.1	116	1.9	5.7	99	---	---	---
21	12.9	320	2.8	7.5	146	3.0	8.0	147	2.4	7.0	138	---	---	---
22	12.2	80	3.1	8.2	255	3.1	8.2	255	3.0	8.3	258	---	---	---
23	22.2	284	---	---	---	4.7	9.3	116	---	---	---	---	---	---
24	14.9	316	---	---	---	2.7	6.7	155	1.9	5.8	150	---	---	---
25	19.3	110	4.0	8.4	285	4.1	8.4	283	4.0	8.4	285	---	---	---
26	23.5	290	4.8	9.2	116	5.4	10.1	122	4.7	9.2	114	---	---	---
27	16.6	324	2.9	7.0	141	3.9	8.4	147	2.0	5.8	143	---	---	---
28	9.5	117	2.5	7.4	281	2.5	7.5	279	2.4	7.4	283	---	---	---
29	15.8	310	3.7	8.4	143	3.8	8.6	143	2.4	6.0	128	---	---	---
30	14.2	320	---	---	---	3.2	7.5	146	---	---	---	---	---	---

8.0 EXTREMAL ANALYSIS OF HINDCAST DATA

8.1 BASIC APPROACH

Given the typical configuration of the mean ice edge in the Canadian Beaufort and the importance of northwesterly and westerly winds on the extreme wind climate, it is natural to expect that the ice climate and the storm climate both affect the extreme wave climate. A proper treatment of this interaction has never been implemented for several reasons. Most of all, the interaction of the cyclone properties (tracks, frequencies, intensities) and the ice climate, if any, is not well understood in most areas. On the one hand, if they are linked as most approaches assume, then one need only to hindcast historical events in which the joint occurrence of strong storms and open ice conditions provide the high wave occurrence. Extrapolation of the population of occurrences above a threshold provides the extreme wave climate, then severe historical storms which happened in a short historical period not to have occurred jointly with open-water, would have not been properly considered. Given a long enough period of history, perhaps 100 years, this probably would not matter. But given only 20 years, we believe the possibility that the storm and ice climates are independent should be considered more rigorously. As discussed in chapter 2.0, Empirical Orthogonal Function (EOF) technique may be used in this case. However this is beyond the scope of this study and should be the subject of future investigations.

A relatively simple treatment of the joint probabilities may be formulated as follows:

1. Select an extreme storm population without regard to the actual ice cover except, of course, only select storms from within the calendar period susceptible to open water (i.e. June - October); it would be desirable that the size of the population be large enough to include also the top-ranked storms which occurred jointly with fairly open-water conditions and which therefore represent the high-wave events within the 20-30 years period sampled;

2. Develop effective over-water wind fields for each storm;

3. Hindcast each storm a number of times (i.e. 4 in the present study): one with the actual ice cover and the rest with an ice edge specified at positions with a given probability of occurrence (i.e. 98%, 50%, 30%) such as shown in Appendix C which corresponds to the bi-weekly intervals;

4. At each target grid point of interest subject the population of peak storm wave heights generated to the following extrapolations, using an appropriate extremal distribution:

   a) N storms in Y years (where N is the actual number of storms and Y is the actual number of years, i.e. 20), for sub-population generated in hindcasts which used the actual ice edge.

   b) N storms in Y years for the code of the three separate sub-populations developed for the ice edge for each probability level.

   c) N x 3 storms in Y x 3 years, where all peaks corresponding to all probability levels are grouped together (i.e. 90 storms in 60 years).

Each of the above analyses will yield a series of extreme significant wave heights as a function of return period. The first series (a) corresponds more or less to the traditional approach. The second series (b) may be quite useful in defining extremes for certain engineering problems where the extreme wave climate conditioned on a specified ice condition (say the ice conditions in a year in which a certain construction project is to be carried out) is more important than the long term extreme wave climate. The third series (c) will correspond to the best estimate of the true extreme wave distribution if the storm climatology and the ice cover climatology are taken as independent, which we may expect to be the case in the Canadian Beaufort.

For each series of hindcasts stratified as above, the usual approaches to estimating

parameters associated with the extreme significant waves may be followed. Our standard extremal analysis software accounts for variable storm build-up and decay rates in the specification of maximum individual wave height (H_{max}), crest height (H_c), and estimates peak periods using correlations developed from the hindcast database. It includes different distributions (e.g. Gumbel, Borgman) and a number of fitting techniques (e.g. Linear regression, method of moments and maximum likelihood method). It provides graphical representation of results with 90% and 95% confidence limits plotted. For the present study, and in order to be consistent with other similar studies we carried out for the east and west coasts, Gumbel distribution with method of moment fit is used to provide extreme value estimates as described below.

8.2 ANALYSIS TECHNIQUE

The wave model provided time histories of the following quantities at each grid point of the selected 51 sites which are used in the statistical analysis of extremes:

H_s	=	significant wave height (m)
T_p	=	spectral peak period (s)
θd	=	vector mean wave direction (degrees-going towards)
W_s	=	wind speed (m/s)
θw	=	wind direction (degrees-coming from)

The basic approach was to carry out site specific extremal analysis of hindcast peaks-over-threshold (POT), at each of the selected grid locations. Site averaging was not considered necessary or desirable for the following reasons:

1) a reasonably large number of storms were hindcast, thereby providing a reasonably large population of peaks at each grid location;

2) the meteorological properties of storms responsible for wave generation vary gently across basins. This tends to minimize the kind of sampling variations which site averaging is intended to suppress; and

3) the site specific approach may preserve real variations in extremes of wave height and period, associated with fine-scale variations in the complicated shoreline geometry which bounds the study area.

The objective of the analysis was to determine long term statistical distributions of significant and maximum individual wave height, crest height, and associated wind speed, for sub-populations of storms stratified into sectors of wave approach direction for selected grid points, and omni-directional extremes at all points. It was found, however, that no more than two broad directional sectors (NW and NE) could be justified at any point based upon the given hindcast population of storms. The number of storms in each directional sector was not sufficient to provide reasonable population for directional extreme analysis. Therefore only omni-directional extreme analysis was carried out in the present study. Finally, estimates of extremes for quantities which were not extrapolated, such as T_p, and quantities extrapolated, such as H_s were provided. Correlations were developed from the hindcast data at each grid point between such quantities.

In the remainder of this section, a more detailed description of each of the key steps of the statistical analysis is given. The statistical models and fitting techniques are well established and have been described in several previous studies (e.g. Muir and El-Shaarawi, 1986, see also CCC, 1991).

8.3 CALCULATION OF MAXIMUM AND CREST HEIGHTS

It is by now well known that the statistics of individual wave heights and crest heights in naturally occurring sea states deviate from predictions of the theoretical Rayleigh distribution. A large number of alternative distributions have been proposed. We have adopted the empirical distribution of Forristall (1978) for maximum individual wave height, and the Jahns-Wheeler distribution with Haring, Osborne, and Spencer's (HOS) empirical constants (Haring and Heideman, 1978) for crest height in a wide range of water depths. HOS have also proposed a distribution of maximum individual wave heights which nominally provides maximum heights

about 2 percent lower than Forristall's, but whose constants may be adjusted slightly to provide essentially the same results as Forristall (1978).

The various distributions cited above provide estimates of maximum wave height (H_{max}) and crest height (H_c) in runs of n individual waves, expressed usually as zero-crossing waves. In our standard approach, we use Borgman's (1973) integral expression to account for the effect of the actual buildup and decay for each individual storm on the effective number of waves in a storm at a site. This expression used significant wave period, T_s, to relate the period properties of the seaway to the effective number of individual waves. Other approaches have included the use of an average normalized buildup and decay for all storms, or the simple adoption of a constant storm duration. The computation may also be carried out with different relationships between T_s and zero-crossing period, T_z, and properties of the hindcast spectrum, such as T_p or the spectral moments.

In the calculation of H_{max} in this study, the distribution of Forristall (1978) and the method of Borgman (1973) was applied throughout. The adopted H_{max} at each site and in each storm was taken as the median of the fitted distribution. This method uses the significant wave period, T_s, directly from the hindcast spectrum as computed from the zeroth and first moments (M_0 and M_1).

In the calculation of H_c, the method of HOS was adopted, except that as for H_{max} the actual buildup and decay in each storm was used following the method of Borgman (1973). In this calculation, T_z was calculated from T_p using the constant ratio T_z/T_p of 0.74 found empirically to characterize storm sea states in extratropical storms.

The analysis techniques were described in more detail in the Canadian Climate Centre (1991). It should be noted here that the above techniques are derived for deepwater wave conditions. Other techniques may be applied to site specific shallow water sites.

8.4 EXTREMAL ANALYSIS METHODS

The objective of the extremal analysis was to describe extremes at all contiguous (51) grid locations (see Figure 7.1):

- H_s versus risk (i.e. annual exceedance probability or return period)
- W_s versus risk (wind speed which corresponds to the peak H_s in each storm).

At a selected subset of grid locations a more detailed analysis of the extremes was carried out in order to determine:

1) effective ratios of H_{max}/H_s and H_c/H_s based on the analysis described above;
2) H_{max} and H_c versus risk (or return period); and
3) peak spectral periods T_p associated with peak H_s from the relation $T_p = A\ (H_s)^B$.

At these "representative" grid locations, a further analysis of the extremes was considered. This included sensitivity of extremes to assumed distribution, fitting thresholds, and directional stratification.

The results of the above analyses were presented in both tabular and graphical forms. The following methods were applied in the analysis.

Extreme Value Distribution

The recommended extreme value distribution is the Gumbel:

$$Pr\ \{x \leq X\} = \exp\ [-\exp\ (-(x-a)/b]$$

Borgman distribution was also applied for comparison with Gumbel:

$$Pr\ \{x \leq X\} = \exp\ [-\exp\ (-x^2-a)/b)]$$

where x is the parameter to be fitted (e.g. H_s); a and b are constants determined from the fitting of the hindcast data.

The chosen fitting scheme is the method of moments (MOM). This is in line with what AES use in their Marine Statistics (MAST) System and also previous hindcast studies carried out by MPL/OWI for the east coast and west coast of Canada. The Maximum Likelihood Method (MLM) was also checked and was found to produce results similar to those produced by the Method of Moments.

For most environmental data, the Gumbel distribution, fitted by the method of moments has been accepted as appropriate for representing the probability distribution for extremes. As described by Muir and El-Shaarawi (1986), the method of moments is simple, robust, and is unbiased for the Gumbel type distribution. The method involves equating the sample moments (i.e. mean and variance) to the moments derived from the distribution and solving for the estimated parameters. In the present study, the so-called plotting position was determined using the "exact" expression given by Carter and Challenor (1983).

Return Period

The return period, T, is calculated from the cumulative distribution function:

$$P_T = 1 - \frac{Y}{NT}$$

where N is the number of samples from Y years. Correlating the candidate distribution, Pr $\{x \leq X\}$, to the above distribution of return period T yields:

$$X_T = [a - b \ln (-\ln (P_T))]^c$$

where c = 1 for Gumbel and 0.5 for Borgman distributions.

Numerical Solution

The Gumbel distribution fitted to the extreme value series (whether annual maximum or peak-over-threshold) by the method of moments is simply represented by:

$$X_T = x_{mean} + K_T.s$$

where X_T is the value of the variable equalled or exceeded once in the return period T; x_{mean} and s are the mean and the standard deviation respectively, of the hindcast series of extremes; K_T is a frequency factor dependent on the return period obtained from:

$$K_T = -(\sqrt{6}/\pi) \{0.5772 + \ln [\ln(T/(T-1))]\}$$

Confidence Limits

The extreme values calculated from the above approach represent the "best fit" estimates. However it is necessary to provide the confidence intervals for this estimate (e.g. 90% or 95%). The confidence interval is given by the range:

$$X_T - t(\alpha)s_e \text{ to } X_T + t(\alpha)s_e$$

where: $s_e = ß \cdot s/n$

$$ß = (1 + 1.14 K_T + 1.1 K_T^2)$$

and $t(\alpha)$ is the student t-distribution value corresponds to confidence level α for n samples.

The span of the upper limit (UL) to Lower Limit (LL) values normalized by the best fit (i.e., [UL - LL]/mean) is a relative measure of the goodness-of-fit. It should be noted that these confidence limits address only statistical characteristics of input data, and not the possible errors in storm selection and hindcast accuracy.

All other parameters (i.e. T_p, H_{max} and H_c) are derived from the estimated extreme H_s for given return periods (or probability of occurrence). The derived values are based on the mean or best-fit values of H_s and the methods described in the previous section. The above equations were used to provide the desired extremes both in tabular and graphical forms as shown in the following section.

8.5 ANALYSIS RESULTS

The hindcast peak significant wave height for each storm at each of the selected 51 grid points (Appendix E) were input to the extremal analysis program to produce the expected design values for the following return periods:

2, 5, 10, 25, 50 and 100 years.

This was done for the four groups of ice edge scenarios:

1) actual ice edge
2) 98% occurrences of ice edge
3) 50% occurrences of ice edge
4) 30% occurrences of ice edge

Additional run was made using all storms with the three climatological ice edge combined, i.e.total number of storms N = 30 storms x 3 ice edge scenarios = 90 storms, total number of years Y = 20 years x 3 ice edges = 60 years. It should be noted that the number of storms (N) at a given grid point in each group depends on the location of the site (grid point) with respect to ice field (i.e. if the grid point in question happened to be in the ice, there will be no hindcast value for this particular storm, and the total valid events or storms would be 29, and so on).

8.5.1 Sensitivity Analysis

Detailed extremal analysis was carried out at a number of grid points in the study

area. The results are discussed below. The grid points at which the detailed analysis was carried out are:

Grid Point #	Latitude	Longitude	Model Water Depth (m)	
360	70.84	132.79	56.50	
384	69.88	134.15	10.10	
437	69.61	136.17	8.65	closest to Minuk
463	69.30	137.20	18.60	
492	69.99	138.05	136.30	
574	70.35	141.00	174.10	
435	68.94	136.32	7.50	
464	69.64	137.14	30.15	

The results are presented in Figures 8.1 - 8.5. The results are provided for the actual ice edge scenario.

Effect of Wave Height Threshold

Extremal analysis was carried out with different wave height thresholds for each population at selected grid points. In the selection of the thresholds; first, all events were used in the extremal analysis; second, the thresholds were chosen such that the remaining population produced best fit (best regression correlation).

It was found, in general, the lower thresholds provided slightly higher extreme wave heights than those calculated with higher thresholds, at large return periods (50-100 years).

Gumbel Versus Borgman Distributions

A number of extreme value distributions and fitting techniques were checked (i.e. Gumbel versus Borgman distribution using MOM or MLM fit). Figure 8.1 - 8.5 present the extremal analysis results using Gumbel and Borgman distributions.

GRID POINT 360 AT 70.840 N, 132.79 W

GUMBEL – Method of Moments

23 storms
Wave height threshold = 2.90 m

Return Period (yr)	Best Fit (m)	90% U.L. (m)	Tp (s)	Hmax (m)	Hc (m)
2	3.5	3.6	8.1	6.4	3.6
5	3.9	4.1	8.6	7.1	3.9
10	4.1	4.4	8.9	7.5	4.2
30	4.5	4.9	9.3	8.2	4.6
50	4.6	5.1	9.5	8.5	4.7
100	4.9	5.5	9.7	8.9	5.0

Tp, Hmax, and Hc were calculated using

$Tp = 4.098\ Hs^{0.547}$
$Hmax = 1.826\ Hs$
$Hc = 1.020\ Hs$

Correlation = 0.99

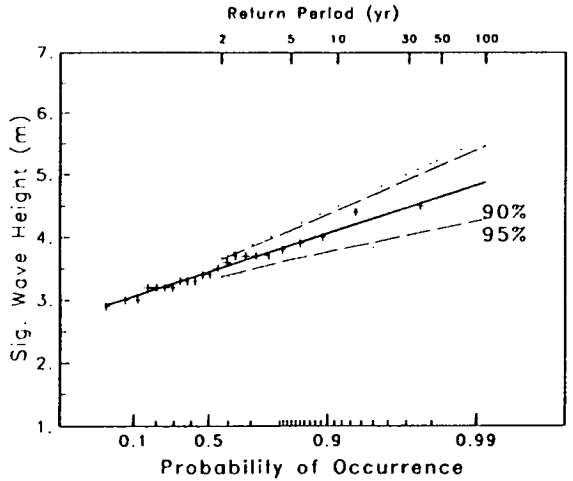

GUMBEL – Method of Moments

26 storms
Wave height threshold = 1.50 m

Return Period (yr)	Best Fit (m)	90% U.L. (m)	Tp (s)	Hmax (m)	Hc (m)
2	3.4	3.6	8.0	6.2	3.5
5	3.9	4.3	8.6	7.2	4.0
10	4.3	4.8	8.9	7.9	4.4
30	4.9	5.5	9.4	8.9	5.0
50	5.1	5.9	9.6	9.4	5.2
100	5.5	6.3	9.9	10.0	5.6

Tp, Hmax, and Hc were calculated using

$Tp = 4.693\ Hs^{0.439}$
$Hmax = 1.825\ Hs$
$Hc = 1.021\ Hs$

Correlation = 0.91

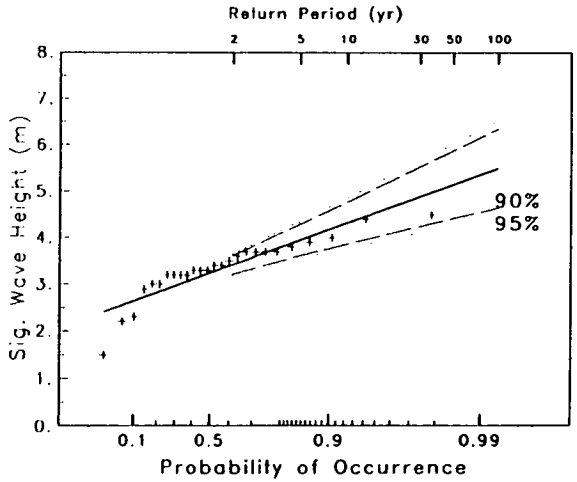

Figure 8.1 Extremal Analysis Results At Grid Point #360 (Actual Ice Edge)

GRID POINT 360 AT 70.840 N, 132.79 W

BORGMAN – Method of Moments

23 storms
Wave height threshold = 2.90 m

Return Period (yr)	Best Fit (m)	90% U.L. (m)	Tp (s)	Hmax (m)	Hc (m)
2	3.5	4.3	8.2	6.5	3.6
5	3.9	4.9	8.6	7.1	4.0
10	4.1	5.3	8.9	7.5	4.2
30	4.4	5.8	9.3	8.1	4.5
50	4.6	6.0	9.4	8.3	4.7
100	4.7	6.3	9.6	8.7	4.8

Tp, Hmax, and Hc were calculated using

$Tp = 4.098\ Hs^{0.547}$
Hmax = 1.826 Hs
Hc = 1.020 Hs

Correlation = 0.99

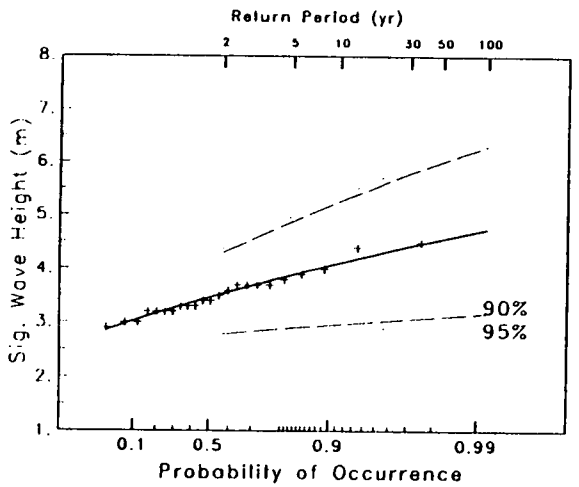

BORGMAN – Method of Moments

26 storms
Wave height threshold = 1.50 m

Return Period (yr)	Best Fit (m)	90% U.L. (m)	Tp (s)	Hmax (m)	Hc (m)
2	3.5	4.3	8.1	6.3	3.5
5	3.9	4.9	8.5	7.2	4.0
10	4.2	5.4	8.8	7.7	4.3
30	4.6	6.0	9.2	8.4	4.7
50	4.8	6.3	9.3	8.7	4.9
100	5.0	6.6	9.5	9.1	5.1

Tp, Hmax, and Hc were calculated using

$Tp = 4.693\ Hs^{0.459}$
Hmax = 1.825 Hs
Hc = 1.021 Hs

Correlation = 0.94

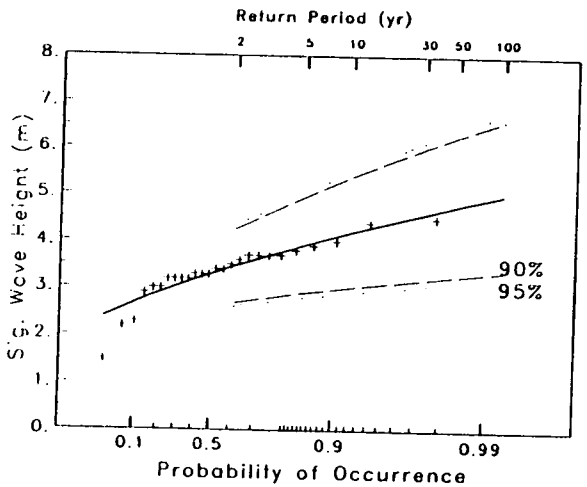

Figure 8.1 (cont'd)

GRID POINT 437 AT 69.612 N, 136.17 W

BORGMAN - Method of Moments

29 storms
Wave height threshold = 1.67 m

Return Period (yr)	Best Fit (m)	90% U.L. (m)	Tp (s)	Hmax (m)	Hc (m)
2	2.8	3.5	8.3	5.0	2.8
5	3.3	4.2	9.0	5.9	3.3
10	3.6	4.7	9.3	6.5	3.6
30	4.0	5.3	9.8	7.2	4.0
50	4.2	5.6	10.0	7.5	4.2
100	4.4	6.0	10.2	8.0	4.4

Tp, Hmax, and Hc were calculated using

$Tp = 5.315\ Hs^{0.439}$
$Hmax = 1.802\ Hs$
$Hc = 0.999\ Hs$

Correlation = 0.98

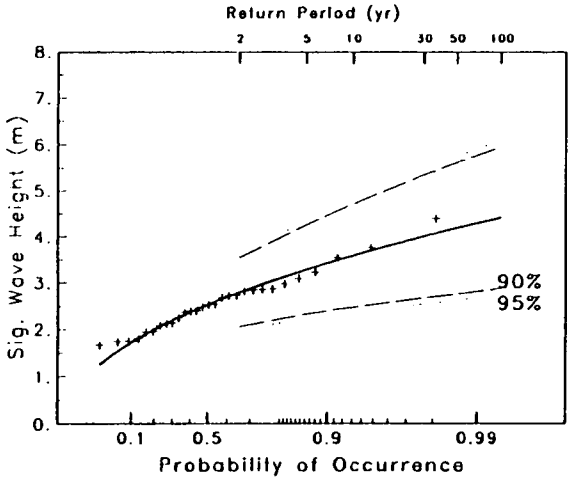

GRID POINT 437 AT 69.612 N, 136.17 W

GUMBEL - Method of Moments

29 storms
Wave height threshold = 1.70 m

Return Period (yr)	Best Fit (m)	90% U.L. (m)	Tp (s)	Hmax (m)	Hc (m)
2	2.7	2.9	8.2	4.9	2.7
5	3.2	3.5	8.9	5.8	3.2
10	3.6	4.0	9.3	6.5	3.6
30	4.1	4.7	9.9	7.5	4.1
50	4.4	5.1	10.1	7.9	4.4
100	4.7	5.5	10.5	8.5	4.7

Tp, Hmax, and Hc were calculated using

$Tp = 5.350\ Hs^{0.432}$
$Hmax = 1.802\ Hs$
$Hc = 0.999\ Hs$

Correlation = 0.99

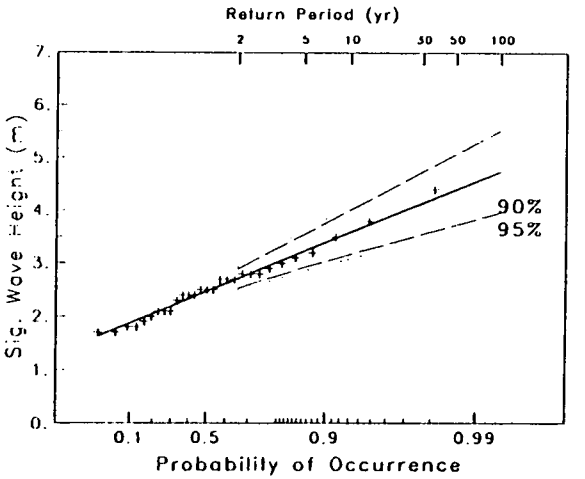

Figure 8.2 Extremal Analysis Results at Grid Point #437 (Actual Ice Edge)

GRID POINT 463 AT 69.300 N, 137.20 W

GUMBEL - Method of Moments

27 storms
Wave height threshold = 2.10 m

Return Period (yr)	Best Fit (m)	90% U.L. (m)	Tp (s)	Hmax (m)	Hc (m)
2	2.9	3.0	7.9	5.2	2.9
5	3.3	3.5	8.5	5.9	3.3
10	3.6	3.9	8.9	6.4	3.6
30	4.0	4.5	9.4	7.3	4.0
50	4.2	4.8	9.6	7.6	4.2
100	4.5	5.1	9.9	8.1	4.5

Tp, Hmax, and Hc were calculated using

$Tp = 4.751\ Hs^{0.491}$
$Hmax = 1.812\ Hs$
$Hc = 1.009\ Hs$

Correlation = 0.99

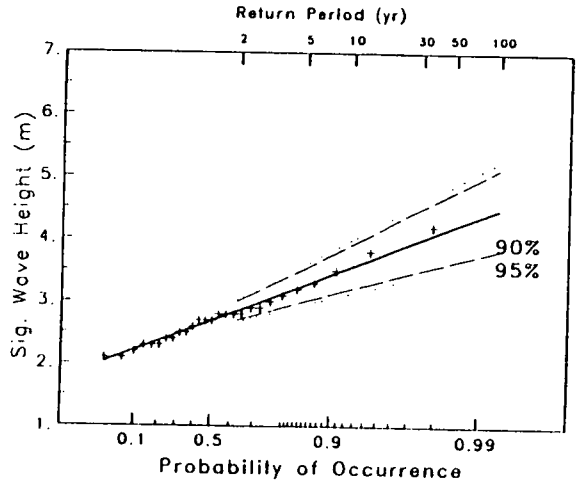

GUMBEL - Method of Moments

29 storms
Wave height threshold = 1.70 m

Return Period (yr)	Best Fit (m)	90% U.L. (m)	Tp (s)	Hmax (m)	Hc (m)
2	2.8	3.0	7.9	5.1	2.9
5	3.3	3.5	8.5	5.9	3.3
10	3.6	4.0	8.9	6.5	3.6
30	4.1	4.6	9.5	7.4	4.1
50	4.3	4.9	9.7	7.8	4.3
100	4.6	5.3	10.0	8.3	4.6

Tp, Hmax, and Hc were calculated using

$Tp = 4.826\ Hs^{0.479}$
$Hmax = 1.812\ Hs$
$Hc = 1.009\ Hs$

Correlation = 0.99

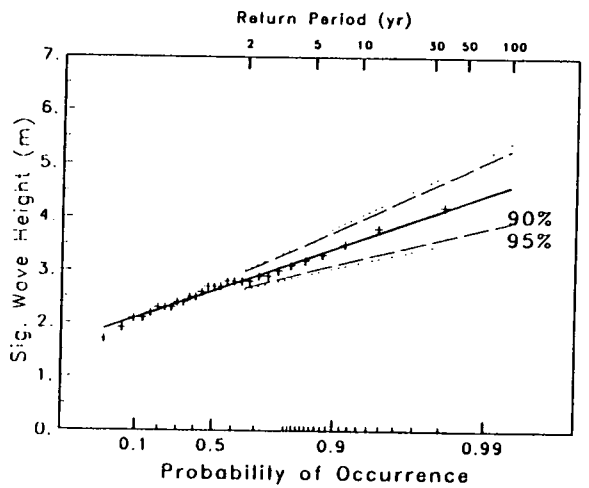

Figure 8.3 Extremal Analysis Results At Grid Point #463 (Actual Ice Edge)

GRID POINT 492 AT 69.990 N, 138.05 W

BORGMAN – Method of Momenls

27 storms
Wave height threshold = 2.20 m

Return Period (yr)	Best Fit (m)	90% U.L. (m)	Tp (s)	Hmax (m)	Hc (m)
2	3.6	4.4	8.2	6.4	3.6
5	4.1	5.2	8.9	7.4	4.1
10	4.5	5.7	9.3	8.0	4.5
30	4.9	6.4	9.9	8.9	5.0
50	5.1	6.7	10.1	9.2	5.2
100	5.4	7.1	10.4	9.7	5.4

Tp, Hmax, and Hc were calculated using

$Tp = 3.928\ Hs^{0.579}$
Hmax = 1.800 Hs
Hc = 1.006 Hs

Correlation = 0.98

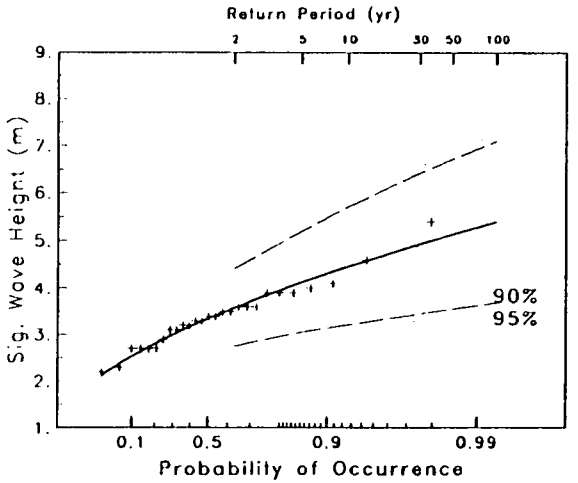

GRID POINT 492 AT 69.990 N, 138.05 W

GUMBEL – Method of Moments

27 storms
Wave height threshold = 2.20 m

Return Period (yr)	Best Fit (m)	90% U.L. (m)	Tp (s)	Hmax (m)	Hc (m)
2	3.5	3.7	8.1	6.3	3.5
5	4.1	4.4	8.9	7.3	4.1
10	4.5	4.9	9.3	8.0	4.5
30	5.1	5.7	10.1	9.1	5.1
50	5.3	6.1	10.4	9.6	5.4
100	5.7	6.6	10.8	10.3	5.8

Tp, Hmax, and Hc were calculated using

$Tp = 3.928\ Hs^{0.579}$
Hmax = 1.800 Hs
Hc = 1.006 Hs

Correlation = 0.98

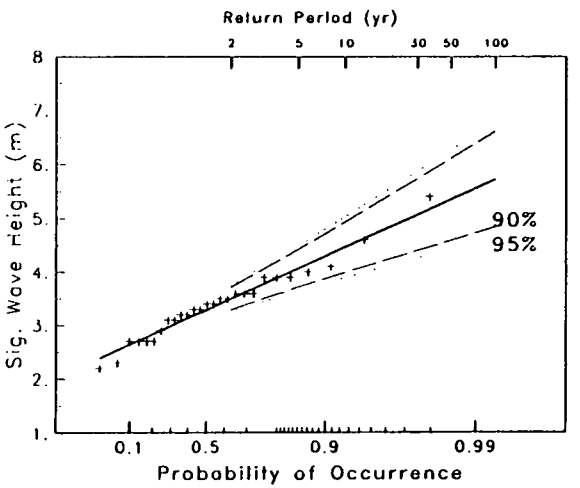

Figure 8.4 Extremal Analysis Results At Grid Point #492 (Actual Ice Edge)

GRID POINT 574 AT 70.350 N, 141.00 W

GUMBEL - Method of Moments

19 storms
Wave height threshold = 2.50 m

Return Period (yr)	Best Fit (m)	90% U.L. (m)	Tp (s)	Hmax (m)	Hc (m)
2	3.3	3.5	8.0	5.9	3.3
5	3.8	4.2	8.5	6.9	3.9
10	4.2	4.7	8.8	7.6	4.2
30	4.7	5.5	9.2	8.5	4.8
50	5.0	5.8	9.4	9.0	5.0
100	5.3	6.3	9.7	9.6	5.3

Tp, Hmax, and Hc were calculated using

$Tp = 4.937\ Hs^{0.403}$
$Hmax = 1.800\ Hs$
$Hc = 1.005\ Hs$

Correlation = 0.99

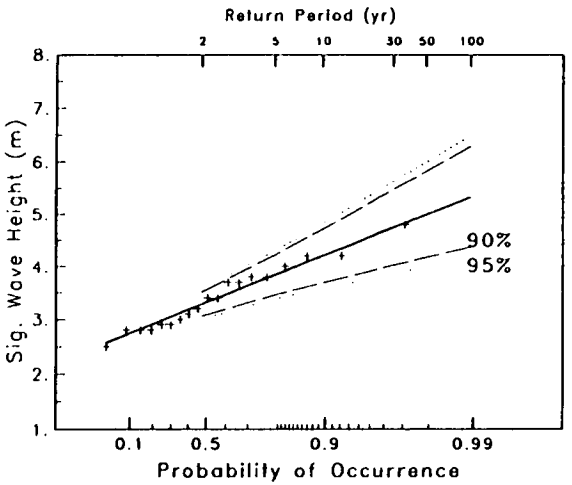

GUMBEL - Method of Moments

20 storms
Wave height threshold = 1.80 m

Return Period (yr)	Best Fit (m)	90% U.L. (m)	Tp (s)	Hmax (m)	Hc (m)
2	3.2	3.5	7.9	5.8	3.2
5	3.8	4.3	8.5	6.9	3.9
10	4.3	4.8	9.0	7.7	4.3
30	4.9	5.7	9.6	8.8	4.9
50	5.2	6.1	9.8	9.3	5.2
100	5.5	6.6	10.2	10.0	5.6

Tp, Hmax, and Hc were calculated using

$Tp = 4.514\ Hs^{0.474}$
$Hmax = 1.801\ Hs$
$Hc = 1.007\ Hs$

Correlation = 0.97

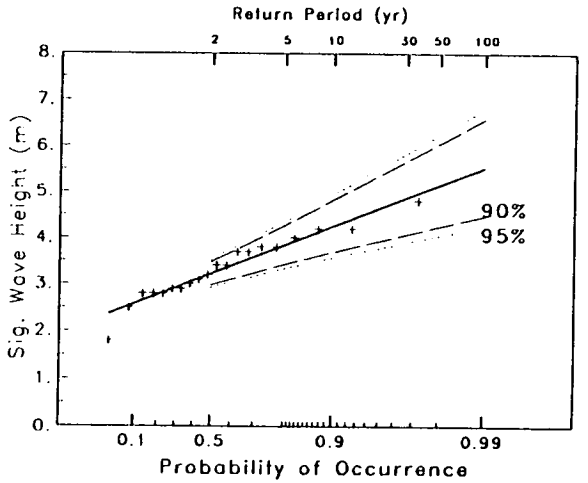

Figure 8.5 Extremal Analysis Results At Grid Point #574 (Actual Ice Edge)

It can be concluded from the above that the extremal analysis results are slightly affected by the type of distribution tested and the threshold value used with Gumbel providing higher values than Borgman. In the final analysis, the Gumbel distribution was used with the top number of storms which produced the best-fit regression line (i.e. the number of storms and the thresholds used in the extremal analysis varied from one grid point to another, for each ice edge scenario, as shown in the next section).

8.5.2 Stratification of Storm Population by Direction

The storm population at each of the three grid points was stratified by wave direction as shown in Figure 8.6 (for actual ice edge and for 98% ice edge). As shown the given size of the population is not sufficient to provide full directional extreme analysis. It can be seen that only two broad directional sectors may be used:

- East to NE and NW (each with 10 - 15 storms)

This is not enough to warrant reliable extremal analysis estimates. Therefore no further analysis was considered.

8.5.3 Final Results

The extremal analysis was then executed for all 51 grid points (Figure 7.1). The results are presented in Tables 8.1 - 8.5 as follows:

1. Maximum wind speed vs. return period (2 - 100 yr.) or risk factor (0.5 - 0.01) (Table 8.1)
2. Significant wave height vs. return period or risk factor: with real ice edge (Table 8.2), 98% ice edge (Table 8.3), 50% ice edge (Table 8.4), and 30% ice edge (Table 8.5). The results in these tables are based on the best fit of regression line to hindcast values, i.e. highest correlation coefficient.

In these Tables only "active" (open-water) grid points are presented (dashed lines indicate the grid point is in ice). The values presented are the best-fit H_s and 90%

DISTRIBUTION OF STORM WAVE HEIGHTS BY DIRECTION

REAL ICE EDGE

Grid Point 360 – 70.84 N, 132.79 W

26 storms

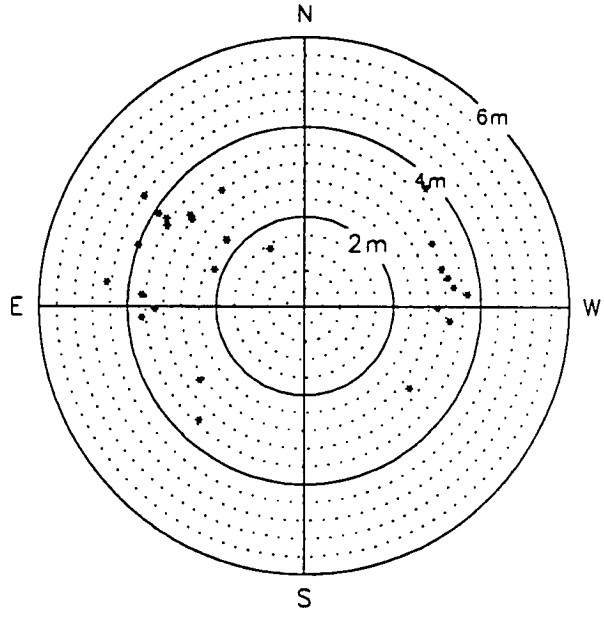

Grid Point 574 – 70.35 N, 141.0 W

20 storms

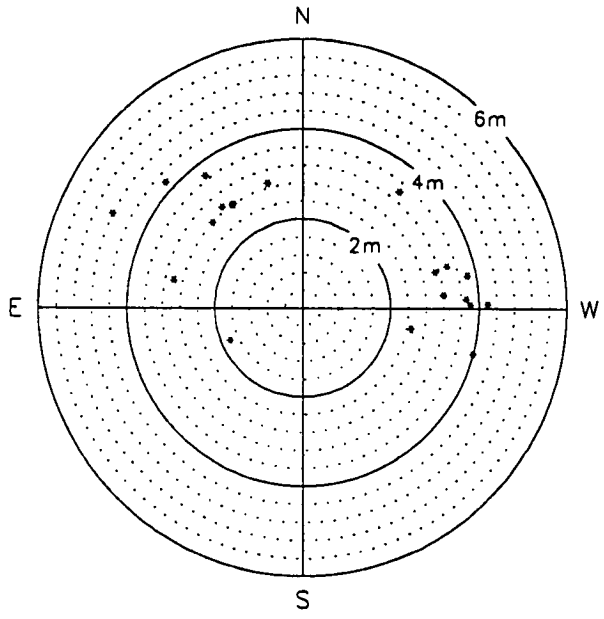

Grid Point 437 – 69.6 N, 136.2 W

29 storms

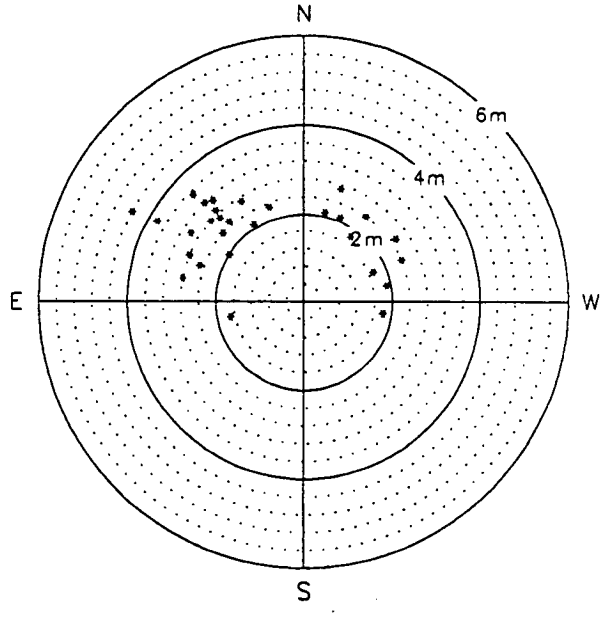

Grid Point 463 – 69.3 N, 137.2 W

29 storms

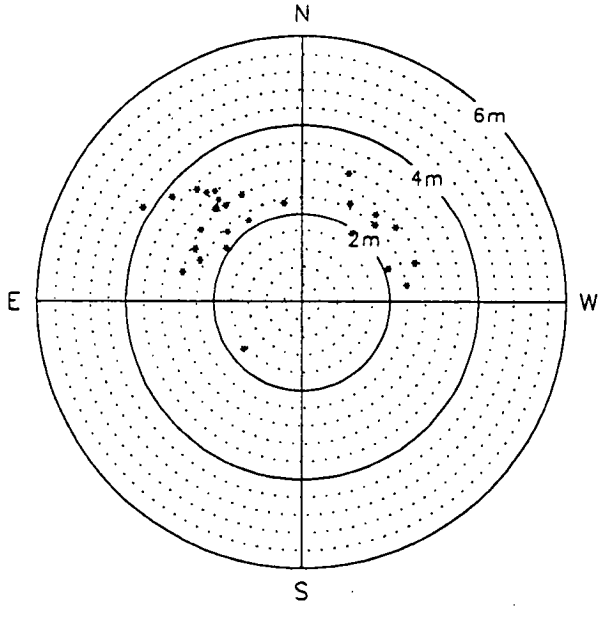

Figure 8.6

DISTRIBUTION OF STORM WAVE HEIGHTS
BY DIRECTION
98% OCCURRENCE OF ICE EDGE

Grid Point 360 – 70.84 N, 132.79 W

30 storms

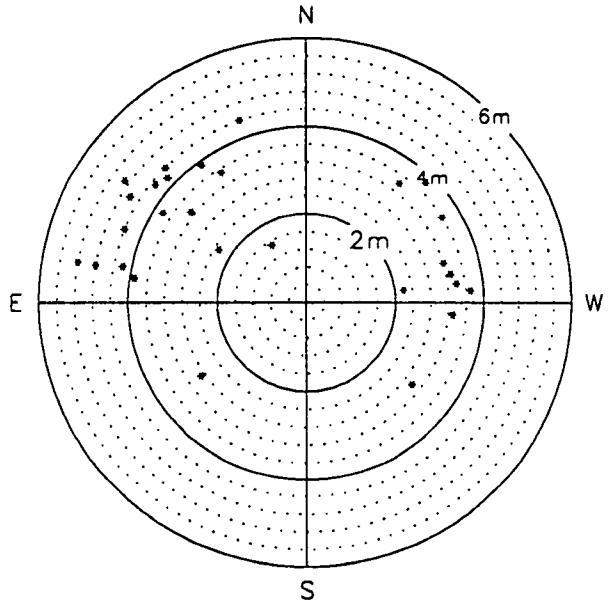

Grid Point 574 – 70.35 N, 141.0 W

30 storms

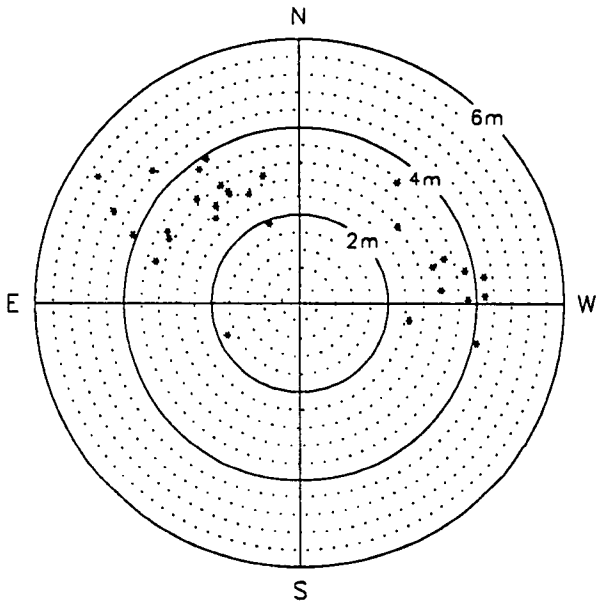

Grid Point 437 – 69.6 N, 136.2 W

30 storms

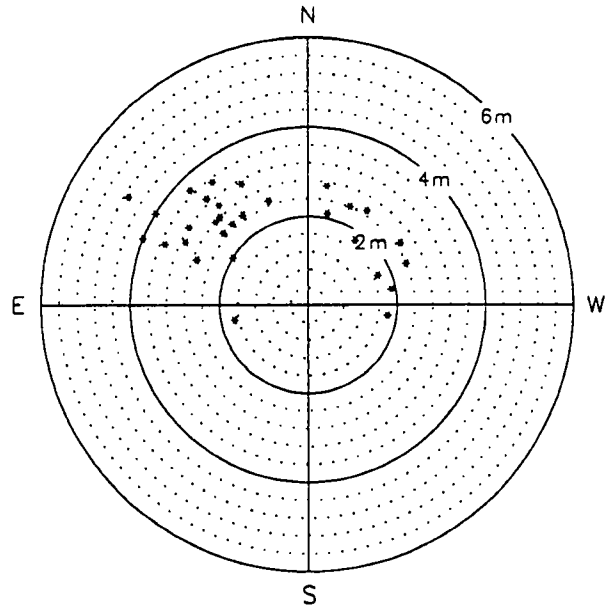

Grid Point 463 – 69.3 N, 137.2 W

30 storms

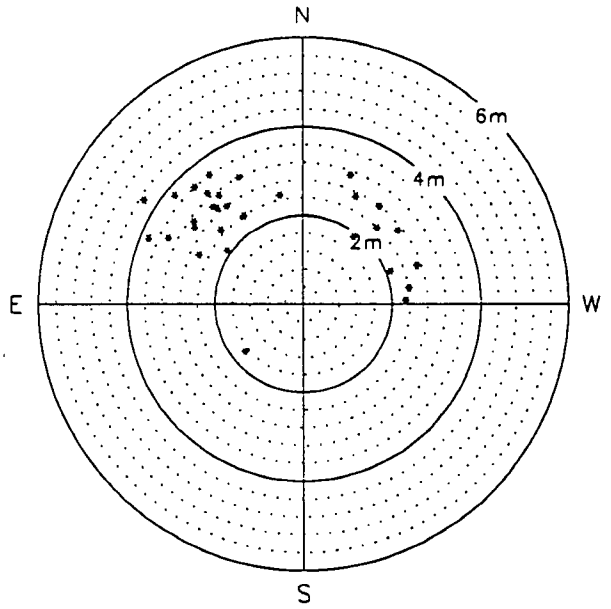

Figure 8.6 (cont'd)

confidence level upper limit for return periods 2, 5, 10, 25, 50 and 100 years. The tables also show the number of storms used in the final analysis at each grid point.

Table 8.6 presents the extremal analysis results for the joint probability scenario where the three climatological ice edges were combined.

The results of the above analyses are also presented graphically on a base map at each of the 51 grid points. Figures 8.7 - 8.11 show the 100 year significant wave height fields for the real ice edge, the 98%, 50% and 30% ice edges, and the overall (combined) three climatological ice edge scenarios i.e. joint probability, respectively.

Table 8.7 provides a summary of the 100 year design significant wave heights at each grid point for all ice edge scenarios studied. The table provides a quick comparison of the extreme wave height estimates for each ice edge scenario.

Detailed analysis results are presented at the previously selected grid points. The results are shown in figures 8-12 - 8-15 for the joint probability case. It provides the design H_s and T_p, H_{max} and H_c for given return periods, and the probability of occurrences vs. H_s curves with 90% and 95% confidence limits shown. The analysis was carried out using all storms available at these points.

Finally, contour presentations of the 100 year return period significant wave height, maximum wave height and the corresponding wind speed are given in Figures 8-16 to 8-18, for actual ice edge. Similar contour maps are provided for the 98% ice edge, and for the combined climatological ice edge (joint probability) case as shown in Figures 8-19 throughout 8-22. The joint probability analysis results provide the design wave parameters in the study area.

Table 8.1 Summary of Extremal Analysis Results At 51 Grid Points

Peak Wind Speed

SUMMARY OF EXTREMAL ANALYSIS RESULTS AT ALL GRID POINTS IN STUDY AREA

MAXIMUM WIND SPEED

risk factor / return period			.50 2 yr		0.20 5 yr		0.10 10 yr		0.04 25 yr		0.02 50 yr		0.01 100 yr		
grid point	Lat (N)	Long (W)	Best Fit m/s	90% U.L. m/s	Best Fit m/s	90% U.L. m/s	Best Fit m/s	90% U.L. m/s	Best Fit m/s	90% U.L. m/s	Best Fit m/s	90% U.L. m/s	Best Fit m/s	90% U.L. m/s	NUM PTS
198	70.47	126.82	15.4	15.9	16.7	17.5	17.6	18.7	18.8	20.3	19.6	21.5	20.5	22.6	25
200	71.12	126.34	15.3	15.8	16.7	17.6	17.6	18.8	18.8	20.4	19.8	21.7	20.7	22.9	25
226	70.87	127.57	15.9	16.4	17.2	18.1	18.1	19.3	19.3	20.9	20.2	22.0	21.1	23.2	25
252	70.61	128.78	16.4	16.8	17.6	18.4	18.4	19.5	19.5	20.9	20.3	22.0	21.1	23.1	24
254	71.27	128.36	16.0	16.5	17.4	18.3	18.3	19.5	19.6	21.2	20.5	22.4	21.4	23.6	25
278	70.35	129.96	16.6	17.1	18.0	18.9	19.0	20.2	20.3	21.9	21.2	23.2	22.1	24.4	25
280	71.01	129.58	16.9	17.4	18.2	19.0	19.1	20.2	20.3	21.8	21.1	22.9	22.0	24.1	25
306	70.74	130.77	17.0	17.5	18.3	19.1	19.1	20.2	20.3	21.7	21.1	22.8	21.9	23.9	26
309	71.73	130.23	16.0	16.4	17.1	17.8	17.8	18.8	18.7	20.1	19.4	21.0	20.1	22.0	22
330	69.80	132.22	17.3	18.0	19.3	20.5	20.7	22.3	22.5	24.7	23.8	26.4	25.2	28.2	29
331	70.13	132.08	17.7	18.4	19.6	20.8	21.0	22.6	22.7	24.8	24.0	26.5	25.3	28.2	28
332	70.46	131.93	17.5	18.1	19.1	20.1	20.2	21.5	21.6	23.4	22.7	24.8	23.7	26.2	27
356	69.51	133.30	16.8	17.5	18.8	20.0	20.2	21.8	21.9	24.1	23.2	25.8	24.5	27.6	28
357	69.84	133.18	17.7	18.4	19.7	20.9	21.1	22.7	22.8	25.0	24.2	26.8	25.5	28.6	29
358	70.17	133.05	17.9	18.6	19.7	20.9	21.0	22.6	22.7	24.7	23.9	26.4	25.2	28.0	28
360	70.84	132.79	17.6	18.1	19.0	19.9	20.0	21.1	21.2	22.8	22.1	24.0	23.0	25.2	26
362	71.50	132.50	16.6	17.1	17.9	18.6	18.7	19.8	19.8	21.2	20.7	22.3	21.5	23.4	27
384	69.88	134.15	18.1	18.8	20.1	21.4	21.6	23.3	23.4	25.7	24.8	27.5	26.1	29.4	27
386	70.55	133.92	17.8	18.4	19.5	20.6	20.7	22.1	22.2	24.1	23.4	25.6	24.5	27.1	28
410	69.58	135.21	17.8	18.5	19.7	20.9	21.0	22.7	22.6	24.9	23.8	26.5	25.0	28.2	22
411	69.92	135.12	18.3	19.2	20.7	22.1	22.3	24.2	24.4	27.0	26.0	29.1	27.6	31.1	29
412	70.25	135.03	18.3	19.0	20.4	21.7	21.9	23.6	23.8	26.1	25.2	27.9	26.6	29.8	29
413	70.59	134.93	18.0	18.7	19.9	21.0	21.1	22.6	22.8	24.8	24.0	26.4	25.2	28.0	28
414	70.92	134.82	17.8	18.4	19.6	20.7	20.9	22.3	22.5	24.5	23.7	26.1	24.9	27.7	28
417	71.92	134.49	16.1	16.5	17.2	18.0	18.0	19.0	18.9	20.3	19.7	21.3	20.4	22.2	22
435	68.94	136.32	16.3	17.0	17.9	19.1	19.0	20.5	20.3	22.4	21.3	23.8	22.3	25.1	18
436	69.28	136.25	16.4	17.2	18.5	19.8	20.0	21.7	21.9	24.2	23.3	26.1	24.7	28.0	28
437	69.61	136.17	17.3	18.1	19.6	20.9	21.2	23.0	23.3	25.8	24.8	27.8	26.4	29.8	30
438	69.95	136.10	18.2	19.0	20.5	21.9	22.2	24.0	24.3	26.8	25.8	28.9	27.4	30.9	30
440	70.62	135.93	17.8	18.4	19.7	20.8	21.0	22.5	22.7	24.7	24.0	26.4	25.2	28.1	30
463	69.30	137.20	16.4	17.1	18.5	19.7	19.9	21.6	21.7	24.1	23.1	25.9	24.5	27.7	27
464	69.64	137.14	17.2	18.0	19.5	20.9	21.2	23.1	23.3	25.9	24.9	28.0	26.5	30.1	30
465	69.97	137.07	18.1	18.9	20.5	21.9	22.2	24.1	24.4	26.9	26.0	29.1	27.6	31.2	30
468	70.98	136.87	17.7	18.3	19.5	20.5	20.7	22.2	22.3	24.3	23.5	25.8	24.7	27.4	30
470	71.65	136.73	16.4	17.0	18.0	18.9	19.1	20.3	20.5	22.2	21.5	23.6	22.6	25.0	29
490	69.32	138.15	16.5	17.2	18.4	19.7	19.8	21.5	21.5	23.8	22.8	25.6	24.1	27.3	25
491	69.65	138.10	17.3	18.2	19.6	20.9	21.1	23.0	23.0	25.6	24.5	27.5	26.0	29.5	26
492	69.99	138.05	18.2	19.1	20.6	22.0	22.2	24.2	24.3	27.0	25.9	29.1	27.4	31.1	27
493	70.33	138.01	17.9	18.8	20.3	21.7	22.0	23.8	24.1	26.6	25.7	28.7	27.3	30.8	30
494	70.66	137.96	17.9	18.6	20.0	21.3	21.5	23.2	23.4	25.7	24.9	27.6	26.3	29.5	30
522	71.01	138.93	17.6	18.4	19.6	20.9	21.0	22.7	22.8	25.1	24.2	26.9	25.5	28.7	27
525	72.02	138.82	15.8	16.4	17.4	18.4	18.5	19.9	20.0	21.8	21.0	23.2	22.1	24.7	27
545	69.68	140.03	16.6	17.5	19.0	20.4	20.6	22.5	22.6	25.3	24.1	27.3	25.7	29.3	26
546	70.01	140.02	17.2	18.2	19.9	21.4	21.7	23.8	24.1	26.9	25.8	29.3	27.6	31.6	29
548	70.68	139.98	17.1	17.9	19.5	21.0	21.2	23.2	23.4	26.0	25.1	28.2	26.7	30.3	30
574	70.35	141.00	16.9	17.8	19.5	21.1	21.4	23.5	23.7	26.6	25.5	28.9	27.2	31.2	29
576	71.02	141.00	17.1	18.0	19.7	21.3	21.5	23.6	23.8	26.7	25.6	29.0	27.3	31.2	29
578	71.69	141.00	15.9	16.7	18.1	19.4	19.6	21.3	21.5	23.9	23.0	25.8	24.4	27.7	29
630	71.01	143.07	15.9	16.8	18.6	20.2	20.4	22.6	22.9	25.8	24.7	28.2	26.5	30.6	29
655	70.33	143.99	14.9	15.9	17.8	19.6	19.9	22.2	22.5	25.7	24.5	28.3	26.5	30.9	30
764	70.55	148.08	12.9	13.8	15.3	16.9	17.0	19.1	19.2	22.0	20.8	24.1	22.4	26.3	26

Table 8.2 Summary of Extremal Analysis Results At 51 Grid Points

Significant Wave Height - Real Ice Edge

SUMMARY OF EXTREMAL ANALYSIS RESULTS AT ALL GRID POINTS IN STUDY AREA

SIGNIFICANT WAVE HEIGHT

A) REAL ICE EDGE

risk factor / return period			.50 / 2 yr		0.20 / 5 yr		0.10 / 10 yr		0.04 / 25 yr		0.02 / 50 yr		0.01 / 100 yr		
grid point	Lat (N)	Long (W)	Best Fit (m)	90% U.L. (m)	Best Fit (m)	90% U.L. (m)	Best Fit (m)	90% U.L. (m)	Best Fit (m)	90% U.L. (m)	Best Fit (m)	90% U.L. (m)	Best Fit (m)	90% U.L. (m)	NUM PTS
198	70.47	126.82	3.1	3.3	3.5	3.8	3.8	4.2	4.2	4.6	4.4	5.0	4.7	5.4	24
200	71.12	126.34	3.2	3.4	3.7	4.0	4.0	4.4	4.4	5.0	4.7	5.4	5.1	5.8	25
226	70.87	127.57	3.4	3.6	3.9	4.2	4.2	4.6	4.6	5.2	4.9	5.6	5.2	6.0	25
252	70.61	128.78	2.8	2.9	3.2	3.5	3.5	3.9	3.9	4.4	4.2	4.7	4.4	5.1	28
254	71.27	128.36	3.3	3.5	3.7	4.0	4.0	4.3	4.3	4.8	4.5	5.1	4.8	5.4	21
278	70.35	129.96	2.5	2.6	2.9	3.2	3.2	3.6	3.6	4.1	3.9	4.5	4.2	4.9	26
280	71.01	129.58	3.4	3.5	3.8	4.0	4.0	4.3	4.3	4.8	4.6	5.1	4.8	5.4	22
306	70.74	130.77	3.3	3.5	3.8	4.0	4.0	4.4	4.4	4.9	4.7	5.2	4.9	5.6	24
309	71.73	130.23	3.0	3.1	3.3	3.5	3.5	3.8	3.7	4.2	3.9	4.4	4.0	4.7	12
330	69.80	132.22	2.2	2.4	2.6	2.9	2.9	3.3	3.3	3.8	3.6	4.1	3.9	4.5	28
331	70.13	132.08	3.2	3.4	3.7	4.0	4.0	4.4	4.4	4.9	4.7	5.3	5.0	5.7	26
332	70.46	131.93	3.4	3.6	3.8	4.1	4.1	4.5	4.5	5.0	4.8	5.4	5.1	5.8	27
356	69.51	133.30	1.6	1.7	1.9	2.1	2.1	2.3	2.4	2.7	2.6	3.0	2.8	3.2	29
357	69.84	133.18	2.7	2.8	3.0	3.2	3.3	3.6	3.6	4.0	3.8	4.3	4.0	4.6	26
358	70.17	133.05	3.4	3.6	3.9	4.1	4.1	4.5	4.5	5.0	4.8	5.3	5.0	5.7	26
360	70.84	132.79	3.5	3.7	3.9	4.1	4.1	4.4	4.4	4.9	4.7	5.2	4.9	5.5	23
362	71.50	132.50	3.1	3.3	3.5	3.7	3.7	4.0	3.9	4.4	4.1	4.7	4.3	4.9	14
384	69.88	134.15	2.9	3.0	3.3	3.5	3.6	3.9	4.0	4.4	4.2	4.8	4.5	5.2	29
386	70.55	133.92	3.5	3.7	3.9	4.2	4.2	4.6	4.6	5.1	4.9	5.4	5.1	5.8	25
410	69.58	135.21	1.9	2.0	2.2	2.4	2.4	2.6	2.7	3.0	2.9	3.3	3.1	3.5	29
411	69.92	135.12	3.2	3.3	3.6	3.9	3.9	4.3	4.3	4.8	4.7	5.2	5.0	5.7	30
412	70.25	135.03	3.5	3.7	3.9	4.2	4.2	4.6	4.6	5.0	4.8	5.4	5.1	5.7	25
413	70.59	134.93	3.5	3.7	4.0	4.2	4.2	4.6	4.6	5.1	4.9	5.4	5.1	5.8	25
414	70.92	134.82	3.5	3.6	3.9	4.1	4.1	4.5	4.4	4.9	4.7	5.2	4.9	5.5	20
417	71.92	134.49	2.2	2.4	2.7	3.0	2.9	3.4	3.3	3.9	3.6	4.3	3.8	4.7	14
435	68.94	136.32	1.2	1.3	1.4	1.5	1.5	1.7	1.7	1.9	1.8	2.1	1.9	2.2	27
436	69.28	136.25	1.9	2.1	2.3	2.6	2.6	2.9	3.0	3.4	3.2	3.8	3.5	4.1	29
437	69.61	136.17	2.7	2.9	3.2	3.5	3.6	4.0	4.1	4.6	4.4	5.1	4.7	5.5	29
438	69.95	136.10	3.3	3.5	3.8	4.1	4.2	4.5	4.6	5.1	4.9	5.5	5.2	5.9	29
440	70.62	135.93	3.5	3.6	3.9	4.2	4.2	4.6	4.6	5.1	4.9	5.5	5.2	5.9	26
463	69.30	137.20	2.8	3.0	3.3	3.5	3.6	3.9	4.0	4.4	4.2	4.8	4.5	5.2	28
464	69.64	137.14	3.2	3.4	3.7	4.0	4.0	4.4	4.5	5.0	4.8	5.5	5.2	5.9	29
465	69.97	137.07	3.4	3.6	3.9	4.2	4.3	4.7	4.7	5.2	5.0	5.7	5.4	6.1	29
468	70.98	136.87	3.4	3.6	4.0	4.3	4.3	4.8	4.8	5.5	5.2	6.0	5.5	6.4	24
470	71.65	136.73	2.7	2.8	3.0	3.2	3.2	3.4	3.4	3.7	3.5	3.9	3.6	4.1	13
490	69.32	138.15	2.5	2.7	2.9	3.1	3.2	3.5	3.5	3.9	3.7	4.2	4.0	4.6	26
491	69.65	138.10	3.4	3.6	3.9	4.2	4.2	4.7	4.7	5.3	5.0	5.7	5.4	6.2	26
492	69.99	138.05	3.5	3.7	4.1	4.4	4.5	4.9	5.0	5.6	5.3	6.1	5.7	6.6	27
493	70.33	138.01	3.5	3.7	4.1	4.4	4.5	4.9	5.0	5.6	5.3	6.1	5.7	6.6	25
494	70.66	137.96	3.5	3.6	3.9	4.2	4.2	4.5	4.5	5.0	4.8	5.4	5.0	5.7	21
522	71.01	138.93	3.0	3.2	3.5	3.8	3.8	4.2	4.2	4.8	4.5	5.2	4.8	5.6	20
525	72.02	138.82	2.4	2.6	2.8	3.1	3.0	3.4	3.2	3.7	3.4	4.0	3.6	4.3	12
545	69.68	140.03	3.0	3.2	3.4	3.7	3.7	4.1	4.1	4.6	4.3	4.9	4.6	5.3	21
546	70.01	140.02	3.3	3.5	3.8	4.2	4.2	4.6	4.6	5.2	4.9	5.7	5.2	6.1	20
548	70.68	139.98	3.1	3.3	3.6	4.0	4.0	4.5	4.5	5.1	4.8	5.6	5.2	6.1	22
574	70.35	141.00	3.3	3.5	3.8	4.2	4.2	4.7	4.6	5.3	5.0	5.8	5.3	6.3	19
576	71.02	141.00	2.8	3.0	3.3	3.6	3.6	4.0	4.0	4.6	4.3	5.0	4.5	5.3	19
578	71.69	141.00	2.5	2.7	3.0	3.3	3.3	3.7	3.6	4.3	3.9	4.7	4.2	5.1	15
630	71.01	143.07	2.9	3.1	3.4	3.8	3.8	4.3	4.2	4.9	4.5	5.3	4.8	5.8	15
655	70.33	143.99	2.4	2.7	3.1	3.5	3.5	4.1	4.1	4.9	4.5	5.4	4.9	6.0	22
764	70.55	148.08	1.7	1.9	2.1	2.4	2.4	2.9	2.8	3.4	3.1	3.8	3.4	4.2	21

Table 8.3 Summary of Extremal Analysis Results At 51 Grid Points

Significant Wave Height - 98% Ice Edge

B) 98% FREQUENCY OF OCCURRENCE ICE EDGE

risk factor / return period			.50 / 2 yr		0.20 / 5 yr		0.10 / 10 yr		0.04 / 25 yr		0.02 / 50 yr		0.01 / 100 yr		
grid point	Lat (N)	Long (W)	Best Fit (m)	90% U.L. (m)	Best Fit (m)	90% U.L. (m)	Best Fit (m)	90% U.L. (m)	Best Fit (m)	90% U.L. (m)	Best Fit (m)	90% U.L. (m)	Best Fit (m)	90% U.L. (m)	NUM PTS
198	70.47	126.82	3.4	3.6	3.9	4.3	4.3	4.8	4.8	5.4	5.1	5.9	5.5	6.4	25
200	71.12	126.34	3.6	3.9	4.3	4.8	4.8	5.4	5.5	6.3	6.0	6.9	6.4	7.6	27
226	70.87	127.57	3.7	4.0	4.4	4.8	4.9	5.5	5.5	6.3	5.9	6.9	6.4	7.5	27
252	70.61	128.78	3.2	3.4	3.8	4.1	4.1	4.6	4.6	5.3	5.0	5.8	5.4	6.3	27
254	71.27	128.36	3.8	4.0	4.5	4.9	5.0	5.5	5.6	6.3	6.0	6.9	6.5	7.5	27
278	70.35	129.96	2.8	3.0	3.4	3.8	3.8	4.3	4.4	5.1	4.8	5.6	5.2	6.1	28
280	71.01	129.58	3.8	4.0	4.4	4.8	4.9	5.4	5.4	6.1	5.8	6.6	6.2	7.2	27
306	70.74	130.77	3.8	4.1	4.5	4.9	4.9	5.4	5.5	6.2	5.9	6.8	6.3	7.3	27
309	71.73	130.23	3.7	4.0	4.3	4.7	4.8	5.2	5.3	6.0	5.7	6.5	6.1	7.0	27
330	69.80	132.22	2.4	2.6	3.0	3.3	3.3	3.7	3.8	4.3	4.1	4.8	4.5	5.2	30
331	70.13	132.08	3.7	3.9	4.3	4.7	4.7	5.2	5.2	6.0	5.6	6.5	6.0	7.0	24
332	70.46	131.93	3.9	4.1	4.5	4.9	5.0	5.5	5.5	6.3	6.0	6.8	6.4	7.4	27
356	69.51	133.30	1.7	1.8	2.1	2.3	2.3	2.6	2.6	3.0	2.8	3.3	3.1	3.6	28
357	69.84	133.18	2.9	3.1	3.3	3.6	3.6	3.9	3.9	4.4	4.2	4.7	4.4	5.1	24
358	70.17	133.05	3.9	4.1	4.5	4.8	4.9	5.4	5.4	6.1	5.8	6.6	6.2	7.1	26
360	70.84	132.79	4.1	4.3	4.7	5.1	5.1	5.7	5.7	6.4	6.1	6.9	6.5	7.5	27
362	71.50	132.50	3.9	4.1	4.4	4.8	4.8	5.3	5.3	6.0	5.7	6.5	6.1	6.9	27
384	69.88	134.15	3.2	3.4	3.7	4.0	4.0	4.5	4.5	5.1	4.8	5.6	5.2	6.0	25
386	70.55	133.92	4.0	4.3	4.7	5.1	5.2	5.7	5.7	6.5	6.2	7.1	6.6	7.6	29
410	69.58	135.21	2.0	2.1	2.3	2.5	2.6	2.8	2.9	3.2	3.1	3.5	3.3	3.8	29
411	69.92	135.12	3.5	3.7	4.1	4.5	4.5	5.1	5.1	5.8	5.5	6.3	5.9	6.8	28
412	70.25	135.03	4.0	4.2	4.6	5.0	5.0	5.5	5.5	6.2	5.9	6.7	6.3	7.2	27
413	70.59	134.93	4.1	4.3	4.7	5.1	5.1	5.6	5.7	6.4	6.1	6.9	6.5	7.5	29
414	70.92	134.82	4.1	4.3	4.7	5.1	5.2	5.7	5.8	6.5	6.2	7.1	6.6	7.6	29
417	71.92	134.49	3.4	3.6	4.0	4.5	4.5	5.1	5.2	5.9	5.6	6.5	6.1	7.1	30
435	68.94	136.32	1.3	1.3	1.4	1.5	1.5	1.6	1.6	1.8	1.7	2.0	1.8	2.1	24
436	69.28	136.25	2.0	2.1	2.4	2.7	2.7	3.0	3.1	3.5	3.4	3.9	3.6	4.3	30
437	69.61	136.17	3.0	3.2	3.6	3.9	4.0	4.4	4.5	5.1	4.9	5.7	5.3	6.2	28
438	69.95	136.10	3.7	3.9	4.2	4.5	4.6	5.1	5.1	5.7	5.5	6.2	5.8	6.7	29
440	70.62	135.93	4.1	4.3	4.7	5.0	5.1	5.6	5.7	6.3	6.1	6.9	6.5	7.4	30
463	69.30	137.20	3.1	3.2	3.5	3.8	3.8	4.2	4.2	4.7	4.5	5.1	4.8	5.5	27
464	69.64	137.14	3.5	3.7	4.0	4.4	4.4	4.9	4.9	5.5	5.3	6.0	5.6	6.5	28
465	69.97	137.07	3.8	4.0	4.3	4.7	4.7	5.2	5.2	5.8	5.6	6.3	6.0	6.8	30
468	70.98	136.87	4.0	4.1	4.5	4.8	4.9	5.3	5.3	5.9	5.7	6.4	6.0	6.8	29
470	71.65	136.73	3.5	3.7	4.1	4.4	4.5	5.0	5.1	5.7	5.5	6.3	5.9	6.8	30
490	69.32	138.15	2.8	2.9	3.1	3.3	3.3	3.6	3.6	4.0	3.8	4.3	4.1	4.6	22
491	69.65	138.10	3.7	3.9	4.2	4.6	4.6	5.0	5.0	5.6	5.4	6.1	5.7	6.5	26
492	69.99	138.05	3.9	4.1	4.5	4.8	4.9	5.4	5.4	6.0	5.8	6.6	6.2	7.1	29
493	70.33	138.01	4.0	4.2	4.5	4.9	4.9	5.3	5.4	6.0	5.8	6.5	6.1	7.0	29
494	70.66	137.96	3.8	4.0	4.3	4.6	4.6	5.0	5.1	5.6	5.4	6.0	5.7	6.4	29
522	71.01	138.93	3.6	3.8	4.1	4.5	4.5	5.0	5.0	5.7	5.4	6.2	5.8	6.7	29
525	72.02	138.82	3.2	3.4	3.7	4.1	4.1	4.5	4.5	5.1	4.9	5.5	5.2	6.0	28
545	69.68	140.03	3.3	3.4	3.7	3.9	3.9	4.3	4.3	4.7	4.5	5.1	4.8	5.4	25
546	70.01	140.02	3.6	3.8	4.1	4.4	4.5	4.9	4.9	5.5	5.2	5.9	5.6	6.3	27
548	70.68	139.98	3.6	3.8	4.2	4.6	4.7	5.2	5.2	5.9	5.6	6.4	6.0	7.0	29
574	70.35	141.00	3.6	3.8	4.2	4.6	4.6	5.1	5.1	5.7	5.5	6.2	5.8	6.7	28
576	71.02	141.00	3.3	3.5	3.8	4.1	4.2	4.6	4.6	5.2	5.0	5.6	5.3	6.1	28
578	71.69	141.00	3.2	3.4	3.8	4.1	4.1	4.5	4.6	5.1	4.9	5.6	5.3	6.1	28
630	71.01	143.07	3.4	3.6	3.9	4.3	4.3	4.8	4.8	5.4	5.1	5.9	5.4	6.4	22
655	70.33	143.99	2.9	3.1	3.4	3.7	3.7	4.1	4.1	4.6	4.3	5.0	4.6	5.4	22
764	70.55	148.08	1.9	2.1	2.4	2.7	2.7	3.1	3.1	3.6	3.4	4.0	3.7	4.4	29

Table 8.4 Summary of Extremal Analysis Results At 51 Grid Points

Significant Wave Height - 50% Ice Edge

C) 50% FREQUENCY OF OCCURRENCE ICE EDGE

risk factor / return period			.50 2 yr		0.20 5 yr		0.10 10 yr		0.04 25 yr		0.02 50 yr		0.01 100 yr		
grid point	Lat (N)	Long (W)	Best Fit (m)	90% U.L. (m)	Best Fit (m)	90% U.L. (m)	Best Fit (m)	90% U.L. (m)	Best Fit (m)	90% U.L. (m)	Best Fit (m)	90% U.L. (m)	Best Fit (m)	90% U.L. (m)	NUM PTS
198	70.47	126.82	3.0	3.1	3.4	3.6	3.6	3.9	3.9	4.4	4.2	4.7	4.4	5.0	23
200	71.12	126.34	2.9	3.1	3.4	3.8	3.8	4.2	4.2	4.8	4.6	5.3	4.9	5.7	23
226	70.87	127.57	3.2	3.3	3.6	3.9	4.0	4.4	4.4	4.9	4.7	5.4	5.0	5.8	25
252	70.61	128.78	2.7	2.8	3.1	3.3	3.3	3.6	3.6	4.1	3.9	4.4	4.1	4.7	27
254	71.27	128.36	2.9	3.1	3.4	3.8	3.8	4.3	4.2	4.9	4.6	5.4	4.9	5.8	22
278	70.35	129.96	2.4	2.6	2.9	3.2	3.2	3.6	3.6	4.2	3.9	4.6	4.3	5.0	28
280	71.01	129.58	3.1	3.3	3.6	3.8	3.9	4.2	4.3	4.8	4.5	5.2	4.8	5.6	25
306	70.74	130.77	3.2	3.3	3.7	4.0	4.0	4.4	4.4	5.0	4.8	5.4	5.1	5.9	28
330	69.80	132.22	2.2	2.4	2.7	2.9	3.0	3.3	3.3	3.8	3.6	4.2	3.9	4.6	26
331	70.13	132.08	3.1	3.3	3.7	4.0	4.0	4.5	4.5	5.1	4.9	5.5	5.2	6.0	28
332	70.46	131.93	3.3	3.5	3.8	4.1	4.1	4.5	4.6	5.1	4.9	5.5	5.2	6.0	28
356	69.51	133.30	1.6	1.7	1.9	2.1	2.1	2.4	2.4	2.8	2.6	3.0	2.8	3.3	27
357	69.84	133.18	2.6	2.8	3.0	3.2	3.2	3.6	3.6	4.0	3.8	4.3	4.1	4.7	25
358	70.17	133.05	3.3	3.5	3.8	4.1	4.2	4.6	4.6	5.2	4.9	5.6	5.3	6.0	28
360	70.84	132.79	3.2	3.4	3.8	4.1	4.2	4.6	4.6	5.2	5.0	5.7	5.3	6.2	27
384	69.88	134.15	2.7	2.9	3.2	3.5	3.5	3.9	3.9	4.4	4.2	4.8	4.5	5.3	29
386	70.55	133.92	3.3	3.5	3.9	4.2	4.2	4.7	4.7	5.3	5.1	5.8	5.4	6.2	28
410	69.58	135.21	1.8	1.9	2.1	2.3	2.3	2.6	2.6	3.0	2.8	3.2	3.0	3.5	27
411	69.92	135.12	3.0	3.2	3.5	3.8	3.8	4.2	4.3	4.8	4.6	5.2	4.9	5.6	29
412	70.25	135.03	3.4	3.6	3.9	4.2	4.2	4.6	4.7	5.2	5.0	5.7	5.4	6.1	29
413	70.59	134.93	3.3	3.5	3.9	4.2	4.2	4.7	4.7	5.3	5.1	5.8	5.4	6.2	28
414	70.92	134.82	3.1	3.3	3.7	4.1	4.1	4.7	4.7	5.4	5.1	6.0	5.5	6.5	24
435	68.94	136.32	1.2	1.3	1.4	1.5	1.5	1.7	1.7	1.9	1.8	2.1	2.0	2.3	25
436	69.28	136.25	1.9	2.1	2.3	2.6	2.6	2.9	3.0	3.4	3.2	3.8	3.5	4.1	27
437	69.61	136.17	2.6	2.8	3.1	3.4	3.5	3.9	3.9	4.5	4.2	4.9	4.6	5.4	27
438	69.95	136.10	3.2	3.3	3.6	3.9	3.9	4.3	4.4	4.9	4.7	5.3	5.0	5.7	29
440	70.62	135.93	3.3	3.5	3.8	4.2	4.2	4.7	4.7	5.4	5.1	5.9	5.5	6.4	28
463	69.30	137.20	2.7	2.9	3.2	3.4	3.5	3.9	3.9	4.4	4.2	4.8	4.5	5.2	27
464	69.64	137.14	3.0	3.2	3.6	3.9	3.9	4.3	4.4	4.9	4.7	5.4	5.0	5.8	27
465	69.97	137.07	3.2	3.4	3.7	4.1	4.1	4.5	4.6	5.1	4.9	5.6	5.2	6.0	28
468	70.98	136.87	2.8	3.1	3.4	3.8	3.8	4.3	4.3	5.0	4.6	5.5	5.0	6.0	22
490	69.32	138.15	2.4	2.5	2.8	3.0	3.0	3.3	3.3	3.8	3.6	4.1	3.8	4.4	25
491	69.65	138.10	3.1	3.3	3.7	4.1	4.1	4.6	4.6	5.3	5.0	5.8	5.4	6.3	27
492	69.99	138.05	3.3	3.5	3.9	4.2	4.3	4.7	4.8	5.4	5.1	5.9	5.5	6.4	28
493	70.33	138.01	3.3	3.5	3.9	4.2	4.3	4.7	4.8	5.4	5.2	5.9	5.5	6.4	27
494	70.66	137.96	3.1	3.3	3.6	3.9	3.9	4.4	4.4	5.0	4.7	5.4	5.0	5.9	24
522	71.01	138.93	1.6	1.9	2.4	2.9	2.8	3.5	3.3	4.2	3.6	4.8	4.0	5.3	11
545	69.68	140.03	2.7	2.9	3.2	3.5	3.5	3.9	3.9	4.5	4.2	4.9	4.5	5.3	21
546	70.01	140.02	3.0	3.2	3.5	3.9	4.0	4.5	4.5	5.2	4.9	5.7	5.3	6.2	25
548	70.68	139.98	2.4	2.7	3.0	3.5	3.4	4.0	3.9	4.7	4.3	5.2	4.7	5.8	17
574	70.35	141.00	2.6	2.9	3.4	3.9	3.9	4.6	4.5	5.5	5.0	6.1	5.5	6.8	21

Table 8.5 Summary of Extremal Analysis Results At 51 Grid Points

Significant Wave Height - 30% Ice Edge

D) 30% FREQUENCY OF OCCURRENCE ICE EDGE

risk factor / return period			.50 / 2 yr		0.20 / 5 yr		0.10 / 10 yr		0.04 / 25 yr		0.02 / 50 yr		0.01 / 100 yr		
grid point	Lat (N)	Long (W)	Best Fit (m)	90% U.L. (m)	Best Fit (m)	90% U.L. (m)	Best Fit (m)	90% U.L. (m)	Best Fit (m)	90% U.L. (m)	Best Fit (m)	90% U.L. (m)	Best Fit (m)	90% U.L. (m)	NUM PTS
198	70.47	126.82	2.6	2.7	2.9	3.1	3.0	3.3	3.3	3.6	3.4	3.9	3.6	4.1	16
226	70.87	127.57	2.0	2.2	2.5	2.9	2.8	3.2	3.1	3.7	3.3	4.0	3.5	4.4	11
252	70.61	128.78	2.2	2.3	2.5	2.7	2.7	2.9	2.9	3.2	3.1	3.5	3.2	3.7	20
278	70.35	129.96	2.1	2.2	2.4	2.7	2.7	3.0	3.0	3.5	3.2	3.8	3.5	4.1	21
306	70.74	130.77	2.3	2.5	2.7	2.9	2.9	3.2	3.1	3.6	3.3	3.9	3.5	4.1	15
330	69.80	132.22	2.1	2.2	2.4	2.6	2.6	3.0	2.9	3.4	3.1	3.7	3.4	4.0	20
331	70.13	132.08	2.7	2.8	3.1	3.4	3.4	3.8	3.7	4.2	4.0	4.6	4.3	5.0	21
332	70.46	131.93	2.6	2.7	2.9	3.2	3.2	3.6	3.5	4.0	3.8	4.3	4.0	4.7	21
356	69.51	133.30	1.5	1.6	1.8	1.9	2.0	2.2	2.2	2.5	2.4	2.8	2.5	3.0	23
357	69.84	133.18	2.3	2.4	2.7	2.9	2.9	3.2	3.2	3.7	3.5	4.0	3.7	4.3	23
358	70.17	133.05	2.8	2.9	3.2	3.5	3.5	3.8	3.8	4.3	4.1	4.7	4.3	5.0	21
384	69.88	134.15	2.3	2.5	2.7	3.0	3.0	3.4	3.4	3.9	3.6	4.2	3.9	4.6	22
386	70.55	133.92	2.0	2.2	2.5	2.9	2.8	3.3	3.1	3.8	3.3	4.1	3.6	4.5	11
410	69.58	135.21	1.6	1.7	1.9	2.1	2.1	2.4	2.4	2.8	2.6	3.1	2.8	3.4	23
411	69.92	135.12	2.6	2.7	3.0	3.2	3.3	3.6	3.6	4.1	3.9	4.4	4.1	4.8	22
412	70.25	135.03	2.6	2.7	3.0	3.2	3.2	3.6	3.5	4.0	3.8	4.4	4.0	4.7	21
435	68.94	136.32	1.1	1.2	1.4	1.5	1.5	1.7	1.7	1.9	1.8	2.1	2.0	2.3	22
436	69.28	136.25	1.8	1.9	2.2	2.4	2.4	2.7	2.7	3.2	3.0	3.5	3.2	3.9	23
437	69.61	136.17	2.2	2.3	2.6	2.9	3.0	3.4	3.4	3.9	3.7	4.3	4.0	4.8	22
438	69.95	136.10	2.6	2.8	3.0	3.3	3.3	3.6	3.6	4.1	3.9	4.5	4.1	4.8	22
463	69.30	137.20	2.3	2.5	2.7	3.0	3.0	3.4	3.3	3.8	3.6	4.2	3.9	4.5	23
464	69.64	137.14	2.5	2.7	3.0	3.3	3.3	3.7	3.7	4.2	4.0	4.6	4.2	5.0	21
465	69.97	137.07	2.5	2.7	2.9	3.2	3.2	3.6	3.5	4.0	3.8	4.4	4.0	4.7	21
490	69.32	138.15	2.0	2.1	2.3	2.5	2.5	2.8	2.7	3.1	2.9	3.3	3.1	3.6	18
491	69.65	138.10	2.5	2.7	3.0	3.3	3.3	3.7	3.7	4.2	4.0	4.7	4.3	5.1	22
492	69.99	138.05	2.2	2.3	2.6	2.8	2.8	3.2	3.1	3.6	3.4	4.0	3.6	4.3	19

Table 8.6 Summary of Extremal Analysis Results At 51 Grid Points

Significant Wave Height - Joint Probability (Combined Ice Edge)

E) JOINT PROBABILITY (98% + 50% + 30% FREQUENCY OF OCCURRENCE ICE EDGE)

risk factor / return period			0.20 / 5 yr		0.10 / 10 yr		0.04 / 25 yr		0.02 / 50 yr		0.01 / 100 yr		
grid point	Lat (N)	Long (W)	Best Fit (m)	90% U.L. (m)	Best Fit (m)	90% U.L. (m)	Best Fit (m)	90% U.L. (m)	Best Fit (m)	90% U.L. (m)	Best Fit (m)	90% U.L. (m)	NUM PTS
198	70.47	126.82	3.5	3.7	4.0	4.3	4.5	5.0	5.0	5.5	5.4	6.0	80
200	71.12	126.34	3.7	4.0	4.2	4.6	4.9	5.5	5.5	6.1	6.0	6.8	66
226	70.87	127.57	3.8	4.1	4.4	4.8	5.1	5.6	5.6	6.2	6.1	6.8	70
252	70.61	128.78	3.3	3.5	3.7	3.9	4.2	4.5	4.6	5.0	4.9	5.5	81
254	71.27	128.36	3.8	4.1	4.4	4.8	5.1	5.7	5.7	6.4	6.2	7.1	55
278	70.35	129.96	3.0	3.2	3.4	3.6	3.9	4.2	4.3	4.7	4.6	5.1	81
280	71.01	129.58	3.8	4.1	4.4	4.8	5.0	5.6	5.5	6.2	6.0	6.8	59
306	70.74	130.77	3.9	4.1	4.4	4.7	5.1	5.5	5.5	6.1	6.0	6.7	77
309	71.73	130.23	3.5	3.9	4.1	4.7	4.9	5.7	5.4	6.4	5.9	7.1	30
330	69.80	132.22	2.7	2.9	3.0	3.2	3.4	3.7	3.7	4.1	4.0	4.4	80
331	70.13	132.08	3.8	4.0	4.2	4.5	4.8	5.2	5.2	5.7	5.7	6.2	81
332	70.46	131.93	4.0	4.2	4.5	4.8	5.1	5.5	5.5	6.1	6.0	6.6	81
356	69.51	133.30	1.9	2.0	2.1	2.3	2.4	2.6	2.6	2.9	2.8	3.1	80
357	69.84	133.18	3.1	3.2	3.4	3.6	3.7	4.0	4.0	4.4	4.3	4.7	80
358	70.17	133.05	4.0	4.2	4.4	4.7	5.0	5.4	5.4	5.8	5.8	6.3	81
360	70.84	132.79	4.1	4.4	4.6	5.0	5.3	5.8	5.7	6.4	6.2	7.0	58
362	71.50	132.50	3.6	4.1	4.2	4.8	4.9	5.7	5.4	6.4	5.9	7.0	30
384	69.88	134.15	3.3	3.5	3.7	3.9	4.1	4.5	4.5	4.9	4.8	5.3	81
386	70.55	133.92	4.1	4.3	4.6	4.9	5.2	5.7	5.7	6.3	6.2	6.9	70
410	69.58	135.21	2.2	2.3	2.4	2.5	2.7	2.9	2.9	3.2	3.1	3.4	80
411	69.92	135.12	3.6	3.8	4.0	4.3	4.5	4.9	4.9	5.3	5.3	5.8	81
412	70.25	135.03	4.0	4.3	4.5	4.8	5.1	5.5	5.5	6.0	6.0	6.5	81
413	70.59	134.93	4.1	4.4	4.6	5.0	5.2	5.7	5.7	6.3	6.1	6.8	63
414	70.92	134.82	4.1	4.4	4.6	5.0	5.2	5.8	5.7	6.4	6.2	7.0	54
417	71.92	134.49	3.2	3.6	3.8	4.3	4.4	5.2	4.9	5.8	5.4	6.4	30
435	68.94	136.32	1.4	1.5	1.5	1.6	1.7	1.9	1.9	2.0	2.0	2.2	80
436	69.28	136.25	2.3	2.4	2.6	2.8	2.9	3.2	3.2	3.5	3.5	3.8	80
437	69.61	136.17	3.2	3.4	3.6	3.8	4.1	4.4	4.4	4.9	4.8	5.3	79
438	69.95	136.10	3.8	3.9	4.1	4.4	4.6	5.0	5.0	5.4	5.4	5.9	81
440	70.62	135.93	4.1	4.4	4.6	4.9	5.1	5.6	5.6	6.2	6.0	6.7	58
463	69.30	137.20	3.2	3.4	3.5	3.8	4.0	4.3	4.3	4.7	4.6	5.0	80
464	69.64	137.14	3.6	3.8	4.0	4.3	4.5	4.9	4.9	5.3	5.3	5.8	79
465	69.97	137.07	3.9	4.1	4.3	4.6	4.8	5.2	5.2	5.7	5.6	6.2	80
468	70.98	136.87	3.9	4.2	4.3	4.7	4.9	5.5	5.4	6.0	5.8	6.6	52
470	71.65	136.73	3.3	3.7	3.8	4.3	4.4	5.1	4.8	5.6	5.2	6.1	30
490	69.32	138.15	2.8	3.0	3.1	3.3	3.5	3.8	3.8	4.1	4.1	4.5	80
491	69.65	138.10	3.8	4.0	4.2	4.5	4.8	5.2	5.2	5.7	5.6	6.2	79
492	69.99	138.05	4.0	4.2	4.5	4.8	5.1	5.6	5.6	6.2	6.1	6.7	79
493	70.33	138.01	4.0	4.3	4.5	4.8	5.1	5.6	5.5	6.1	5.9	6.6	58
494	70.66	137.96	3.8	4.1	4.2	4.6	4.7	5.2	5.1	5.6	5.5	6.1	54
522	71.01	138.93	3.4	3.7	3.9	4.4	4.6	5.2	5.0	5.8	5.5	6.4	41
525	72.02	138.82	3.1	3.4	3.5	4.0	4.1	4.7	4.4	5.2	4.8	5.7	30
545	69.68	140.03	3.3	3.5	3.7	4.0	4.1	4.6	4.5	5.0	4.9	5.4	55
546	70.01	140.02	3.7	3.9	4.1	4.5	4.7	5.2	5.1	5.7	5.5	6.2	56
548	70.68	139.98	3.5	3.9	4.0	4.5	4.7	5.2	5.1	5.8	5.6	6.3	47
574	70.35	141.00	3.6	3.9	4.2	4.6	4.8	5.4	5.3	6.0	5.8	6.6	51
576	71.02	141.00	3.2	3.5	3.7	4.1	4.2	4.9	4.7	5.4	5.1	6.0	37
578	71.69	141.00	3.1	3.4	3.5	4.0	4.1	4.7	4.5	5.2	4.9	5.7	30
630	71.01	143.07	3.1	3.5	3.7	4.2	4.4	5.1	4.9	5.7	5.4	6.4	37
655	70.33	143.99	2.8	3.1	3.2	3.6	3.8	4.3	4.2	4.9	4.6	5.4	40
764	70.55	148.08	1.9	2.1	2.2	2.6	2.7	3.1	3.0	3.5	3.3	3.9	38

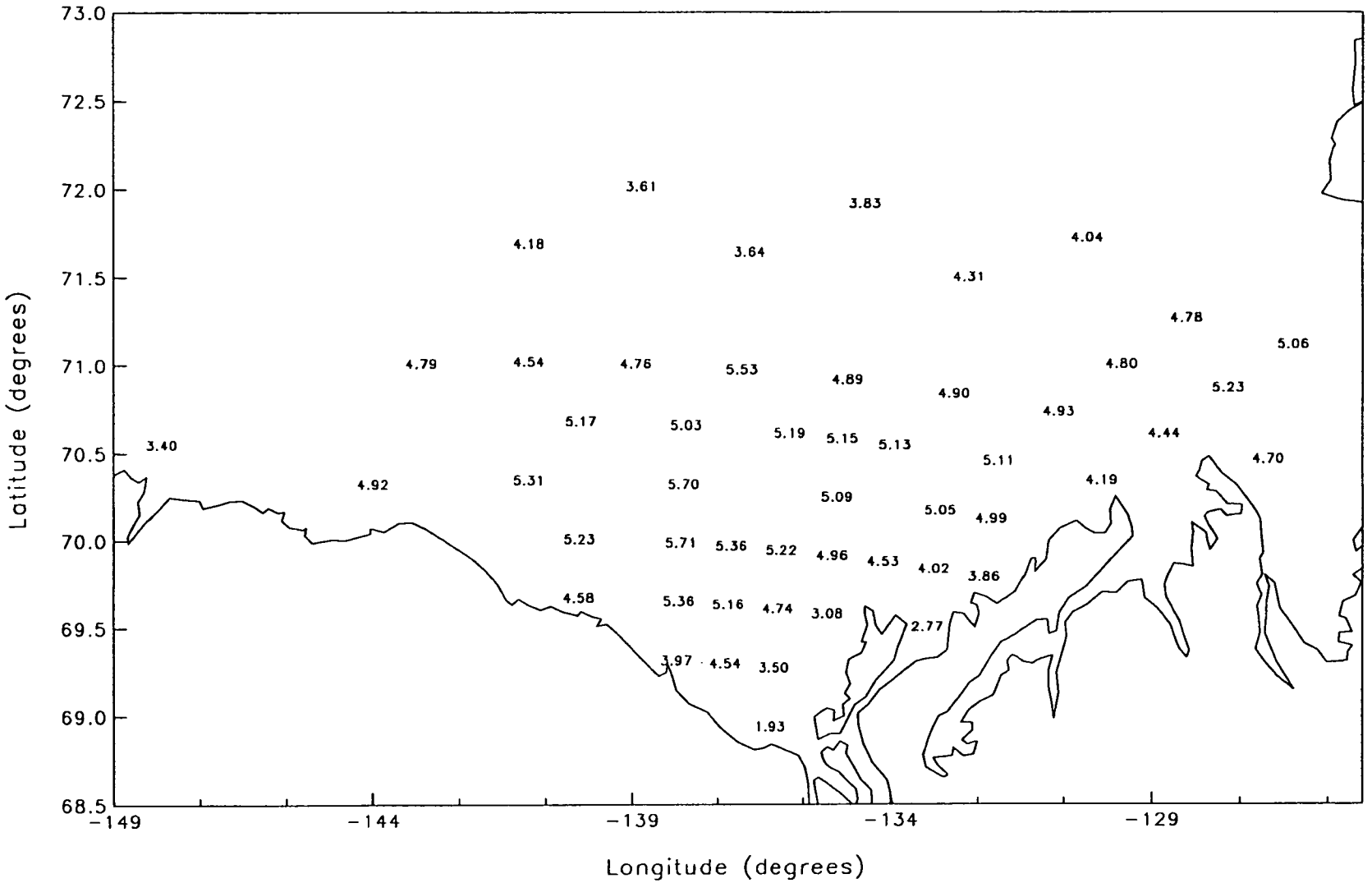

Figure 8.7 100-Year Significant Wave Height - Real Ice Edge

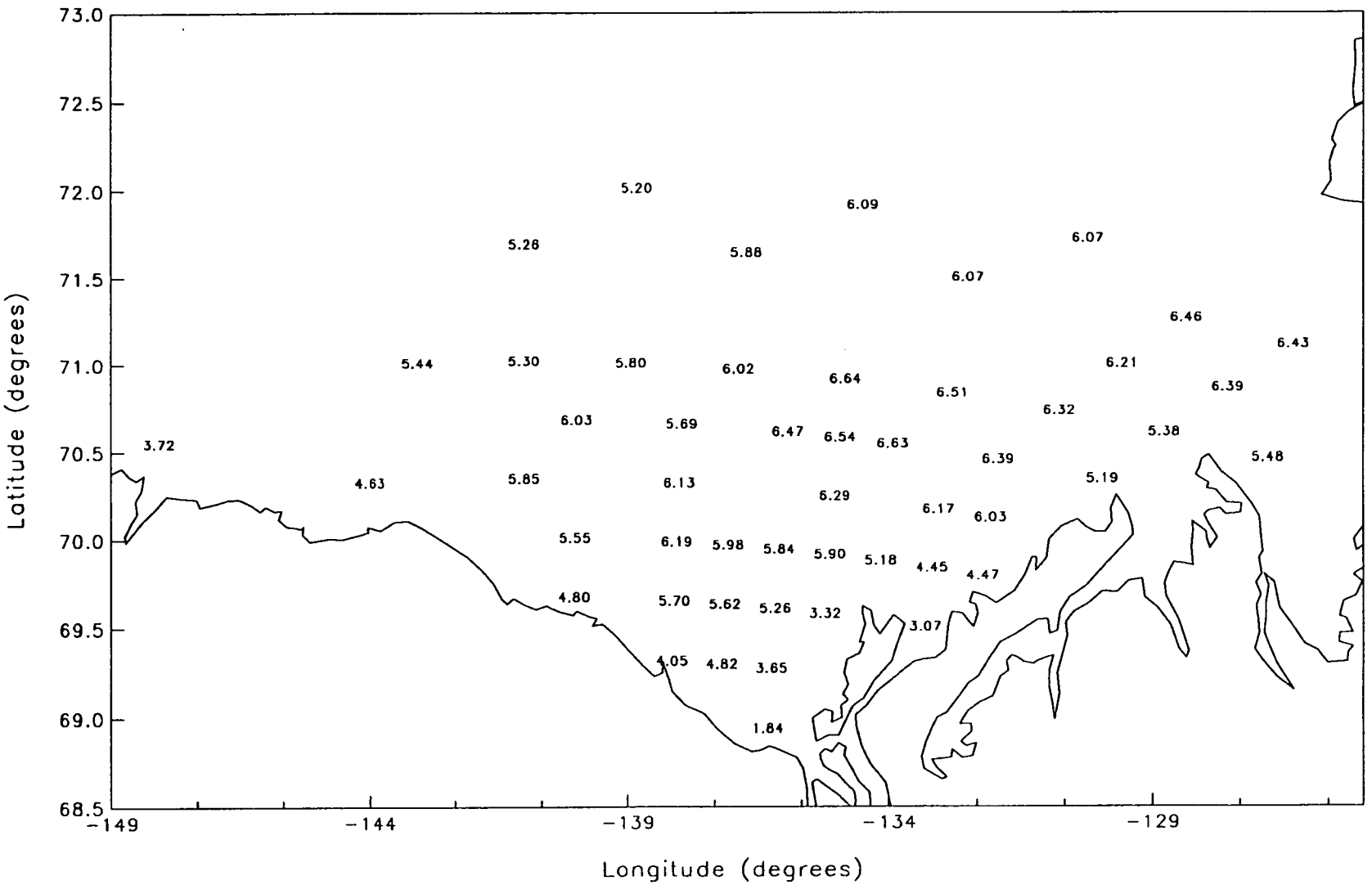

Figure 8.8 100-Year Significant Wave Height - 98% Ice Edge

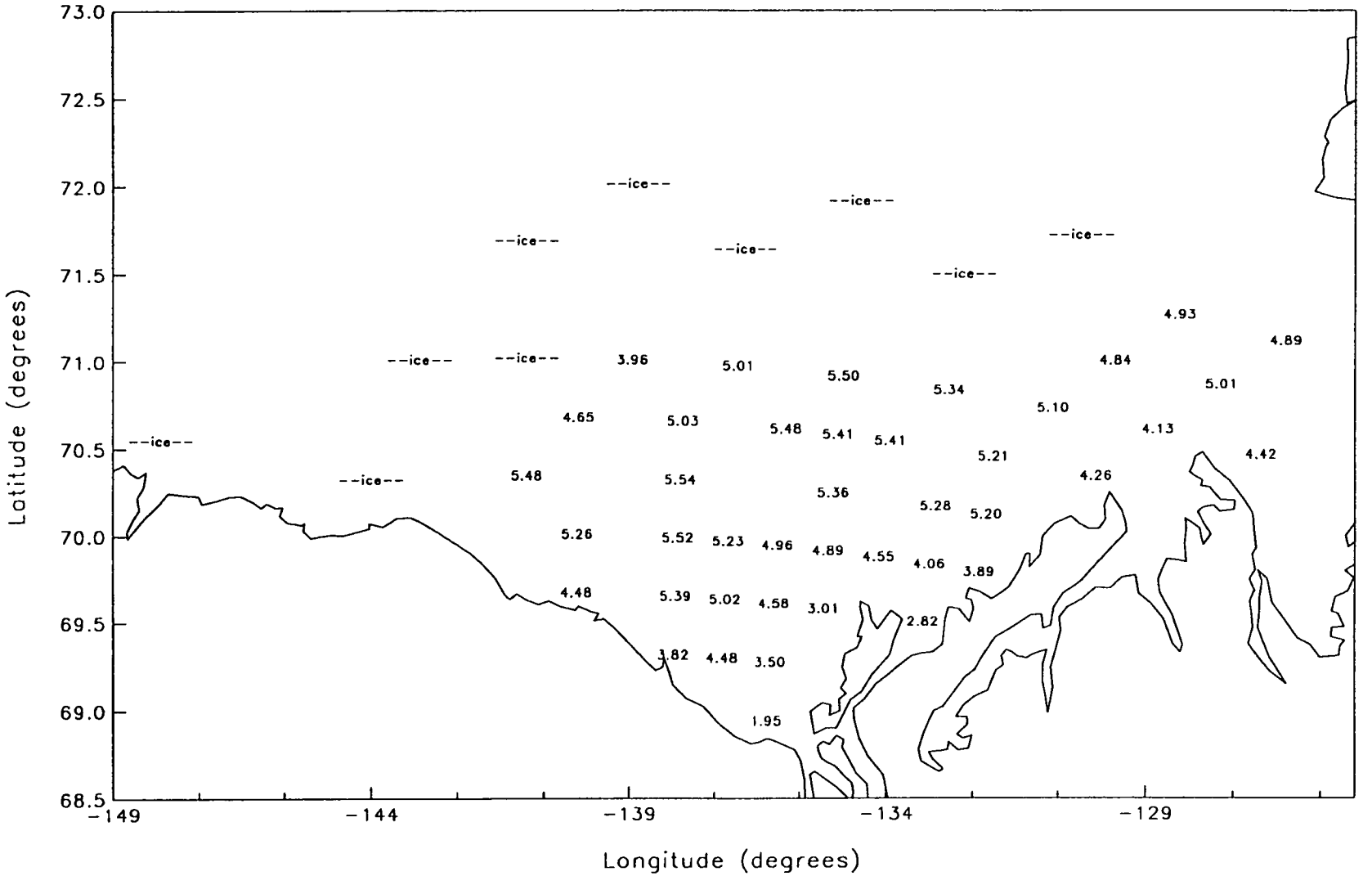

Figure 8.9 100-Year Significant Height - 50% Ice Edge

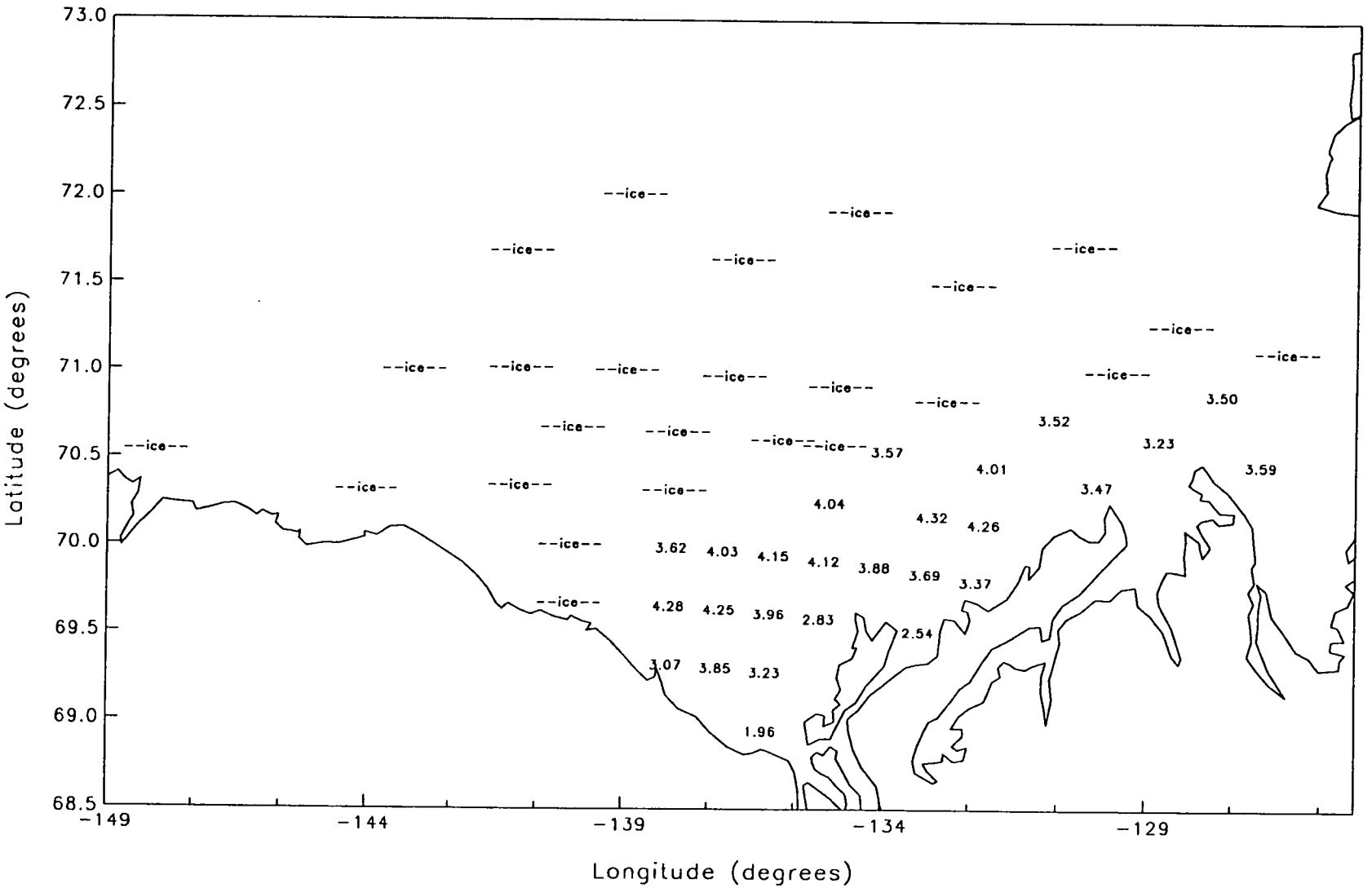

Figure 8.10 100-Year Significant Wave Height - 30% Ice Edge

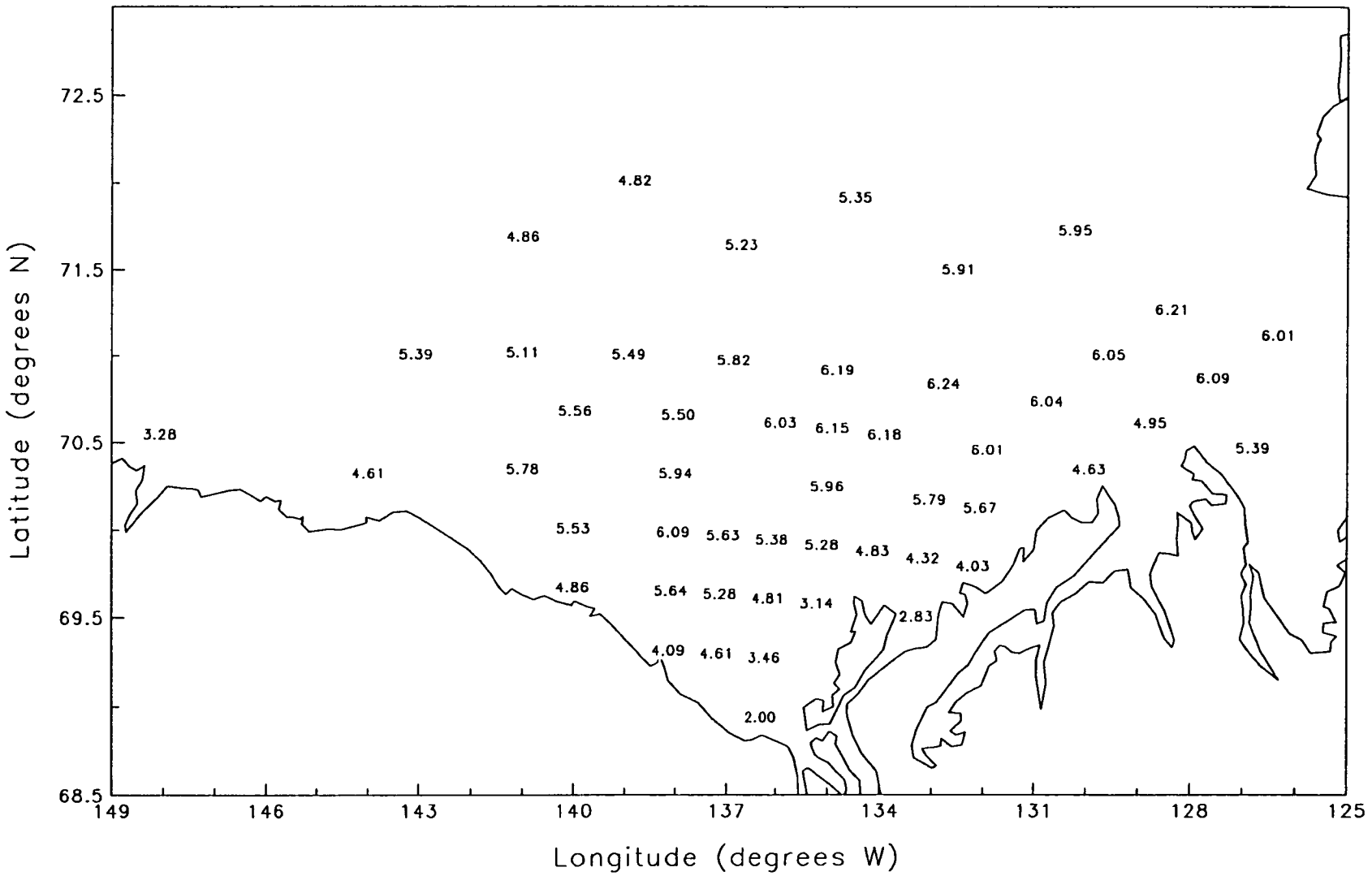

Figure 8.11 100-Year Significant Wave Height - Joint Probability

Table 8.7 Summary of 100 Year Significant Wave Height For Different Ice Edge Scenarios

Grid Point	Latitude (N)	Longitude (W)	Real edge	98% ice edge	50% ice edge	30% ice edge	Joint Probablilty
198	70.47	126.82	4.70	5.48	4.42	3.59	5.4
200	71.12	126.34	5.06	6.43	4.89	----	6.0
226	70.87	127.57	5.23	6.39	5.01	3.50	6.1
252	70.61	128.78	4.44	5.38	4.13	3.23	4.9
254	71.27	128.36	4.78	6.46	4.93	----	6.2
278	70.35	129.96	4.19	5.19	4.26	3.47	4.6
280	71.01	129.58	4.80	6.21	4.84	----	6.0
306	70.74	130.77	4.93	6.32	5.10	3.52	6.0
309	71.73	130.23	4.04	6.07	----	----	5.9
330	69.80	132.22	3.86	4.47	3.89	3.37	4.0
331	70.13	132.08	4.99	6.03	5.20	4.26	5.7
332	70.46	131.93	5.11	6.39	5.21	4.01	6.0
356	69.51	133.30	2.77	3.07	2.82	2.54	2.8
357	69.84	133.18	4.02	4.45	4.06	3.69	4.3
358	70.17	133.05	5.05	6.17	5.28	4.32	5.8
360	70.84	132.79	4.90	6.51	5.34	----	6.2
362	71.50	132.50	4.31	6.07	----	----	5.9
384	69.88	134.15	4.53	5.18	4.55	3.88	4.8
386	70.55	133.92	5.13	6.63	5.41	3.57	6.2
410	69.58	135.21	3.08	3.32	3.01	2.83	3.1
411	69.92	135.12	4.96	5.90	4.89	4.12	5.3
412	70.25	135.03	5.09	6.29	5.36	4.04	6.0
413	70.59	134.93	5.15	6.54	5.41	----	6.1
414	70.92	134.82	4.89	6.64	5.50	----	6.2
417	71.92	134.49	3.83	6.09	----	----	5.4
435	68.94	136.32	1.93	1.84	1.95	1.96	2.0
436	69.28	136.25	3.50	3.65	3.50	3.23	3.5
437	69.61	136.17	4.74	5.26	4.58	3.96	4.8
438	69.95	136.10	5.22	5.84	4.96	4.15	5.4
440	70.62	135.93	5.19	6.47	5.48	----	6.0
463	69.30	137.20	4.54	4.82	4.48	3.85	4.6
464	69.64	137.14	5.16	5.62	5.02	4.25	5.3
465	69.97	137.07	5.36	5.98	5.23	4.03	5.6
468	70.98	136.87	5.53	6.02	5.01	----	5.8
470	71.65	136.73	3.64	5.88	----	----	5.2
490	69.32	138.15	3.97	4.05	3.82	3.07	4.1
491	69.65	138.10	5.36	5.70	5.39	4.28	5.6
492	69.99	138.05	5.71	6.19	5.52	3.62	6.1
493	70.33	138.01	5.70	6.13	5.54	----	5.9
494	70.66	137.96	5.03	5.69	5.03	----	5.5
522	71.01	138.93	4.76	5.80	3.96	----	5.5
525	72.02	138.82	3.61	5.20	----	----	4.8
545	69.68	140.03	4.58	4.80	4.48	----	4.9
546	70.01	140.02	5.23	5.55	5.26	----	5.5
548	70.68	139.98	5.17	6.03	4.65	----	5.6
574	70.35	141.00	5.31	5.85	5.48	----	5.8
576	71.02	141.00	4.54	5.30	----	----	5.1
578	71.69	141.00	4.18	5.26	----	----	4.9
630	71.01	143.07	4.79	5.44	----	----	5.4
655	70.33	144.00	4.92	4.63	----	----	4.6
764	70.55	148.08	3.40	3.72	----	----	3.3

GRID POINT 360 AT 70.840 N, 132.79 W

GUMBEL - Method of Moments

58 storms
Wave height threshold = 1.34 m

Return Period (yr)	Best Fit (m)	90% U.L. (m)	Tp (s)	Hmax (m)	Hc (m)
2	3.2	3.4	7.8	5.9	3.3
5	4.1	4.4	8.8	7.4	4.1
10	4.6	5.0	9.4	8.3	4.7
30	5.4	6.0	10.2	9.8	5.5
50	5.7	6.4	10.6	10.5	5.8
100	6.2	7.0	11.1	11.4	6.3

Tp, Hmax, and Hc were calculated using

$Tp = 4.189\ Hs^{0.532}$
$Hmax = 1.821\ Hs$
$Hc = 1.018\ Hs$

Correlation = 0.99

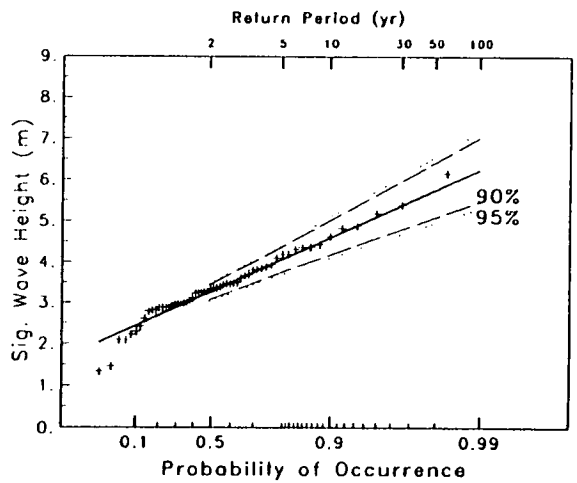

GRID POINT 384 AT 69.882 N, 134.15 W

GUMBEL - Method of Moments

81 storms
Wave height threshold = 1.72 m

Return Period (yr)	Best Fit (m)	90% U.L. (m)	Tp (s)	Hmax (m)	Hc (m)
2	2.7	2.9	7.9	4.9	2.8
5	3.3	3.5	8.8	5.9	3.3
10	3.7	3.9	9.4	6.6	3.7
30	4.2	4.6	10.3	7.6	4.2
50	4.5	4.9	10.7	8.1	4.5
100	4.8	5.3	11.2	8.7	4.8

Tp, Hmax, and Hc were calculated using

$Tp = 4.275\ Hs^{0.610}$
$Hmax = 1.800\ Hs$
$Hc = 1.000\ Hs$

Correlation = 1.00

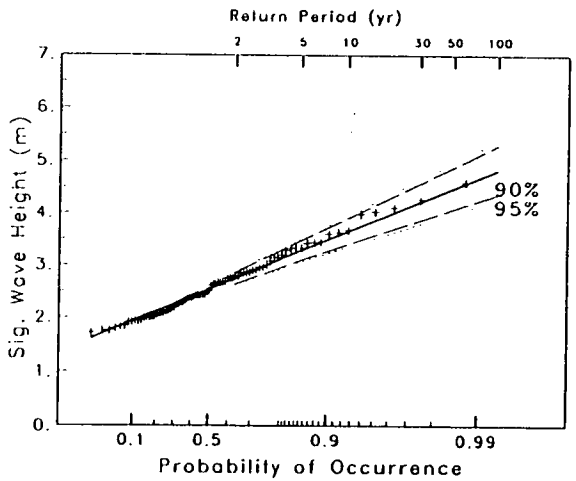

Figure 8.12 Final Extreme Analysis Results - Joint Probability

GRID POINT 435 AT 68.942 N, 136.32 W

GUMBEL – Method of Moments

80 storms
Wave height threshold = 0.68 m

Return Period (yr)	Best Fit (m)	90% U.L. (m)	Tp (s)	Hmax (m)	Hc (m)
2	1.2	1.2	4.7	2.2	1.2
5	1.4	1.5	5.1	2.5	1.4
10	1.5	1.6	5.4	2.8	1.6
30	1.8	1.9	5.8	3.2	1.8
50	1.9	2.0	6.0	3.4	1.9
100	2.0	2.2	6.3	3.6	2.1

Tp, Hmax, and Hc were calculated using

$Tp = 4.275\ Hs^{0.551}$
$Hmax = 1.828\ Hs$
$Hc = 1.031\ Hs$

Correlation = 0.98

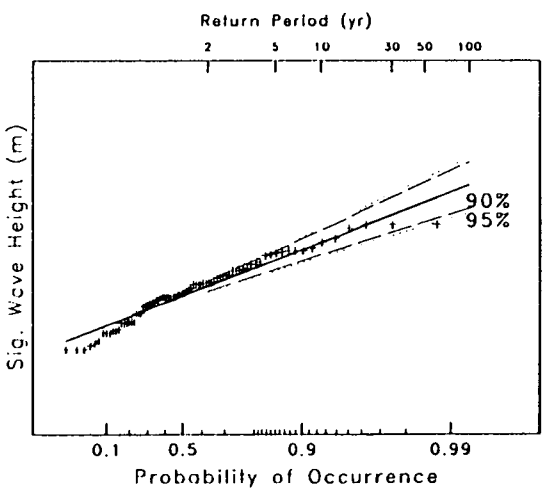

GRID POINT 437 AT 69.612 N, 136.17 W

GUMBEL – Method of Moments

79 storms
Wave height threshold = 1.50 m

Return Period (yr)	Best Fit (m)	90% U.L. (m)	Tp (s)	Hmax (m)	Hc (m)
2	2.6	2.7	7.9	4.7	2.6
5	3.2	3.4	8.8	5.7	3.2
10	3.6	3.8	9.4	6.4	3.6
30	4.2	4.5	10.3	7.5	4.2
50	4.4	4.9	10.7	8.0	4.5
100	4.8	5.3	11.2	8.7	4.8

Tp, Hmax, and Hc were calculated using

$Tp = 4.528\ Hs^{0.576}$
$Hmax = 1.811\ Hs$
$Hc = 1.006\ Hs$

Correlation = 1.00

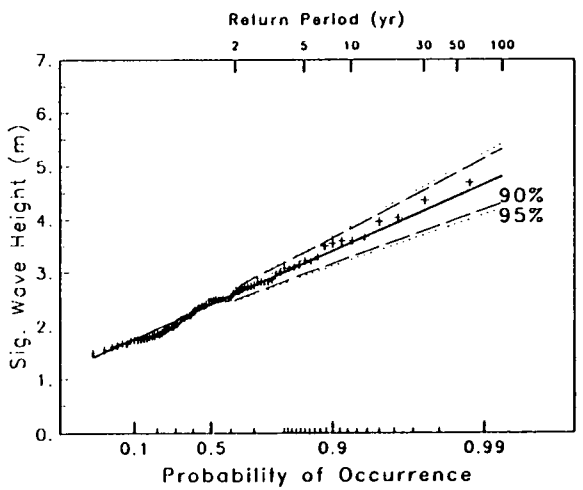

Figure 8.13 Final Extreme Analysis Results - Joint Probabilities

GRID POINT 463 AT 69.300 N, 137.20 W

GUMBEL - Method of Moments

80 storms
Wave height threshold = 1.66 m

Return Period (yr)	Best Fit (m)	90% U.L. (m)	Tp (s)	Hmax (m)	Hc (m)
2	2.7	2.8	7.6	4.9	2.7
5	3.2	3.4	8.4	5.8	3.2
10	3.5	3.8	8.9	6.4	3.6
30	4.1	4.4	9.7	7.4	4.1
50	4.3	4.7	10.0	7.8	4.3
100	4.6	5.0	10.5	8.4	4.7

Tp, Hmax, and Hc were calculated using

$Tp = 4.175\ Hs^{0.601}$
$Hmax = 1.815\ Hs$
$Hc = 1.011\ Hs$

Correlation = 1.00

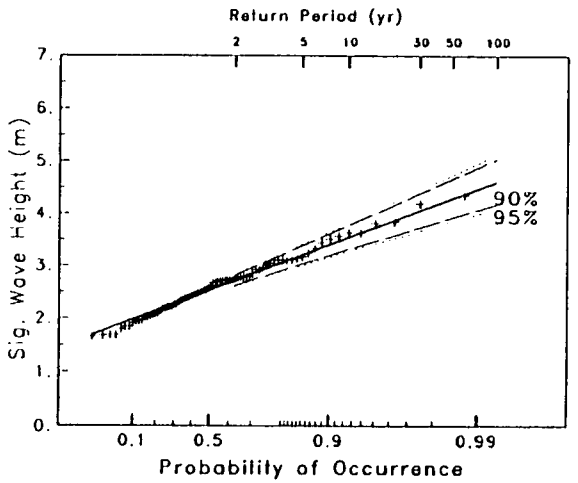

GRID POINT 464 AT 69.635 N, 137.14 W

GUMBEL - Method of Moments

79 storms
Wave height threshold = 1.91 m

Return Period (yr)	Best Fit (m)	90% U.L. (m)	Tp (s)	Hmax (m)	Hc (m)
2	3.1	3.2	7.7	5.5	3.1
5	3.6	3.8	8.5	6.6	3.7
10	4.0	4.3	9.1	7.3	4.1
30	4.6	5.0	9.8	8.4	4.7
50	4.9	5.3	10.2	8.9	5.0
100	5.3	5.8	10.6	9.6	5.3

Tp, Hmax, and Hc were calculated using

$Tp = 4.022\ Hs^{0.583}$
$Hmax = 1.812\ Hs$
$Hc = 1.012\ Hs$

Correlation = 1.00

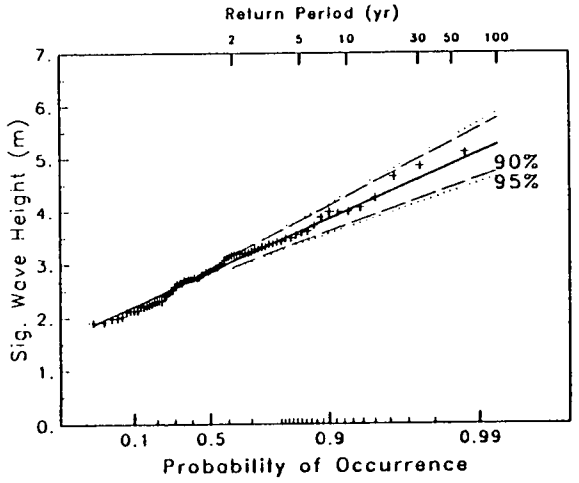

Figure 8.14 Final Extreme Analysis Results - Joint Probability

GRID POINT 492 AT 69.990 N, 138.05 W

GUMBEL – Method of Moments

79 storms
Wave height threshold = 1.43 m

Return Period (yr)	Best Fit (m)	90% U.L. (m)	Tp (s)	Hmax (m)	Hc (m)
2	3.2	3.4	7.8	5.8	3.3
5	4.0	4.2	8.7	7.2	4.0
10	4.5	4.8	9.4	8.1	4.5
30	5.3	5.7	10.3	9.5	5.3
50	5.6	6.2	10.6	10.1	5.7
100	6.1	6.7	11.1	11.0	6.2

Tp, Hmax, and Hc were calculated using

$Tp = 4.015\ Hs^{0.565}$
$Hmax = 1.809\ Hs$
$Hc = 1.011\ Hs$

Correlation = 0.99

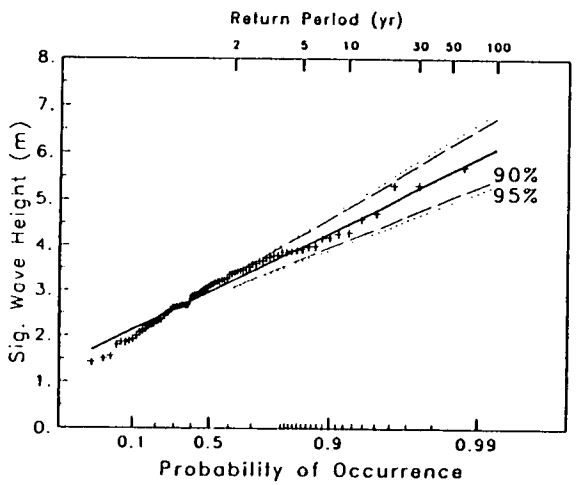

GRID POINT 574 AT 70.350 N, 141.00 W

GUMBEL – Method of Moments

51 storms
Wave height threshold = 1.45 m

Return Period (yr)	Best Fit (m)	90% U.L. (m)	Tp (s)	Hmax (m)	Hc (m)
2	2.8	3.0	7.3	5.1	2.8
5	3.6	3.9	8.4	6.6	3.7
10	4.2	4.6	9.0	7.5	4.2
30	4.9	5.6	9.9	8.9	5.0
50	5.3	6.0	10.3	9.6	5.4
100	5.8	6.6	10.8	10.5	5.9

Tp, Hmax, and Hc were calculated using

$Tp = 4.251\ Hs^{0.530}$
$Hmax = 1.810\ Hs$
$Hc = 1.012\ Hs$

Correlation = 0.98

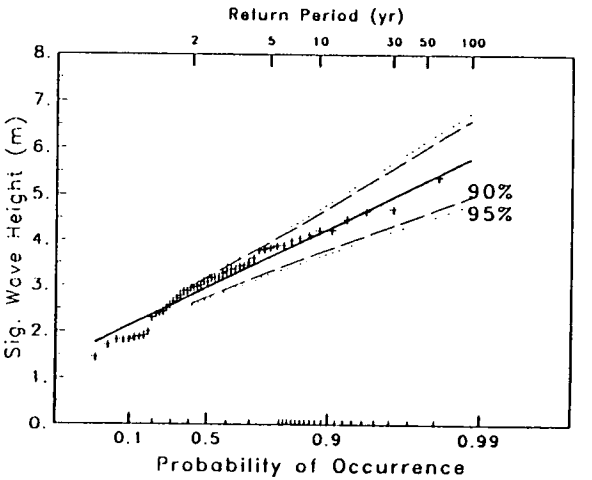

Figure 8.15 Final Extreme Analysis Results - Joint Probability

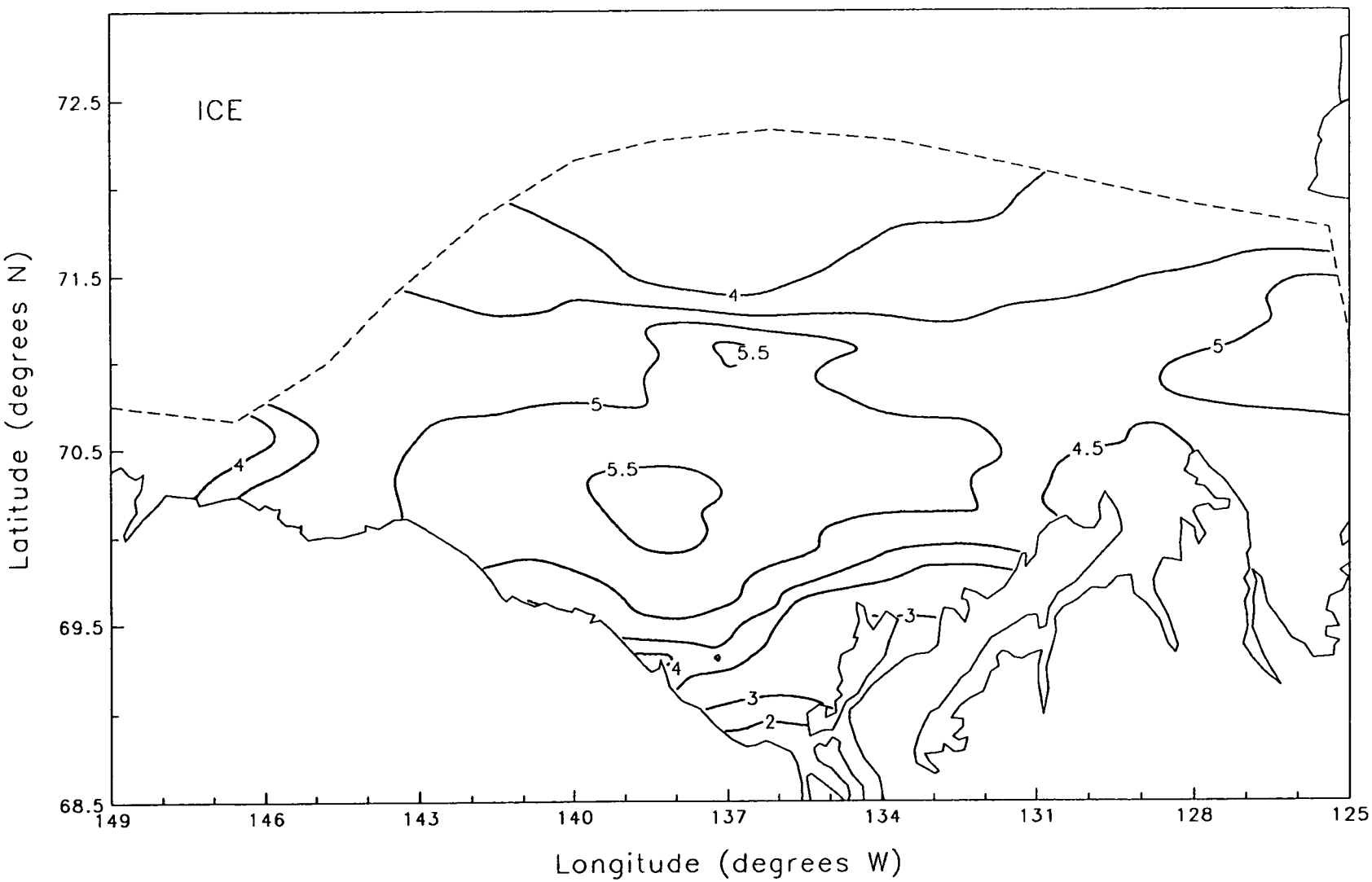
BEAUFORT SEA 100 YR SIGNIFICANT WAVE HEIGHT (m)
REAL ICE EDGE
ICE
72.5
71.5
70.5
69.5
68.5
Latitude (degrees N)
149
146
143
140
137
134
131
128
125
Longitude (degrees W)
4
5.5
5
4.5
3
2

Figure 8.16

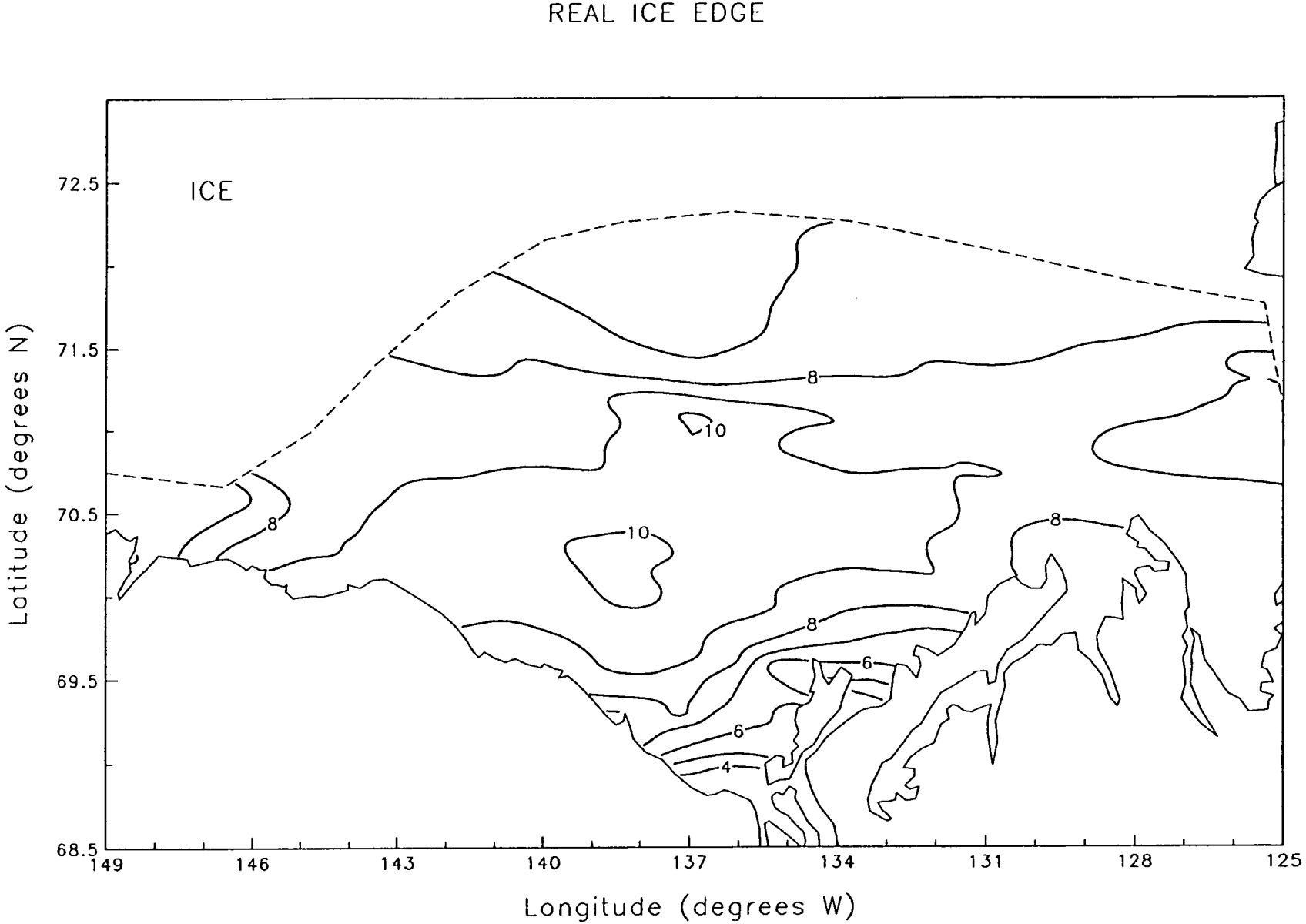
BEAUFORT SEA 100 YR MAXIMUM WAVE HEIGHT (m)
REAL ICE EDGE
ICE
72.5
71.5
70.5
69.5
68.5
Latitude (degrees N)
149
146
143
140
137
134
131
128
125
Longitude (degrees W)
8
10
10
8
8
8
6
6
4

Figure 8.17

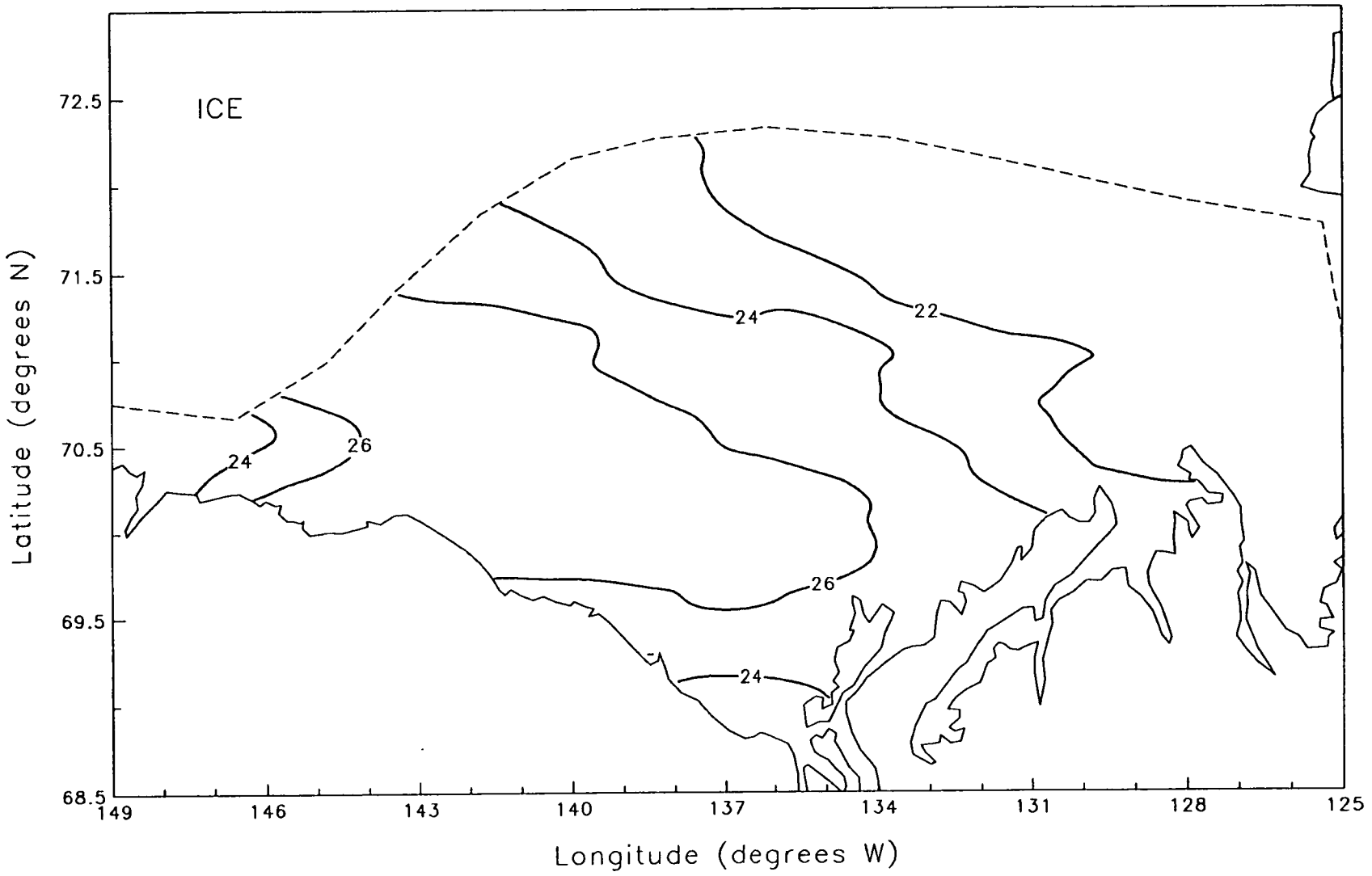
BEAUFORT SEA 100 YR WINDS (m/s)
REAL ICE EDGE
ICE
72.5
71.5
70.5
69.5
68.5
Latitude (degrees N)
24
26
24
22
26
24
149
146
143
140
137
134
131
128
125
Longitude (degrees W)

Figure 8.18

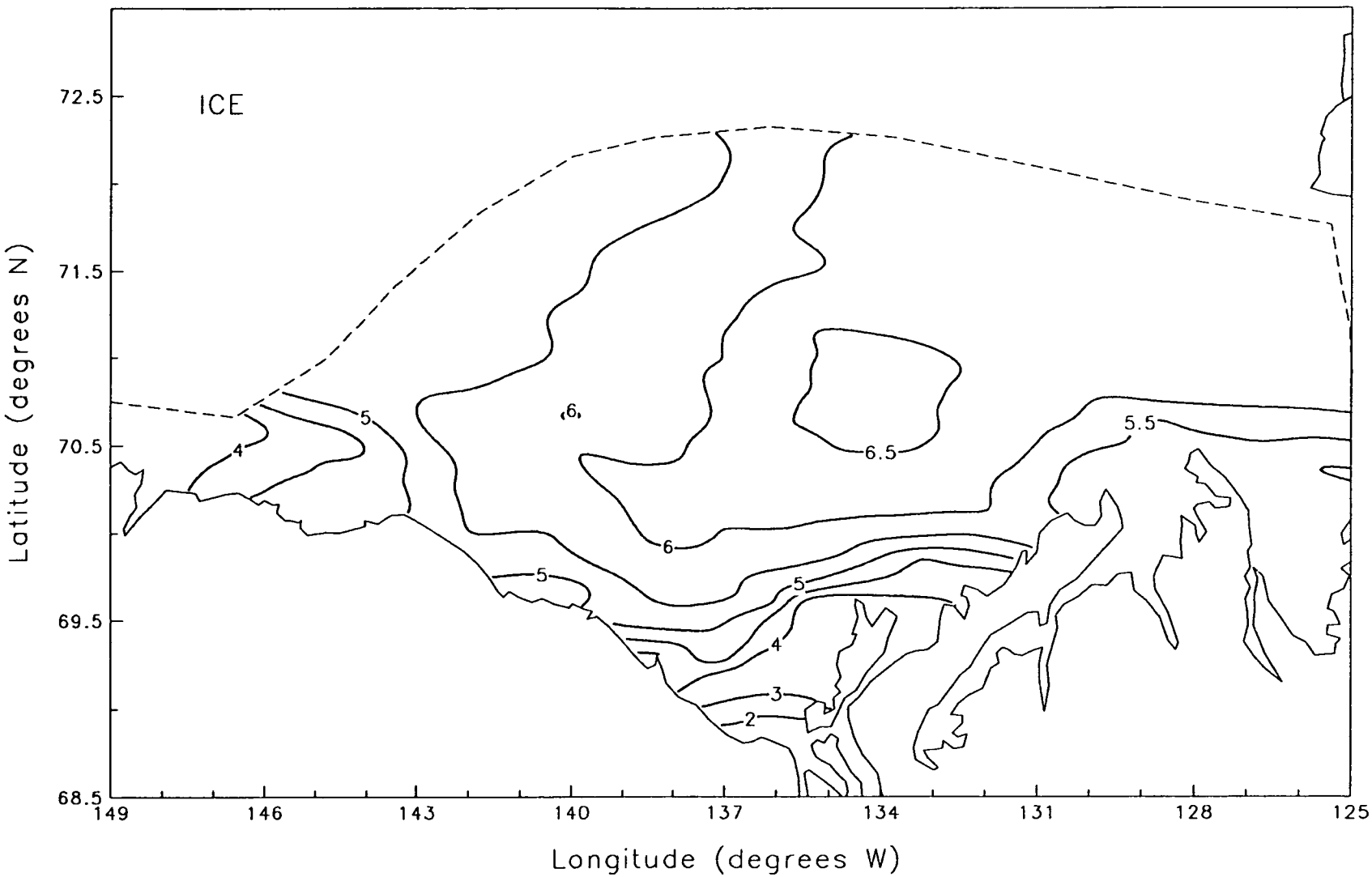
BEAUFORT SEA 100 YR SIGNIFICANT WAVE HEIGHT (m)
98% Occurrence of Ice Edge
ICE
72.5
71.5
70.5
69.5
68.5
Latitude (degrees N)
149
146
143
140
137
134
131
128
125
Longitude (degrees W)
6
6.5
5.5
5
4
3
2

Figure 8.19

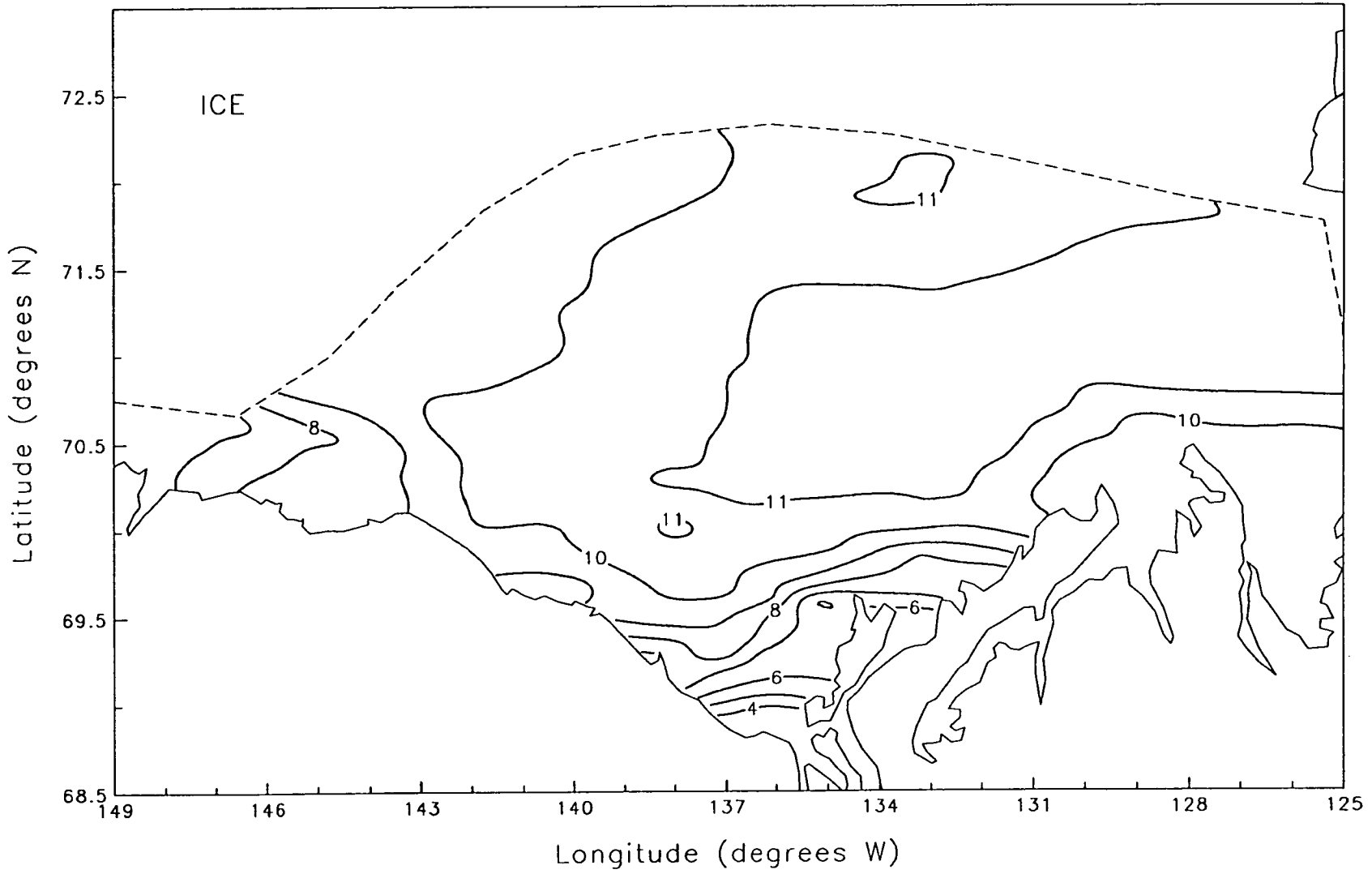
BEAUFORT SEA 100 YR MAXIMUM WAVE HEIGHT (m)
98% Occurrence of Ice Edge
ICE
11
10
8
6
4
72.5
71.5
70.5
69.5
68.5
149
146
143
140
137
134
131
128
125
Latitude (degrees N)
Longitude (degrees W)

Figure 8.20

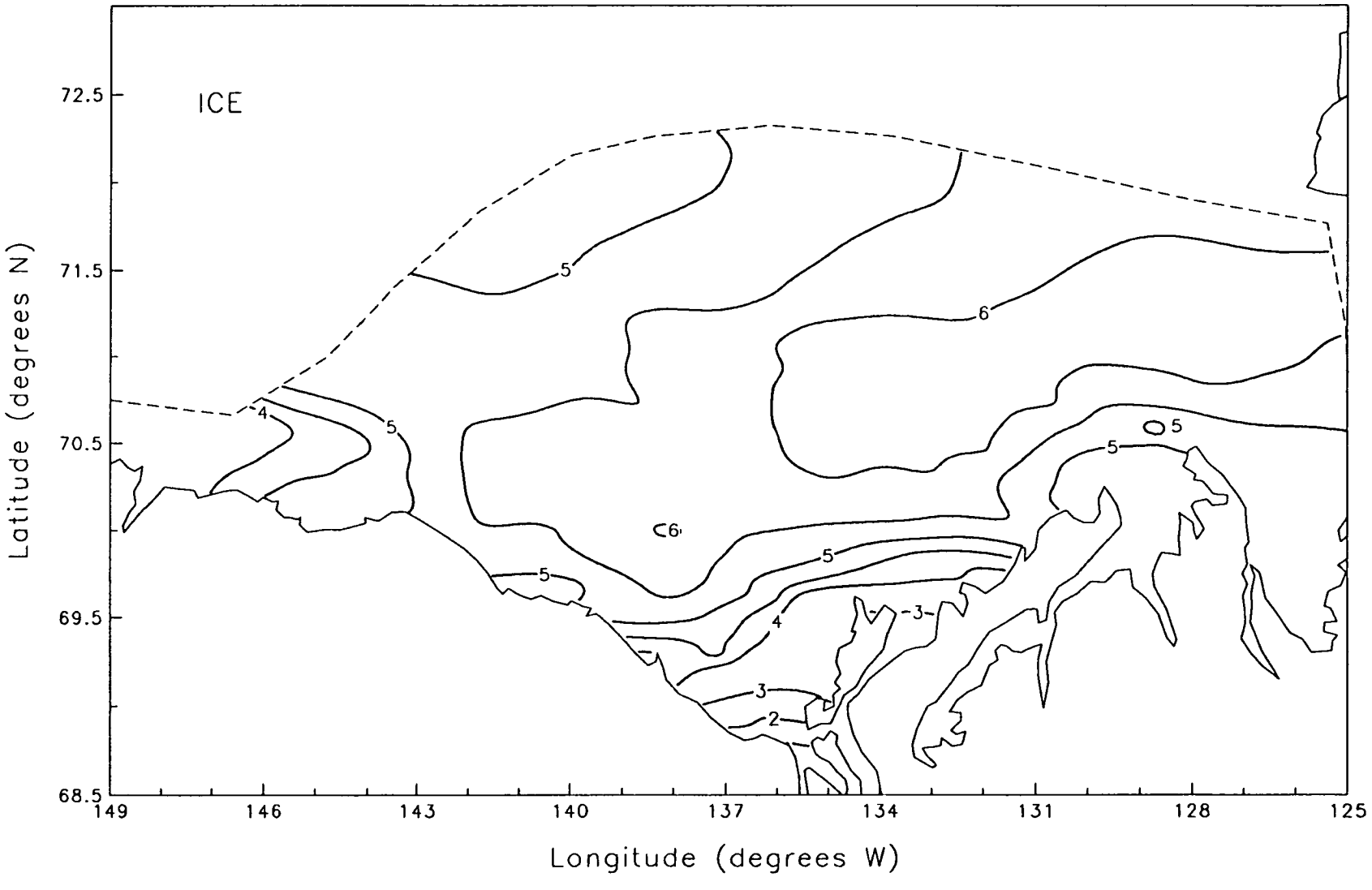
BEAUFORT SEA 100 YR SIGNIFICANT WAVE HEIGHT (m)
JOINT PROBABILITY (98% + 50% + 30% ICE EDGE)
ICE
72.5
71.5
70.5
69.5
68.5
Latitude (degrees N)
149
146
143
140
137
134
131
128
125
Longitude (degrees W)
6
5
4
3
2

Figure 8.21

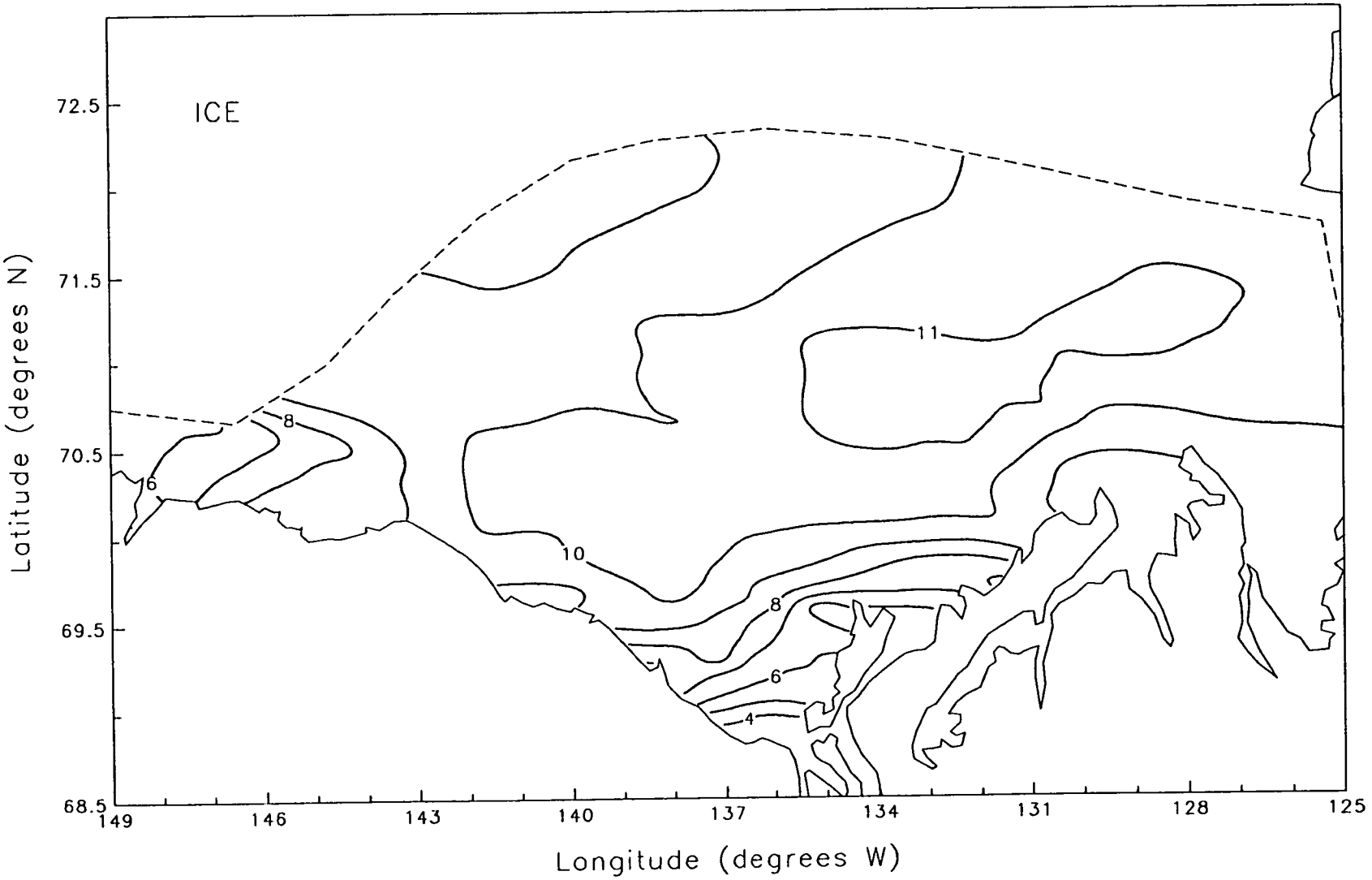
BEAUFORT SEA 100 YR MAXIMUM WAVE HEIGHT (m)
JOINT PROBABILITY (98% + 50% + 30% ICE EDGE)
ICE
11
10
8
8
6
6
4
72.5
71.5
70.5
69.5
68.5
Latitude (degrees N)
149
146
143
140
137
134
131
128
125
Longitude (degrees W)

Figure 8.22

8.6 DISCUSSION

The extremal analysis results presented in previous sections provided the expected design parameter's values at different risk levels (or return periods) in the open water region of the Canadian Beaufort. The analysis was provided for different ice edge scenarios, real ice and climatological ice. The hindcast storms with real ice edge were slightly higher than those hindcast with median (50% occurrence) ice edge. This is due to the storm selection criteria which biased the larger open water conditions. The 98% ice edge (which represents the maximum open water conditions in the Canadian Beaufort) provided extreme value results which were found to be in the range from 5% to 60%, with an average of about 20%, higher than those obtained using actual ice edge. As shown the effect of the extent of the ice edge on storm hindcasts and in turn the extremal analysis results varies from one site to another, with the largest differences are in the northern and middle parts of the study area. The 100 year significant wave height for 98% ice edge was found to be as high as 2.25 m greater than that estimated with the real ice edge at some locations (see Table 8.7).

The results of the joint probability scenario provided values which are lower than those obtained using 98% ice edge (i.e. maximum open water) scenario and higher than those obtained using real ice edge as one would expect. The following table provides a comparison between the results at the locations of the highest values for each scenario.

Table 8.8 Maximum 100 Year H_s (m) For Different Ice Edge Scenarios

		Real Ice Edge		98% Ice Edge		Joint Probability	
Grid Point	Corresponding Wind Speed (m/s)	Most Prob.	90% U.L.	Most Prob.	90% U.L.	Most Prob.	90% U.L.
492	18.2	5.7*	6.6	6.2	7.1	6.1	6.7
414	17.8	4.9	5.5	6.6*	7.6	6.2*	7.0
360	17.6	4.9	5.5	6.5	7.5	6.2*	7.0

* Maximum value in study area for each ice edge scenario.

As shown, the joint probability extreme values seem to reasonably represent the design wave parameters in the Beaufort Sea. It is therefore, suggested that these values be used as recommended design wave parameters for the study area. The extreme wind speeds which correspond to extreme wave heights are also provided for calculation of combined loads on offshore structures.

The results presented in this study were compared with the previous studies. Figure 8.23 shows a comparison of extreme value distribution of significant wave heights from various hindcast studies including the present study. As shown, the present study provided estimates of the extreme wave heights which lie between Seaconsult (1989) and Hydrotechnology (1980) estimates. Our values presented in Figure 8.23 represent three different locations: the first is in relatively shallow water at grid point #464 (30 m depth) which is near Tarsiut exploration site, the second at G.P. #437 in very shallow water (8.65 m depth) near Minuk, and the third provides the offshore deepwater location at G.P #360 (see Figure 7.1 for map location).

Minuk Storm (September 16-18, 1985)

The present hindcast results of the Minuk storm agree well with the previous extensive studies by Seaconsult (1987, 89) and Baird & Associates (1987). The best estimates of the peak H_s and T_p as suggested by these studies were 4.2 m and 10.5 s, respectively with dominant direction = 300°. Our peak hindcast values for this storm are H_s = 4.4 m, T_p = 10.6 s and vector mean wave direction = 298°. From the present extreme analysis results (Figures 8.13 and 8.14 for the nearest grid points #437 and 464) it is estimated that the Minuk storm would have had a return period between 25-50 years. The 100 year H_s at this site is estimated to be in the order of 5.0 m and T_p = 10.5 s, which is close to the values suggested in previous studies.

The final contour presentations of 100 year values (Figures 8.21 and 8.22) show the spatial variation of the design values in the study area. Detailed extreme value distributions are given for selected grid points which represent a variety of wave climate conditions in the study area. The maximum 100 year significant wave height in the study area is 6.2 $\pm$ 0.8 m for 90% confidence limits.

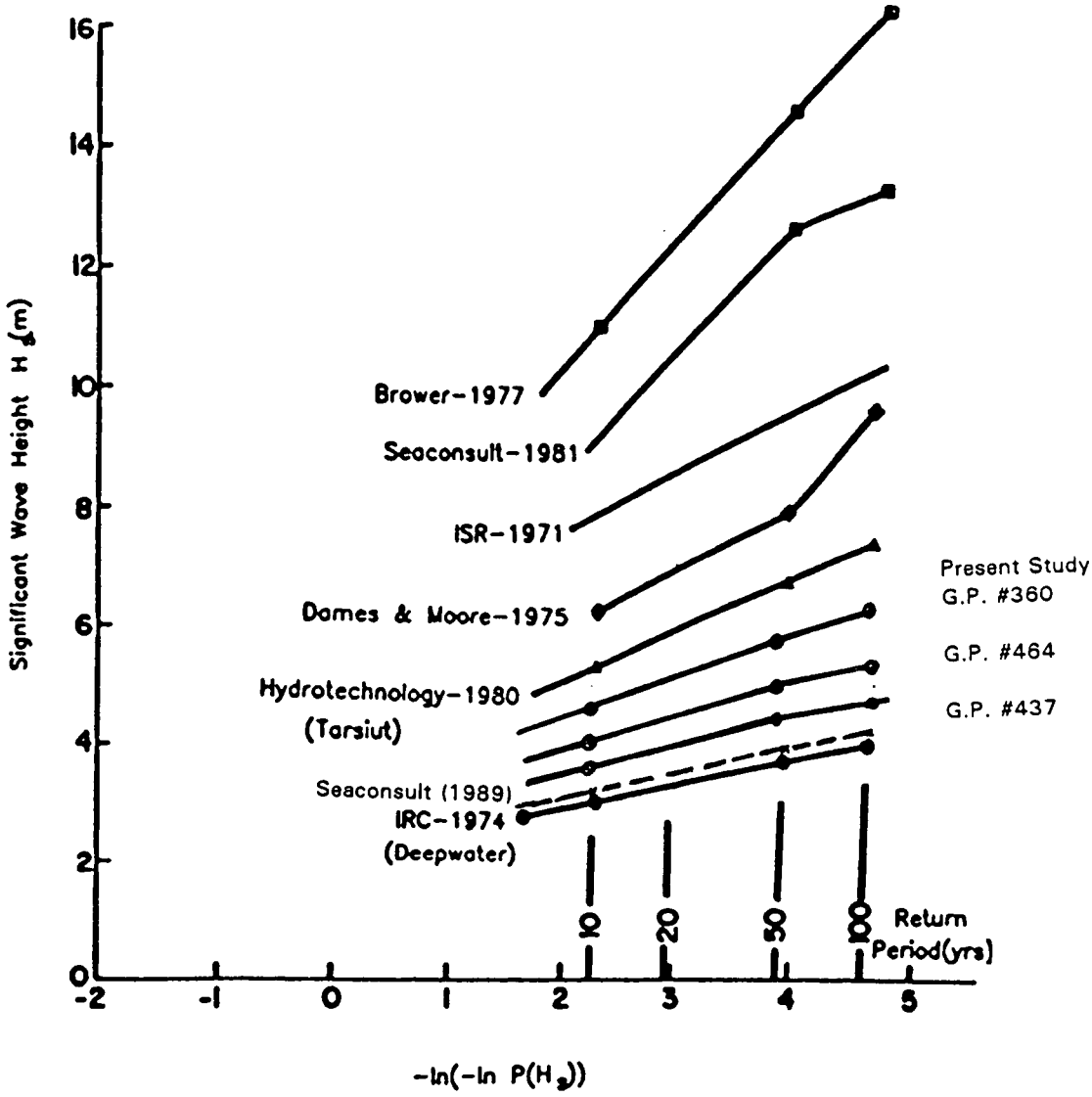

Figure 8.23 Comparison of Extreme Value Distribution of Significant Wave Heights for the Beaufort Sea from Various Hindcast Studies.

9.0 SUMMARY AND RESULTS

9.1 SUMMARY

The objective of this study was to develop new and definitive estimates of the extreme wave climate in the Canadian Beaufort Sea, with emphasis on offshore exploration areas in deep and shallow water. A hindcast approach was adopted, which includes the following traditional steps: (1) assembly of a comprehensive data base of archived historical meteorological data, wave measurements and ice cover; (2) identification and ranking of historical storm occurrences during the potential open-water season, over as long an historical period as allowed by the data, and selection of a population of storms for hindcasting; (3) adaptation and validation of the most accurate numerical hindcasting procedures to specify time histories of surface wind fields, surface wave fields and directional spectra in each hindcast storm; (4) hindcast of 30 selected historical storms; (5) statistical analysis of hindcast extremes at selected model grid points in order to estimate the significant wave height, maximum individual wave height and crest height, and associated wind speed and wave period, associated with rare return intervals.

The Beaufort Sea presents a number of special problems, not normally encountered in extreme wave climate studies of Northern Hemisphere mid-latitude basins. The main problems are: (1) the relative scarcity of historical meteorological data, including almost a total absence of transient ship reports, which are the main data source in mid-latitude problems; (2) the highly variable and complex nature of sea-ice cover, which can be expected to exert a significant control over the wave field. The lack of data complicates both the storm selection process, and the ability to accurately specify wind fields in selected historical storms. The presence of sea ice also complicates the storm selection process, and the hindcast process, since accurate hindcasts depend to some extent on the ability to specify ice-cover in selected events accurately.

The study was divided into two Phases. Phase I included an extensive literature review, assembly of historical meteorological data and offshore data including wave

measurements, and sea-ice data, the main stages of the storm selection process, and adaption and validation of the hindcast methodology. Phase II included final selection of the hindcast storms, the production hindcasts themselves, and the extremal analysis.

The review of all known previous wind/wave climate studies of the Canadian Beaufort confirmed the need for a new study. For example, estimates of the 100-year maximum significant wave height in deep water varied among the studies published to date from about 4m to nearly 16m with no indication that a consensus was emerging from the many studies carried out over the past decade. Previous studies, however, did contribute information useful to the data assembly and storm selection tasks.

The data base assembly was intended to be comprehensive. In addition to data contributed in previous studies, the data assembly tapped raw data sources in so far as possible, including the archives of the Atmospheric Environment Service (AES), the NOAA National Climatic Data Centre (NCDC), the Marine Environmental Data Service (MEDS), and the offshore industry. The data base assembled includes microfilm series of weather maps prepared in real-time at the AES Beaufort Weather Office and NOAA's National Meteorological Centre (NMC), digital files of surface observations from land stations, transient ships, and offshore drilling rigs, and wave observations from MEDS buoys moored near exploratory rigs. The processing facilities of the AES Climate Centre (CCAH), including MAST, LAST, DUST and CRISP were also extensively utilized. Where data could not be obtained or accessed in computer compatible form, hard copies were obtained (e.g selected maps not microfilmed, and logs of offshore observations from rigs (MANMAR).

The storm selection work was designed to identify historical storms based upon their ability to generate high sea-states within the study area. Thus, while a number of storms which may be high ranked for their ability to generate strong ocean currents and cause significant erosion of artificial islands are included in the storm selection, the hindcast population does not necessarily include the top-ranked members of the population of "erosion" storms.

The first step in the process was to identify all storms which occurred in the potential ice-free part of the year (June 15 - Nov 15), between 1957 - 1988. The first pass through all of the data sources noted above provided a Master Candidate List (MCL) of 1,087 events. The MCL was distilled in stages to a final list of 50 hindcast candidates from which the actual population of 30 storms hindcast was selected. The distillation process used both objective storm intensity and ranking procedures, and subjective assessments made by experienced synoptic meteorologists.

The presence of ice complicated the storm selection, since it is not known whether, during the warm season, the storm climatology and ice cover climatology of the basin are coupled. The location of the ice edge relative to long term normals was evaluated in the 50 storms selected, and the ice edge was found to lie offshore of climatology in the mean. This could be attributed to the fact that measured wave heights influenced the storm selection. To better account for the variability and uncertainty of extremes associated with ice edge effects, it was decided to hindcast each storm with four different ice-edge specifications, taking in each instance the 5/10 concentration as the limiting boundary for wave generation and propagation purposes. The four specifications were: (1) the actual ice edge during the storm, taken as fixed during the whole event; (2) climatological ice edges for three probability levels: 98%, 50% and 30% occurrences. Actual ice edges were produced from careful analysis of the AES daily and weekly ice charts, whereas climatological ice edges were taken from the semi-monthly charts also produced at AES. Separate extremal analyses were carried for each population of hindcasts, and for the combined probabilistic ice edge hindcasts.

The wind and wave hindcast methodology adapted to the basin has already undergone substantial refinement and validation in previous studies of this type, including several studies in Arctic basins, including the Chukchi Sea and U.S. Beaufort Seas. The wind field analysis procedure has been also applied recently in several Canadian Beaufort studies. The specification of wind fields includes a complete reanalysis of the evolution of the surface pressure field, starting with the best archived maps assembled, and adding additional ship and offshore rig data which may not have been available in real time. Wind fields are calculated from the pressure fields using a

proven marine planetary boundary layer model (MPBL). The domain of the analysis is 68-76N, 120-162W on a grid of points spaced 1 degree latitude by 3 degrees longitude. In areas where direct wind observations reveal deficiencies in the MPBL winds, kinematic analysis is carried out, the resulting streamline and isotach analyses are hand-gridded and the kinematic winds then supersede the MPBL winds.

The ODGP wave hindcast model, as adapted recently to shallow water, is used for the wave hindcasts. The grid spacing is 20 n. mi. While the model has been validated in several previous studies carried out in Canada, including studies associated with the CASP and LEWEX and LIMEX programs, and the major PERD East Coast and West Coast extreme wave climate studies, this study included a substantial validation of the wave hindcasts in the Canadian Beaufort. The validation involved hindcasting five storms of the types which characterize the selected storm population, and comparing hindcast and measured sea states at several sites located in different water depths, in each event.

The validation showed that when wind fields verify well against measured winds at offshore sites, and the ice edge location is well known and sharply defined, the wave hindcasts verify well. Comparisons of measured and hindcast time histories indicate hindcast errors of 24% in significant wave height (H_S) and 25% in spectral peak period (T_P) or 0.44m and 2 RMS, respectively. The statistical and time series comparisons show a high degree of agreement between the measured and hindcast wave parameters.

For external analysis, however, the most important aspect of the model is its ability to predict the storm peak accurately. Therefore, the peak to peak comparisons are considered to be of significant importance for evaluating model predictions.

Comparisons of hindcast and measured storm peaks at evaluation sites, yield an average bias (mean difference) of -0.06m in H_S and +0.24s in T_P, and RMS differences of 0.38m in H_S and 1.2s in T_P with scatter indices of 14.7% and 15.5% in H_S and T_P respectively. These results, taken together with skillful time history comparisons, compare favourably with those exhibited in other recent comprehensive hindcast

studies carried out in mid-latitude regions.

The production phase of the study included the hindcast of 30 storms, which, for four perturbations on ice edge, required 120 separate runs. Time histories of wind fields and selected integrated properties of the wave spectrum were archived at all model grid points for each run. At a subset of 51 grid points, distributed mainly over the parts of the Canadian Beaufort of interest to offshore hydrocarbon exploration operations, more detailed model results were saved, including all of the integrated properties as well as the full directional wave spectrum.

The extremal analysis was carried out at each of the 51 points on a site-specific basis. That is, no site-averaging or smoothing of extremes was deemed necessary given the fairly smooth spatial distribution of hindcast storm peaks, which itself is believed to be due to the scale of forcing wind field and the regularity of the bottom topography. At each point, five separate populations of storm peaks were subjected to the analysis, one for each of the four ice edge treatments, and one which combined the populations of the hindcasts for the three climatological ice edge specifications, the latter serving to approximate the true extremal wave distribution under the assumption that the storm climatology and the ice cover climatology are independent.

While resolution of the extremes into directional sectors was investigated, it was deemed that only omni-directional extremes could be reliably estimated. Prior to the site-specific analysis, peaks of maximum individual wave height (H_M) and crest height (H_C) were calculated for each storm at each point using well known statistical distributions, which operate on the entire time history of sea state at a site in a storm. These results were used to estimate the effective ratios of H_M/H_S and H_C/H_S at each point, to be applied later to extrapolated H_S.

The extrapolation of hindcast peak H_S and maximum wind speed (WM) for each subpopulation of peaks at each point was based upon the GUMBEL distribution, using the method of moments to fit the distribution, and varying the threshold of admittance of storm peaks until the fit was achieved which maximized the correlation coefficient of the best-fit regression line. Sensitivity analysis on the effect of the distribution (the

Borgman distribution was also tried) and the fitting method were carried out before the final scheme was adopted. The sensitivity of the final extremes, however, to distribution, fitting scheme and threshold were small in general.

9.2 RESULTS

The results of the extremal analysis constitute the principal study product. At 51 points, these include estimates of extreme WM for return period between 2 and 100 years, and estimates of extreme H_S (best fit and upper 90% confidence level) for the same return periods, and for each ice edge dependent subpopulation, That is, real ice edge, 98% probability, 50% probability and 30% probability, and all three climatological ice edges combined. Results for the sensitivity studies as noted above, and an assessment of the directional distribution of hindcast (not extrapolated) extremes is presented for 8 grid points.

For the population of hindcast peaks using the actual ice-edge, extreme 100-year H_S varied from about 2m at the shallowest depths modelled (about 7.5m depth) to 5.7m in deep water. These extremes turned out to be slightly higher than the extremes derived for those derived from hindcasts made with the median (50%) ice edge. As expected, extremes derived from the hindcast peaks with the 98% ice edge (which represents maximum open water) were higher, ranging between 5% and 60% higher with an average increase of 20%. In real terms the increase was as great as 2.25m in H_S. The results of the joint ice edge probability analysis provided extremes lower than those obtained using 98% ice edge and higher than those using the real ice edge. These results (i.e. from ice edge probability analysis) are the recommended extremes for design, i.e. the 100-year extreme H_S of 6.2+/- 0.8m for 90% confidence limits. Comparison of these new results with existing estimates indicate that our extremes are at the lower end of the wide range of extremes provided by previous studies.

10.0 REFERENCES

Agnew, T., L. Spicer and B. Maxwell, 1987. Marine Climatological Atlas - Canadian Beaufort Sea. A publication of Canadian Climate Centre, AES, 196 pp.

Agnew, T., B. Eid, W. Skinner, and V. Cardone, 1989. Beaufort Sea Wind/Wave-storm Hindcasting. Proceedings and 2nd International Workshop on Wave Hindcast Forecast, April 1989, Vancouver, B.C., 192-202 pp.

Baird & Associates Engineering Ltd. 1987. Estimation of the Wave Climate at Minuk I-53 During the Storm of September 16-18, 1985. Report for ESSO Resources Canada Limited.

Baird, W.F., J.S. Readshaw, and O.J. Sayao, 1986. Nearshore Sediment Transport Predictions, Stanhope Lane, P.E.I. Report No. C2S2-21, NRCC No. 25830, National Research Council of Canada, May, 1986.

Borgman, L.E. 1973. Probabilities for the highest wave in a hurricane. J. Waterways, Harbours and Coastal Engineering Div., ASCE, 185-207.

Bouws, E., J. J. Ephraums, J. A. Ewing, P. E. Francis, H. Gunther, P.A. Janssen, G.J. Komen, W. Rosenthal, and W. J. deVoogt, 1985. A shallow water intercomparison of three numerical wave prediction models (SWIM). Qrtly. J. Royal Met. Soc., III, 1087, 1112.

Brower, W.A. Jr., H.W. Searby, and J.L. Ulise, 1977. Climatic atlas of the outer continental shelf waters and coastal regions of Alaska, Vol.III, Chukchi and Beaufort Sea. U.S. Department of Commerce, NOAA/OCSEAP, 3:409.

Buckley, J.R. and W.P. Budgell, 1988. Meteorologically Induced Currents in the Beaufort Sea, Institute of Ocean Sciences, Sydney, B.C.

Canadian Climate Centre, 1990. Marine Climate Directory Datasets and Services. Hydrometeorology Division, Internal Report No. 90-1, 1990.

Cardone, V.J., 1969. Specification of the wind field distribution in the marine boundary layer for wave forecasting. Report TR-69-1, Geophys. Sci. Lab., New York University.

Cardone, V., W.J. Pierson, and E.G. Ward, 1976. Hindcasting the Directional Spectrum of Hurricane Generated Waves. J. of Petrol. Tech., 28, 385-394.

Cardone, V.J., 1978. Specification and prediction of the vector wind on the United States continental shelf for application to an oil slick trajectory forecast program. Final Report, contract T-35430, NOAA, U.S. Dept. of Commerce, Silver Spring, Maryland.

Cardone, V.J., A.J. Broccoli, C.V. Greenwood, and J.A. Greenwood, 1980. Error Characteristics of Extratropical Storm Wind Fields Specified from Historical Data. J. of Petrol. Tech., 32, 873-850.

Carter, D.J.T. and P.G. Challenor, 1983. Methods of fitting the Fisher-Tippett Type 1 extreme value distribution. Ocean Engng. 10(3), 191-199.

Cote, J., J. O. Davis, W. Marks, R. J. McGough, E. Mehr, W. J. Pierson, J. F. Ropek, G. Stephenson, and R. C. Vetter, 1960. The directional spectrum of wind generated sea as determined from data obtained by the Stereo Wave Observation Project (SWOP). Meteorological Papers, 2, 6, New York University, College of Engineering. New York University Press, NY, 88 pp.

Eid, B.M. and V.J. Cardone, 1987. Operational test of wave forecasting models during the Canadian Atlantic Storms Program (CASP). Environmental Studies Research Funds, Report Series No. 076. Ottawa, 111 p. & appendices

Forristall, G.J., 1978. On the statistical distribution of wave heights in a storm. J. of Geophys. Res. 83, 2353-2358.

Grant, W.D. and O.S. Madsen, 1982. Movable bed roughness in unsteady oscillatory flow. J. of Geophys. Res., 87, C2, 469-481.

Greenwood, J.A., V.J. Cardone and L.M. Lawson, 1985. Intercomparison test version of the SAIL Wave Model. In Ocean Wave Modelling. Plenum Press, New York, 221-233.

Gumbel, E.J., 1958. Statistics of Extremes. Columbia University Press, New York, 375 pp.

Haring, R.E. and J.C. Heideman, 1978. Gulf of Mexico rare wave return periods. Offshore Technology Conference Paper 3230.

Haring, R.E., A.R. Osborne, and L.P. Spencer. 1976. Extreme wave parameters based on continental shelf storm wave records. Proceedings of the 15th Coastal Engineering Conference, Honolulu, July 11 - 17.

Kozo, T.L., and Robe, R.Q. Modelling Winds and Open-Water Buoy Drift Along the Eastern Beaufort Sea Coast, Including the Effects of the Brooks Range. Journal of Geophysical Research, Vol. 91, N. C11, 1986.

Lindsay, D.G., 1977. Sea Ice Atlas of Arctic Canada, 1969-1974. Department of Energy, Mines, and Resources, Ottawa.

MacLaren Plansearch Limited, 1985. Evaluation of Spectral Ocean Wave Model (SOWM) for supporting Real-Time Wave Forecasting in the Canadian East Coast Offshore. Report submitted to AES, Downsview, January, 1985.

MacLaren Plansearch Limited, 1987. Objective and Kinematic analyses of meteorological records and the production of wind data of selected storms in the Beaufort Sea. Report submitted to MEDS/AES.

MacLaren Plansearch Limited, 1988. Development and Evaluation of a Wave Climate Database for the East Coast of Canada. Report submitted to Marine Environmental Data Services, under SSC Contract #FP802-62574 101-SS.

MacLaren Plansearch Limited, 1989. Beaufort Sea winter storms hindcast. Report to Atmospheric Environment Service, Downsview, Ontario.

Manak, D.K., 1988. Climate study of Arctic sea ice extent and anomalies. Climate Research Group Report No. 88-10, McGill University, Montreal, Quebec.

Markham, W.E., 1981. Ice atlas Canadian Arctic waterways. Department of Supply and Services, Ottawa.

Muir, L.R. and A.H. El-Shaarawi, 1986. On the Calculation of Extreme Wave Heights: A Review Ocean Energy, 13 (1), 93-118.

Murray, M.A. and M. Maes, 1986. Beaufort Sea extremal wave studies assessment. Environment Studies Revolving Funds (ESRF), Report Series No. 023.

Pierson, W.J., L.J. Tick and L. Baer, 1966. Computer-based procedures for preparing global wave forecasts and wind field analyses capable of using wave data obtained by a space craft. Sixth Naval Hydrodynamics Symposium, ACRO-136, Office of Naval Research, Dept. of the Navy, Washington, D.C., pp. 499-532.

Readshaw, J.S. Beaufort Sea Hindcast Study, 1970 to 1982, APOA Project 203. Final report submitted to Gulf Canada Resources Inc., December, 1983.

Reece, A.M. and V.J. Cardone, 1982. Test of wave hindcast model results against measurements during four different meteorological systems. Offshore Technology Conference Paper 4323.

Resio, D. T., 1981. The estimation of wind-wave generation in a discrete spectral model. J. of Phys. Oceanography, 11, 510 - 525.

Seaconsult Marine Research Limited, 1986. Analysis of the ADGO Wave Measurements for the Storm of September 15-18, 1985. Report submitted to ESSO Resources Canada Limited, October 1986.

Seaconsult Marine Research Limited, 1986b. An Extreme Value Analysis of Storm Wave Power at Minuk. Report to ESSO Resources Canada Limited, September 1986.

Seaconsult Marine Research Limited, 1987. Wave heights and durations during severe storm events in the Beaufort Sea. Report submitted to ESSO Resources Canada Limited, February 1987.

Seaconsult Marine Research Limited, 1989: Amauligak Development Studies 1988/89: Design Storm Characteristics, Amauligak Region, Beaufort Sea. Confidential Report, Gulf Canada Resources Limited.

Swail, V., V.J. Cardone and B. Eid, 1989. An extremes wind and wave hindcast off the East Coast of Canada. Proceedings, 2nd International workshop on Wave Hindcasting and Forecasting. Vancouver, B.C., pp. 151-160.

SWAMP (see Wave Modelling Project) Group, 1985. Ocean wave modelling. Plenum Press, New York, 256 pp.

Szabo, D., V. Cardone and B. Callahan, 1989. Severe storms identification for extreme criteria determination by hindcasting. Proceedings 2nd International Workshop of Wave Hindcasting and Forecasting. Vancouver, B.C., April 25-18, 1989, pp. 89-99.

APPENDIX A
CANDIDATE STORM LISTS

TABLE A.1

MASTER CANDIDATE LIST
Top 512 storms for the Beaufort Sea

Sources:

A Severe storms over the Canadian Western High Arctic 1957-1983 Report #87-2
B Beaufort Weather and Ice Office Annual Summaries (1976-1985)
C Arctic petroleum Operator's Association,1983:Beaufort Sea Hindcast Study 1970-1982. APOA study 203
D Seaconsult 1986: An extreme value analysis of storm wave power at Minuk
E BAIRD & Associates,1987: Estimation of the wave power at Minuk I-53 1960-1985
F Bucley and Budgell, 1988: Meteorologically induced currents in the Beaufort Sea.
G Seaconsult 1989: Design storm characteristic, Amiligak Region, Beaufort Sea
H Maclaren Plansearch database
I Seaconsult 1987: Wind and wave Hindcast for the storm of September 15 to 19, 1985
J Seaconsult 1986: Analysis of the ADGO Wave measurements for the storm of September 15 to 19, 1985
K Baird & Associates, 1987: Estimation of the wave climate at Minuk I-53 during the storm of September 15 to 19, 1985.
L COADS.wave waves >= 1.5 m
M COADS.wind winds >= 25 kts
N LAST.wind winds >= 25 kts
P RIG.wave waves >= 1.5 m
R RIG.wind winds >= 25 kts
S SPASM central pressure <= 970 mb
T MPL HINDCAST
V MEDS

	START YYMMDDHH	END YYMMDDHH	DUR	OBS	WIND SPD (kts)	WIND DIR	COMBINED HS (m)	COMBINED TP (s)	SEA DIR	SEVERITY INDEX	MINT CENT PRESSURE (mb)	WAVERIDER HS (m)	WAVERIDER TP (s)	SOURCES
1	57071206	57071509	75	17	34.	100	1.5	5.0	070	2550				L,M,N
2	57072518	57072706	36	4	23.	330	2.5	8.0	340	828				L
3	57072821	57072821	1	1	10.	270	2.0	6.0	200	10				L
4	57080603	57080706	27	3	20.	070	1.5	5.0	070	540				L
5	57080900	57080915	15	5	34.	230	3.0	8.0	230	510				L,M
6	57081809	57081809	1	1	12.	070	5.5	5.0	200	12				L
7	57082703	57082806	27	3	23.	110	2.0	6.0	050	621				L
8	57091623	57091705	6	2	30.	320				180				N
9	57092717	57092820	27	6	35.	110				945				N
10	57100205	57100220	15	4	30.	230				450				N
11	57102820	57102823	3	2	26.	090				78				N
12	57110411	57110423	12	5	32.	070				384				N
13	58072017	58072020	3	2	26.	090	0.0	6.0	020	78				M,N
14	58080412	58080506	18	2	15.	050	1.5	6.0	040	270				L
15	58081608	58081617	9	4	28.	090				252				N
16	58082318	58082500	30	5	23.	050	2.5	6.0	030	690				L
17	58090606	58090606	1	1	23.	200	1.5	5.0	210	23				L
18	58092506	58100800	306	52	25.	320				7650	962.5			N,S
19	58101317	58101411	18	4	30.	050				540				N
20	58102818	58110314	140	26	35.	090				4900	966.8			N,S
21	58110620	58110723	27	7	32.	110				864				N
22	59070911	59071017	30	4	31.	250				930				N

TABLE A.1 (continued)

23	59071417-59071505	12	2	32.	340				384		N
24	59071717-59072011	66	7	45.	360	0.0	6.0	020	2970		M,N
25	59072615-59072800	33	9	40.	290	1.5	6.0	290	1320		L,M
26	59072911-59072923	12	2	35.	020				420		N
27	59080111-59080211	24	6	30.	360	0.0	6.0	290	720		M,N
28	59080905-59081003	22	2	28.	270	0.5	5.0	300	616		M,N
29	59082815-59082900	9	2	30.	120	0.0	5.0	300	270		M
30	59082909-59082912	3	2	21.	160	1.5	5.0	170	63		L
31	59090403-59090406	3	2	20.	090	1.5	5.0	090	60		L
32	59090417-59090611	42	10	30.	050				1260		N
33	59091017-59091217	48	7	43.	230				2064		N
34	59091218-59091218	1	1	15.	180	2.0	6.0	210	15		L
35	59092503-59092703	48	14	28.	290				1344		N
36	59093006-59100216	58	38	39.	140				2262		N
37	59100317-59100523	54	36	37.	360				1998		N
38	59101300-59101511	59	26	35.	270				2065		N
39	59101717-59102005	60	14	34.	230				2040		N
40	59102100-59102500	96	17	28.	110				2688	956.8	N,S
41	59102913-59103011	22	24	40.	090				880		N
42	59103117-59110417	96	43	48.	230				4608		N
43	59110905-59111017	36	5	30.	270				1080		N
44	59111405-59111514	33	13	32.	320				1056		N
45	60071111-60071117	6	2	32.	270				192		N
46	60071906-60071918	12	2	39.	320	0.0	5.0	100	468		M
47	60072017-60072117	24	3	30.	320				720		N
48	60072300-60072306	6	2	31.	060	0.0	5.0	100	186		M
49	60072600-60072906	78	12	58.	070	0.0	5.0	100	4524		M,N
50	60073118-60080115	21	4	26.	090	2.0	6.0	040	546		L,N
51	60080418-60080600	30	5	47.	110	0.0	5.0	100	1410		M
52	60081917-60082200	55	8	31.	320	3.5	5.0	310	1705		L,M,N
53	60082320-60082605	57	20	37.	290				2109		N
54	60082818-60083018	48	3	39.	320	0.0	8.0	290	1872		M
55	60091211-60091512	73	20	55.	135	0.0	8.0	290	4015		M,N
56	60091706-60091718	12	2	25.	090	0.0	8.0	290	300		M
57	60091815-60091918	27	9	27.	320	2.0	6.0	280	729		L,M
58	60092217-60092411	42	28	30.	090				1260		N
59	60092700-60092900	48	7	29.	270	1.5	8.0	250	1392		L,M
60	60100517-60101112	139	23	33.	230				4587	970.0	N,S
61	60101711-60101714	3	2	26.	140				78		N
62	60101910-60101912	2	2	27.	240	0.0	8.0	250	54		M
63	60102022-60102318	68	15	49.	110	0.0	8.0	250	3332		M
64	60103012-60103018	6	2	25.	050	0.0	8.0	250	150		M
65	60110302-60110406	28	4	28.	050	0.0	8.0	250	784		M
66	60110522-60110609	11	8	30.	110				330		N
67	60110818-60110906	12	4	30.	090	0.0	8.0	250	360		M
68	60110911-60111017	30	8	48.	270				1440		N
69	61061611-61061711	24	2	30.	320				720		N
70	61062211-61062314	27	5	29.	090				783		N
71	61062811-61062817	6	2	26.	320				156		N
72	61071100-61071106	6	2	28.	100	1.0	5.0	100	168		M
73	61071212-61071218	6	2	33.	240	1.0	5.0	240	198		M

TABLE A.1 (continued)

74	61071317-61071500	31	6	48. 320	2.1	5.0	342	1488		M,N
75	61071700-61071800	24	2	28. 130	0.5	5.0	130	672		M
76	61081217-61081317	24	5	30. 320				720		N
77	61082300-61082303	3	2	26. 360	1.0	5.0	350	78		M
78	61082423-61082520	21	22	37. 050				777		N
79	61082715-61082806	15	4	35. 090	2.0	5.0	130	525		L,M,N
80	61090615-61090706	15	4	32. 200	1.1	5.0	144	480		M
81	61090717-61090810	17	4	28. 090				476		N
82	61091209-61091212	3	2	32. 160	1.5	0.0		96		L,M
83	61111411-61111523	36	4	35. 230				1260		N
84	62062719-62062801	6	5	28. 090				168		N
85	62071900-62071906	6	3	24. 080	2.0	5.0	090	144		L
86	62072115-62072506	87	20	50. 290	4.0	5.0	080	4350		L,M
87	62072506-62072506	1	1	26. 080	4.0	5.0	080	26		M
88	62072511-62072603	16	3	28. 140				448		N
89	62072805-62072917	36	9	39. 290				1404		N
90	62080311-62080317	6	6	28. 090				168		N
91	62081816-62081919	27	5	27. 070				729		N
92	62082200-62082203	3	2	22. 020	1.5	5.0	050	66		L
93	62082618-62082619	1	2	28. 290				28		N
94	62083108-62083117	9	9	30. 360				270		N
95	62090311-62090715	100	34	56. 310	9.5	16.0	310	5600		L,M,N
96	62090805-62090811	6	2	26. 270				156		N
97	62090903-62091106	51	14	48. 250	8.0	6.0	230	2448		L,M
98	62091618-62091623	5	4	27. 090				135		N
99	62092617-62092705	12	3	30. 250				360		N
100	62092706-62100118	108	19	26. 110				2808	968.5	N,S,T
101	62101200-62101205	5	3	28. 050				140		N
102	62101300-62101606	78	14	26. 160				2028	957.2	N,S
103	62102419-62102611	40	20	33. 140				1320		N
104	62110112-62110718	150	26	30. 090				4500	961.6	N,S
105	63061817-63061823	6	2	43. 270				258		N
106	63062408-63062518	34	13	30. 090				1020		N
107	63070523-63070617	18	5	29. 270				522		N
108	63072503-63072506	3	2	24. 090	1.5	5.0	090	72		L
109	63072805-63073017	60	9	31. 320				1860		N
110	63081605-63081711	30	13	35. 290				1050		N
111	63082311-63082323	12	2	52. 230	5.5	16.0	220	624		L,M,N
112	63091418-63091506	12	3	25. 100	2.5	6.0	120	300		L,M
113	63100217-63100423	54	27	39. 250				2106		N
114	63100905-63100923	18	8	30. 140				540		N
115	63101406-63101718	84	15	33. 340				2772	963.9	N,S
116	63102006-63102306	72	13	25. 070				1800	949.2	N,S
117	63102900-63102923	23	5	27. 020				621		N
118	63103012-63110518	150	34	41. 090				6150	953.1	N,S
119	64062505-64062605	24	14	35. 270				840		N
120	64062711-64062717	6	2	30. 270				180		N
121	64062911-64062923	12	2	28. 270				336		N
122	64071111-64071117	6	2	27. 360				162		N
123	64071311-64071323	12	3	30. 290				360		N
124	64081218-64081317	23	2	26. 090				598		N

TABLE A.1 (continued)

125	64082011-64082217	54	23	43. 250				2322			N
126	64090323-64090417	18	6	32. 320				576			N
127	64091105-64091123	18	4	30. 320				540			N
128	64102211-64102310	23	6	30. 140				690			N
129	64102618-64103006	84	16	30. 140				2520	969.7		N,S
130	65061620-65061705	9	4	26. 090				234			N
131	65071500-65071509	9	4	33. 070	3.5	5.0	050	297			L,M
132	65080215-65080221	6	3	29. 110	2.0	5.0	120	174			L,M
133	65080617-65080706	13	5	32. 320				416			N
134	65092101-65092211	34	6	30. 290				1020			N
135	65100515-65100611	20	20	31. 110				620			N
136	65101500-65101906	102	18	30. 290				3060	964.3		N,S
137	65102305-65102405	24	22	33. 110				792			N
138	65102523-65102623	24	4	30. 320				720			N
139	65102923-65103105	30	5	34. 270				1020			N
140	65110505-65110505	1	1	39. 270				39			N
141	65110711-65110717	6	2	30. 270				180			N
142	65111217-65111305	12	4	40. 230				480			N
143	65111312-65111600	60	11	28. 110				1680	969.0		N,S
144	66061923-66062017	18	4	30. 320				540			N
145	66081921-66082006	9	4	22. 090	1.5	5.0	090	198			L
146	66082912-66082918	6	2	31. 040	3.4	6.0	066	186			L,M
147	66091017-66091023	6	2	32. 290				192			N
148	66091411-66091417	6	2	32. 320				192			N
149	66091500-66092021	141	21	27. 320	1.5	5.0	270	3807	959.2		L,M,N,S
150	66102912-66110300	108	19	23. 190	2.9	10.0	116	2484	965.7		L,S
151	66110511-66110517	6	2	28. 290				168			N
152	67081912-67081912	1	1	8. 030	4.0	5.0	030	8			L
153	67090121-67090221	24	8	30. 040	1.0	5.0	060	720			M
154	67091112-67091206	18	3	32. 080	1.0	10.0	080	576			M
155	67091518-67091600	6	3	25. 060	1.5	8.0	060	150			L,M
156	67091811-67091817	6	2	30. 090				180			N
157	67100311-67100323	12	2	30. 320				360			N
158	67100523-67100611	12	3	35. 180				420			N
159	67100612-67101118	126	22	27. 260	1.5	5.0	260	3402	957.9		L,M,S
160	67101611-67101911	72	10	39. 290				2808			N
161	67102912-67110606	186	32	21. 150	3.6	5.0	150	3906	958.9		L,S
162	68063017-68070111	18	2	30. 320				540			N
163	68071403-68071406	3	2	30. 050	2.2	5.0	040	90			M
164	68081700-68081706	6	2	27. 080	2.0	6.0	090	162			L
165	68081706-68081706	1	1	27. 080	2.0	6.0	080	27			M
166	68090706-68090803	21	4	30. 270	3.8	6.0	270	630			L,M
167	68092112-68092200	12	3	26. 200	5.6	6.0	271	312			L,M
168	68092306-68092318	12	3	32. 250	1.8	14.0	239	384			L,M
169	68100323-68100405	6	2	27. 290				162			N
170	68100418-68100418	1	1	16. 060	3.6	12.0	059	16			L
171	68101712-68101719	7	7	31. 090				217			N
172	68102503-68102600	21	22	30. 070				630			N
173	68102600-68102600	1	1	30. 160	3.6	14.0	167	30			M
174	68102701-68102817	40	42	39. 090				1560			N
175	68110612-68111112	120	21	30. 090				3600	969.2		N,S

TABLE A.1 (continued)

176	68111511-68111523	12	3	28.	290				336				N
177	69071603-69071621	18	3	25.	280	0.0	14.0	167	450				M
178	69072611-69072623	12	3	30.	290				360				N
179	69080505-69080523	18	3	30.	320				540				N
180	69080709-69080806	21	4	37.	140	0.0	14.0	167	777				M
181	69082023-69082105	6	2	27.	360				162				N
182	69090403-69090418	15	2	28.	110	0.0	14.0	167	420				M
183	69091003-69091109	30	9	33.	070	2.0	5.0	070	990				L,M
184	69091818-69092000	30	6	30.	100	1.5	5.0	120	900				L,M
185	69092708-69092711	3	2	27.	180				81				N
186	69100218-69100900	150	26	30.	290				4500	966.7			N,S
187	69102417-69102717	72	18	32.	270				2304				N
188	69110116-69110314	46	31	32.	090				1472				N
189	70072818-70072900	6	3	30.	070	0.0	5.0	060	180				M
190	70073012-70073019	7	6	28.	110				196				N
191	70080206-70080318	36	6	30.	300	2.0	5.0	280	1080				L,M,N
192	70080506-70080518	12	3	26.	110	2.0	6.0	110	312				M
193	70080518-70080612	18	5	26.	110	2.0	6.0	110	468				L
194	70080812-70080906	18	4	20.	030	1.5	5.0	030	360				L
195	70082721-70083000	51	5	25.	310	2.5	5.0	325	1275				L,M
196	70090218-70090716	118	37	45.	110	4.5	12.0	330	5310		3.6	8	C,L,M,N
197	70090921-70091105	32	4	30.	210	1.5	5.0	250	960				L,M,N
198	70091313-70091512	47	28	63.	240	5.6	7.0	284	2961	968	2.5	6	A,C,L,N,N,T
199	70091706-70091812	30	3	23.	320	2.0	5.0	180	690				L
200	70100618-70100618	1	1	26.	050	2.0	5.0	050	26				L
201	70101211-70101302	15	4	30.	320				450				N
202	70101512-70101512	1	1	33.	060	1.0	5.0	060	33				M
203	70101816-70101905	13	10	35.	160				455				N
204	70102017-70102123	30	25	35.	160				1050				N
205	70110117-70110123	6	4	35.	270				210				N
206	70110300-70110307	7	5	26.	070				182				N
207	70110700-70111212	132	23						0	962.7			S
208	71070100-71070100	1	1	40.	300	10.6	22.0	282	40				L,M
209	71072806-71072806	1	1	19.	260	1.5	5.0	260	19				L
210	71072900-71073003	27	9	30.	270	0.0	22.0	282	810				C,M,N
211	71080303-71080315	12	6	28.	360	2.6	6.7		336				C,N
212	71080318-71080708	86	18	37.	250	0.0	22.0	282	3182				M
213	71082218-71082306	72	5	26.	360	2.9	7.1		2520		2.9	7	C,N
214	71090306-71090412	30	26	34.	090	0.0	22.0	282	1020				M,N
215	71090806-71090806	1	1	27.	200	1.1	5.0	099	27				M
216	71092312-71092312	1	1	12.	350	6.0	5.0	350	12				L
217	71100200-71100200	1	1	24.	220	2.0	12.0	220	24				L
218	71102100-71102118	18	5	35.	260				630				N
219	71103000-71103018	18	2	29.	290				522				N
220	71110106-71110418	84	8	37.	270				3108				N
221	71111021-71111212	39	39	32.	090				1248				N
222	72081302-72081400	22	2	25.	320	1.0	5.0	100	550				M
223	72081418-72081500	6	2	16.	100	1.5	5.0	100	96				L
224	72081806-72081900	18	2	25.	100	1.5	8.0	110	450				L
225	72081900-72081906	6	2	27.	110	1.5	6.0	100	162				M
226	72082012-72082012	1	1	30.	090	2.0	5.0	090	30	1001			A,L

TABLE A.1 (continued)

227	72082012-72082112	24	5	50.	320	2.0	5.0	090	1200			M,N,T
228	72082400-72082522	46	17	35.	320	0.0	5.0	090	1610			M,N
229	72083000-72083006	6	2	17.	110	2.0	5.0	110	102			L
230	72090110-72090209	23	12	40.	290	3.7	7.0		920			C,L,N
231	72090506-72090506	1	1	15.	100	1.5	6.0	100	15			L
232	72090700-72090806	30	4	24.	090	1.5	6.0	080	720			L
233	72091012-72091018	6	2	23.	080	1.5	6.0	080	138			L
234	72091200-72091318	42	1			2.7	6.6		0			C
235	72091606-72091706	24	2	31.	340	2.5	5.0	330	744			L,M
236	72091914-72092002	12	2	34.	250	0.0	6.0	340	408			M
237	73072100-73072112	12	6	48.	280				576			N,T
238	73090200-73090218	18	4	27.	090	2.9	8.0	135	486			L,M
239	73090406-73090412	6	2	26.	130	1.1	5.0	156	156			M
240	73090612-73090718	30	5	25.	100	6.5	12.0	103	750			L,M
241	73090912-73091006	18	4	27.	300	1.5	5.0	330	486			L,M,N
242	73091500-73091700	48	6	32.	270	3.5	7.0	300	1536			L,M,N
243	73092515-73092515	1	1	3.	180	3.0	5.0	180	3			L
244	74080115-74080215	24	4	40.	250	0.0	6.0	250	960			M
245	74080618-74080700	6	2	36.	090	0.0	6.0	250	216			M
246	74080919-74081121	50	26	42.	250	0.0	6.0	250	2100			M,N
247	74081400-74081510	34	25	30.	290	0.0	6.0	250	1020			M,N
248	74081800-74081803	3	2	20.	320	1.5	5.0	320	60			L
249	74081805-74082006	49	22	37.	290	1.5	5.0	310	1813			L,M,N
250	74082321-74082321	1	1	20.	090	1.5	5.0	090	20			L
251	74083106-74083106	1	1	10.	090	5.5	6.0	090	10			L
252	74090214-74090214	1	1	26.	300				26			N
253	74090317-74090403	10	11	35.	260				350			N
254	74090406-74090500	18	4	43.	340	0.0	5.0	330	774			M
255	74090606-74090618	12	2	26.	100	1.5	5.0	100	312			M
256	74090618-74090812	42	3	26.	100	2.0	6.0	080	1092			L
257	74091000-74091000	1	1	20.	090	1.5	5.0	090	20			L
258	74091606-74091700	18	4	29.	100	2.6	5.8		522			C,L,M
259	74101108-74101313	53	17	30.	240				1590			N
260	74101512-74101714	50	14	30.	270				1500			N
261	74102310-74102410	24	25	43.	270				1032			N
262	74102512-74102912	96	71	36.	090				3456			N
263	74103012-74103118	30	7	30.	080				900	969.5		N,S
264	74110319-74110406	11	12	30.	070				330			N
265	75071906-75071910	4	3	27.	290				108			N
266	75072022-75072120	22	15	29.	290				638			N
267	75072603-75072609	6	3	30.	050	0.0	6.0	100	180			M
268	75072909-75072918	9	3	26.	240	4.5	9.0	360	234			M
269	75080615-75080621	6	3	26.	340	1.5	5.0	340	156			L,M
270	75080815-75081118	75	29	40.	280	4.7	10.0	310	3000		2.4 6	L,M,V
271	75080908-75081108	48	5	28.	300				1344			N
272	75080921-75081203	1	1			2.4			0			D
273	75081800-75081903	27	4	61.	310	1.5	5.0	040	1647			L,M
274	75082606-75082814	56	29	45.	230	5.0	0.0	270	2520		2.2 6	D,L,M,N,V
275	75083003-75083015	12	2	56.	090	0.0	0.0	270	672			M
276	75090112-75090200	12	4	28.	270	1.5	5.0	270	336			L,M,N
277	75090606-75090800	42	7	34.	050	2.0	5.0	030	1428			L,M,N

TABLE A.1 (continued)

278	75091212-75091400	36	4	29.	260	2.9	6.0	230	1044					L,M,N
279	75091712-75092312	144	15	33.	230	4.0	6.0	070	4752					L,M,N
280	75092421-75092701	52	27	35.	270	1.0	5.0	120	1820					M,N
281	76080922-76081005	7	7	25.	100	2.0	6.0		175					P,R
282	76081121-76081423	72	61	35.	050	4.3	6.2		2520		2.8	6		B,C,D,L,M,N,P,R,V
283	76081422-76081615	41	14	29.	130	1.5	0.0		1189					R
284	76082109-76082213	28	42	40.	270	2.0	5.0		1120		2.2	6		D,L,M,N,P,R,V
285	76082312-76082400	12	5	30.	300	0.5	5.0		360					N,R
286	76082510-76082904	90	41	34.	090	2.0	5.0		3060					M,N,P,R
287	76090501-76090514	13	12	30.	280	2.0	5.0		390					P,R
288	76090816-76091009	41	67	32.	090	3.0	6.0		1312					M,N,P,R
289	76091018-76091203	1	1			2.6			0		2.6	7		D,V
290	76091204-76091707	123	148	30.	120	3.0	6.0		3690	963.0	1.8	8		M,N,P,R,S
291	76091907-76092218	80	88	37.	120	3.0	5.0	220	2960		1.7	6		L,M,N,P,R
292	76092323-76092706	79	55	38.	090	4.6	7.0	073	3002					L,M,N,P,R
293	76092814-76100208	90	166	32.	070	4.0	6.0	070	2880		1.9	6		L,M,P,R,V
294	76100412-76100500	12	2	33.	050	0.0	6.0	070	396					M
295	76101017-76101110	17	22	25.	290	2.0	6.0		425					P,R
296	76101112-76101812	168	29	35.	190	1.5	5.0		5880	965.4				N,P,R,S
297	76101813-76102012	47	26	35.	290	0.0	5.0		1645					N,R
298	77080600-77081306	174	152	33.	090	2.2	6.0	080	5742		1.8	6		L,M,N,P,R
299	77081308-77081713	101	87	37.	100	1.5	5.0	080	3737					N,P,R
300	77081718-77081800	6	2	28.	300	0.0	6.0	080	168					M
301	77082105-77082509	100	36	35.	090	2.0	6.0	130	3500					L,M,R
302	77082512-77082918	102	59	41.	320	3.4	6.9		4182				3.2	8 B,C,D,E,F,L,M,N,P,R,T,V
303	77083115-77090201	58	31	32.	310	2.5	6.0	320	1856					D,P,R
304	77090318-77090318	1	2	23.	240	1.5	5.0	240	23					L
305	77090506-77090512	6	2	17.	280	1.5	5.0	280	102					L
306	77090603-77090921	90	55	36.	120	2.5	6.0	350	3240					D,L,M,P,R,V
307	77091100-77091522	118	33	32.	130	3.5	6.0	055	3776					D,L,M,P,R,V
308	77091903-77091905	2	2	26.	080	1.0	5.0	080	52					R
309	77092018-77092100	6	2	20.	060	2.0	5.0	030	120					L
310	77092100-77092214	38	60	42.	270	3.0	6.0	290	1596				2.9	7 D,N,P,R,V
311	77092309-77092808	119	173	40.	160	3.0	6.0	150	4760					D,F,L,M,N,P,R,T,V
312	77092818-77100411	137	60	32.	280	3.0	5.0	020	4384					D,L,M,N,P,R,T,V
313	77100515-77101213	166	179	45.	130	3.5	5.0	120	7470				2.2	8 B,D,F,N,P,R,T,V
314	77101306-77101309	3	4	17.	360	1.5	5.0	040	51					P
315	77101400-77101613	61	32	31.	060	2.6	6.1		1891	960.3				C,N,P,R,S
316	77101720-77101913	41	28	30.	110	2.0	5.0		1230					P,R
317	77102100-77102306	54	22	54.	150	2.5	6.0	100	2916	950.2				N,P,R,S
318	78081715-78081715	1	1	10.	340	1.5	5.0	340	10					L
319	78082017-78082112	19	13	33.	220	0.0	5.0		627					R
320	78082304-78082712	104	54	40.	300	3.1	6.7		4160					C,E,N,R
321	78082900-78090900	240	211	40	090	2.7	6.0	037	9600				2.7	8 B,C,D,F,L,M,N,R,T,V
322	78090906-78091412	126	54	38.	030	6.3	8.0	062	4788	969.0			1.9	7 L,M,R,S,V
323	78091519-78091715	44	31	47.	310	3.4	8.0	003	2068					D,L,N,R,P,V
324	78091812-78091812	1	1	23.	090	2.0	5.0	090	23					L
325	78091900-78092206	91	99	40.	070	7.5	12.0	098	3640				3.6	10 B,C,D,L,M,N,R,V
326	78092900-78100303	99	98	45.	280	3.5	5.0		4455				2.4	9 M,N,R,T,V
327	78100600-78101004	100	162	50		3.5	7.0		5000					B,F,M,N,R,T
328	78101206-78102412	294	62	42.	220				12348	968.4				M,N,R,S

TABLE A.1 (continued)

329	79081310-79081904	138	279	38.	100	4.5	5.0	070	5244			D,L,M,N,P,R,V
330	79082002-79082600	142	94	37.	100	3.0	5.0	280	5254			D,F,L,M,N,P,R,T,V
331	79090709-79090719	10	11	20.	110	2.0	6.0	100	200			L,P
332	79090900-79090913	13	14	12.	300	1.5	5.0	290	156			L,P
333	79091110-79091923	205	448	36.	070	4.0	6.0	090	7380		2.5	9 D,L,M,N,P,R,V
334	79092106-79100705	383	339	95.	100	4.5	6.0	100	36385	965.2	2.4	7 B,C,D,E,F,L,M,N,P,R,S,T,V
335	79100800-79101720	236	441	40.	110	4.5	6.0	080	9440		2.0	6 B,D,L,M,N,P,R,V
336	79101820-79101923	27	60	27.	100	2.5	8.0	110	729			L,M,P,R
337	79102112-79102606	114	122	45.	060	0.5	5.0	070	5130	953.9		M,N,R,S,T
338	79102718-79102816	22	4	27.	080	1.5	5.0	040	594			L,M,N
339	79103012-79103021	9	4	30.	130	0.0	5.0	070	270			M,R
340	80071300-80071418	42	25	31.	090	2.0	5.0	080	1302			M,N,P,R
341	80071915-80072006	15	3	25.	070	1.5	5.0	070	375			L,M
342	80072504-80072700	44	37	30.	290	2.6	6.9		1320			C,L,N,P,R
343	80073000-80080120	81	67	29.	070	2.7			2349			B,L,M,P,R
344	80080613-80080713	24	13	30.	130	1.5	5.0	140	720			L,P,R
345	80081021-80081101	4	5	16.	080	1.5	5.0	040	64			P
346	80081515-80081902	83	59	26.	300	2.0	5.0	060	2158			N,P,R
347	80082308-80082310	2	3	26.	150	0.5	5.0	140	52			R
348	80082510-80082511	1	2	0.	000	1.5	5.0	300	0			P
349	80082722-80082800	2	2	27.	250	1.0	5.0	260	54			R
350	80082800-80082816	120	12	22.	280	2.0	5.0	240	2640		3.3	8 P,T,V
351	80082900-80090503	171	117	40.	280	3.7			6840			B,D,F,N,P,R
352	80090621-80090713	16	8	30.	220	1.5	5.0	240	480			P,R
353	80090906-80090909	3	3	25.	290	0.5	5.0	300	75			R
354	80091321-80091800	99	56	40.		3.7			3960			B,N,P,R
355	80092102-80092106	4	3	25.	340	1.5	5.0	350	100			P,R
356	80092306-80092318	12	2	33.	270				396			N
357	80092704-80100918	302	59	35.	080	2.5	6.0	080	10570	955.3		B,M,N,P,R,S
358	80101012-80101112	24	2	28.	120				672			N
359	80101606-80101712	30	4	36.	240				1080			N
360	80102306-80102513	55	31	31.	100				1705			N
361	81071600-81072104	124	108	34.	100	5.0	5.0	110	4216			B,M,N,P,R
362	81072214-81072300	10	11	18.	130	1.5	5.0	130	180			P
363	81072414-81072420	6	9	19.	100	1.5	5.0	080	114			P
364	81072503-81072513	10	12	28.	140	1.0	5.0	120	280			R
365	81072615-81073023	104	153	38.	130	4.0	5.0	110	3952			B,L,M,N,P,R,V
366	81080200-81080421	70	201	40		4.0			2800			B,D,E,F,L,M,N,P,R,T,V
367	81080705-81081021	88	140	32.	090	3.0	5.0	090	2816			D,L,M,N,P,R
368	81081218-81081418	48	52	30.	120	2.5	5.0	090	1440			L,M,P,R
369	81081600-81081812	60	125	45.	290	6.0	5.0	290	2700			B,D,E,F,L,M,N,P,R,T,V
370	81081900-81082523	167	212	35.	310	3.5	6.0	080	5845	967.3		C,D,E,L,M,N,P,R,S,V
371	81082808-81090212	124	299	45.	240	4.0	8.0	270	5580			B,C,D,F,L,M,N,P,R,T,V
372	81090405-81090612	55	40	35.	330	2.5	5.0	330	1925			M,N,P,R
373	81090704-81091013	81	94	30.	090	3.0	6.0	100	2430			N,P,R
374	81091506-81092106	144	268	36.	080	4.5	8.0	090	5184			B,C,D,E,L,M,N,P,R,V
375	81092523-81092606	7	8	18.	050	5.0	5.0	090	126			P
376	81092700-81100811	275	710	36.	040	5.0	8.0	020	9900			B,C,D,E,F,M,N,P,R,T,V
377	81100913-81100913	1	1	22.	130	10.0	5.0	120	22			P
378	82071901-82072217	88	67	35.	350	3.0	6.3		3080			B,C,E,N,R
379	82072321-82072507	34	20	36.	300	0.0	5.0	100	1224			R

TABLE A.1 (continued)

380	82072614-82072912	70	111	50.		5.0	6.4		3500	1008	A,B,N,P,R,T,V
381	82073018-82080706	180	142	32.	250	2.5	5.0		5760		P,R
382	82081208-82081211	3	3	26.	080				78		N
383	82081215-82081300	9	3	27.	090	3.5	6.0	090	243		L,M
384	82081300-82081422	46	137	43.	150	3.0	6.0		1978		N,P,R
385	82081703-82081912	57	23	30.	310	2.0	5.0		1710		N,P,R
386	82081912-82082309	93	121	38.	280	3.5	6.0		3534		B,D,E,M,N,P,R,V
387	82082505-82082702	45	45	32.	110	1.5	5.0		1440		P,R
388	82083000-82090110	58	129	34.	070	2.5	5.0		1972		P,R
389	82090218-82090900	160	310	34.	050	2.5	6.0		5440		D,N,P,R,V
390	82090914-82091315	97	229	34.	100	2.7			3298		D,M,P,R,V
391	82091522-82091802	52	53	41.	230	3.0	5.0		2132		B,D,N,P,R,V
392	82091900-82092321	117	268	41.	110	4.0	6.0	110	4797		B,D,F,L,M,N,P,R,T,V
393	82092623-82092700	1	2	25.	010	1.5	5.0		25		P,R
394	82100101-82100200	23	29	20.	030	1.5	5.0		460		P
395	82100200-82101000	192	151	34.	290	3.0			6528	965.3	B,E,N,P,R,S
396	82101000-82101612	156	127	36.	320	3.0	6.0		5616	964.4	B,N,P,R,S
397	82101717-82102806	253	147	54.	270	4.0			13662	967.3	B,F,N,P,R,S,T
398	82102918-82103118	48	6	36.	220				1728		N
399	83070100-83070200	24	2	28.	320	0.0	6.0	110	672		M
400	83070118-83070216	22	2	28.	090				616		N
401	83070217-83070318	25	0	30		1.0			750		B
402	83071220-83071300	4	5	20.	320	1.5	5.0		80		P
403	83071521-83071700	27	17	20.	320	1.5	5.0		540		P
404	83072006-83072018	12	13	18.	080	1.5	5.0		216		P
405	83072500-83073000	120	119	32.	100	15.0	6.0		3840		B,P,R
406	83080105-83080505	96	195	32.	260	13.5	5.0	297	3072		L,M,N,P,R
407	83080606-83080606	1	1	14.	080	5.0	0.0	080	14		L
408	83080701-83081022	93	91	31.	140	3.0	5.0		2883		B,M,P,R
409	83081422-83081712	62	67	27.	080	4.0	6.0		1674		L,P,R,V
410	83081812-83081812	1	1	14.	160	2.0	5.0		14		P
411	83081900-83081906	6	2	20.	140	2.1	5.0	150	120		L
412	83082012-83082412	88	75	30.	110	6.8	6.0	110	2640		B,L,P,R,V
413	83082413-83082414	1	2	20.	350	3.0	5.0		20		P
414	83082718-83082800	6	3	20.	310	2.0	5.0		120		L,P
415	83082917-83091200	295	179	45.	280	5.4	6.0	262	13275		B,D,L,M,N,P,R,V
416	83091422-83091618	44	25	30.	330	2.0	5.0		1320		B,M,N,P,R
417	83092012-83092014	2	2	28.	170	1.5	5.0		56		P,R
418	83110700-83111212	132	24	45.	150	0.0	5.0	310	5940	962.3	B,F,M,N,R,S,T
419	83111512-83111612	24	3	30.	310	0.0	5.0	310	720		M
420	83112118-83112200	6	2	33.	160	0.0	5.0	310	198		M
421	84061522-84061522	1	1	25.	070				25		N
422	84061621	11	0						0		H
423	84062221-84062404	31	24	25.	070	2.0	5.0		775		P,R
424	84062505	41	0			2.0			0		H
425	84062521-84062712	39	23	30.	080	3.0	5.0		1170		H,P,R
426	84062900-84062900	1	1	26.	090				26		N
427	84062913	18	0			2.0			0		H
428	84062915-84063008	17	32	27.	080	2.0	5.0		459		P,R
429	84070120-84070223	27	18	25.	010	2.0	5.0		675		H,P,R
430	84070701	8	0			1.0			0		H

TABLE A.1 (continued)

431	84070913	18	0		0.5			0					H
432	84070919-84070935	16	0		2.5			0					H
433	84070920-84070920	1	1	26. 100	1.0	5.0		26					R
434	84070920-84071021	25	37	24. 080	2.5	5.0		600					P
435	84071221-84071401	28	26	22. 270	1.5	5.0		616					H,P
436	84071709-84072009	72	55	35. 250	2.0	5.0		2520					H,N,P,R
437	840722	0	0					0					H
438	84072509	26	0					0					H
439	84072515-84072622	31	17	29. 100	0.0	5.0		899					R
440	84072901	30	0		1.5			0					H
441	84072911-84073008	21	7	26. 230	1.5	5.0	080	546					H,R
442	84073100-84073100	1	1	16. 340	2.0	5.0		16					P
443	84080409-84080420	11	12	19. 060	1.5	5.0		209					P
444	84080810-84081213	99	88	36. 180	2.5	6.0	270	3564			2.0	5	D,H,N,P,R,V
445	84081318-84082105	179	98	37. 100	1.5	5.0		6623					H,N,P,R
446	84082400-84082800	96	122	38. 360	2.5			3648			2.2	6	E,H,N,P,R
447	84090218-84090218	1	1	25. 110	0.0	5.0	310	25					M
448	84090803-84090803	1	1	22. 090	1.5	5.0	090	22					H,L
449	84090806-84090809	3	2	28. 100	0.0	5.0	310	84					M
450	84090908-84091100	40	9	29. 080	3.0	20.0		1160					P,R
451	84091106-84091106	1	1	25. 120	1.0	5.0		25					R
452	84091223	10	0		1.0			0					H
453	84091303-84091304	1	3	26. 110	1.0	5.0		26					R
454	84091509-84091923	110	143	38. 090	2.5	5.0	100	4180			2.5	5	H,L,M,N,P,R
455	84092411-84092603	40	89	38. 150	3.2	8.0	190	1520					H,L,P,R
456	84092803-84100120	89	131	34. 110	4.0	5.0	350	3026			2.5	5	H,N,P,R
457	84100200-84101218	258	52	30. 080	0.0	5.0		7740	962.0				H,N,R,S
458	84101618-84101906	60	9	37. 200	0.0	5.0		2220					H,N,R
459	84102218-84102906	156	65	45. 280	0.0	5.0		7020					H,N,R
460	84110106-84110112	6	2	31. 210				186					N
461	84110302	19	0					0					H
462	84110312-84110400	12	3	36. 270				432					N
463	84110512-84110518	6	2	26. 270				156					N
464	84110806-84110906	24	4	27. 110				648					N
465	84111001	16	0					0					H
466	85080612-85080917	77	66	32. 130	1.0			2464			2.0	5	G,M,N,R
467	85081505-85081706	49	18	30. 290	2.5	5.0	323	1470					G,L,N,P,R
468	85082010-85082207	45	38	37. 120	1.0	5.0		1665					G,R
469	85082208-85082218	10	4	24. 110	1.5	5.0	050	240					L,P
470	85082423-85082514	15	9	35. 100	1.0	5.0		525					R
471	85082723-85082914	39	16	34. 130	0.5	5.0		1326					N,R
472	85083018-85083118	24	7	26. 120				624					N
473	85090103-85090318	63	40	34. 110	1.5	5.0		2142			3.5	5	B,L,P,R
474	85090418-85090618	48	7	34. 330				1632					N
475	85091221-85091906	153	312	50. 280	6.0	6.0		7650			E,F,G,I,J,K,L,M,N,P,R,T		
476	85092013-85092211	46	34	35. 220	2.0	5.0		1610					M,N,P,R
477	85092512-85092600	12	12	22. 330	1.5	5.0		264					P
478	85092622-85093014	88	64	42. 270	2.0	5.0	080	3696					L,M,N,P,R
479	85100211-85100223	12	10	19. 050	1.5	5.0		228					P
480	85110700-85111418	186	36	45. 140	0.0	5.0		8370	969.0				G,N,R,S
481	85111518-85112118	144	63	42. 270				6048					N

TABLE A.1 (continued)

482	86081918-86082006	12	2	30.	290				360				N
483	86082118-86082512	90	26	36.	320	5.1	9.0	331	3240				M,N
484	86082612-86082612	1	1	20.	160	1.5	5.0	160	20				L
485	86090306-86090306	1	1	20.	100	2.5	8.0	100	20				L
486	86090312-86090412	24	7	30.	270				720				N
487	86090706-86091712	246	32	32.	120	4.0	8.0	110	7872		3.2	5	L,M,N
488	86091912-86091918	6	2	25.	200				150				N
489	86092100-86092118	18	10	30.	340	0.0	14.0	160	540				M,N
490	86093000-86100100	18	24	30.					540		3.5	6	H
491	87082400-87082512	36	4	25.	290	2.5	6.0	280	900				L,M,N,V
492	87082800-87090106	102	68	46.	270	6.5	6.0	260	4692		3.5	9	L,M,N,V
493	87090500-87090618	42	11	35.	320	2.0	6.0	300	1470				L,M,N
494	87090817-87090822	5	5	33.	240				165				N
495	87090906-87090906	1	1	24.	280	1.5	5.0	280	24				L
496	87091300-87091418	42	7	34.	320	4.5	8.0	260	1428				L,M,N,V
497	87101400-87101606	54	19	33.	110				1782				N
498	87102106-87102900	186	32	30.	250				5580	959.2			N,S
499	87103118-87110118	24	3	34.	260				816				N
500	87110406-87110606	48	5	30.	090				1440				N
501	87110712-87111600	204	30	28.	110				5712	968.4			N,S
502	88061618-88061816	46	7	26.	090				1196				N
503	88062920-88070318	94	21	29.	080	0.0	8.0	260	2726				M,N
504	88071206-88071206	1	1	23.	090	2.0	5.0	090	23				L
505	88071212-88071219	7	6	27.	090				189				N
506	88072206-88072212	6	2	25.	290				150				N
507	88080103-88080500	93	61	38.	310	4.3	8.0	288	3534		2.7		L,M,N
508	88101218-88101406	36	12	36.	110	4.5	5.0	110	1296				L,M,N
509	88101512-88101806	66	47	43.	260				2838				N
510	88102000-88102318	90	16	45.	220				4050				N
511	88111400-88111412	12	2	26.	090				312				N

TABLE A.2

TOP 160 - Storm list for the Beaufort Sea

(Storms selected from top 512 storms. Selction criteria : Hs .GE 2.0 m or if there is only one observation, wind speed .GE.30.)

SOURCES:

A Severe storms over the Canadian Western High Arctic 1957-1983 Report #87-2
B Beaufort Weather Office Annual Summaries (1976-1985)
C Arctic Petroleum Operator's Association, 1983: Beaufort Sea Hindcast Study 1970-1982. APOA Study 203
D Seaconsult, 1986: An extreme value analysis of Storm Wave Power at Minuk.
E Baird & Associates, 1987: Estimation of the Wave Climate of Minuk I-53 1960-1985
F Buckley and Budgell, 1988:Meteorologically Induced Currents in the Beaufort Sea
G Sea Consult, 1989: Design Storm Characteristic, Amuligak Region, Beaufort Sea
H Maclaren Plansearch Database
I Seaconsult 1987: Wind and wave Hindcast for the storm of September 15 to 19, 1985
J Seaconsult 1986: Analysis of the ADGO Wave Measurements for the storm of September 15 to 18,1985
K Baird $ Associates, 1987: Estimation of the Wave Climate at Minuk I-53 during the storm of September 15 to 19,1985
L COADS.wave waves >= 1.5 m
M COADS.wind winds >= 25 kts
N LAST.wind winds >= 25 kts
P RIG.wave waves >= 1.5 m
R RIG.wind winds >= 25 kts
S SPASM central pressure <= 970 mb
T MPL HINDCAST
V MEDS

		START YYMMDDHH	END YYMMDDHH	DUR	OBS	WIND SPD (kts)	WIND DIR	COMBINED SEA HS (m)	COMBINED SEA TP (s)	COMBINED SEA DIR	SEVERITY INDEX	MINT CENT PRESSURE (mb)	WAVERIDER HS (m)	WAVERIDER TP (s)	SOURCE
	2	57072518	57072706	36	4	23.	330	2.5	8.0	340	828				L
	5	57080900	57080915	15	5	34.	230	3.0	8.0	230	510				L,M
	6	57081809	57081809	1	1	12.	070	5.5	5.0	200	12				L
	52	60081917	60082200	55	8	31.	320	3.5	5.0	310	1705				L,M,N
	74	61071317	61071500	31	6	48.	320	2.1	5.0	342	1488				L,M,N
*	86	62072115	62072506	87	20	50.	290	4.0	5.0	080	4350				L,M
*	87	62072506	62072506	1	1	26.	080	4.0	5.0	080	26				L,M
	95	62090311	62090715	100	34	56.	310	9.5	6.0	310	5600				L,M
	97	62090903	62091106	51	14	48.	250	8.0	6.0	230	2448				L,M
	100	62092706	62100118	108	19	26.	110				2808	968.5			M,N,S,T
	111	63082311	63082323	12	2	52.	230	5.5	6.0	220	624				L,M,N
	131	65071500	65071509	9	4	33.	070	3.5	5.0	050	297				L,M
	146	66082912	66082918	6	2	31.	040	3.4	6.0	066	186				L,M
	150	66102912	66110300	108	19	23.	190	2.9	10.0	116	2484	965.7			L,S
	152	67081912	67081912	1	1	8.	030	4.0	5.0	030	8				L
	161	67102912	67110606	186	32	21.	150	3.6	5.0	150	3906	958.9			L,S
	163	68071403	68071406	3	2	30.	050	2.2	5.0	040	90				L,M

TABLE A.2 (continued)

166	68090706-68090803	21	4	30.	270	3.8	6.0	270	630				L,M
167	68092112-68092200	12	3	26.	200	5.6	6.0	271	312				L,M
183	69091003-69091109	30	9	33.	070	2.0	5.0	070	990				L,M
196	70090218-70090716	118	37	45.	110	4.5	12.0	330	5310		3.6	8	C,L,M,N,V
198	70091313-70091512	47	28	63.	240	5.6	7.0	284	2961	968	2.5	6	A,C,L,M,N,T,V
208	71070100-71070100	1	1	40.	300	8.0	22.0	282	40				L,M
210	71072900-71073003	27	9	30.	270	2.9	7.0	282	810		2.9	7	C,M,N,V
211	71080303-71080315	12	6	28.	360	2.6	6.7		336		2.6	7	C,N,V
*213	71082218-71082306	12	5	26.	360	2.9	7.1		312		2.9	7	C,N,V
*216	71092312-71092312	1	1	12.	350	6.0	5.0	350	12				L
226	72082012-72082012	1	1	30.	090	2.0	5.0	090	30	1001			A,L
227	72082012-72082112	24	5	50.	320	2.0	5.0	090	1200				L,M,N,T
230	72090110-72090209	23	12	40.	290	3.7	7.0	310	920				C,L,N
234	72091200-72091318	42	1			2.7	6.6		0				C
235	72091606-72091706	24	2	31.	340	2.5	5.0	330	744				L,M
237	73072100-73072112	12	6	48.	280				576				L,M,T
238	73090200-73090218	18	4	27.	090	2.9	8.0	135	486				L,M
240	73090612-73090718	30	5	25.	100	6.5	12.0	103	750				L,M
242	73091500-73091700	48	6	32.	270	3.5	7.0	300	1536				L,M,N
251	74083106-74083106	1	1	10.	090	5.5	6.0	090	10				L
258	74091606-74091700	18	4	29.	100	2.6	5.8	100	522				C,L,M
268	75072909-75072918	9	3	26.	240	4.5	9.0	360	234				L,M
270	75080815-75081118	75	29	40.	280	4.7	10.0	310	3000		2.4	6	L,M,V
274	75082606-75082814	56	29	45.	230	5.0	0.0	270	2520		2.2	6	D,L,M,N,V
277	75090606-75090800	42	7	34.	050	2.0	5.0	030	1428				L,M,N
278	75091212-75091400	36	4	29.	260	2.9	6.0	230	1044				L,M,N
279	75091712-75092312	144	15	33.	230	4.0	6.0	070	4752				L,M,N
282	76081121-76081423	72	61	35.	050	4.3	6.2		2520		2.8	6	B,C,D,L,M,N,P,R,V
284	76082109-76082213	28	42	40.	270	2.2	6.0	290	1120		2.2	6	D,L,M,N,P,R,V
286	76082510-76082904	90	41	34.	090	2.0	5.0		3060				M,N,P,R
288	76090816-76091009	41	67	32.	090	3.0	6.0		1312		2.0	6	M,N,P,R,V
289	76091018-76091203	1	1			2.6			0		2.6	7	D,V
290	76091204-76091707	123	148	30.	120	3.0	6.0		3690	963.0	1.8	8	M,N,P,R,S,V
291	76091907-76092218	80	88	37.	120	3.0	5.0	220	2960		1.7	6	L,M,N,P,R
292	76092323-76092706	79	55	38.	090	4.6	7.0	073	3002				L,M,N,P,R
293	76092814-76100208	90	166	32.	070	4.0	6.0	070	2880		1.9	7	L,M,P,R,V
298	77080600-77081306	174	152	33.	090	2.2	6.0	080	5742		1.8	6	L,M,N,P,R
301	77082105-77082509	100	36	35.	090	2.0	6.0	130	3500				L,M,R
302	77082512-77082918	102	59	41.	320	3.4	6.9	290	4182		3.2	8	B,C,D,E,F,L,M,N,P,R,T,V
303	77083115-77090201	58	31	32.	310	2.5	6.0	320	1856		2.2		D,P,R
306	77090603-77090921	90	55	36.	120	2.5	6.0	350	3240		2.3	7	D,L,M,P,R,V
307	77091100-77091522	118	33	32.	130	3.5	6.0	055	3776		2.1	6	D,L,M,P,R,V
310	77092100-77092214	38	60	42.	270	3.0	6.0	290	1596		2.9	7	D,N,P,R,V
311	77092309-77092808	119	173	40.	160	3.0	6.0	150	4760		2.6	6	D,F,L,M,N,P,R,T,V
312	77092818-77100411	137	60	32.	280	3.0	5.0	020	4384		2.2	7	D,L,M,N,P,R,T,V
313	77100515-77101213	166	179	45.	130	3.5	5.0	120	7470		2.2	8	B,D,F,N,P,R,T,V
315	77101400-77101613	61	32	31.	060	2.6	6.1	060	1891	960.3	1.9	7	C,N,P,R,S
317	77102100-77102306	54	22	54.	150	2.5	6.0	100	2916	950.2			N,P,R,S
320	78082304-78082712	104	54	40.	300	3.1	6.7		4160				C,E,N,R
321	78090100-78090900	240	211	40	090	2.7	6.0	037	9600		2.7	8	B,C,D,F,L,M,N,R,T,V
322	78090906-78091412	126	54	38.	030	6.3	8.0	062	4788	969.0	1.9	7	L,M,R,S,V
323	78091519-78091715	44	31	47.	310	3.4	8.0	003	2068		2.4	8	D,L,N,R,V

TABLE A.2 (continued)

325	78091900-78092206	91	99	40. 070	7.5	12.0	098	3640		3.6	10	B,C,D,L,M,N,R,V
326	78092900-78100303	99	98	45. 280	3.5	5.0		4455		2.4	9	M,N,R,T,V
327	78100600-78101004	100	162	50 080	3.5	7.0		5000				B,F,M,N,R,T
329	79081310-79081904	138	279	38. 100	4.5	5.0	070	5244		2.4	7	D,L,M,N,P,R,V
330	79082002-79082600	142	94	37. 100	3.0	5.0	280	5254		2.4	8	D,F,L,M,N,P,R,T,V
333	79091110-79091923	205	448	36. 070	4.0	6.0	090	7380		2.5	8	D,L,M,N,P,R,V
334	79092118-79092412	66	42	35. 080	4.5	6.0	100	2310	965.2	2.4	7	B,C,D,E,F,L,M,N,P,R,S,V
334a	79092900-79100806	246	68	42. 080	3.5	6.0		10332				B,C,D,E,F,L,M,N,P,R,S,T
335	79100800-79101720	236	441	40. 110	4.5	6.0	080	9440		2.0	6	B,D,L,M,N,P,R,V
336	79101820-79101923	27	60	27. 100	2.5	8.0	110	729				L,M,P,R
337	79102112-79102606	114	122	45. 060	0.5	5.0	070	5130	953.9			M,N,R,S,T
342	80072504-80072700	44	37	30. 290	2.6	6.9	070	1320				C,L,N,P,R
343	80073000-80080120	81	67	29. 070	2.7	6.0	070	2349				B,L,M,P,R
350	80082800-80082816	16	12	22. 280	3.3	8.0	240	352		3.3	8	G,P,T,V
351	80082900-80090503	171	117	40. 280	3.7	8.0	280	6840		3.3	8	B,D,F,N,P,R,V
354	80091321-80091800	99	56	40. 130	3.7	6.0	100	3960		1.9	6	B,N,P,R
357	80092704-80100918	302	59	35. 080	2.5	6.0	080	10570	955.3			B,M,N,P,R,S
361	81071600-81072104	124	108	34. 100	5.0	5.0	110	4216		2.0	6	B,M,N,P,R
365	81072615-81073023	104	153	38. 130	4.0	5.0	110	3952		1.9	6	B,L,M,N,P,R,V
366	81080200-81080421	70	201	40 310	4.0	5.0	310	2800		2.7	7	B,D,E,F,L,M,N,P,R,T,V
367	81080705-81081021	88	140	32. 090	3.0	5.0	090	2816		2.0	7	D,L,M,N,P,R
368	81081218-81081418	48	52	30. 120	2.5	5.0	090	1440				L,M,P,R
369	81081600-81081812	60	125	45. 290	6.0	5.0	290	2700		3.4	8	B,D,E,F,L,M,N,P,R,T,V
370	81081900-81082523	167	212	35. 310	3.5	6.0	080	5845	967.3	2.3	7	C,D,E,L,M,N,P,R,S,V
371	81082808-81090212	124	299	45. 240	4.0	8.0	270	5580		2.4	7	B,C,D,F,L,M,N,P,R,T,V
372	81090405-81090612	55	40	35. 330	2.5	5.0	330	1925				M,N,P,R
373	81090704-81091013	81	94	30. 090	3.0	6.0	100	2430				N,P,R
374	81091506-81092106	144	268	36. 080	4.5	8.0	090	5184		2.3	7	B,C,D,E,L,M,N,P,R,V
375	81092523-81092606	7	8	18. 050	5.0	5.0	090	126				P
376	81092700-81092912	275	710	36. 040	5.0	8.0	020	9900		2.8	8	B,C,D,E,F,M,N,P,R,T,V
377	81100913-81100913	1	1	22. 130	10.0	5.0	120	22		3.5		P
378	82071901-82072217	88	67	35. 350	3.0	6.3		3080		2.5	6	B,C,E,N,R
380	82072614-82072912	70	111	50. 280	5.0	6.4		3500	1008	3.4	8	A,B,N,P,R,T,V
381	82073018-82080706	180	142	32. 250	2.5	5.0		5760		1.8	9	P,R
383	82081215-82081300	9	3	27. 090	3.5	6.0	090	243				L,M
384	82081300-82081422	46	137	43. 150	3.0	6.0		1978		2.0	6	N,P,R
386	82081912-82082309	93	121	38. 280	3.5	6.0		3534		2.8		B,D,E,M,N,P,R,V
388	82083000-82090110	58	129	34. 070	2.5	5.0		1972				P,R
389	82090218-82090900	160	310	34. 050	2.5	6.0		5440		2.3	6	D,N,P,R,V
390	82090914-82091315	97	229	34. 100	2.7	7.0		3298		2.7	7	D,M,P,R,V
391	82091522-82091802	52	53	41. 230	3.0	5.0		2132		2.4	7	B,D,N,P,R,V
392	82091900-82092321	117	268	41. 110	4.0	6.0	110	4797		3.3	8	B,D,F,L,M,N,P,R,T,V
395	82100200-82101000	192	151	34. 290	3.0	8.0		6528	965.3			B,E,N,P,R,S
396	82101000-82101612	156	127	36. 320	3.0	6.0		5616	964.4			B,N,P,R,S
397	82101717-82102806	253	147	54. 270	4.0	5.0		13662	967.3			B,F,N,P,R,S,T
405	83072500-83073000	120	119	32. 100	2.0	6.0		3840				B,P,R
406	83080105-83080505	96	195	32. 260	2.0	5.0	297	3072				B,L,M,N,P,R
407	83080606-83080606	1	1	14. 080	5.0	0.0	080	14				L
408	83080701-83081022	93	91	31. 140	3.0	5.0		2883				B,M,P,R
409	83081422-83081712	62	67	27. 080	4.0	6.0	020	1674		1.5	6	L,P,R,V
412	83082012-83082412	88	75	30. 110	6.8	6.0	110	2640		1.8	6	B,L,P,R,V
415	83082917-83091200	295	179	45. 280	5.4	6.0	262	13275				B,D,L,M,N,P,R,V

TABLE A.2 (continued)

418	83110700-83111212	132	24	45. 150			310	5940	962.3				B,F,M,R,S,T
422	84061621-84061710	11		21. 045				231					B
425	84062521-84062712	39	23	30. 080	3.0	5.0		1170					B,P,R
428	84062915-84063008	17	32	27. 080	2.0	5.0		459		2.0	5		P,R
429	84070120-84070223	27	18	25. 010	2.0	5.0		675		2.0	5		B,P,R
436	84071709-84072009	72	55	35. 250	2.0	5.0		2520		2.0	5		B,N,P,R
440	84072901-84073006	30	7	23. 230	1.5	5.0		690		1.5	5		B,R
444	84080810-84081213	99	88	36. 180	2.5	6.0	270	3564		2.2	6		D,B,N,P,R,V
445	84081318-84082105	99	88	37. 100	1.5	5.0		6623		1.7	6		B,N,P,R,V
446	84082400-84082800	96	122	38. 360	2.5	5.0	280	3648					E,B,N,P,R
447	84090218-84090218	1	1	25. 110			310	25					M
448	84090803-84090803	1	1	22. 090	1.5	5.0	090	22					B,L
450	84090908-84091100	40	9	29. 080	3.0	5.0		1160		3.0	5		P,R
452	84091223-84091309	10		23. 090	1.0	5.0		230					B,R
454	84091509-84091923	110	143	38. 090	2.5	5.0	100	4180					B,L,M,N,P,R
455	84092411-84092603	40	89	38. 150	3.2	8.0	190	1520					B,L,P,R
456	84092803-84100120	89	131	34. 110	4.0	5.0	350	3026					B,N,P,R
457	84100200-84101218	258	52	30. 080	3.0	5.0	040	7740	962.0				B,N,R,S
458	84101618-84101906	60	9	37. 200				2220					B,N,R
459	84102218-84102906	156	65	45. 280				7020					B,N,R
461	84110302-84110321	19		23. 315				437					B
465	84111001-84111017	16		22. 315				352					B
466	85080612-85080917	77	66	32. 130	2.0	5.0		2142					B, R
467	85081505-85081706	49	18	30. 290	2.5	5.0	323	1470					B,L,N,P,R
473	85090103-85090318	63	40	34. 110	3.5	5.0		2520		3.5	5		B,L,P,R
475	85091221-85091906	153	312	50. 280	6.0	6.0	280	7650					B,E,F,I,J,K,L,M,N,P,R,T
476	85092013-85092211	46	34	35. 220	2.0	5.0		1610					M,N,P,R
478	85092622-85093014	88	64	42. 270	2.0	5.0	280	3696					L,M,N,P,R
480	85110700-85111418	186	36	45. 140				8370	969.0				B,N,R,S
483	86082118-86082512	90	26	36. 320	5.1	9.0	331	3240		3.2	5		H,M,N
485	86090306-86090306	1	1	20. 100	2.5	8.0	100	20		2.2	5		H,L,V
487	86090706-86091712	246	32	32. 120	4.0	8.0	110	7872		3.0	9		H,L,M,N
490	86093000-86100100	18	24	30. 100	3.5	6.0	100	540		3.5	6		H,L
*491	87082400-87082512	36	4	25. 290	2.5	6.0	280	900		2.0	7		L,M,N,V
*492	87082800-87090106	102	68	46. 270	6.5	6.0	260	4692		3.5	9		L,M,N,V
493	87090500-87090618	42	11	35. 320	2.0	6.0	300	1470					L,M,N
496	87091300-87091418	42	7	34. 320	4.5	8.0	260	1428		1.7	6		L,M,N,V
507	88080103-88080500	93	61	38. 310	4.3	8.0	288	3534		2.7			L,M,N
508	88101218-88101406	36	12	36. 110	4.5	5.0	110	1296					L,M,N

* Combined into one event in the final top 50 storms
Note : Events 334 and 334a are two seperates storms which were considered as one in the top 500 list.

APPENDIX B
ODGP SHALLOW WATER SPECTRAL GROWTH/DISSIPATION ALGORITHM

ODGP SHALLOW WATER SPECTRAL GROWTH/DISSIPATION

In recent years, two new concepts have been introduced to describe shallow-water wave transformations. The first concept follows from the theoretical finding that non-linear wave-wave interactions, which are now generally believed to play an important role in the deep-water spectral energy balance, are greatly enhanced in shallow water. Over a sloping bottom these interactions, though intrinsically energy conserving, effectively act to cause attenuation of wave height, as energy transferred from the vicinity of the spectral peak to higher frequencies is lost through wave breaking in the so-called saturation range of the spectrum. The second new concept is turbulent bottom friction, which depends sensitively on bottom-sediment properties and sediment-transport processes. These newer bottom friction theories, for which there is increasing experimental support, predict much higher friction coefficients than molecular viscosity theories.

These concepts have led to the introduction of a number of new shallow-water wave prediction models, but the properties of these models vary widely, and a number of controversial issues which affect the quantitative performance of these models in storm situations have yet to be resolved. This had led to a number of intercomparison studies involving alternate models. Several such studies are underway in the U.S., Canada, and Europe which may provide a clearer picture of he relevant physics for shallow-water transformation (the first phase of one of the most extensive intercomparisons, known as SHIP and supported by a consortium of U.S. oil companies, has been completed, and a second Phase, SHIP2, will proceed this year). One of the seeming consequences of the dominance of one or both of the above source terms in the process of shallow-water transformations (over the classical effects of shoaling and refraction which, except in highly inhomogeneous bottom conditions, are relatively slight in comparison) is the recent finding that wind/wave spectra in shallow water follow a self-similar form that can be described by the so-called TMA spectrum (Bouws et al., 1984).

The TMA spectrum, which has been shown to fit well literally thousands of measured spectra from the North Sea and Atlantic continental shelf, has been interpreted by Bouws et al. (1985) as an upper limit to finite-depth spectra in wind seas propagating through sloping bottoms typical of those over which the TMA spectrum was defined.

A second apparent source term of importance, especially for wave components of longer period than that of the spectral peak, is bottom friction due to bottom-sediment properties, ripple formations, and sediment transport to be modelled.

Mechanisms Modelled

The growth algorithm, called CMPE28GG, can be explained by starting with CMPE24. The following changes are made to the algorithm of CMPE24 to yield that of CMPE28A.

1. The reference spectrum is computed as Pierson-Moskowitz without an ω^{-4} range. Several traditional approximations in the numerics combine to yield

$$\alpha = 8.18559 \times 10^{-3}.$$

2. The Pierson-Moskowitz peak frequency is computed from the wind speed:

$$\omega = 0.8790132 \frac{g}{U_{19.5}}$$

where $U_{19.5}$ is wind speed at 19.5 m above sea level. This numeric implies that the constant ß in the P-M spectral formula, nominally 0.74, is here taken as 0.7462625. The corresponding shallow-water wave number (k) is obtained as

$$\hat{K} \tanh(\hat{k}d) = \frac{\omega^2}{g}$$

and the fully-developed shallow-water total variance as

$$E_{tot} = 0.2 \; x \; 8.18559 \; x \; 10^{-3} \; x \; k^{-2}$$

3. At the beginning of each time step, the rms bottom excursions and rms bottom velocity are computed from

$$a^2_{rms} = \sum \frac{s(i)}{\sinh^2 k_i d}$$

$$U^2_{rms} = \sum \frac{s(i)\omega^2_i}{\sinh^2 k_i d}$$

where s(i) is the variance component (<u>not</u> the spectral density), integrated over all directions, in frequency bin i; ω_i is the nominal radian frequency $(2 \pi f)$ in that bin; d is water depth (in feet in the code used; but the combination kd is dimensionless); and k_i is the scalar wave number computed from the shallow-water dispersion relation

$$\frac{\omega^2}{g} = k \tanh kd$$

4. The α used in computing the tail of the spectrum is allowed to float according to Resio's (1981) correlation:

$$\alpha = \alpha_o \left(\frac{E}{E_{pm}}\right)^{-.23}$$

where

$$\alpha_o = 8.18559 \times 10^{-3} \text{ and } E_{pm} = 0.2\alpha_o g^2 \omega^{-4}$$

5. A bottom-friction factor, FW, is computed, following Grant and Madsen (1982), as the greatest of three tentative factors:

   a) a smooth-flow friction factor depending on the Reynolds number

$$Re = 2.005^2 \frac{U_{rms} a_{rms}}{\nu}$$

   where υ is the kinematic viscosity of sea water (a_{rms} is rms value of bottom excursion and U_{rms} is bottom orbital velocity). (For very small values of bottom excursion, the code is in SHALLOW3 yields an unphysically high value of FW).

   b) a skin-friction factor, depending on the ratio of bottom excursion to sand-grain diameter (a sand-grain diameter of 0.2 mm was assumed throughout).

   c) a friction factor reflecting the ability of the bottom velocity to raise ripples; it is a non-dimensional function of bottom excursion, bottom velocity, gravity, sand-grain diameter, and excess of the density of sand over the density of water.

6. For each frequency band, the rate of dissipation, with dimension T^{-1}, is computed as

$$-FW \times U_{rms} \times \frac{\sinh^2 k_i}{g\omega_i^2}$$

7. The A-term (linear growth) is computed as in CMPE24; the B-term (exponential growth) is a function of $\frac{u_*}{c}$, where c is now the shallow-water celerity

$$c = (\frac{g}{\omega}) \tanh (\omega \frac{d}{c})$$

8. Fore each frequency-direction bin, the algebraic sum of B-term and dissipation is taken: this can be positive, negative or zero. (The case where growth exactly balances bottom friction must be regarded to prevent division by zero). Because the growth rate can be arbitrarily close to zero, the function

$$exp(B\ \Delta t)\ -\ 1,$$

naturally occurring in the growth algorithm, is used in the floating-point computational form

$$exp(B\ \Delta t)-1\ =\ 2\ exp(B\ \frac{\Delta t}{2})\ \sinh(B\ \frac{\Delta t}{2})$$

9. After upwind components are dissipated, as in CMPE24, to total variance, E, is computed by summing over 360 frequency-directional bins. The floating α is recomputed from

$$\alpha\ -\ 8.18559\ 10^{-3}(\frac{E}{E_{tot}})^{-.23}$$

where E_{tot} was defined in equation (1) above. The bands to the right of the P-M peak are now computed to the k-scaled tail density

$$\frac{dS}{dk} = \frac{1}{2}\ \alpha\ k^{-3},$$

frequency-direction bins (in downwind directions) that exceed the integral of this density, spread into directions according to the SWOP (Cote et al., 1960) distribution, are cut back.

References:

Bouws, E., J. J. Ephraums, J. A. Ewing, P. E. Francis, H. Gunther, P.A. Janssen, G. J. Komen, W. Rosenthal, and W. J. deVoogt. 1985. A shallow water intercomparison of three numerical wave prediction models (SWIM). Qrtly. J. Royal Met. Soc., III, 1087, 1112.

Cote, J., J. O. Davis, W. Marks, R. J. McGough, E. Mehr, W. J. Pierson, J. F. Ropek, G. Stephenson, and R. C. Vetter. 1960. The directional spectrum of wind generated sea as determined from data obtained by the Stereo Wave Observation Project (SWOP). Meteorological Papers, 2, 6, New York University, College of Engineering. New York University Press, NY, 88 pp.

Grant, W. D. and O. S. Madsen. 1982. Movable bed roughness in unsteady oscillatory flow. J. of Geophys. Res., 87, C2, 469 - 481.

Resio, D. T. 1981. The estimation of wind-wave generation in a discrete spectral model. J. of Phys. Oceanography, 11, 510 - 525.

APPENDIX C
ICE CHARTS

- **Top 30 Hindcast Storms**
- **Climatology Charts**

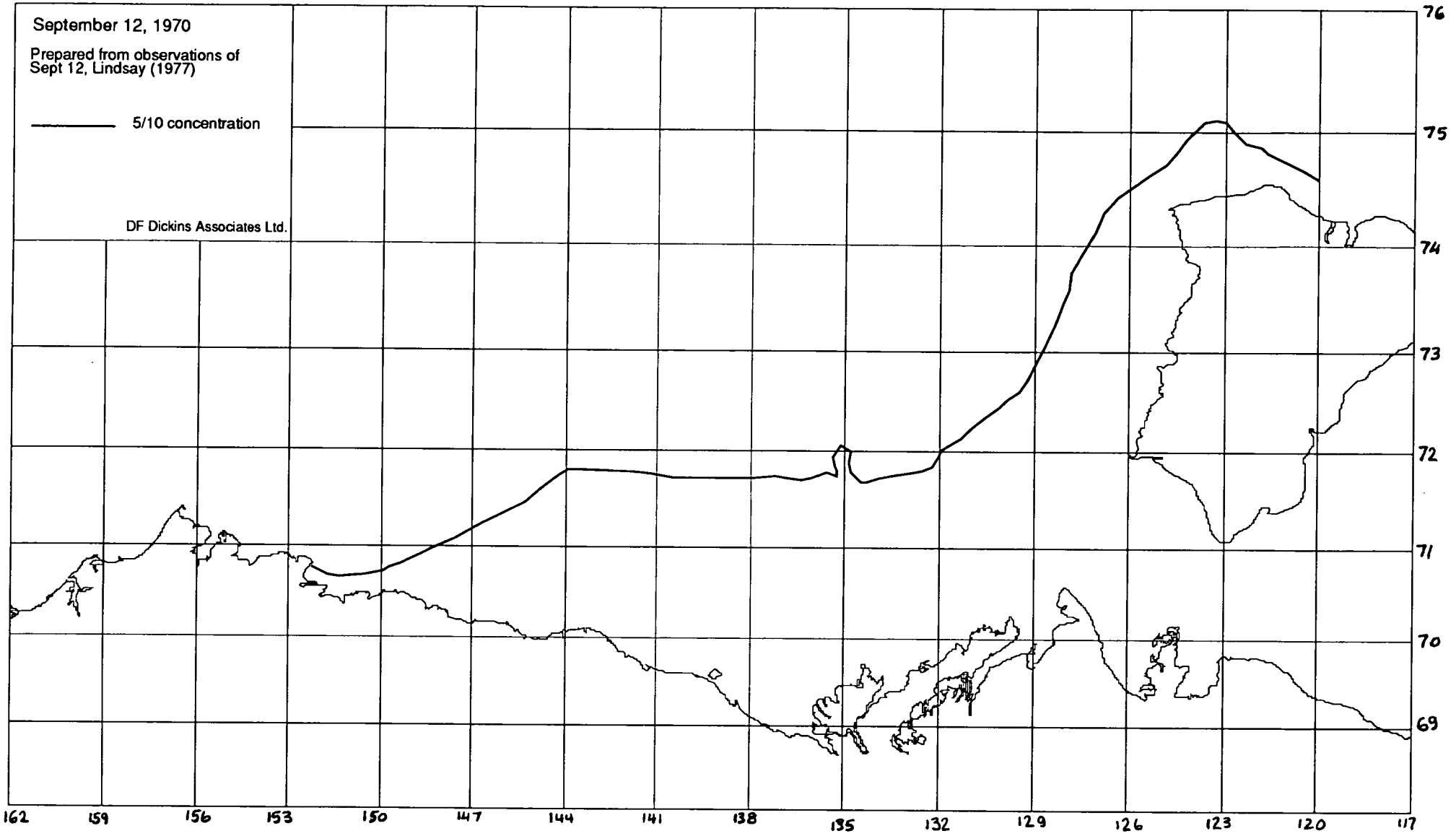
September 12, 1970
Prepared from observations of Sept 12, Lindsay (1977)
5/10 concentration
DF Dickins Associates Ltd.
76
75
74
73
72
71
70
69
162
159
156
153
150
147
144
141
138
135
132
129
126
123
120
117

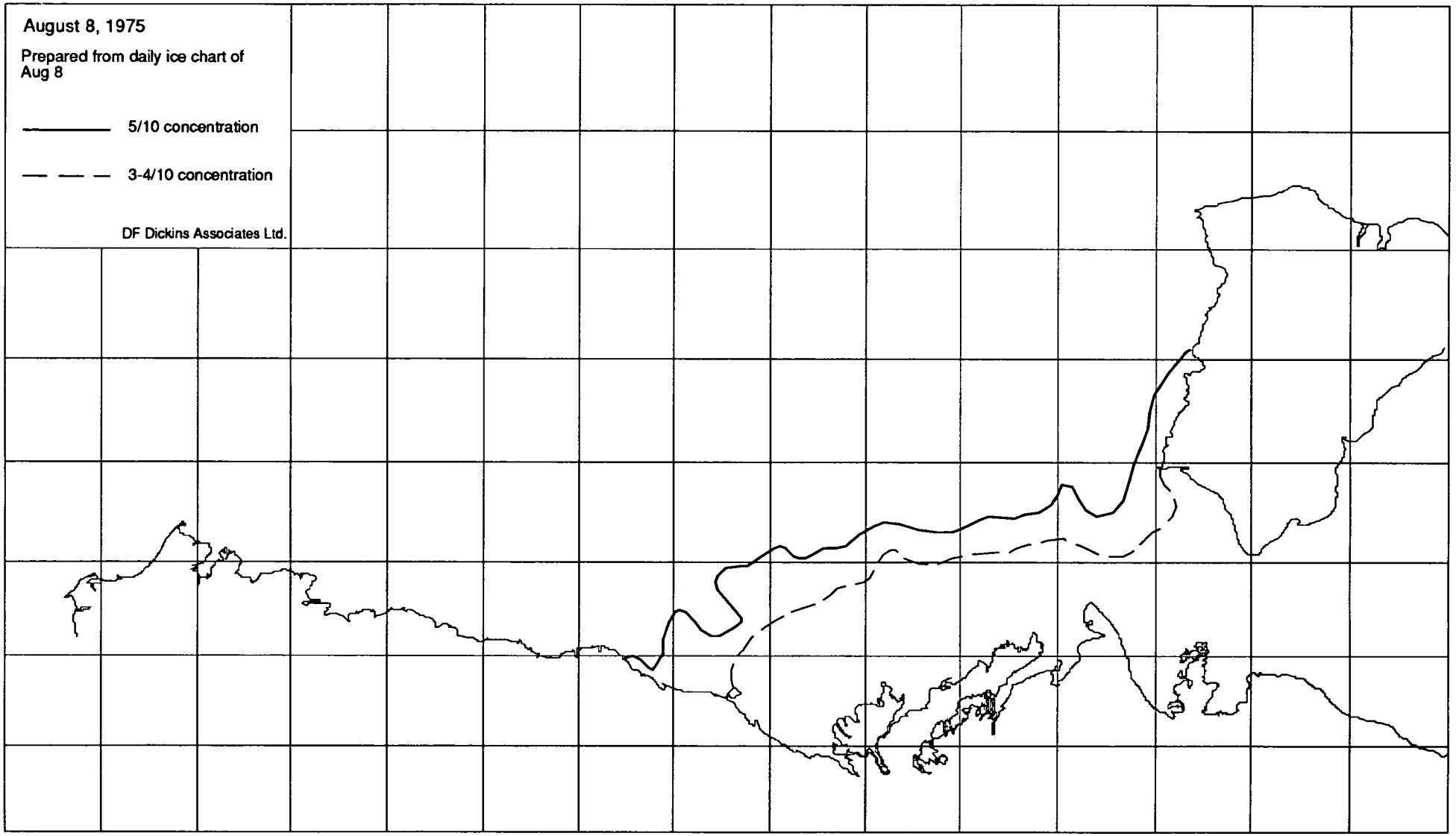
August 8, 1975
Prepared from daily ice chart of Aug 8
5/10 concentration
3-4/10 concentration
DF Dickins Associates Ltd.

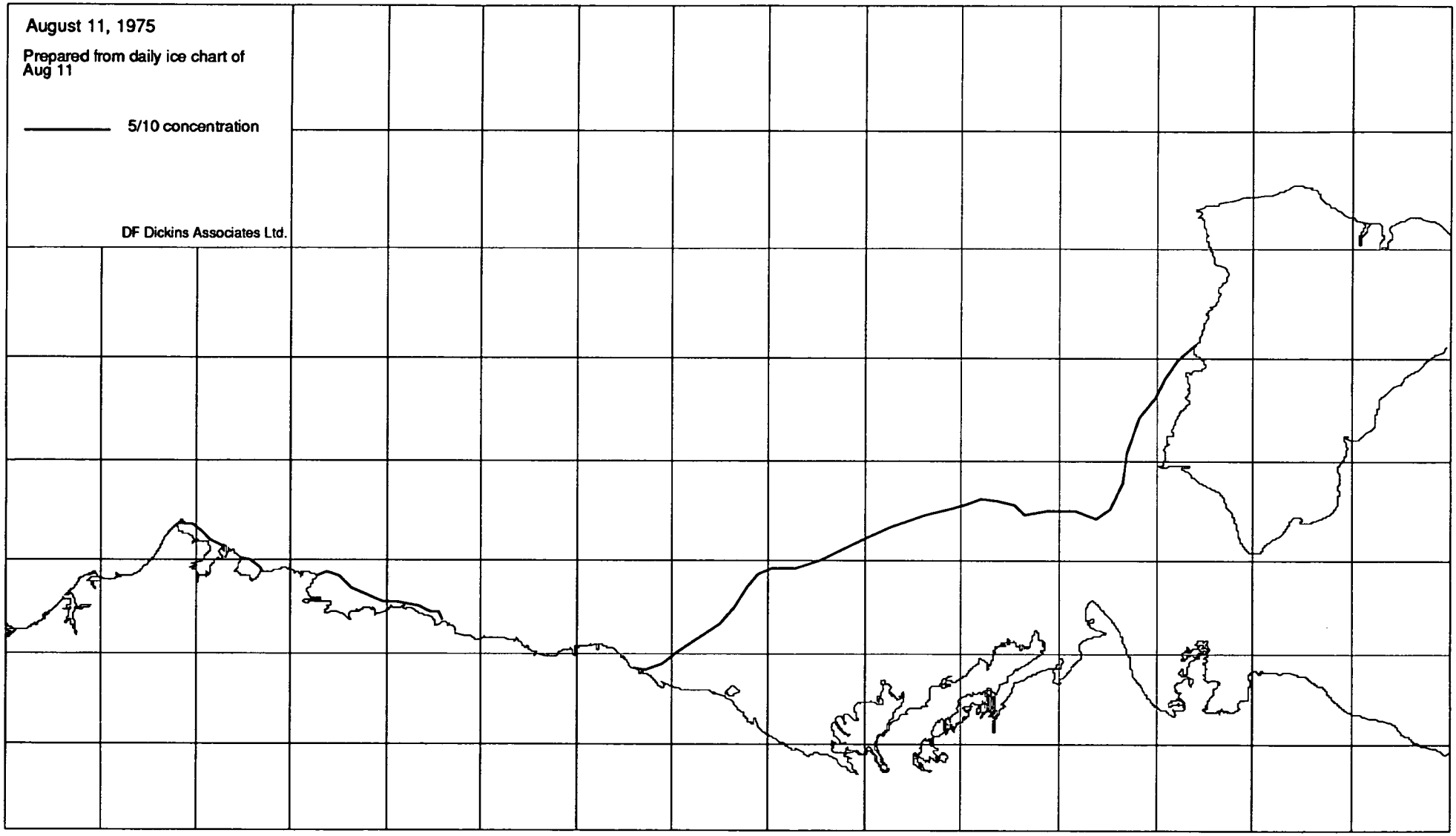
August 11, 1975
Prepared from daily ice chart of Aug 11
5/10 concentration
DF Dickins Associates Ltd.

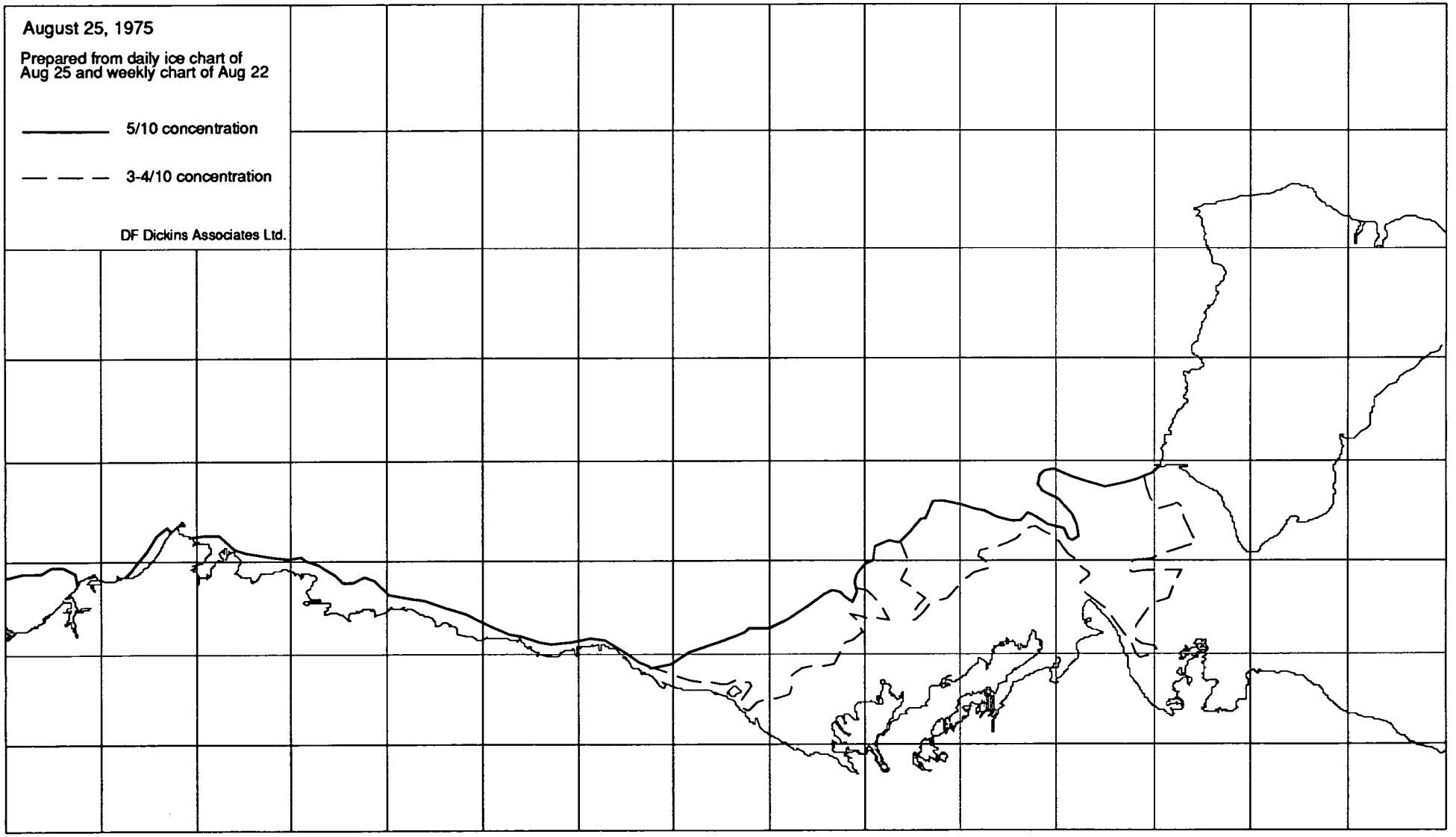
August 25, 1975
Prepared from daily ice chart of
Aug 25 and weekly chart of Aug 22
5/10 concentration
3-4/10 concentration
DF Dickins Associates Ltd.

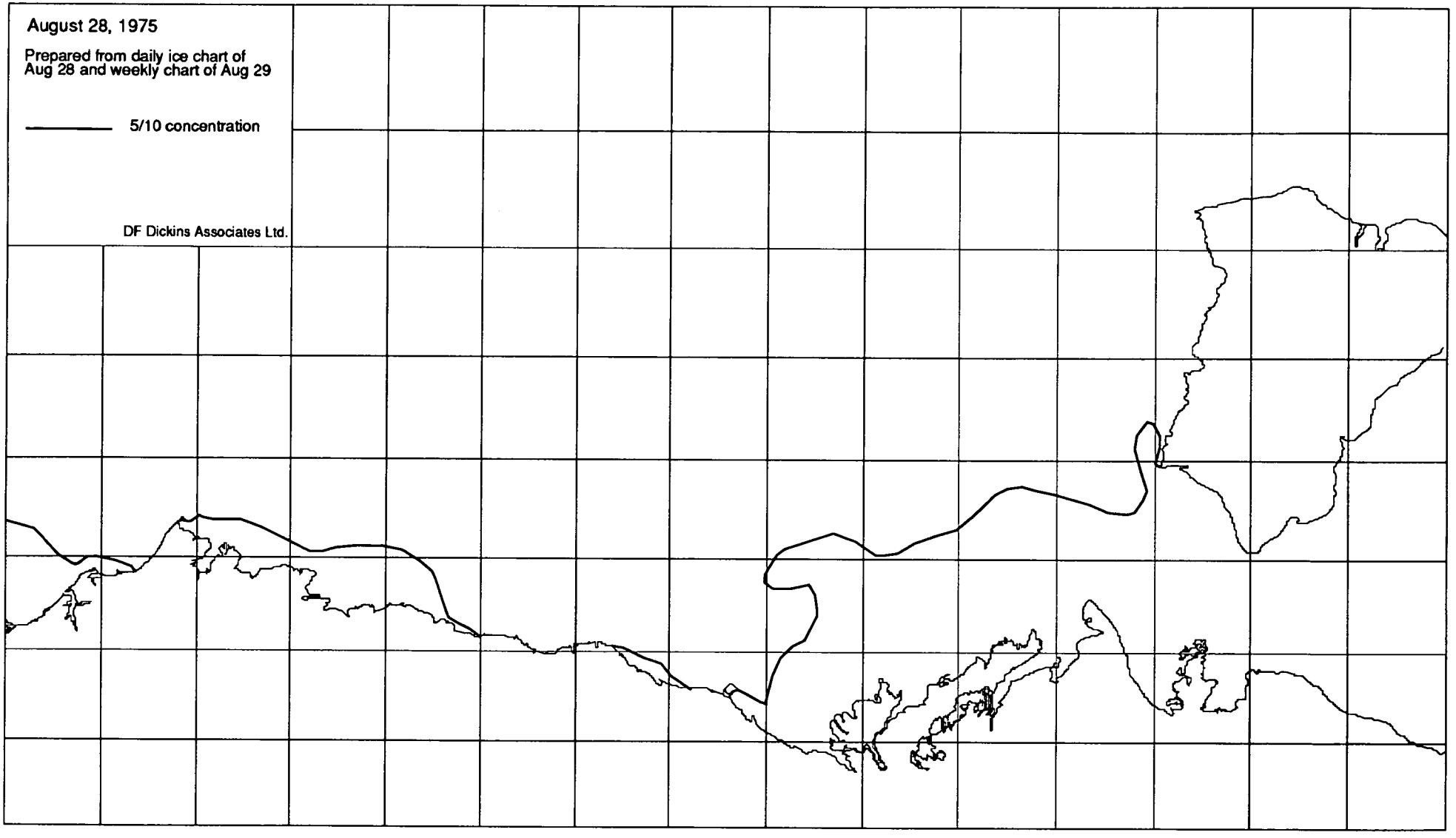
August 28, 1975
Prepared from daily ice chart of
Aug 28 and weekly chart of Aug 29
5/10 concentration
DF Dickins Associates Ltd.

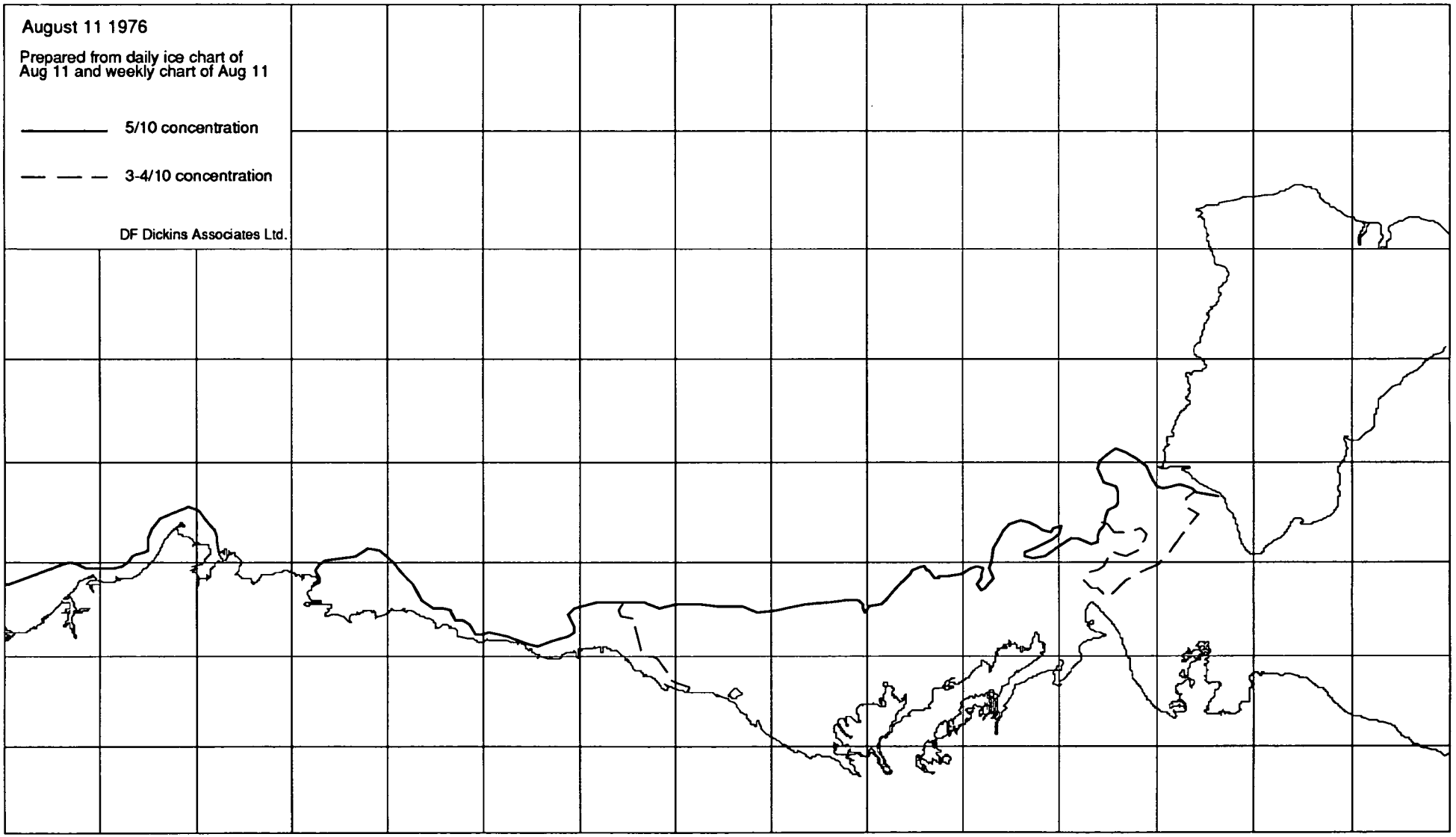
August 11 1976
Prepared from daily ice chart of
Aug 11 and weekly chart of Aug 11
5/10 concentration
3-4/10 concentration
DF Dickins Associates Ltd.

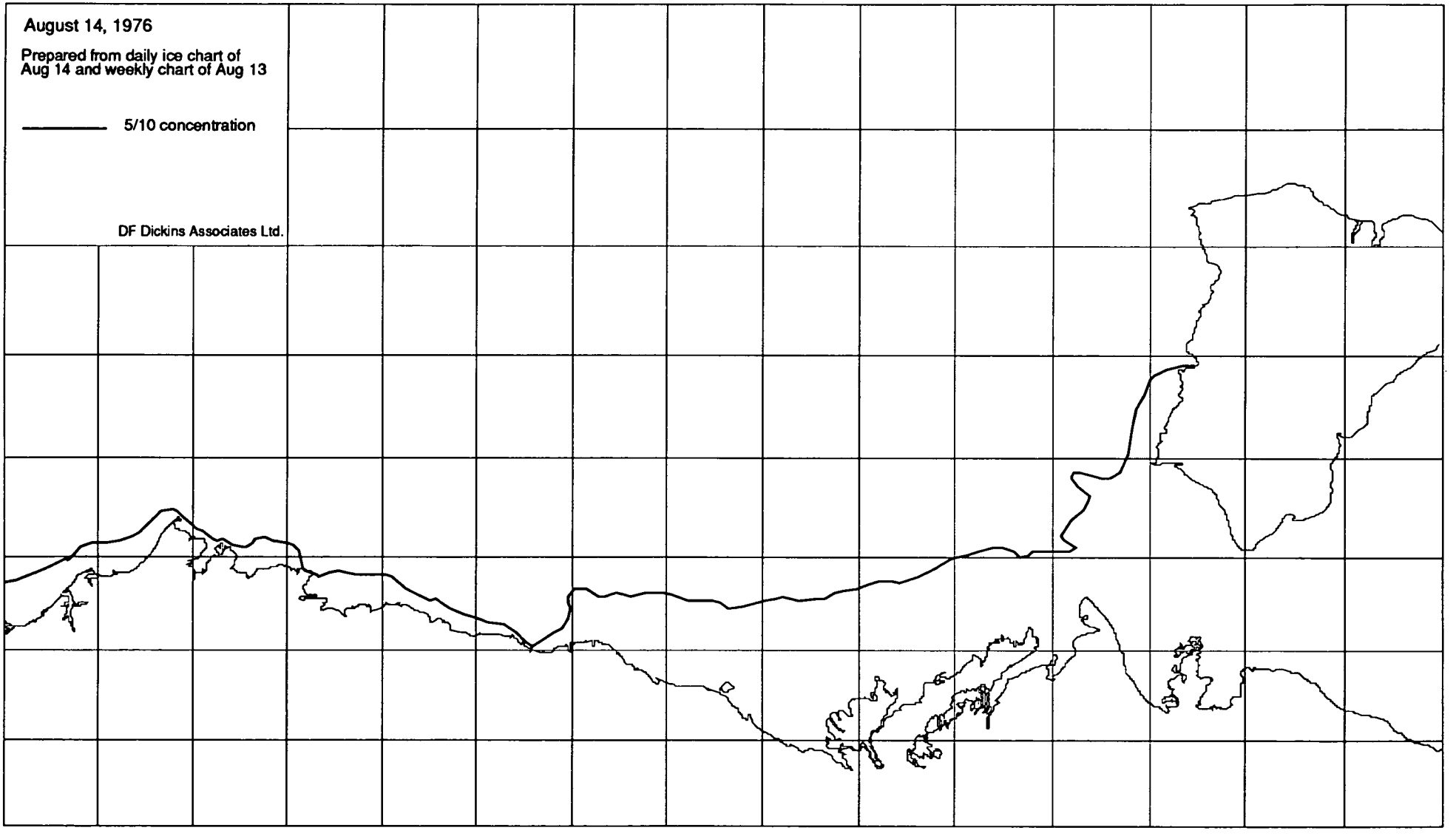
August 14, 1976
Prepared from daily ice chart of
Aug 14 and weekly chart of Aug 13
5/10 concentration
DF Dickins Associates Ltd.

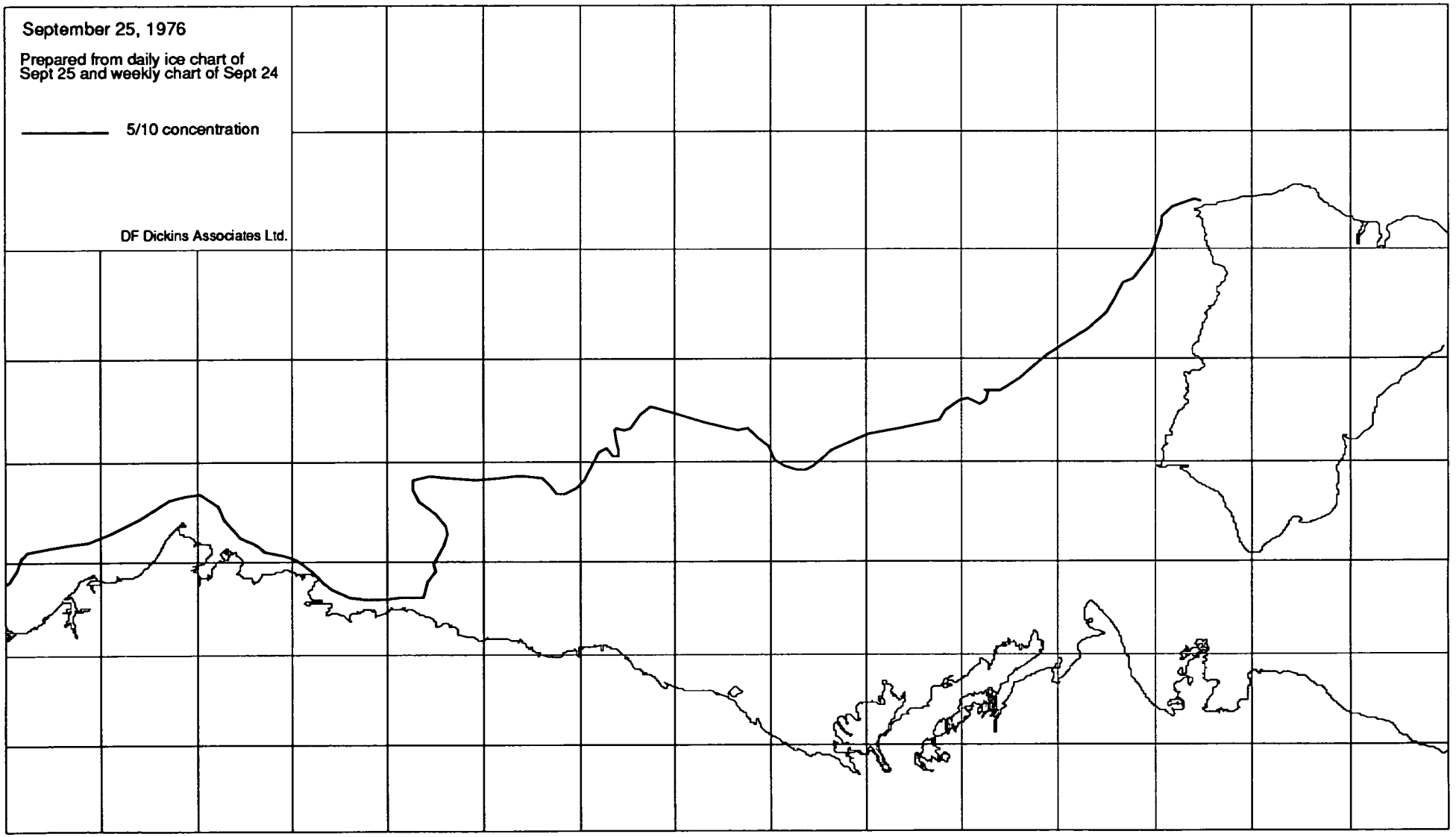
September 25, 1976
Prepared from daily ice chart of
Sept 25 and weekly chart of Sept 24
5/10 concentration
DF Dickins Associates Ltd.

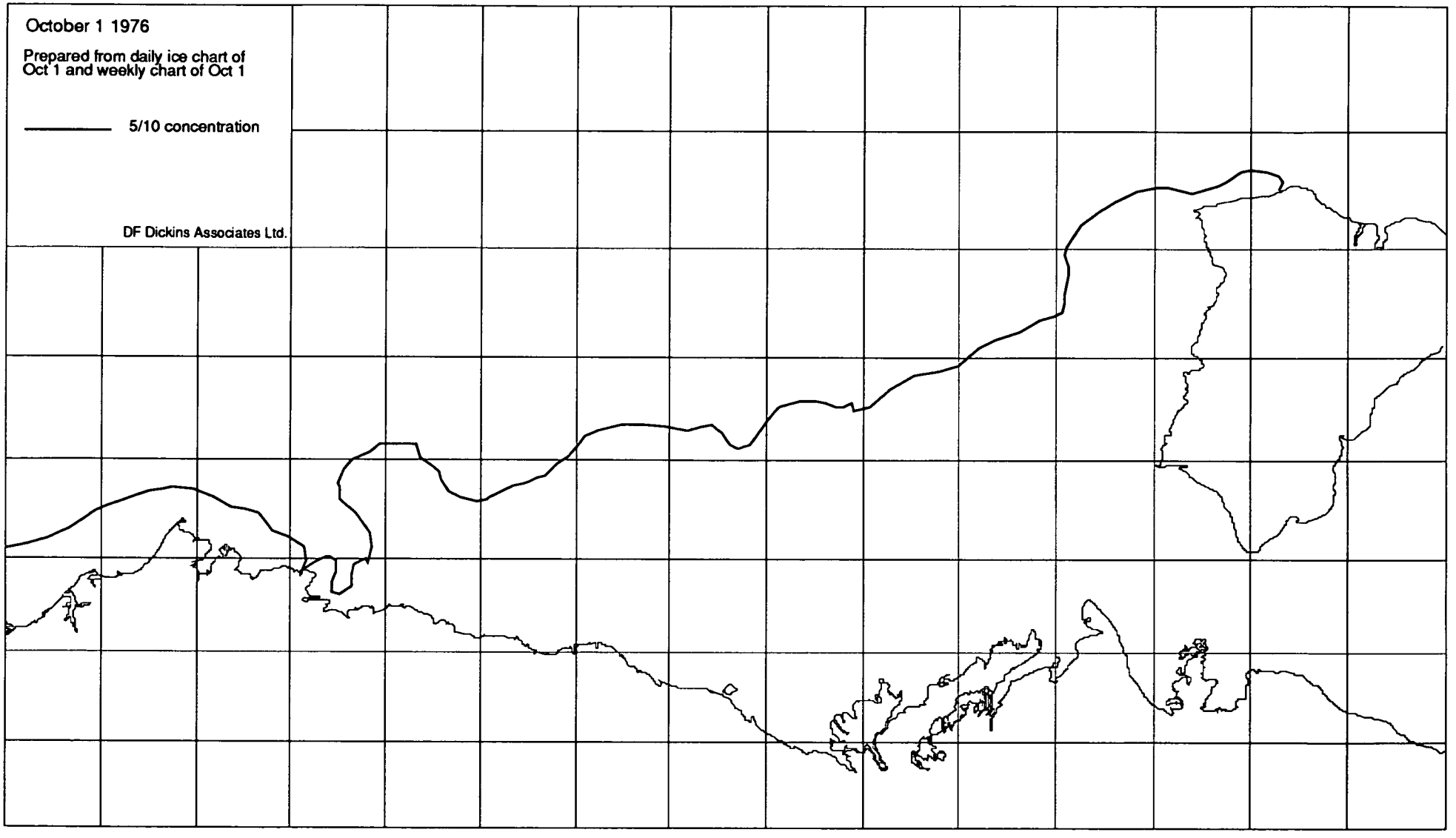
October 1 1976
Prepared from daily ice chart of
Oct 1 and weekly chart of Oct 1
5/10 concentration
DF Dickins Associates Ltd.

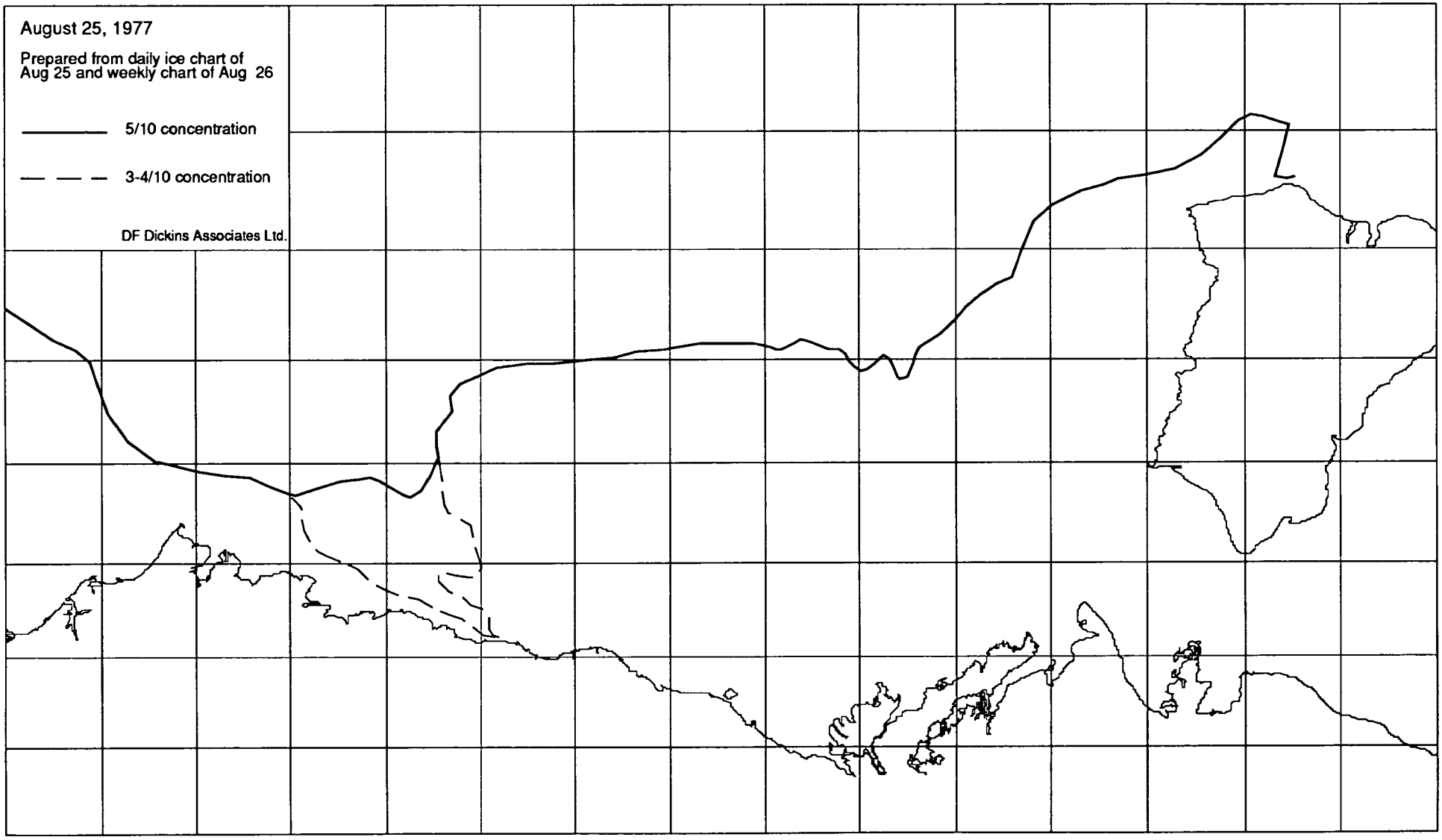
August 25, 1977
Prepared from daily ice chart of Aug 25 and weekly chart of Aug 26
5/10 concentration
3-4/10 concentration
DF Dickins Associates Ltd.

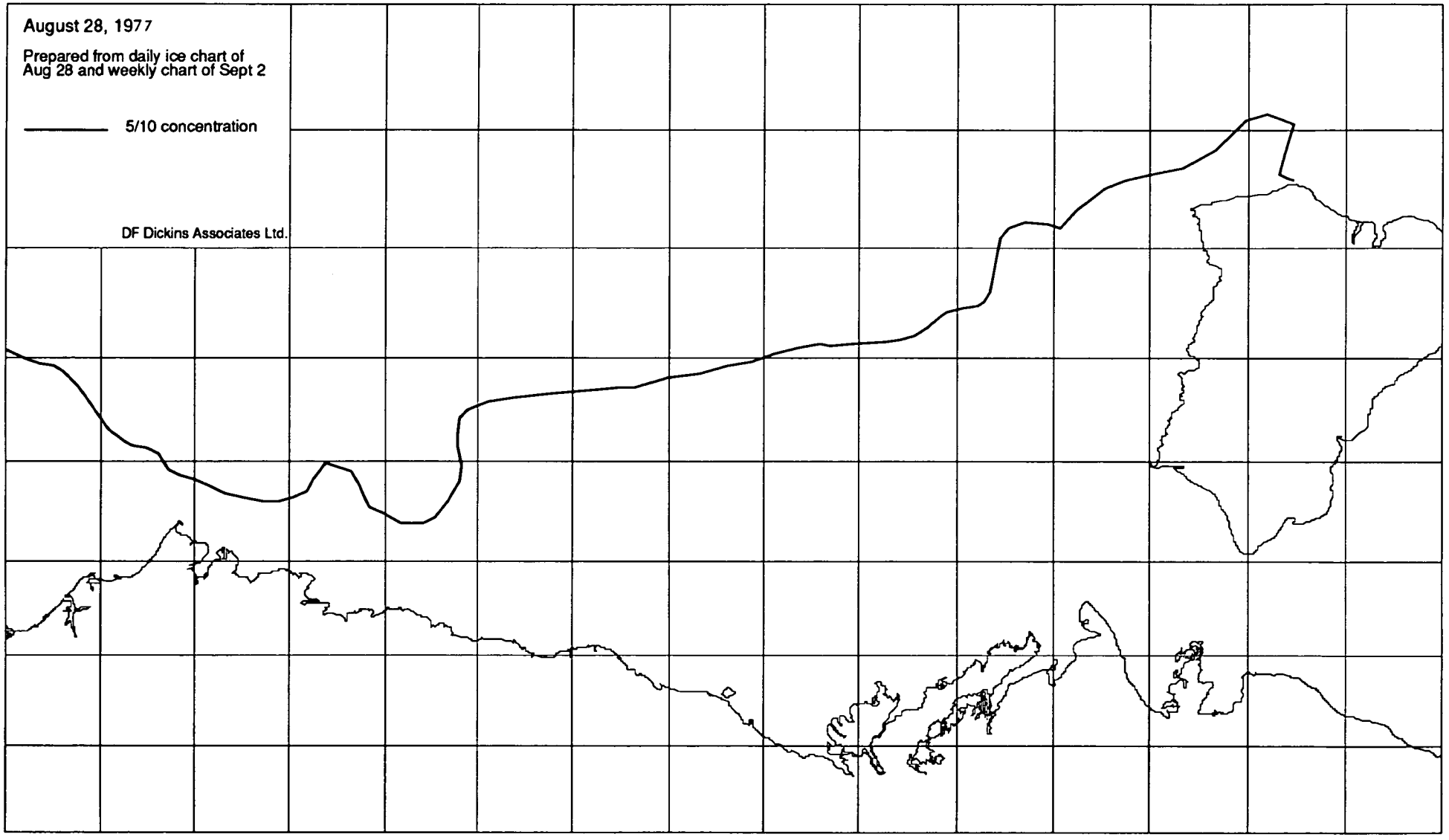
August 28, 1977
Prepared from daily ice chart of
Aug 28 and weekly chart of Sept 2
5/10 concentration
DF Dickins Associates Ltd.

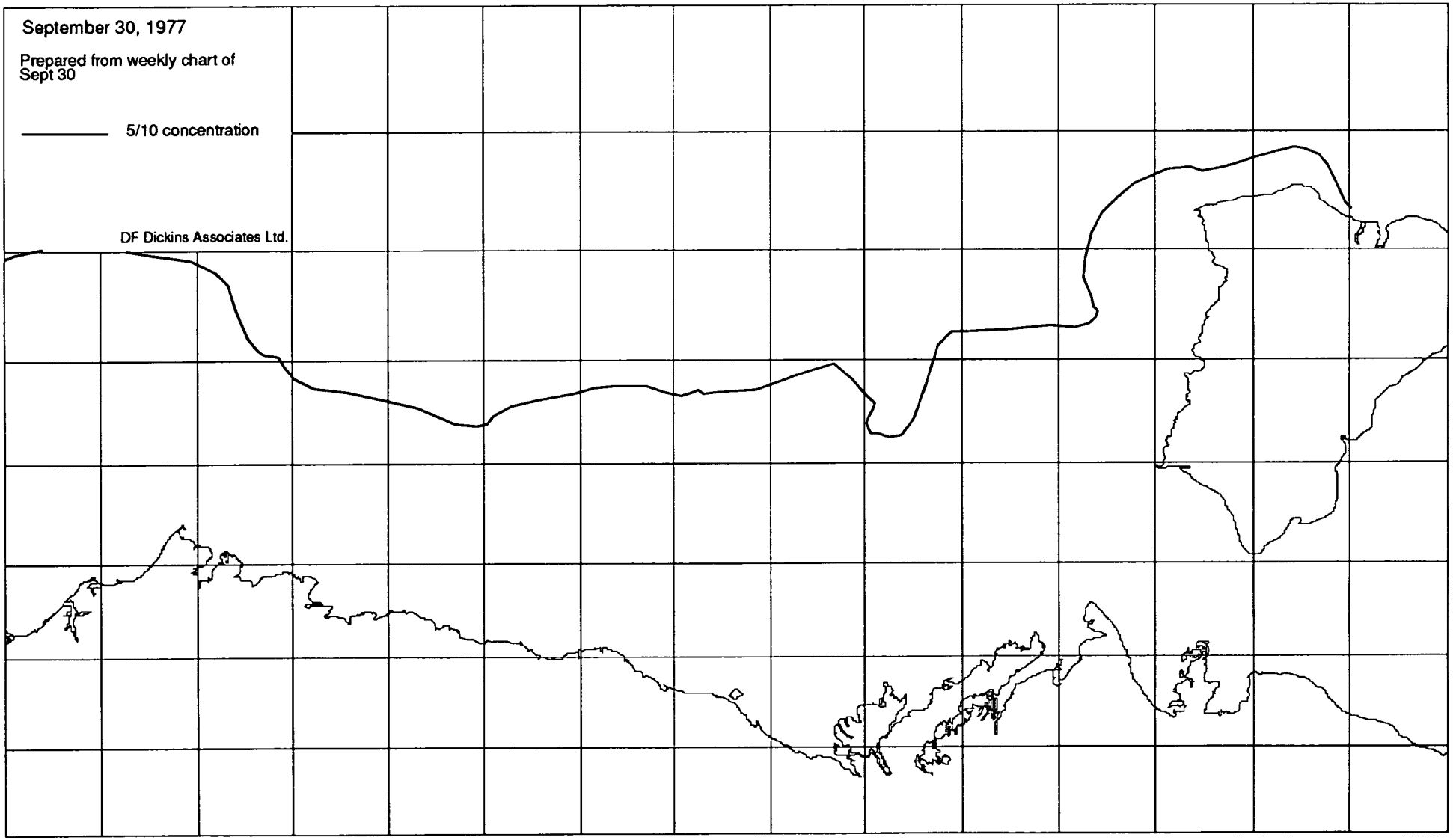
September 30, 1977
Prepared from weekly chart of Sept 30
5/10 concentration
DF Dickins Associates Ltd.

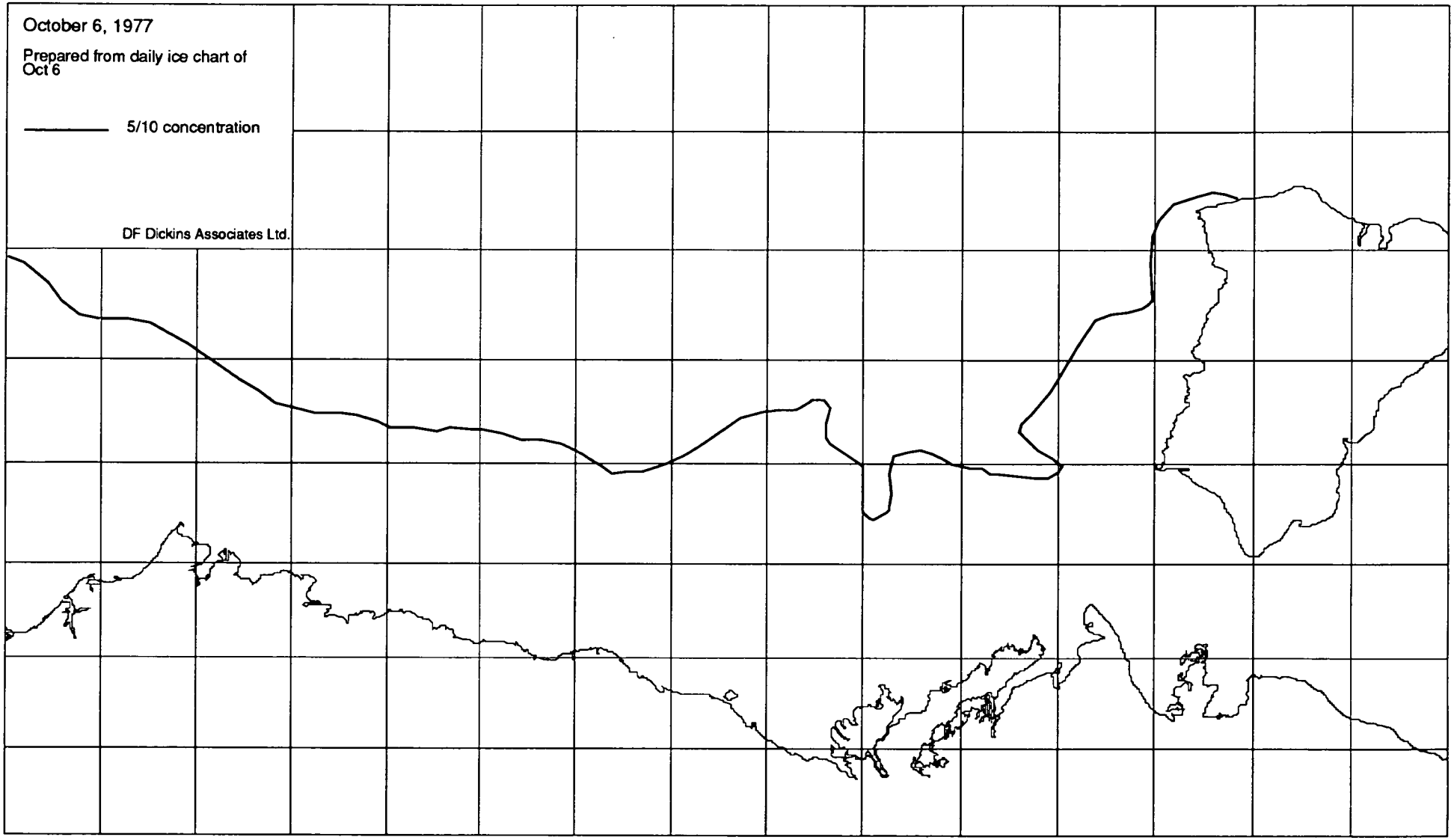
October 6, 1977
Prepared from daily ice chart of Oct 6
5/10 concentration
DF Dickins Associates Ltd.

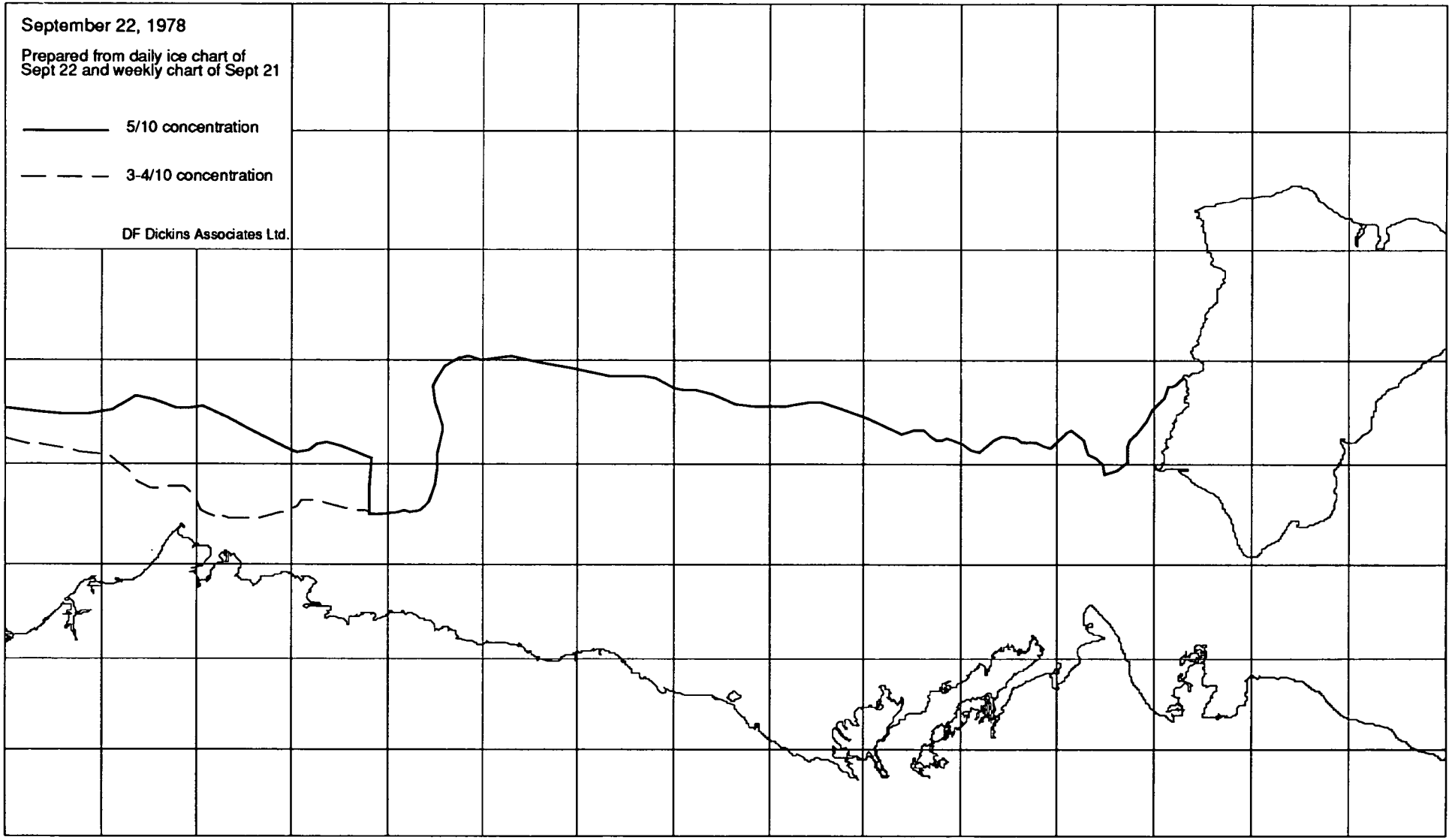
September 22, 1978
Prepared from daily ice chart of Sept 22 and weekly chart of Sept 21
5/10 concentration
3-4/10 concentration
DF Dickins Associates Ltd.

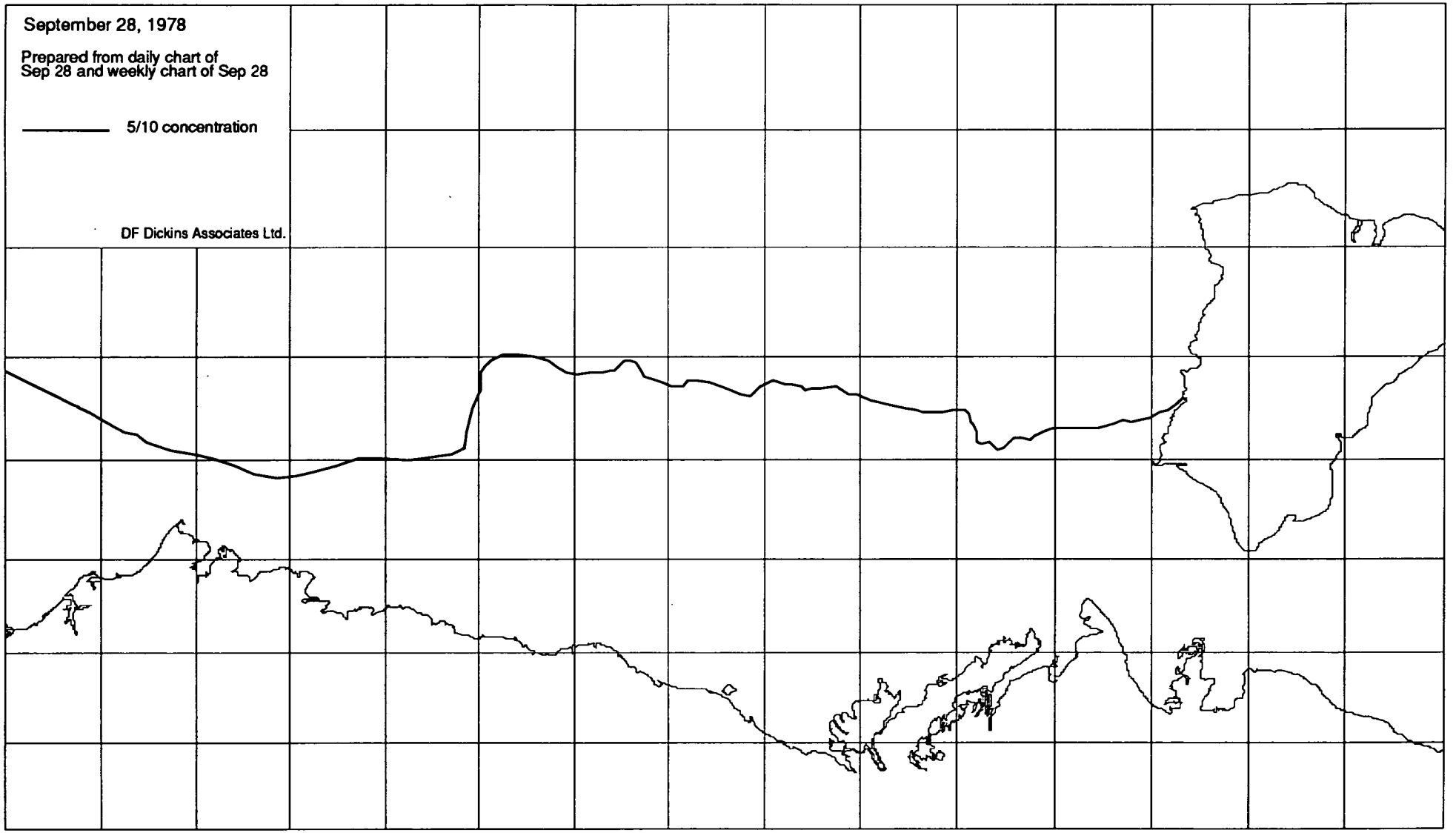
September 28, 1978
Prepared from daily chart of
Sep 28 and weekly chart of Sep 28
5/10 concentration
DF Dickins Associates Ltd.

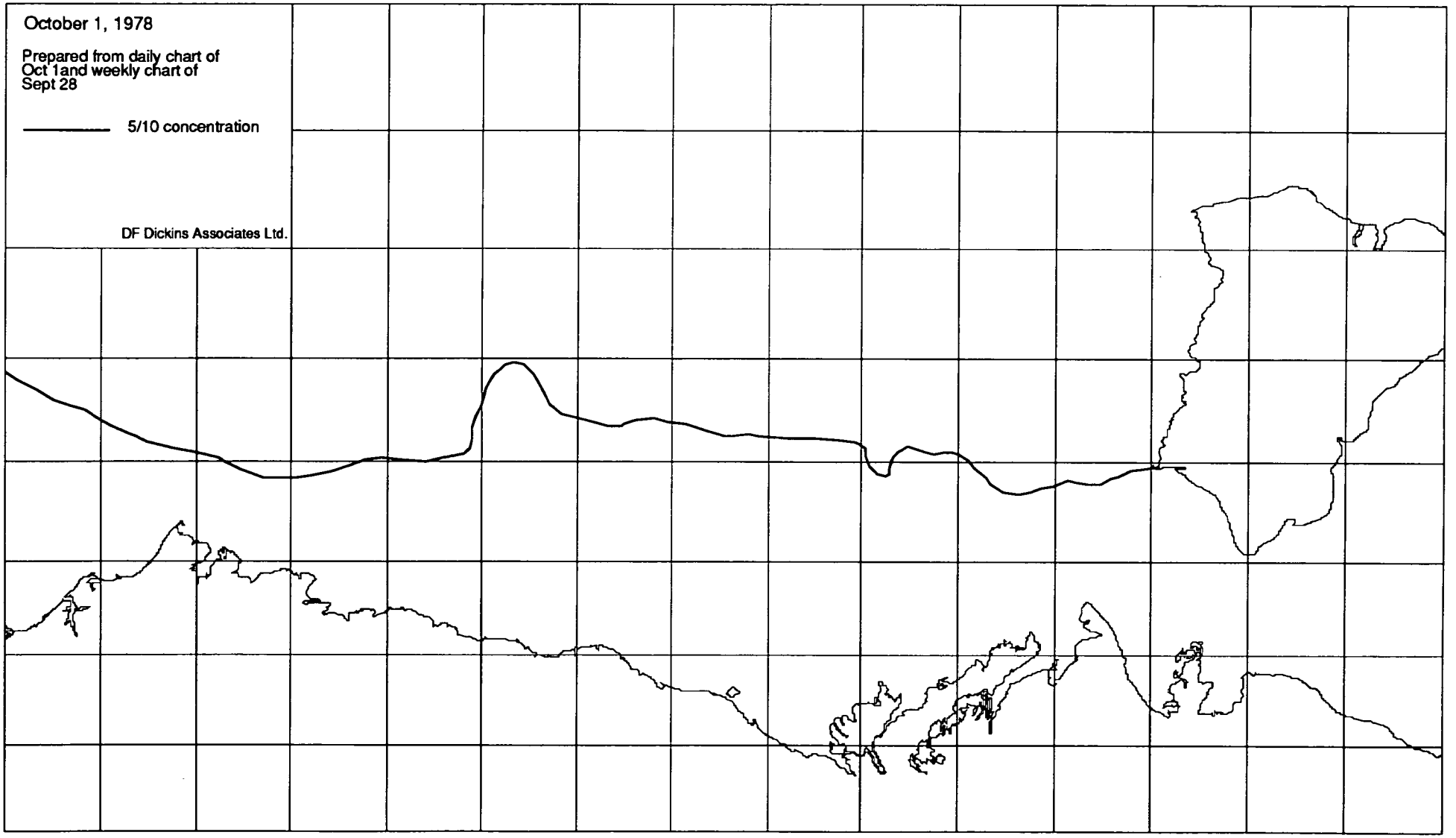
October 1, 1978
Prepared from daily chart of
Oct 1and weekly chart of
Sept 28
5/10 concentration
DF Dickins Associates Ltd.

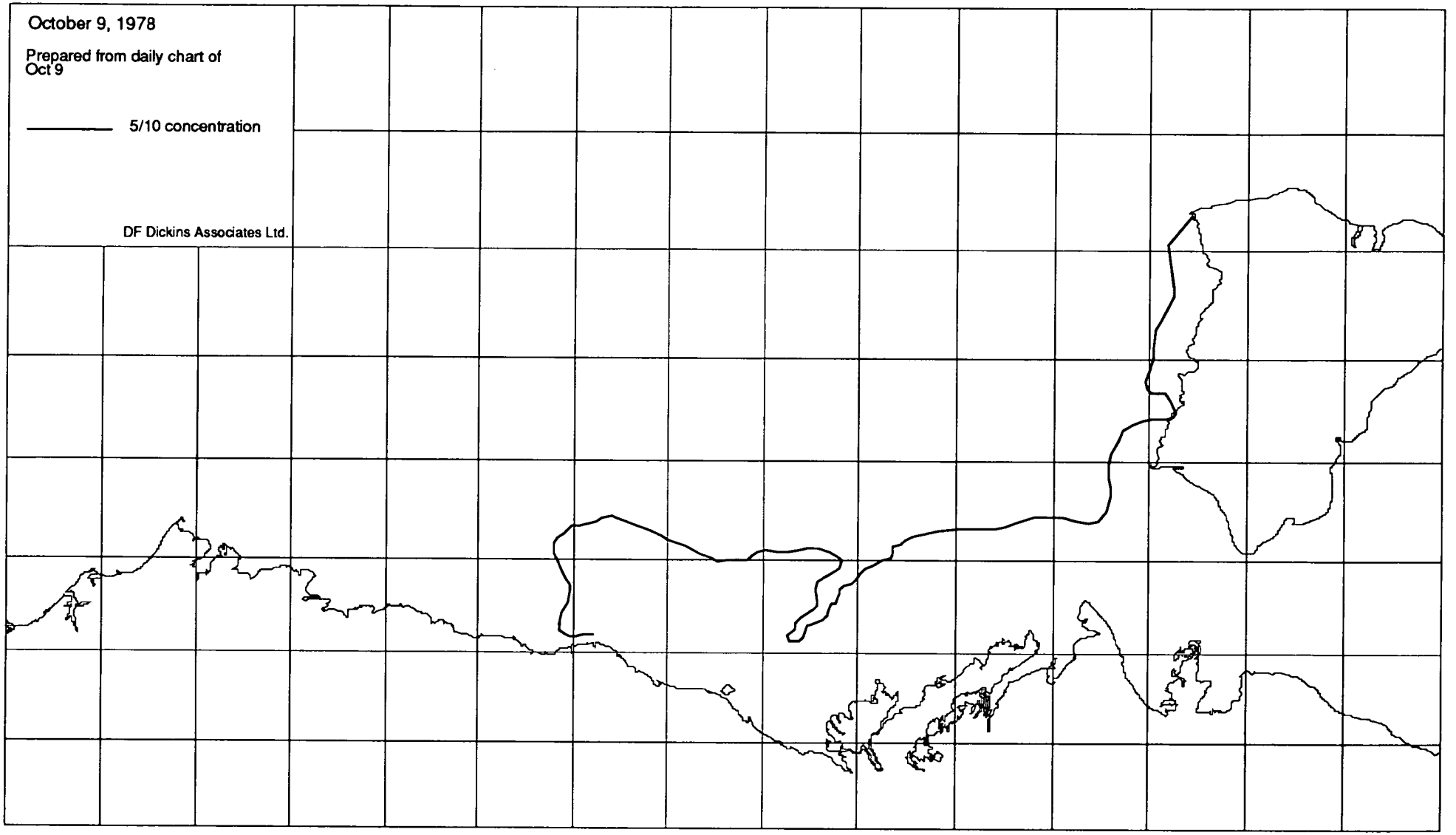
October 9, 1978
Prepared from daily chart of Oct 9
5/10 concentration
DF Dickins Associates Ltd.

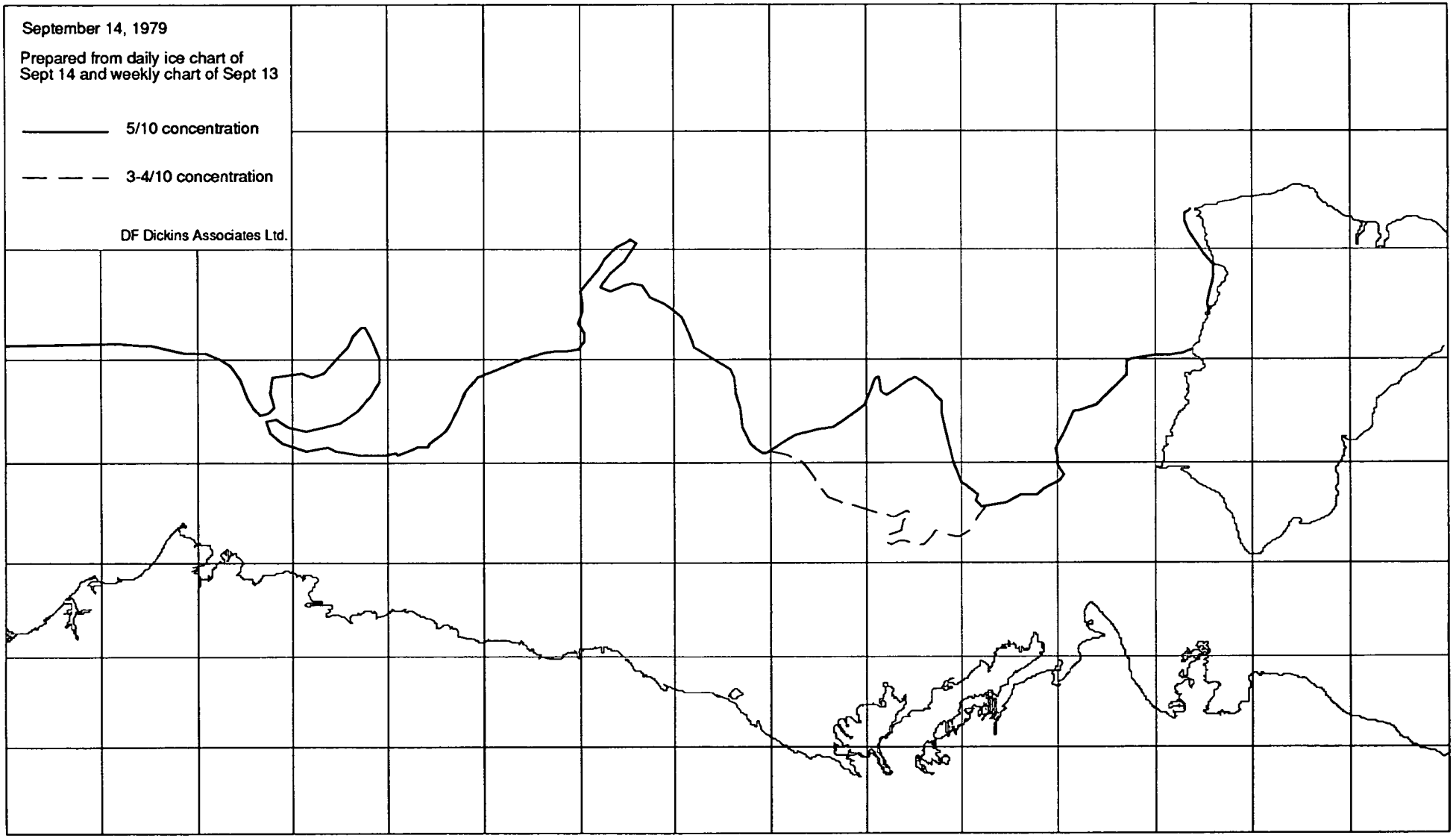
September 14, 1979
Prepared from daily ice chart of
Sept 14 and weekly chart of Sept 13
5/10 concentration
3-4/10 concentration
DF Dickins Associates Ltd.

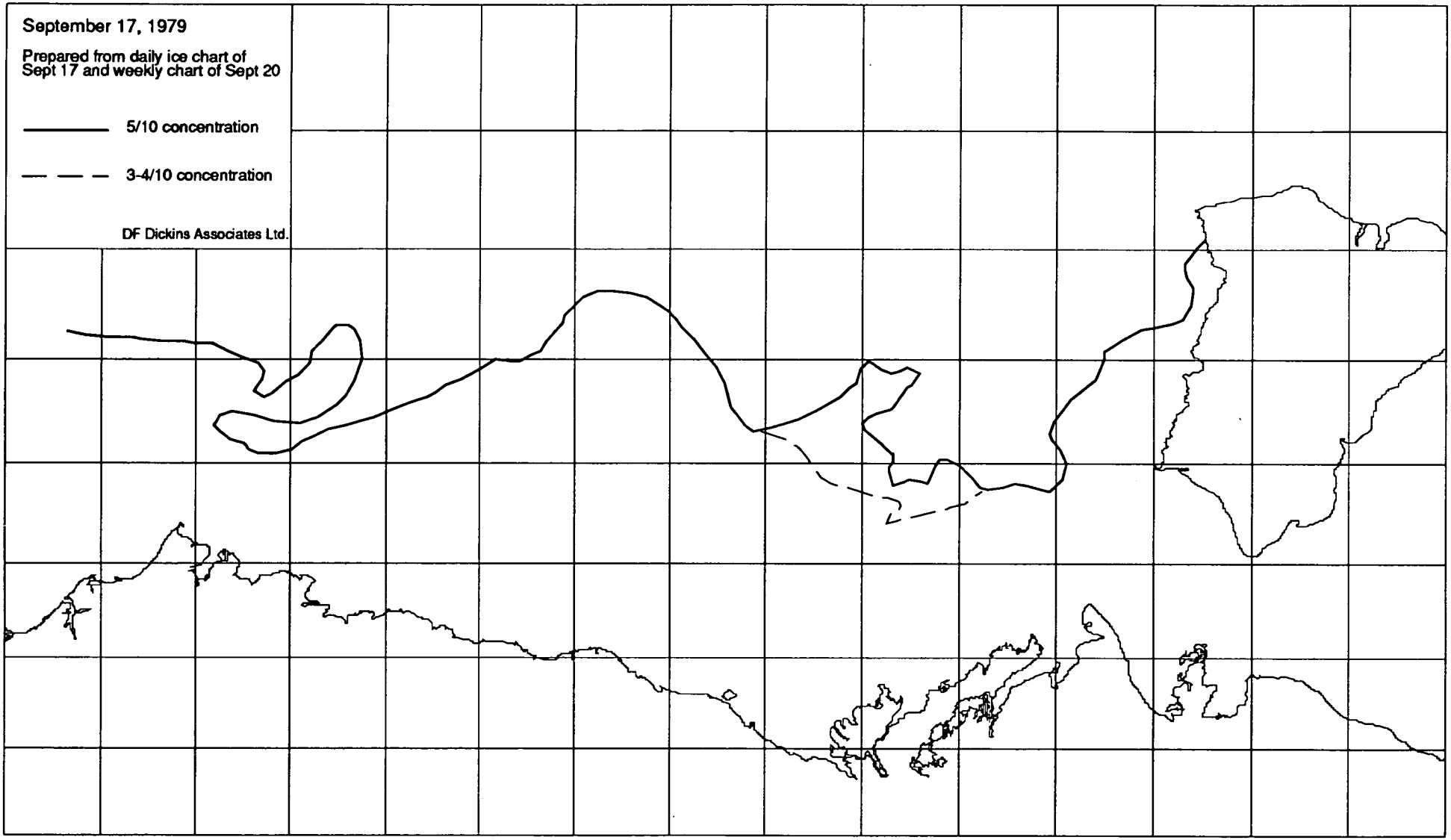
September 17, 1979
Prepared from daily ice chart of Sept 17 and weekly chart of Sept 20
5/10 concentration
3-4/10 concentration
DF Dickins Associates Ltd.

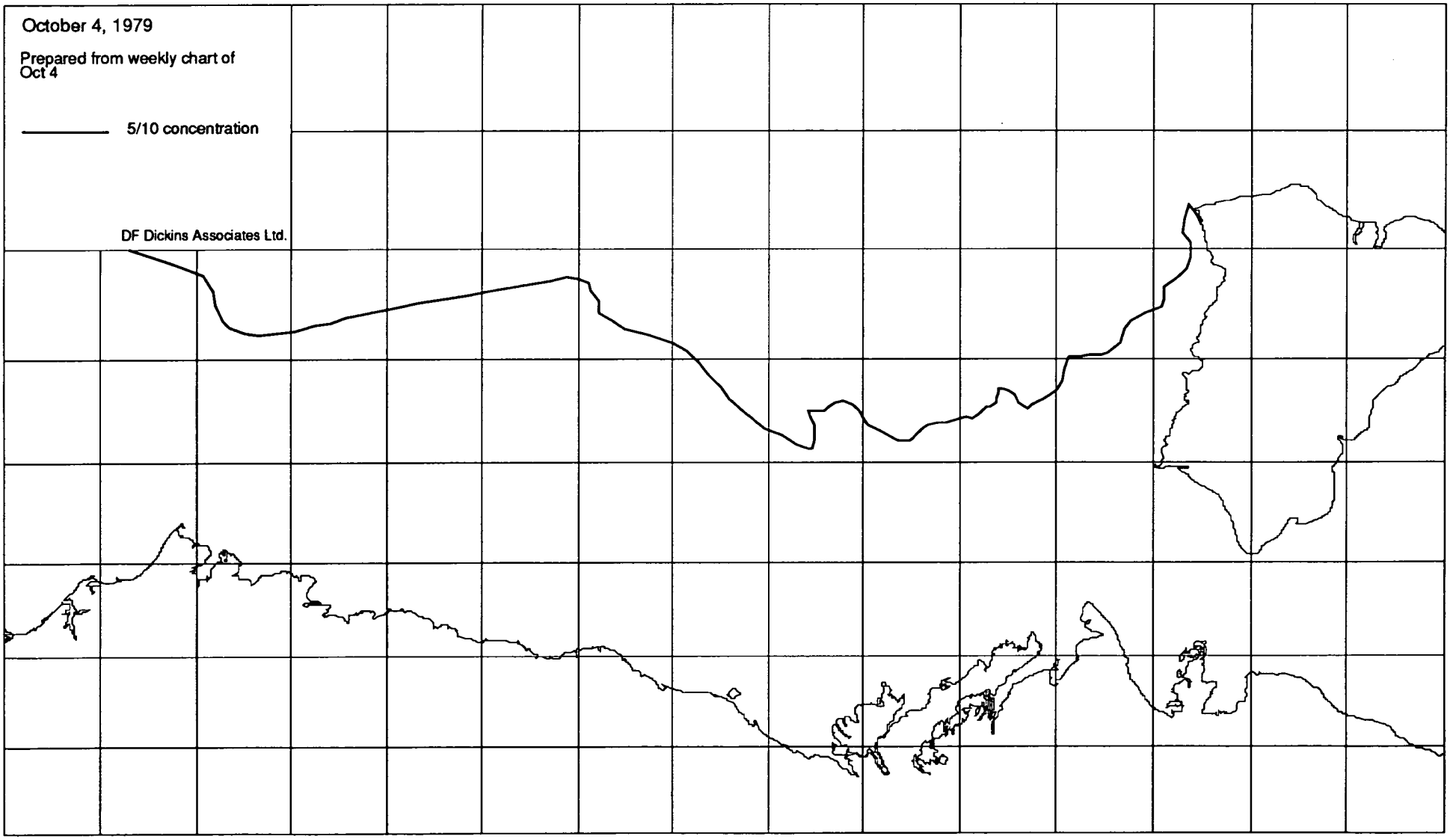
October 4, 1979
Prepared from weekly chart of Oct 4
5/10 concentration
DF Dickins Associates Ltd.

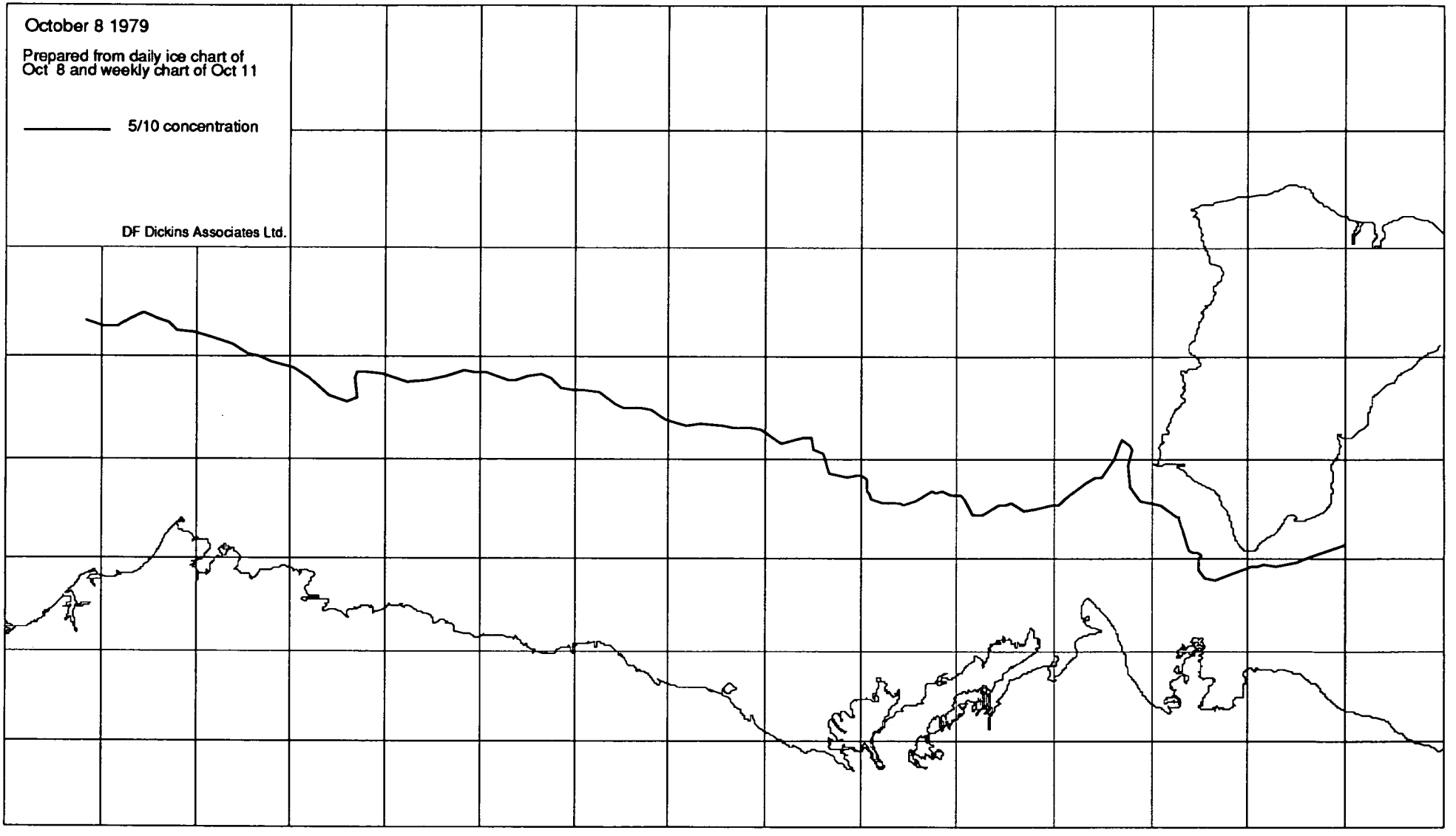
October 8 1979
Prepared from daily ice chart of Oct 8 and weekly chart of Oct 11
5/10 concentration
DF Dickins Associates Ltd.

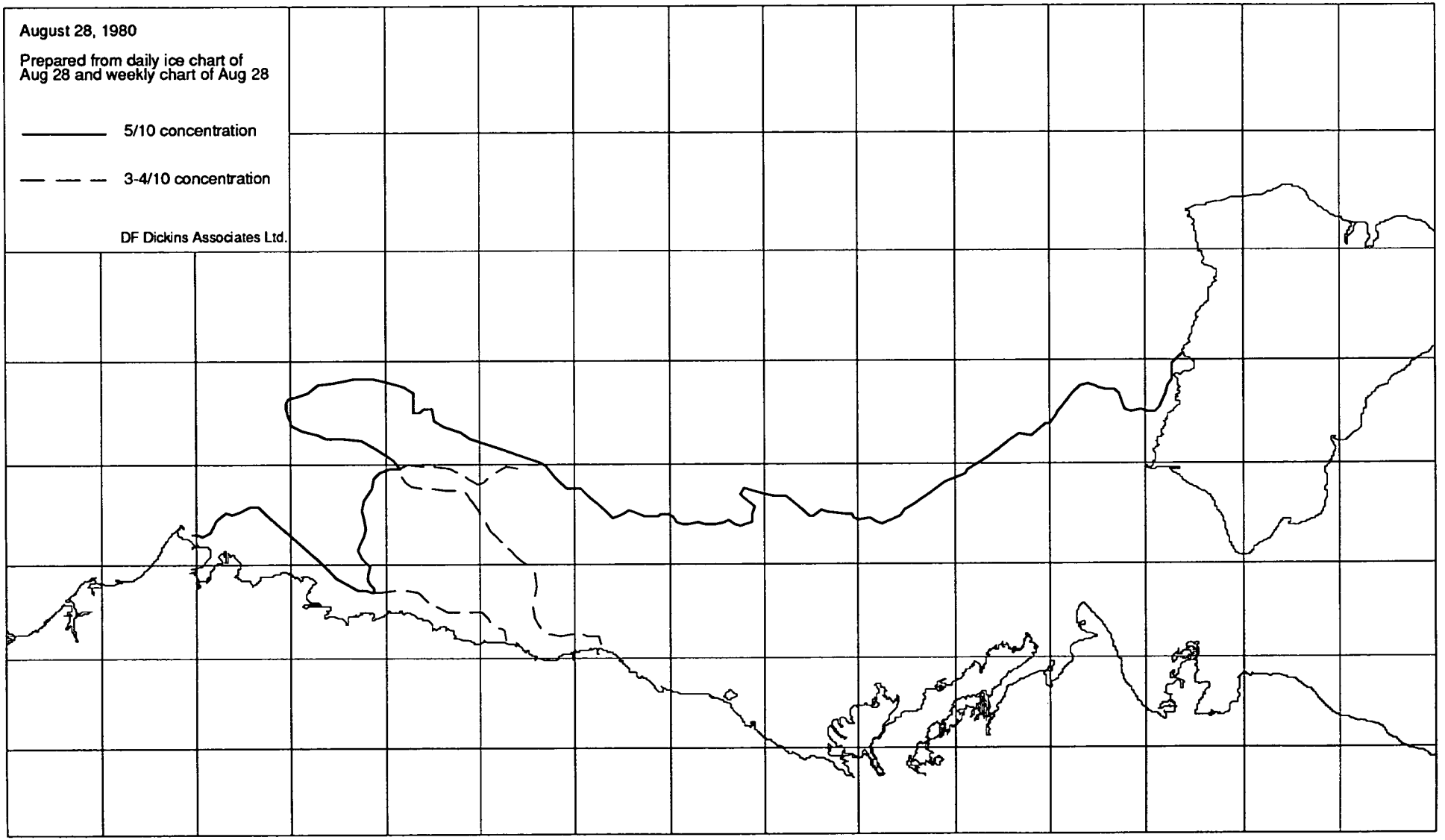
August 28, 1980
Prepared from daily ice chart of
Aug 28 and weekly chart of Aug 28
5/10 concentration
3-4/10 concentration
DF Dickins Associates Ltd.

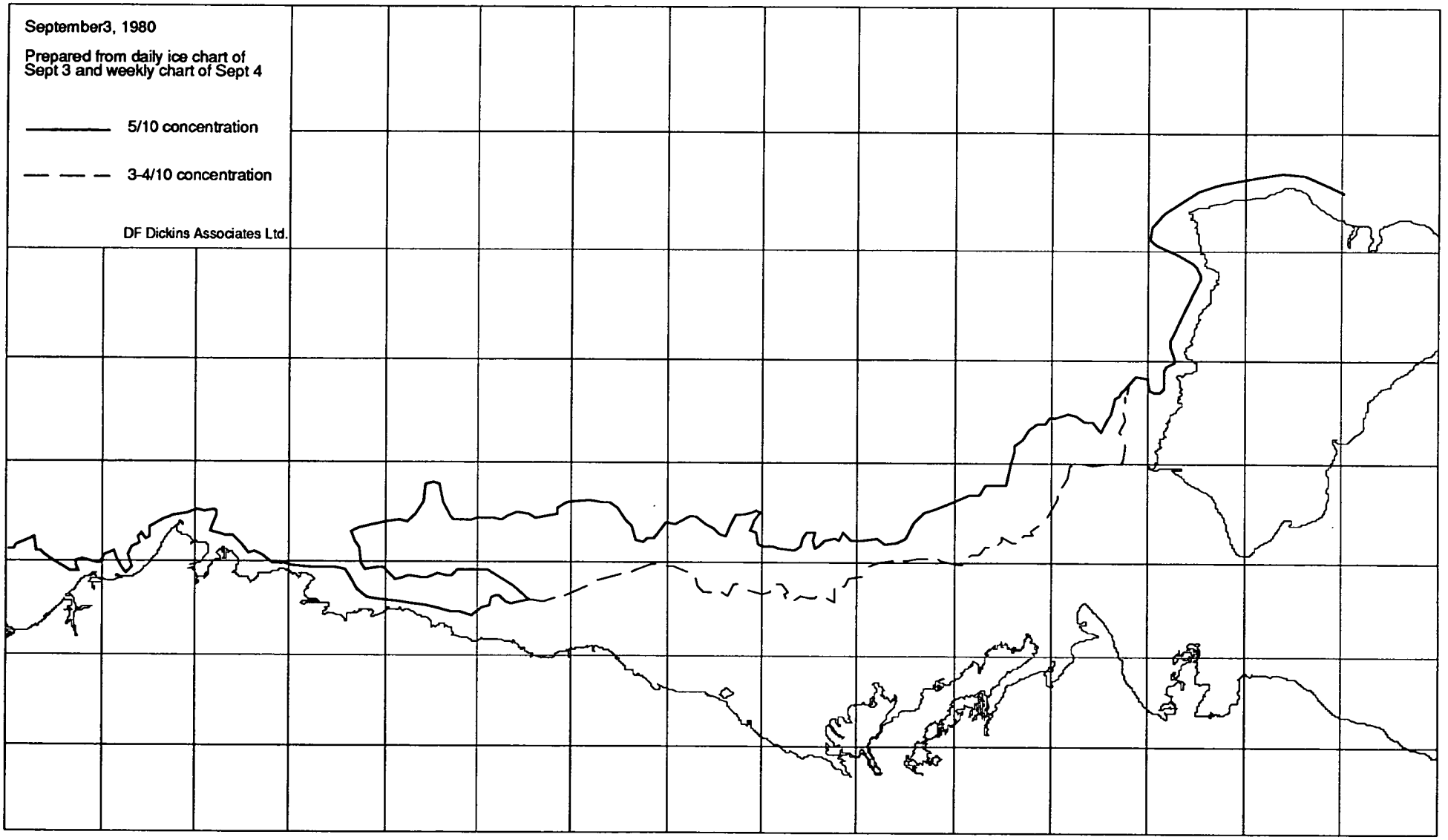
September3, 1980
Prepared from daily ice chart of Sept 3 and weekly chart of Sept 4
5/10 concentration
3-4/10 concentration
DF Dickins Associates Ltd.

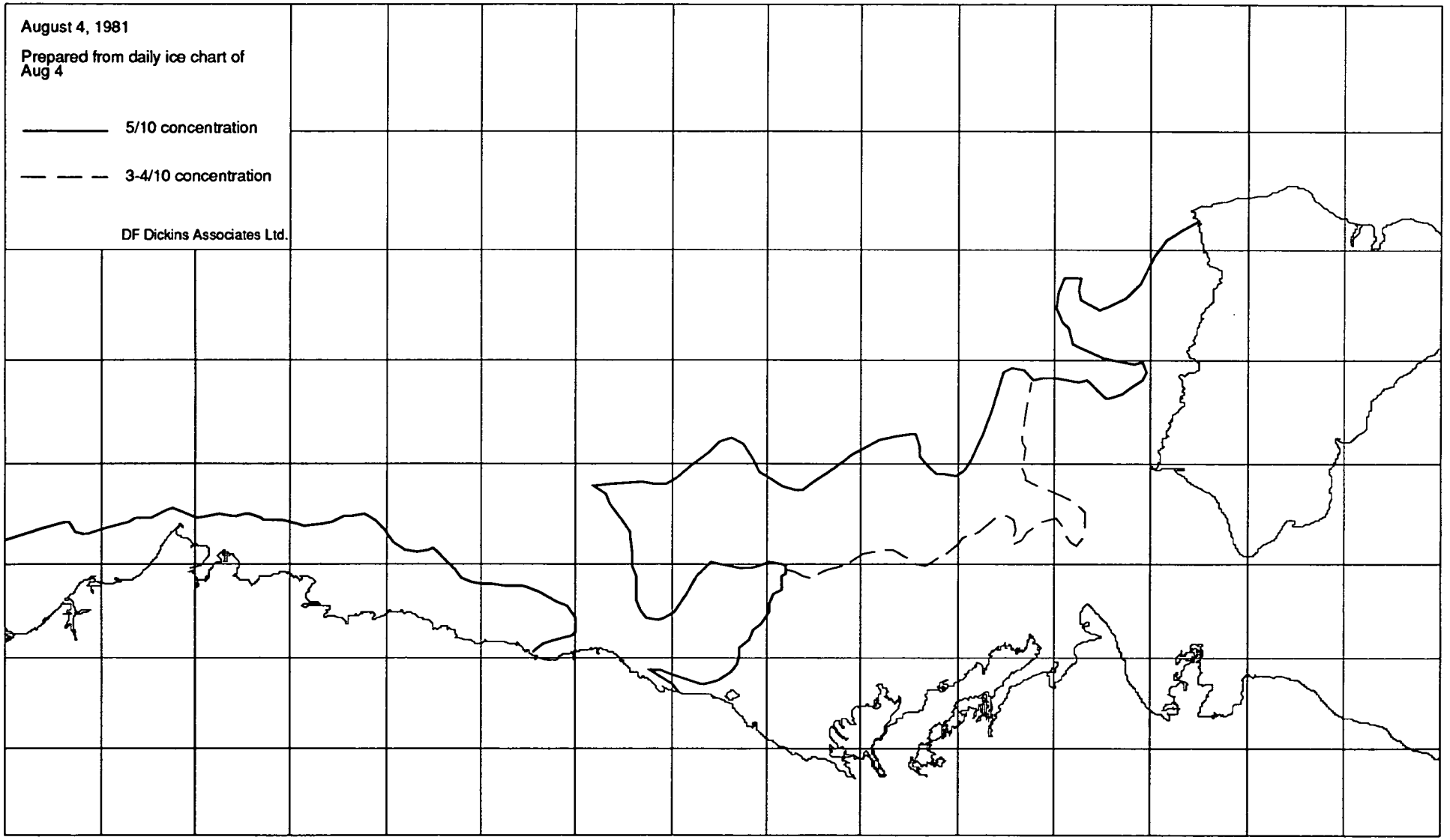
August 4, 1981
Prepared from daily ice chart of Aug 4
5/10 concentration
3-4/10 concentration
DF Dickins Associates Ltd.

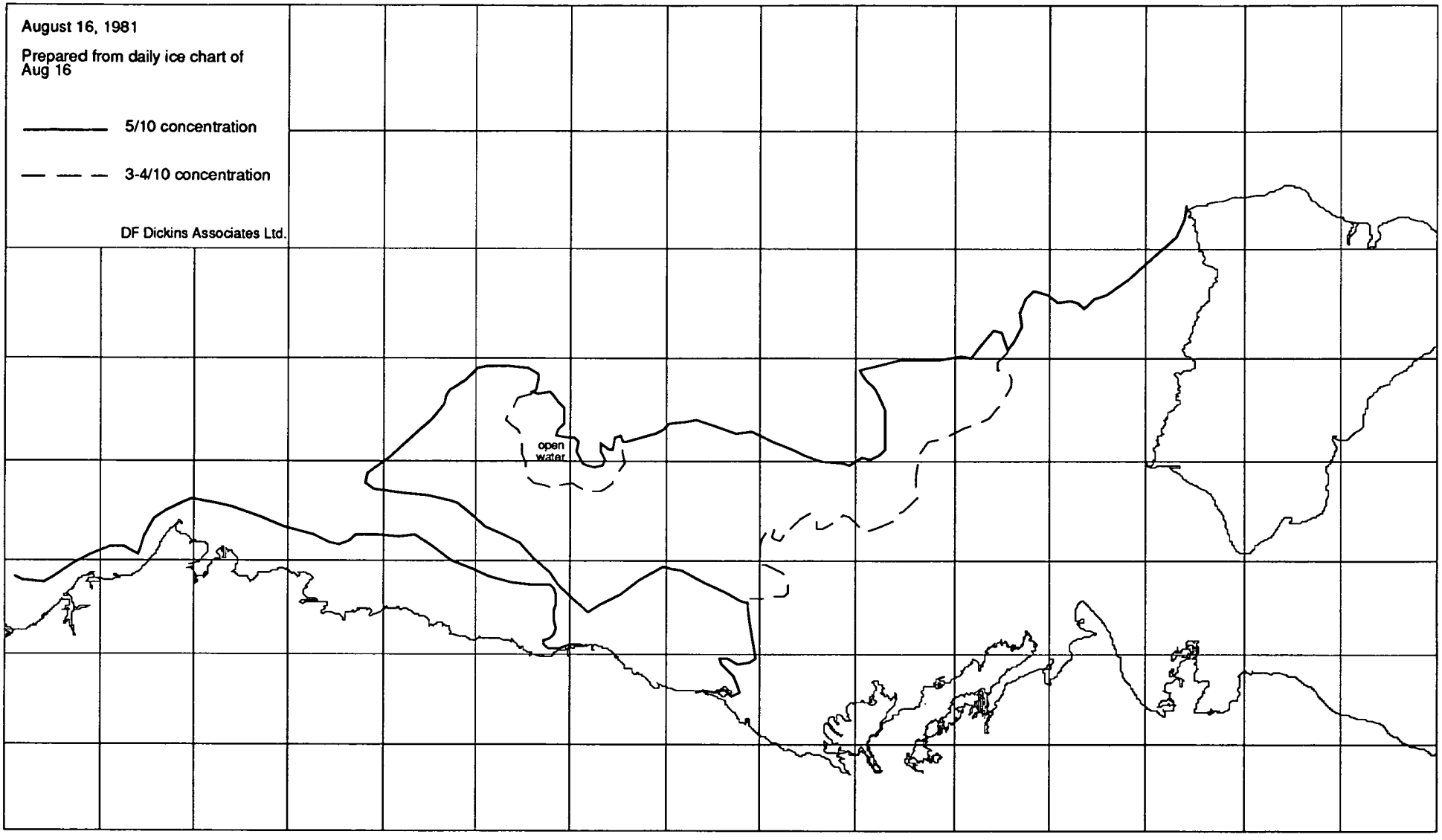
August 16, 1981
Prepared from daily ice chart of Aug 16
5/10 concentration
3-4/10 concentration
DF Dickins Associates Ltd.
open water

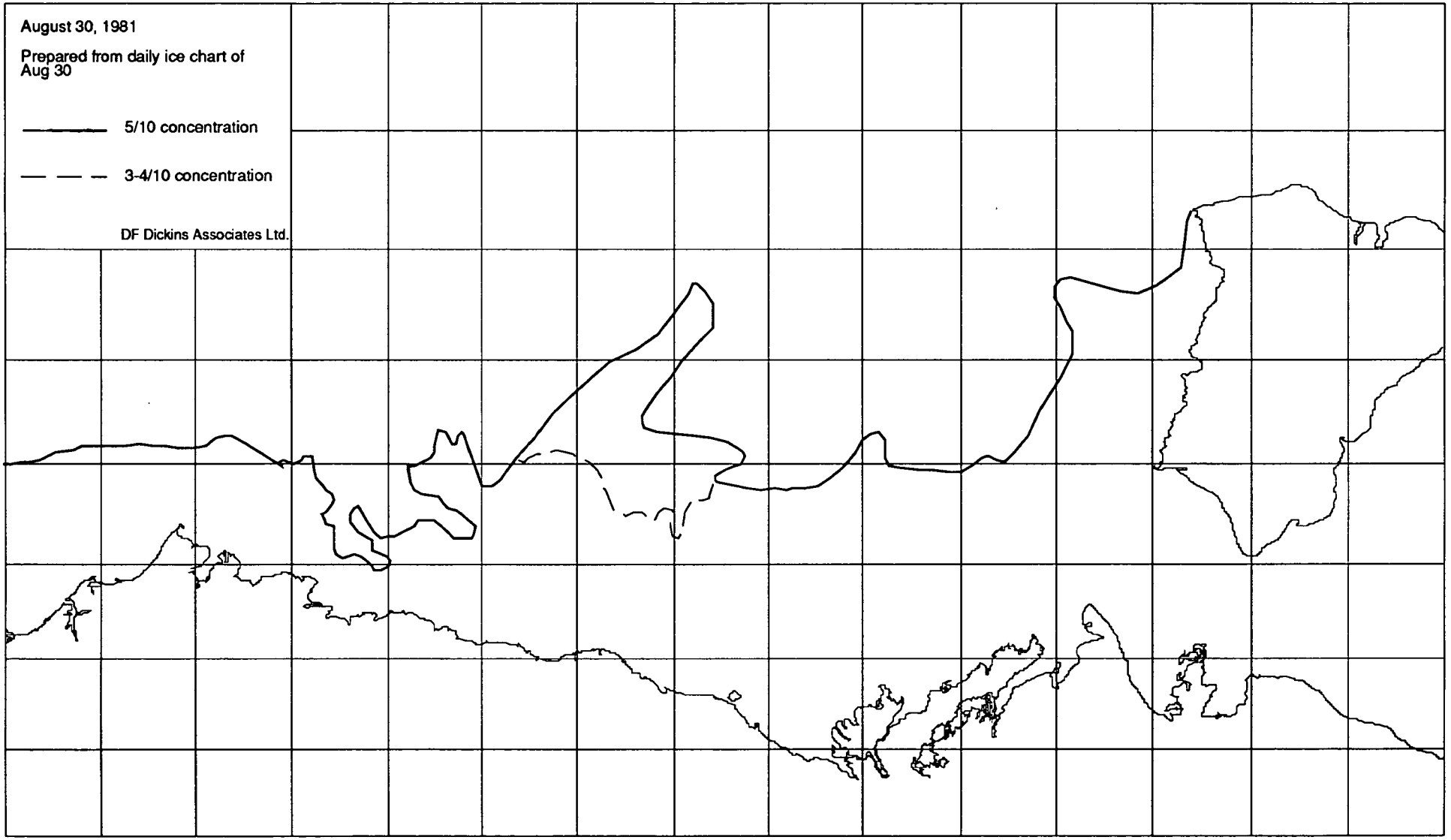
August 30, 1981
Prepared from daily ice chart of Aug 30
5/10 concentration
3-4/10 concentration
DF Dickins Associates Ltd.

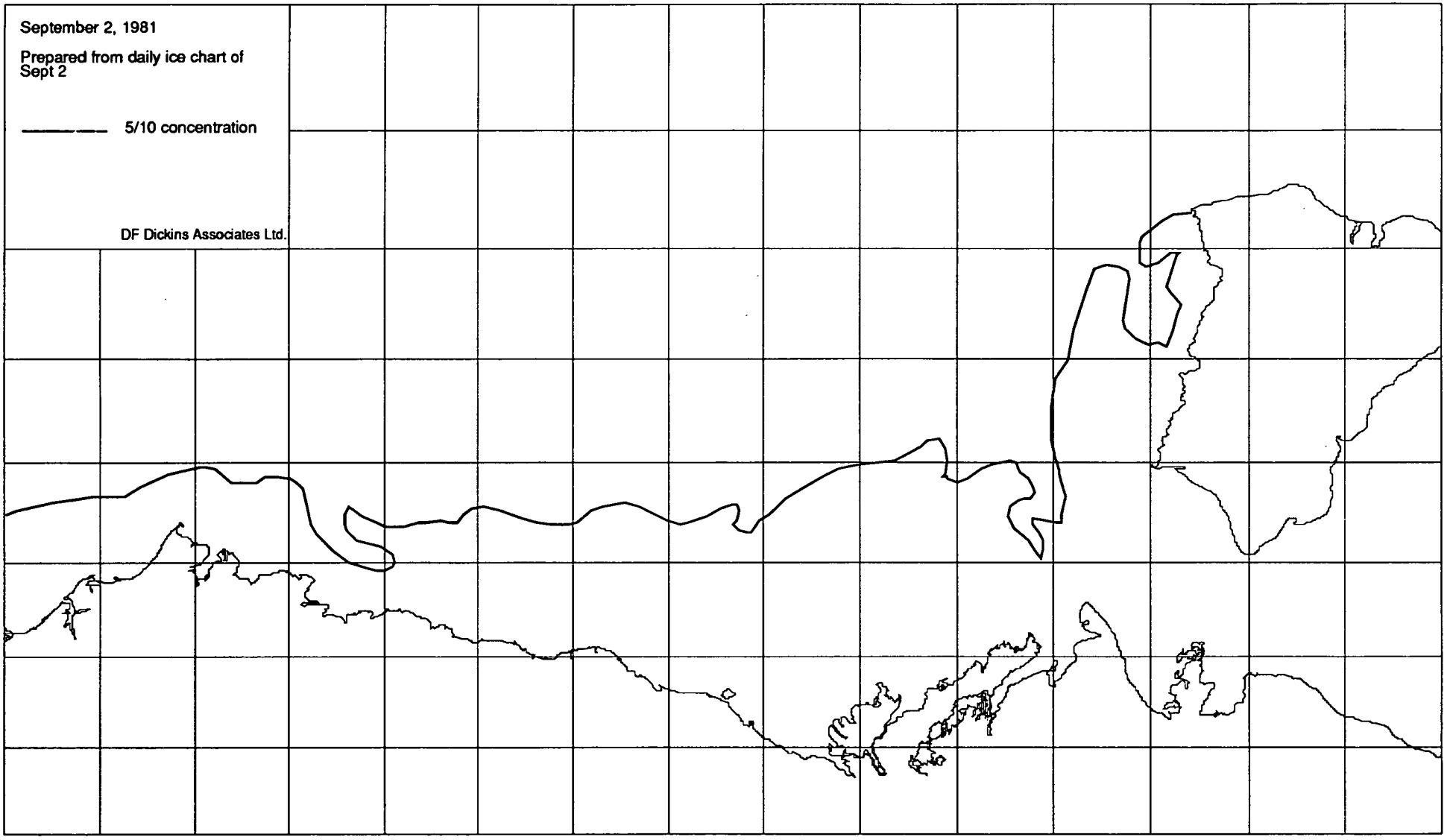
September 2, 1981
Prepared from daily ice chart of Sept 2
5/10 concentration
DF Dickins Associates Ltd.

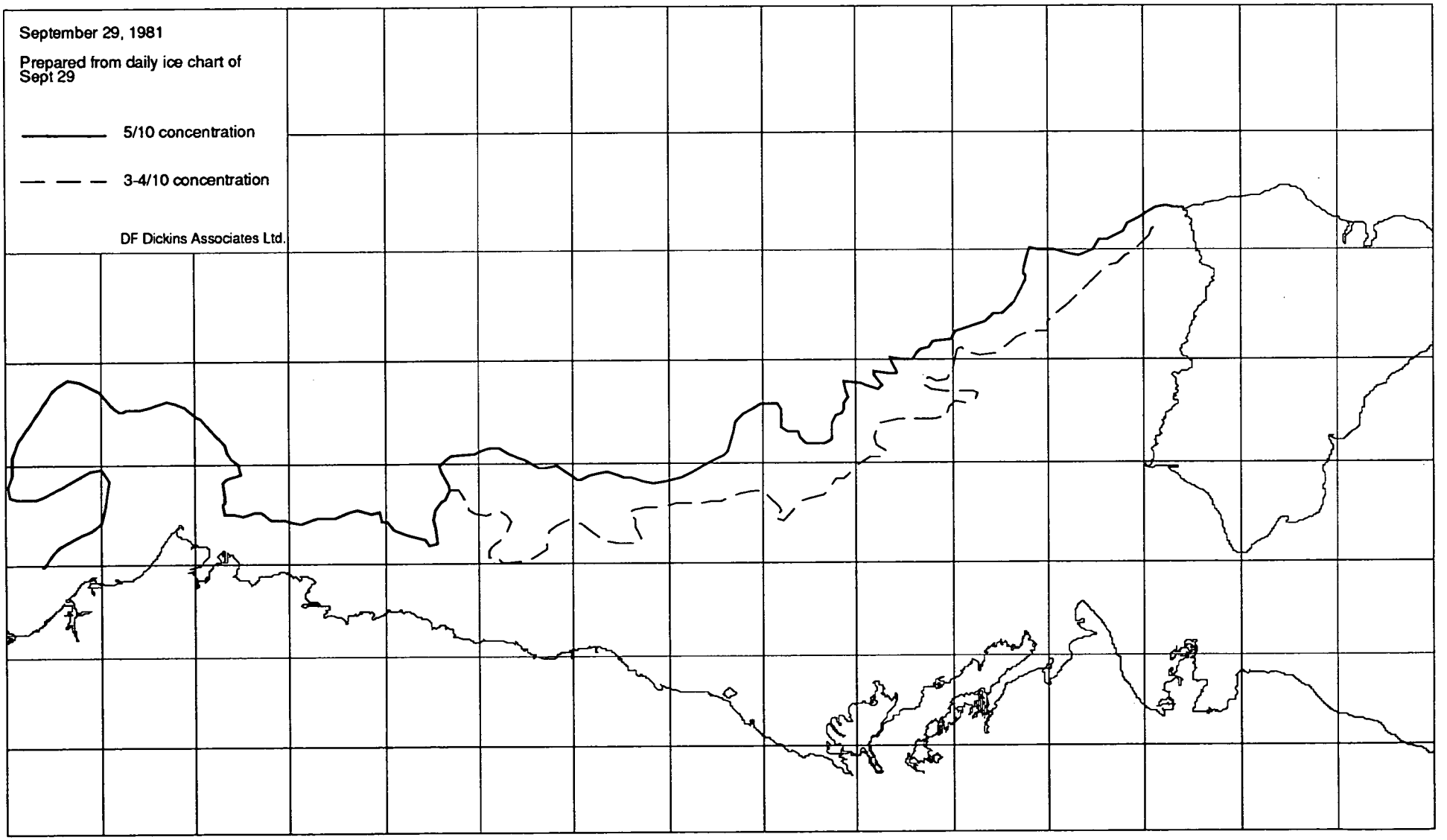
September 29, 1981
Prepared from daily ice chart of Sept 29
5/10 concentration
3-4/10 concentration
DF Dickins Associates Ltd.

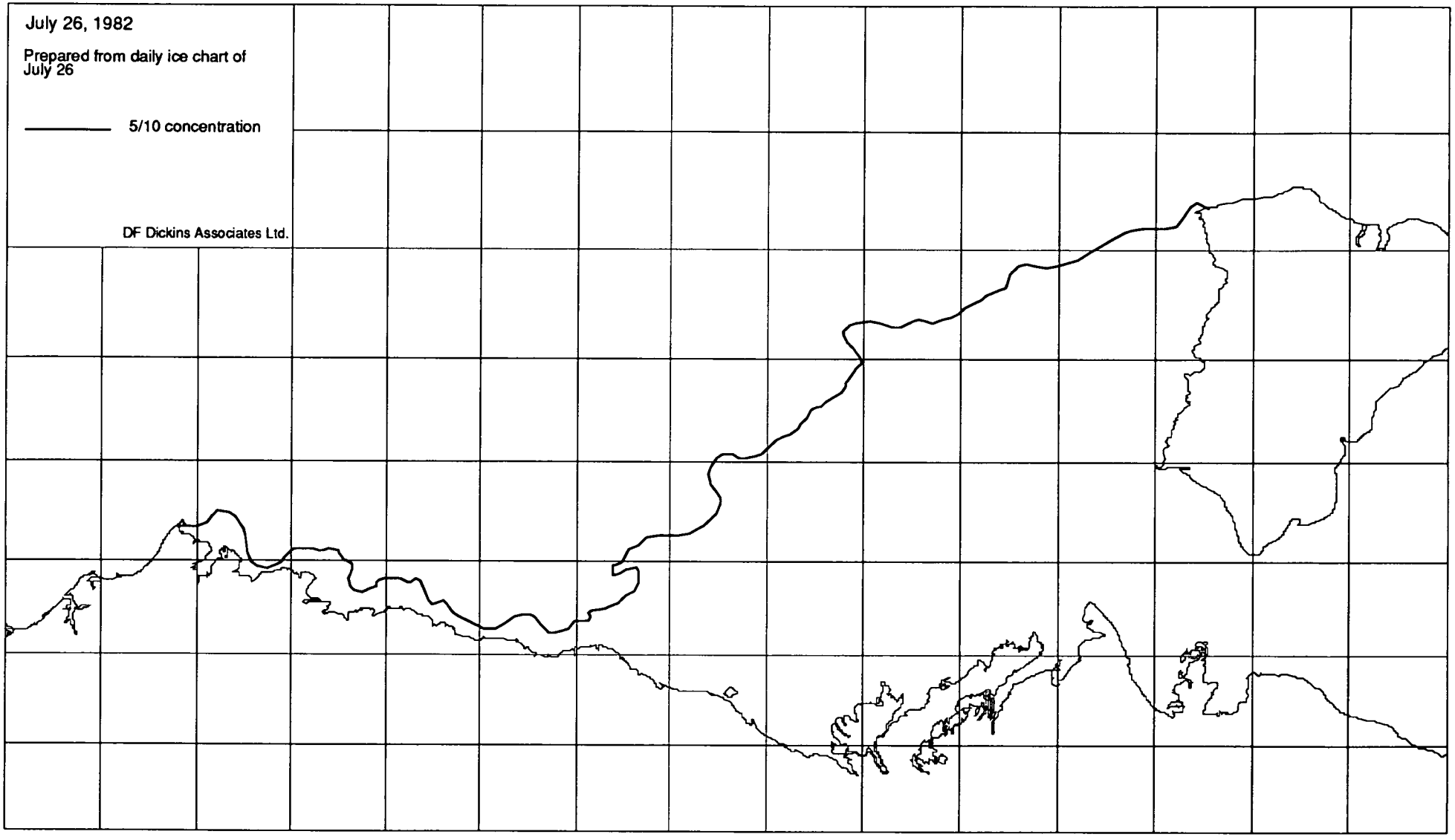
July 26, 1982
Prepared from daily ice chart of July 26
5/10 concentration
DF Dickins Associates Ltd.

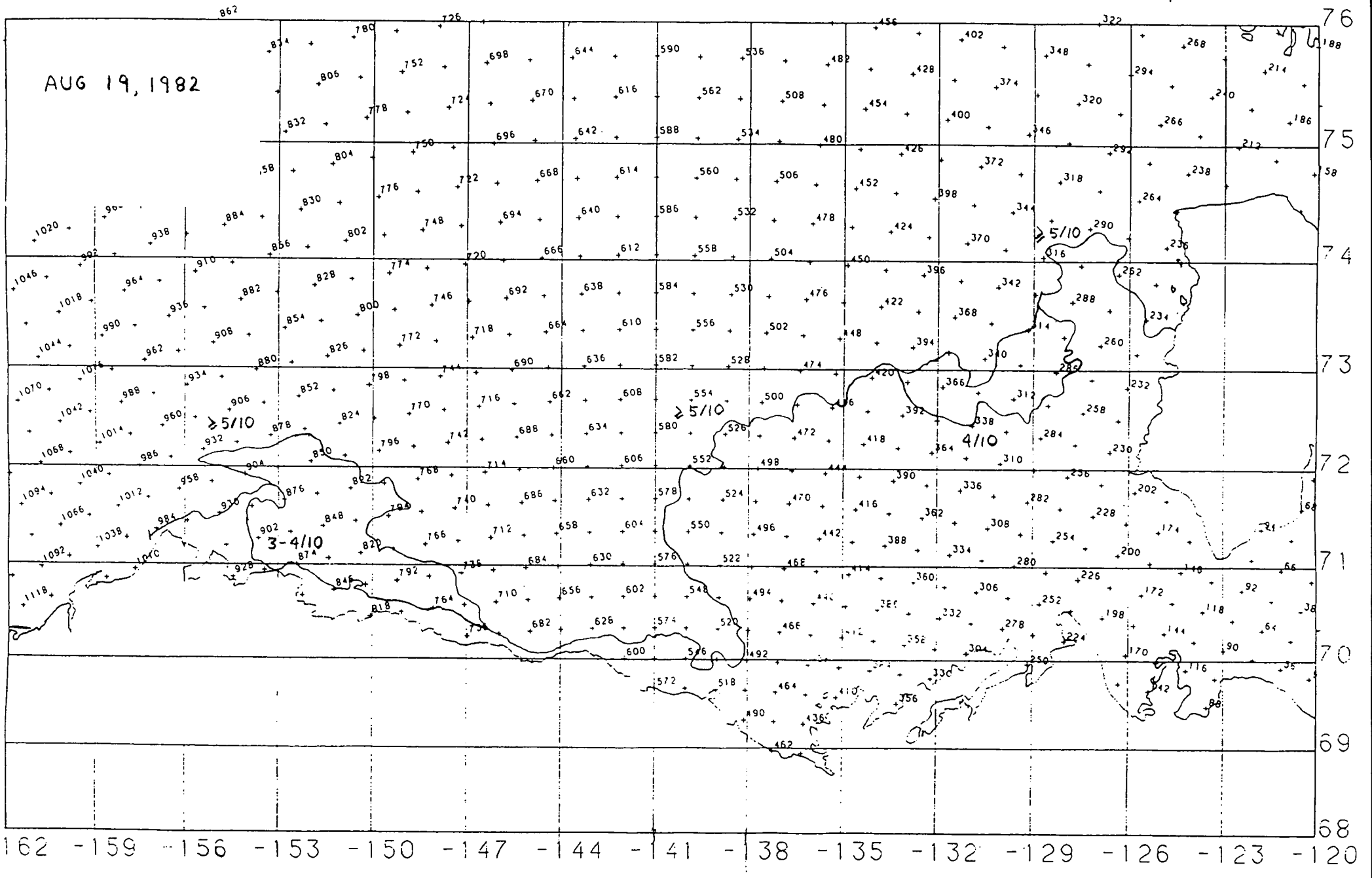
AUG 19, 1982
≥5/10
≥5/10
≥5/10
4/10
3-4/10
76
75
74
73
72
71
70
69
68
162 -159 -156 -153 -150 -147 -144 -141 -138 -135 -132 -129 -126 -123 -120

AUG 19/82

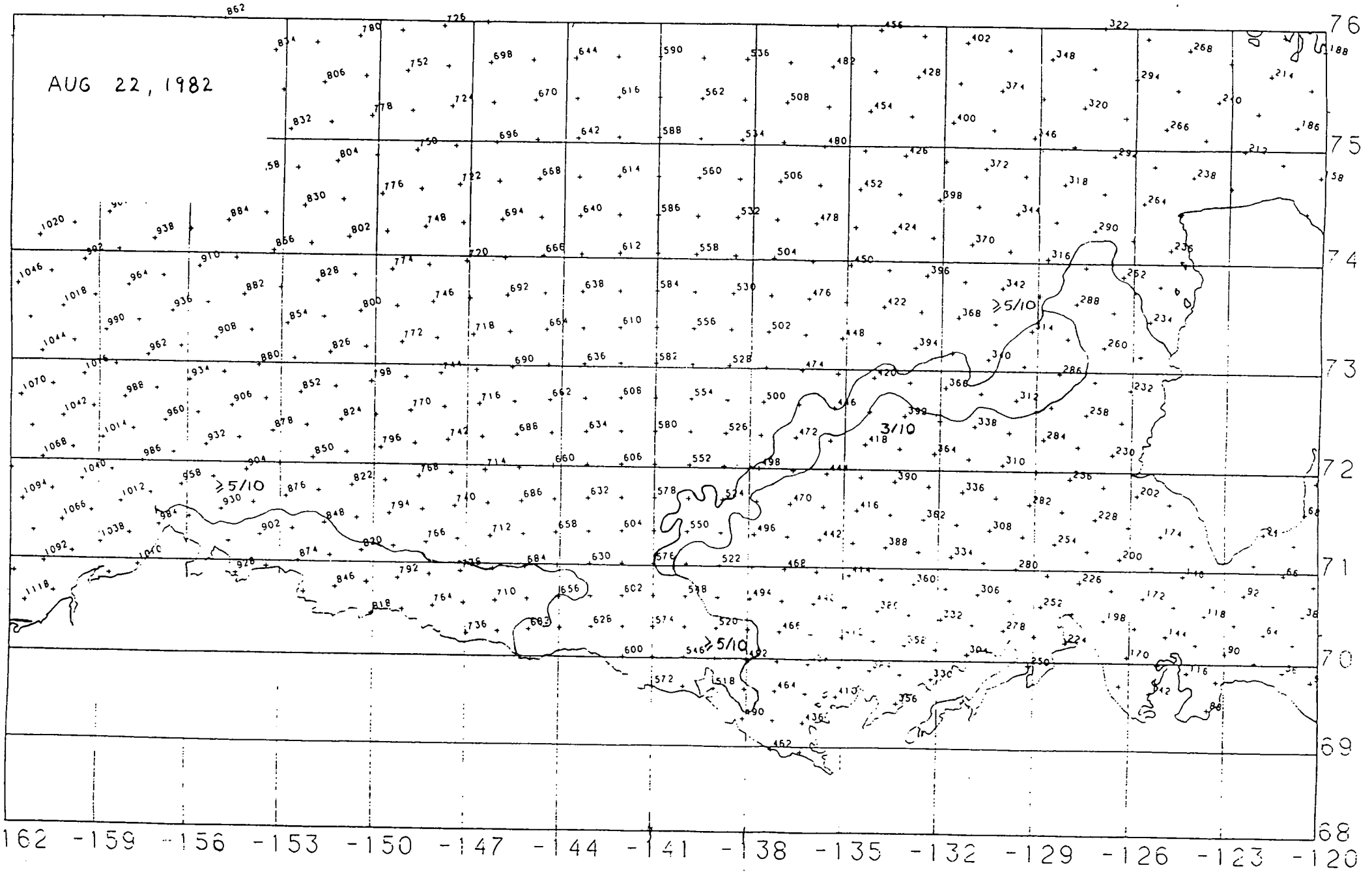
AUG 22, 1982
≥5/10
3/10
≥5/10
76
75
74
73
72
71
70
69
68
162 -159 -156 -153 -150 -147 -144 -141 -138 -135 -132 -129 -126 -123 -120

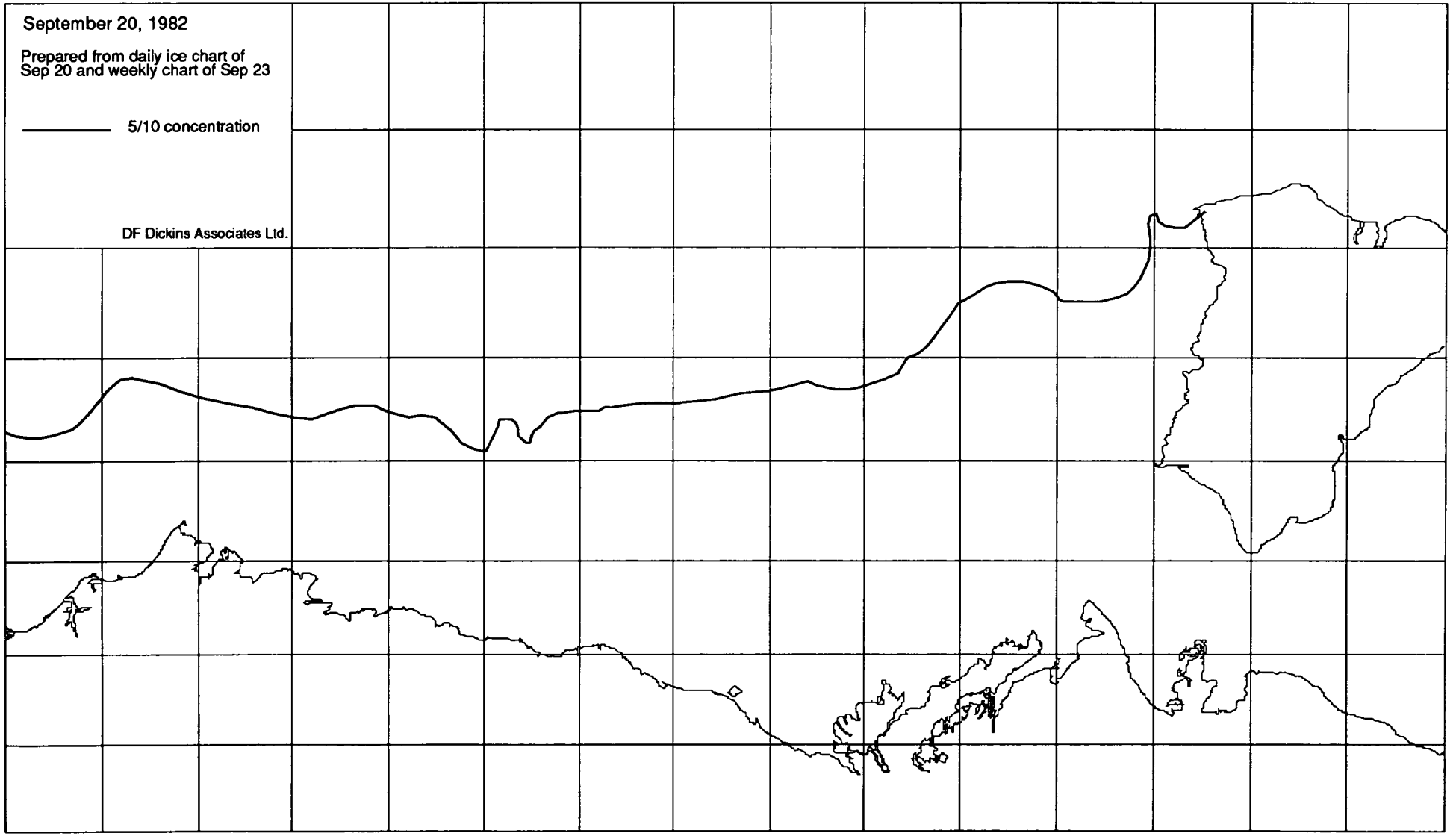
September 20, 1982
Prepared from daily ice chart of
Sep 20 and weekly chart of Sep 23
5/10 concentration
DF Dickins Associates Ltd.

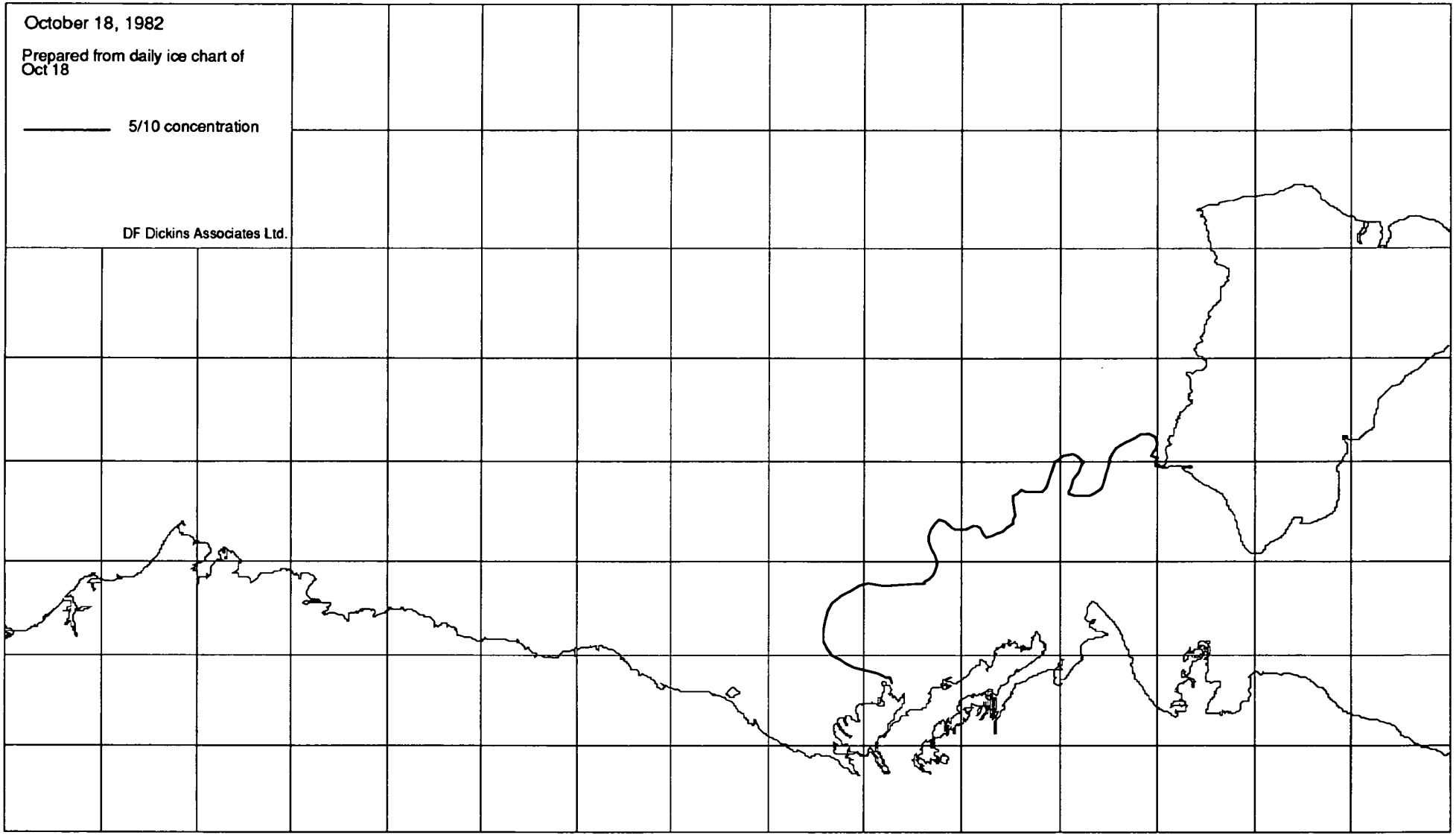
October 18, 1982
Prepared from daily ice chart of Oct 18
5/10 concentration
DF Dickins Associates Ltd.

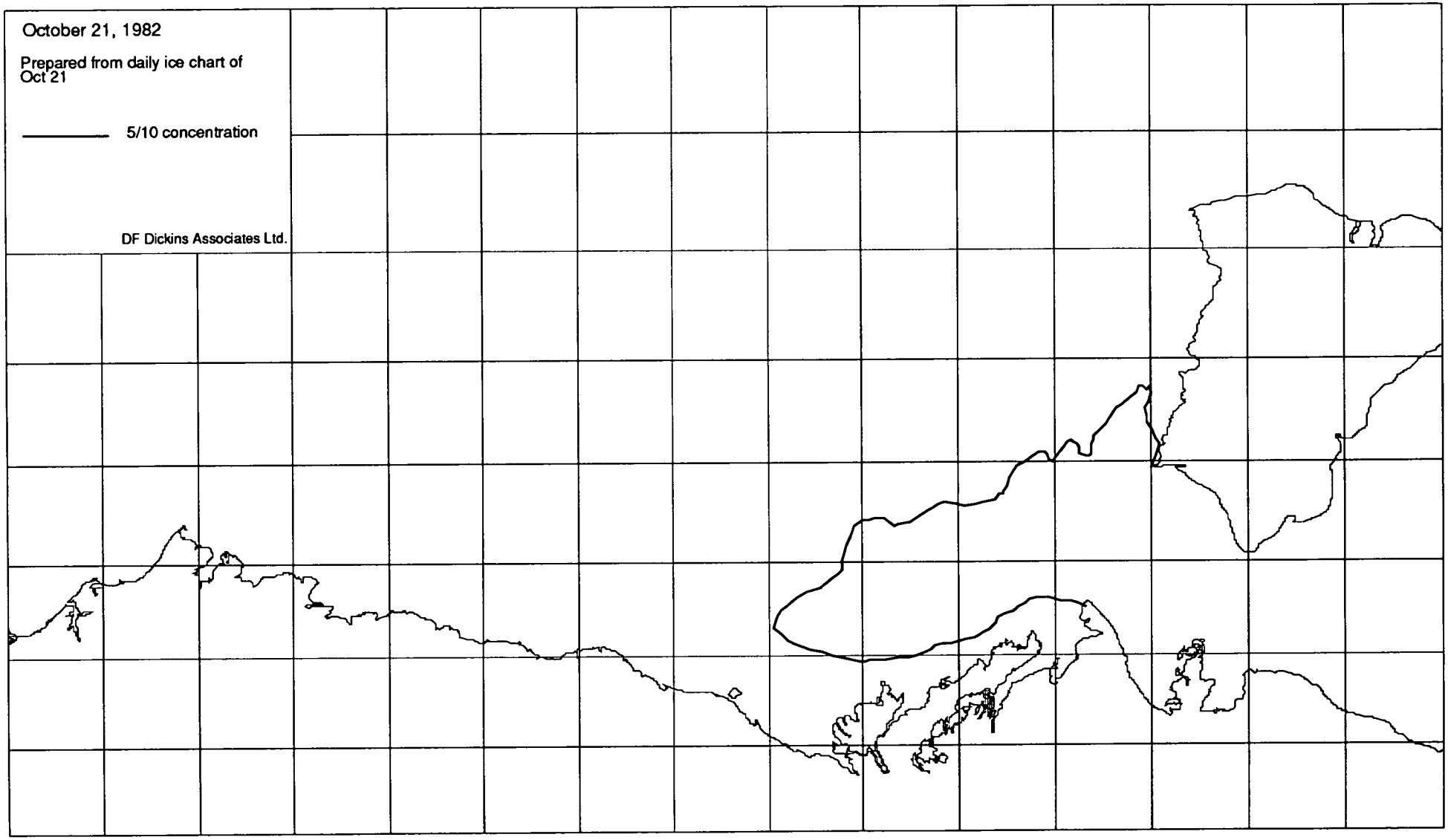
October 21, 1982
Prepared from daily ice chart of Oct 21
5/10 concentration
DF Dickins Associates Ltd.

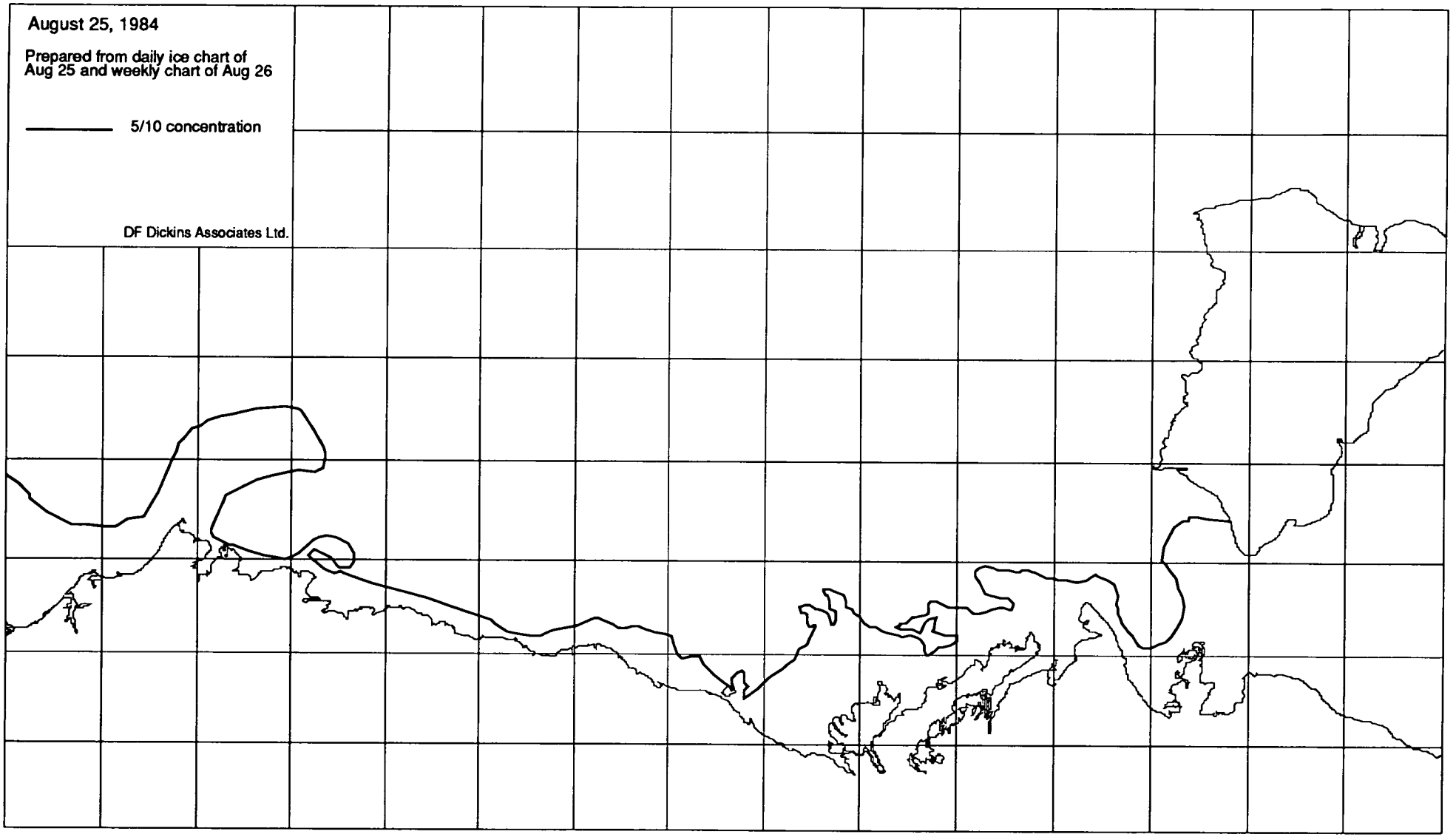
August 25, 1984
Prepared from daily ice chart of
Aug 25 and weekly chart of Aug 26
5/10 concentration
DF Dickins Associates Ltd.

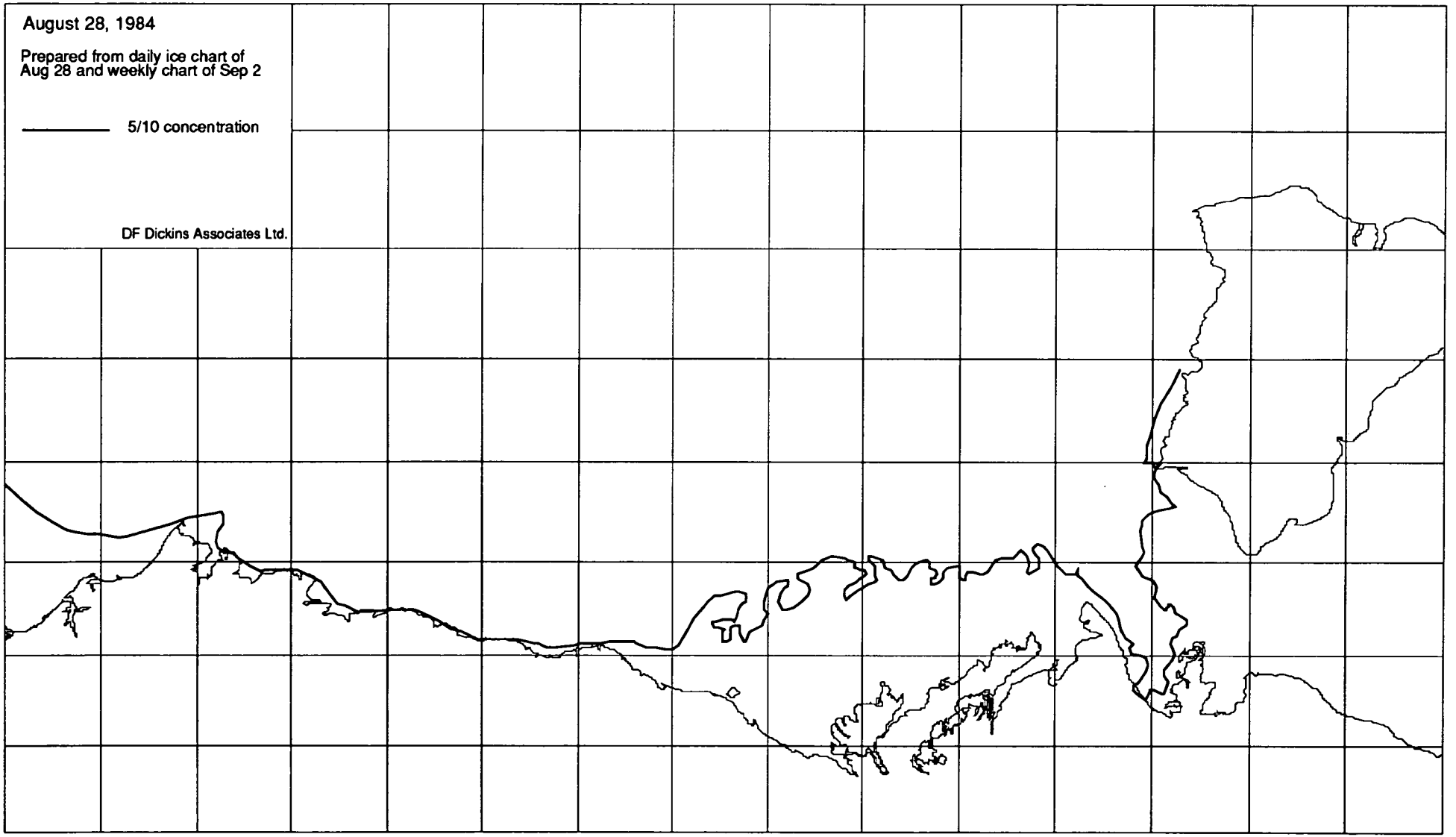
August 28, 1984
Prepared from daily ice chart of
Aug 28 and weekly chart of Sep 2
5/10 concentration
DF Dickins Associates Ltd.

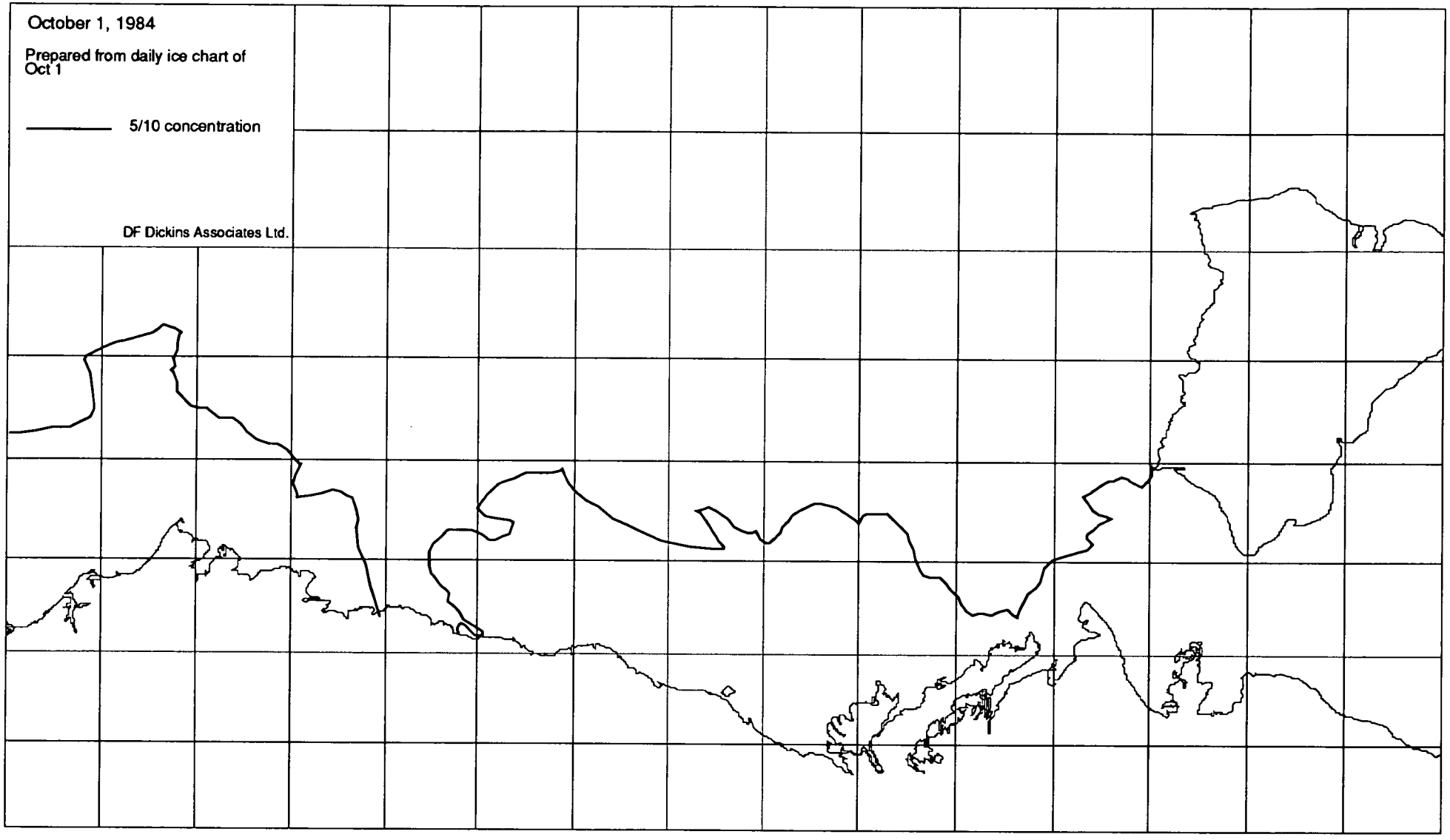
October 1, 1984
Prepared from daily ice chart of Oct 1
5/10 concentration
DF Dickins Associates Ltd.

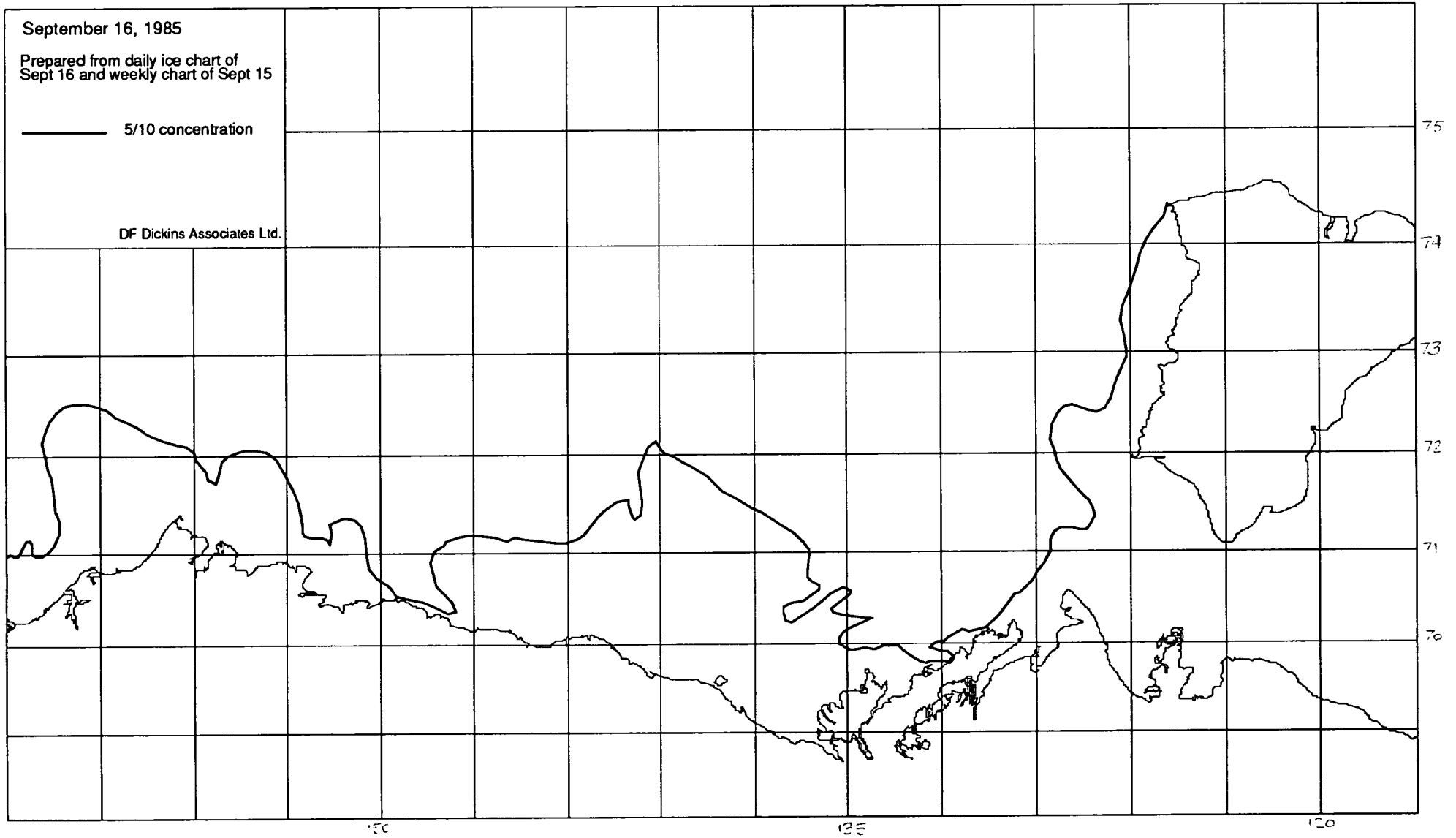
September 16, 1985
Prepared from daily ice chart of Sept 16 and weekly chart of Sept 15
5/10 concentration
DF Dickins Associates Ltd.
75
74
73
72
71
70
130
135
120

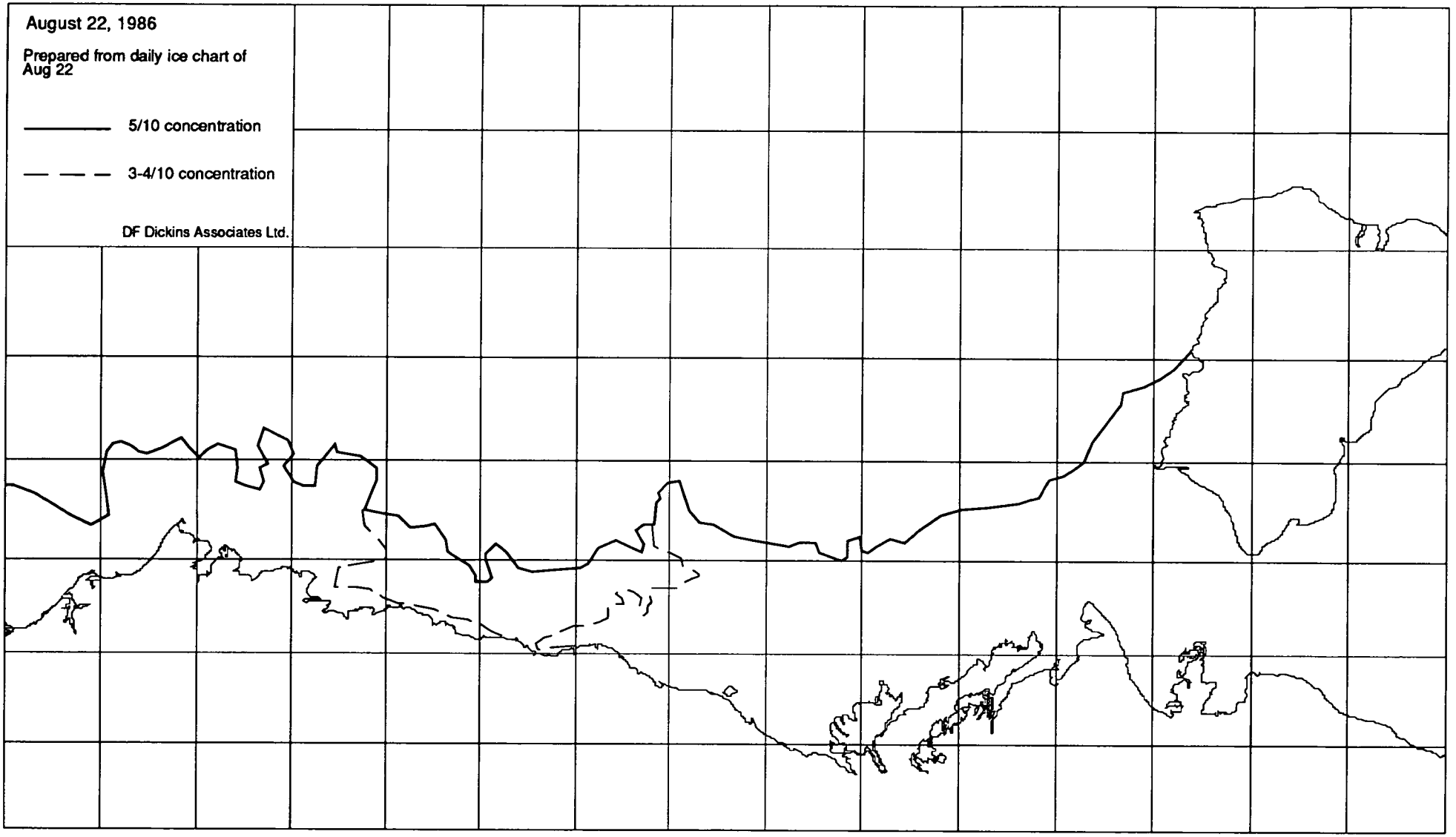
August 22, 1986
Prepared from daily ice chart of Aug 22
5/10 concentration
3-4/10 concentration
DF Dickins Associates Ltd.

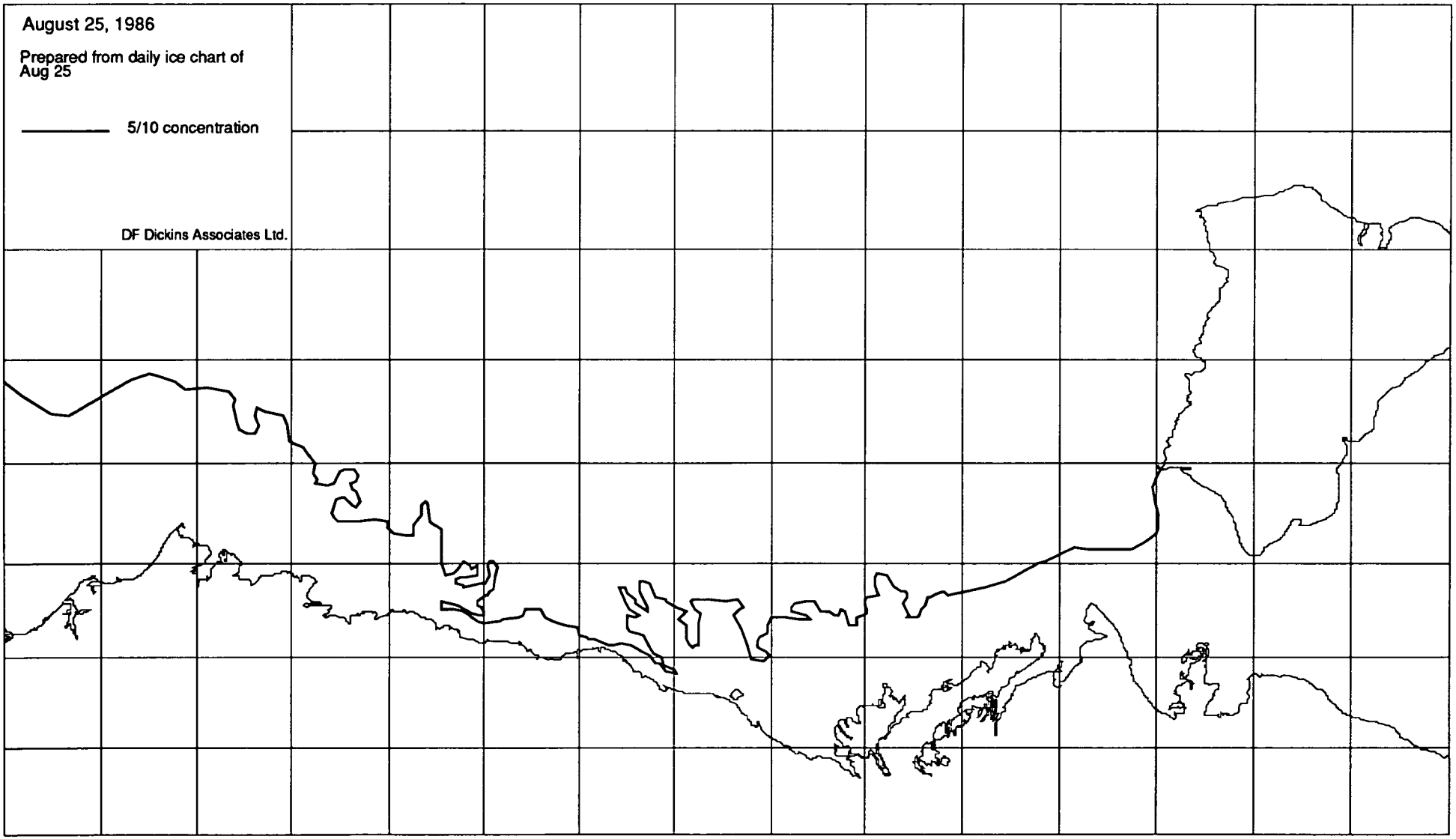
August 25, 1986
Prepared from daily ice chart of Aug 25
5/10 concentration
DF Dickins Associates Ltd.

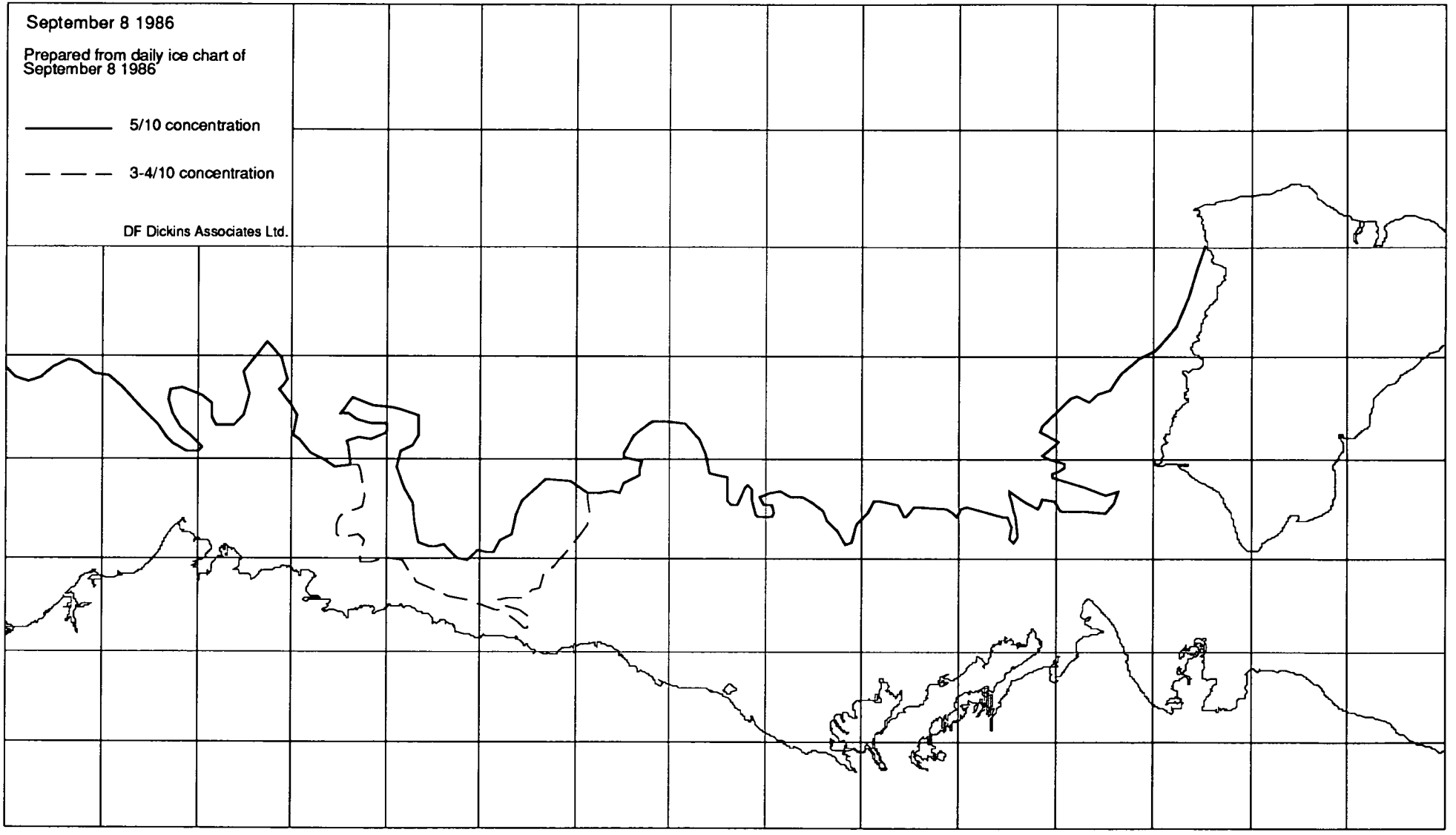
September 8 1986
Prepared from daily ice chart of September 8 1986
5/10 concentration
3-4/10 concentration
DF Dickins Associates Ltd.

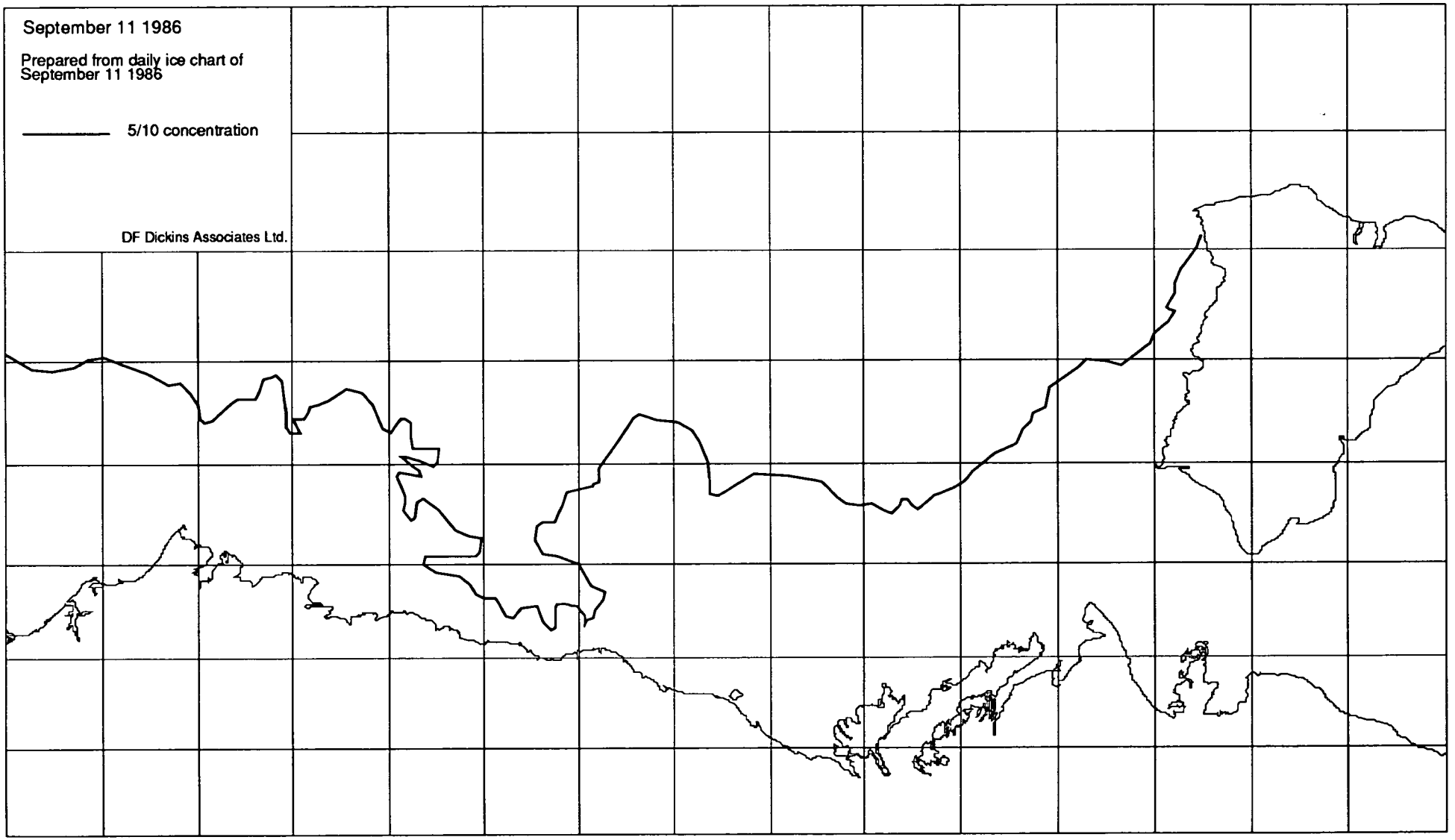
September 11 1986
Prepared from daily ice chart of September 11 1986
5/10 concentration
DF Dickins Associates Ltd.

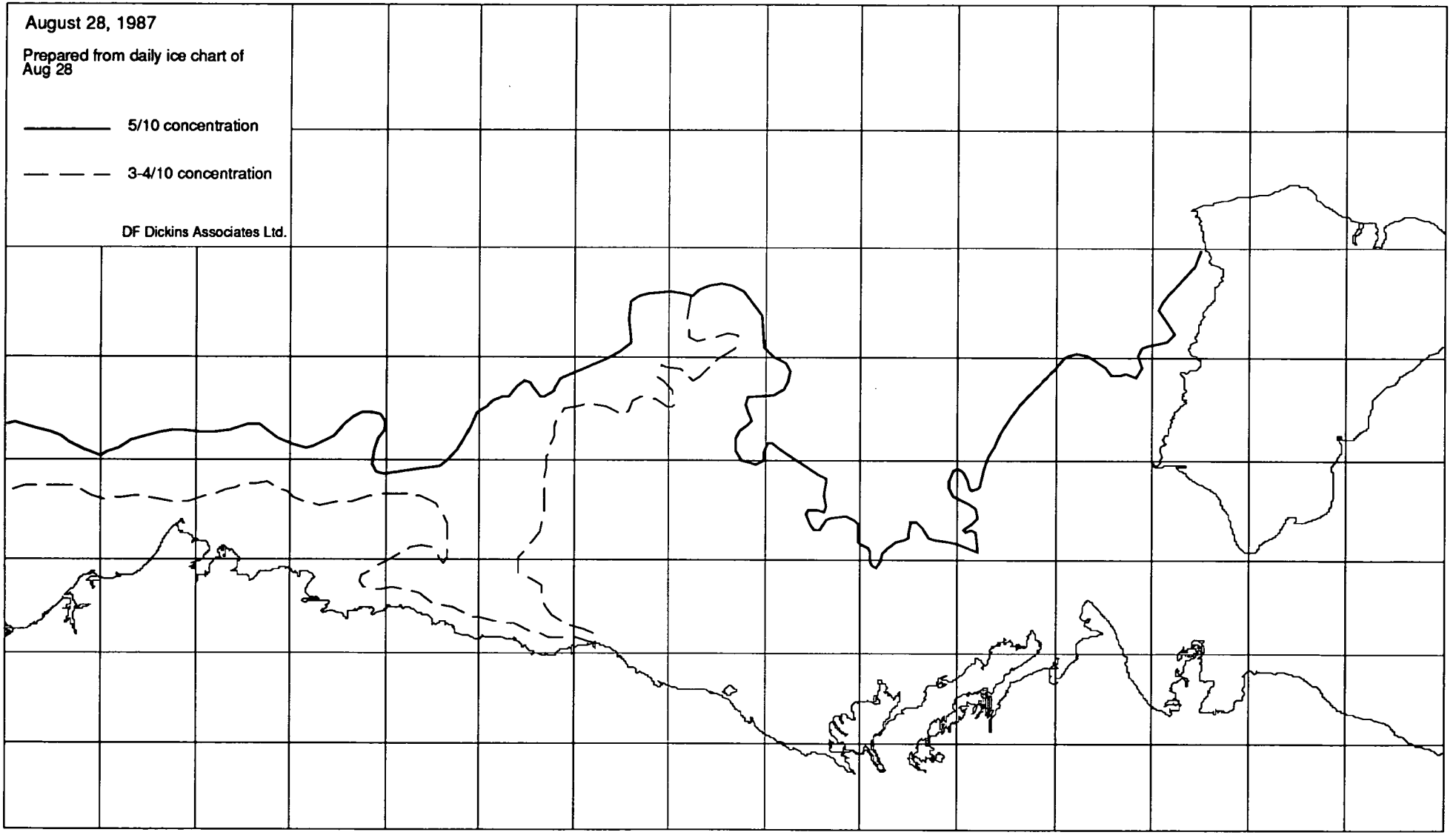
August 28, 1987
Prepared from daily ice chart of Aug 28
5/10 concentration
3-4/10 concentration
DF Dickins Associates Ltd.

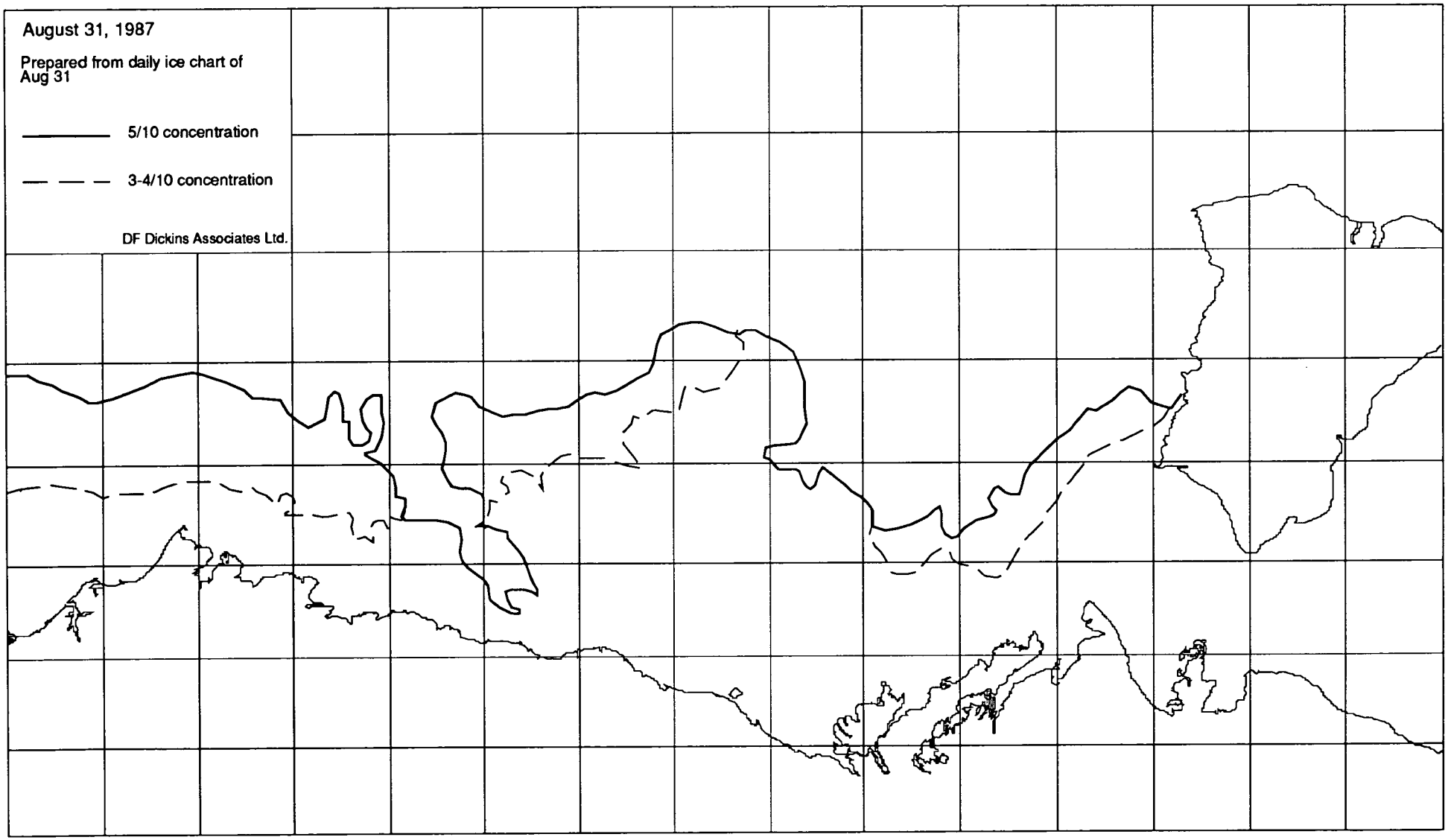
August 31, 1987
Prepared from daily ice chart of Aug 31
5/10 concentration
3-4/10 concentration
DF Dickins Associates Ltd.

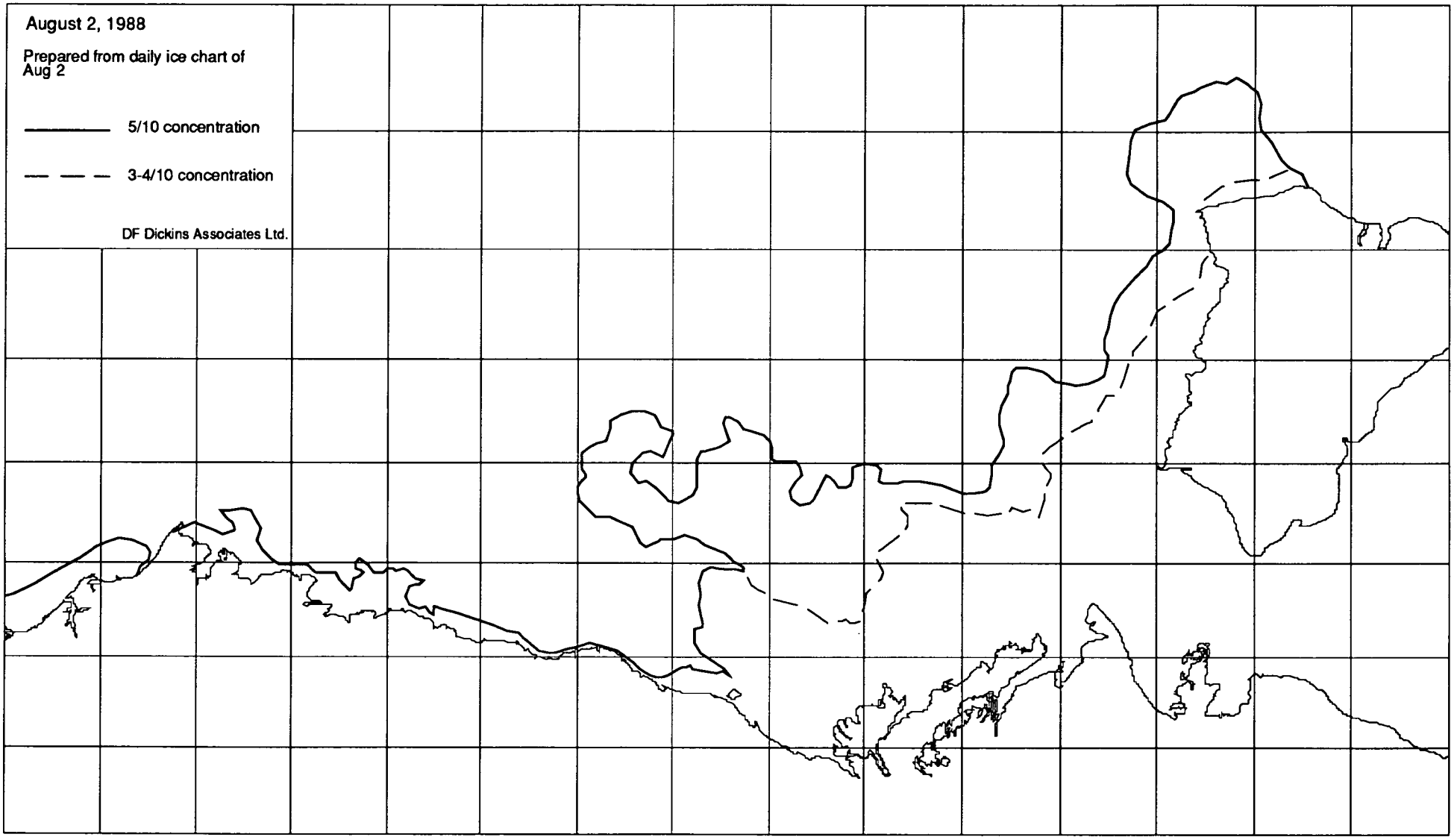
August 2, 1988
Prepared from daily ice chart of Aug 2
5/10 concentration
3-4/10 concentration
DF Dickins Associates Ltd.

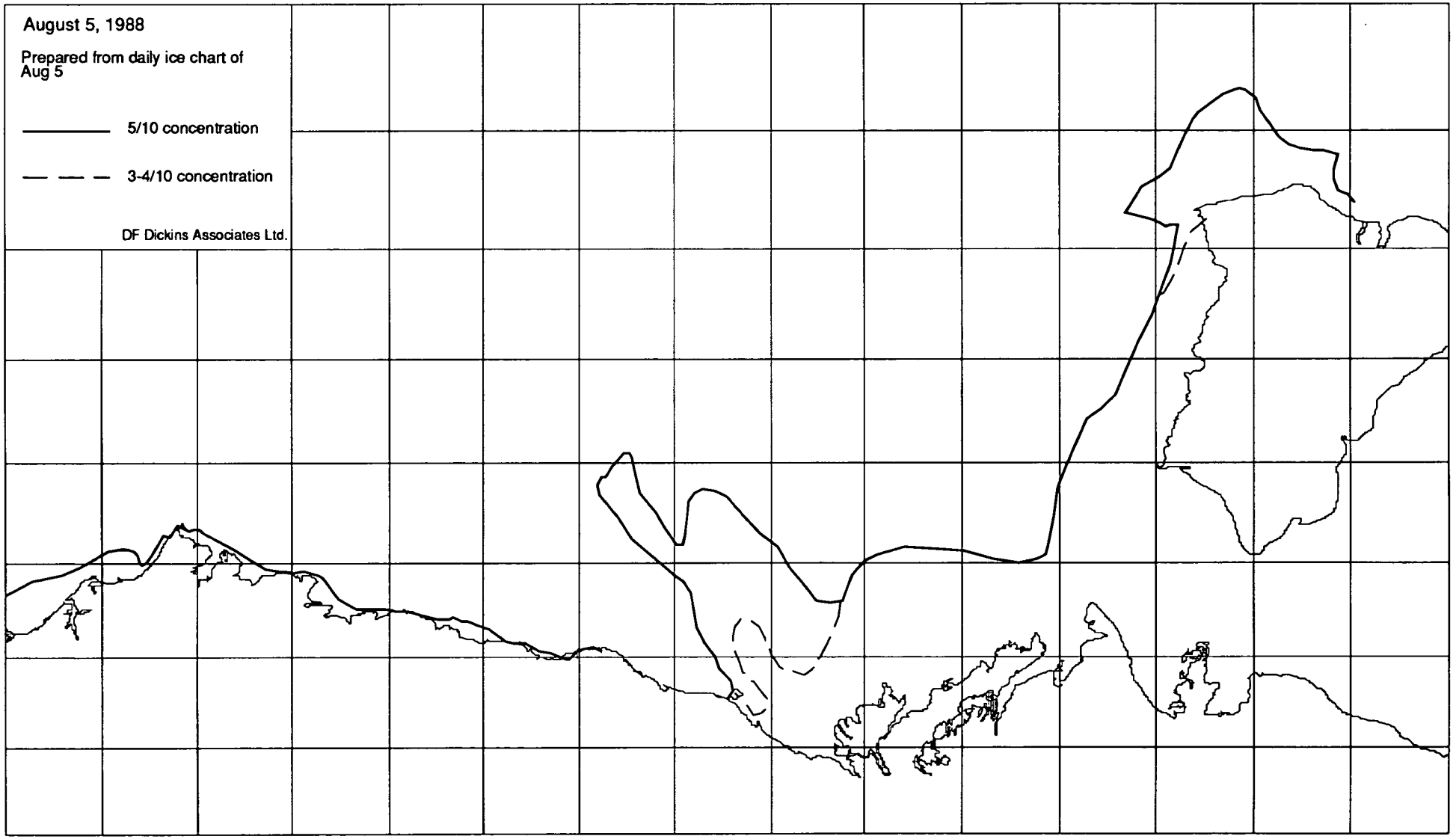
August 5, 1988
Prepared from daily ice chart of Aug 5
5/10 concentration
3-4/10 concentration
DF Dickins Associates Ltd.

PERCENTAGE OCCURRENCE OF ANY ICE

JUL 16 – JUL 31

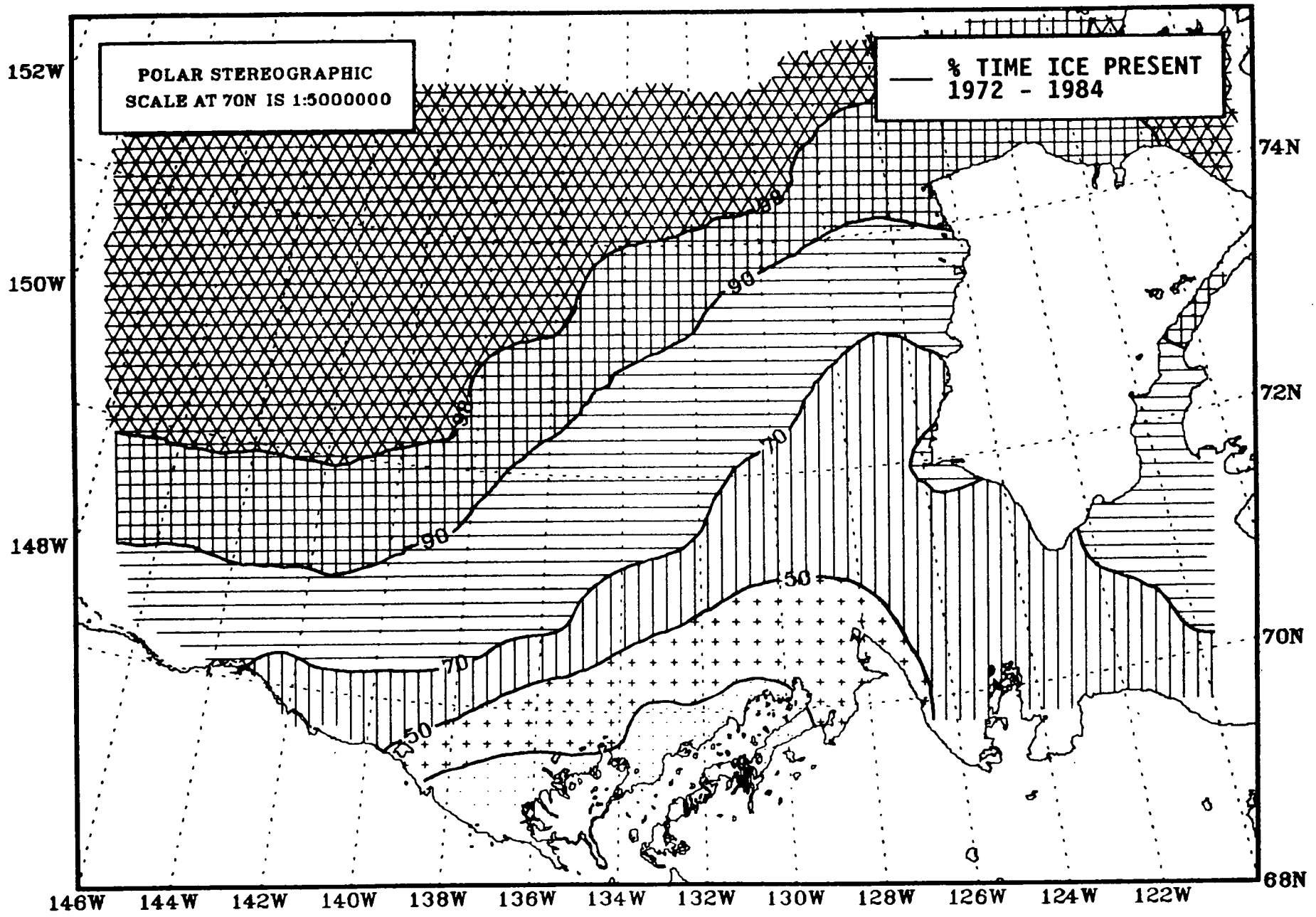

PERCENTAGE OCCURRENCE OF ANY ICE

AUG 1 – AUG 15

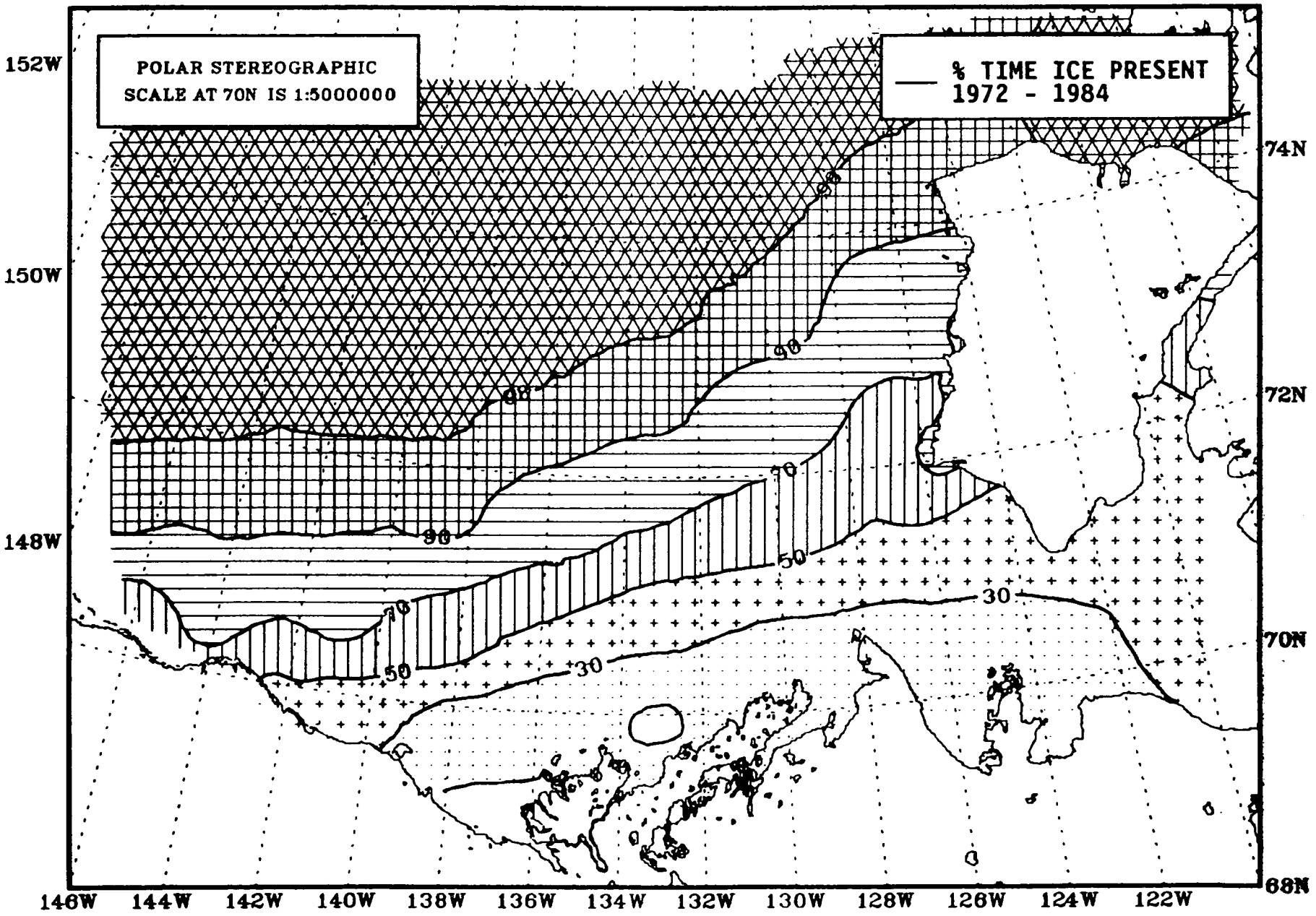

PERCENTAGE OCCURRENCE OF ANY ICE

AUG 16 – AUG 31

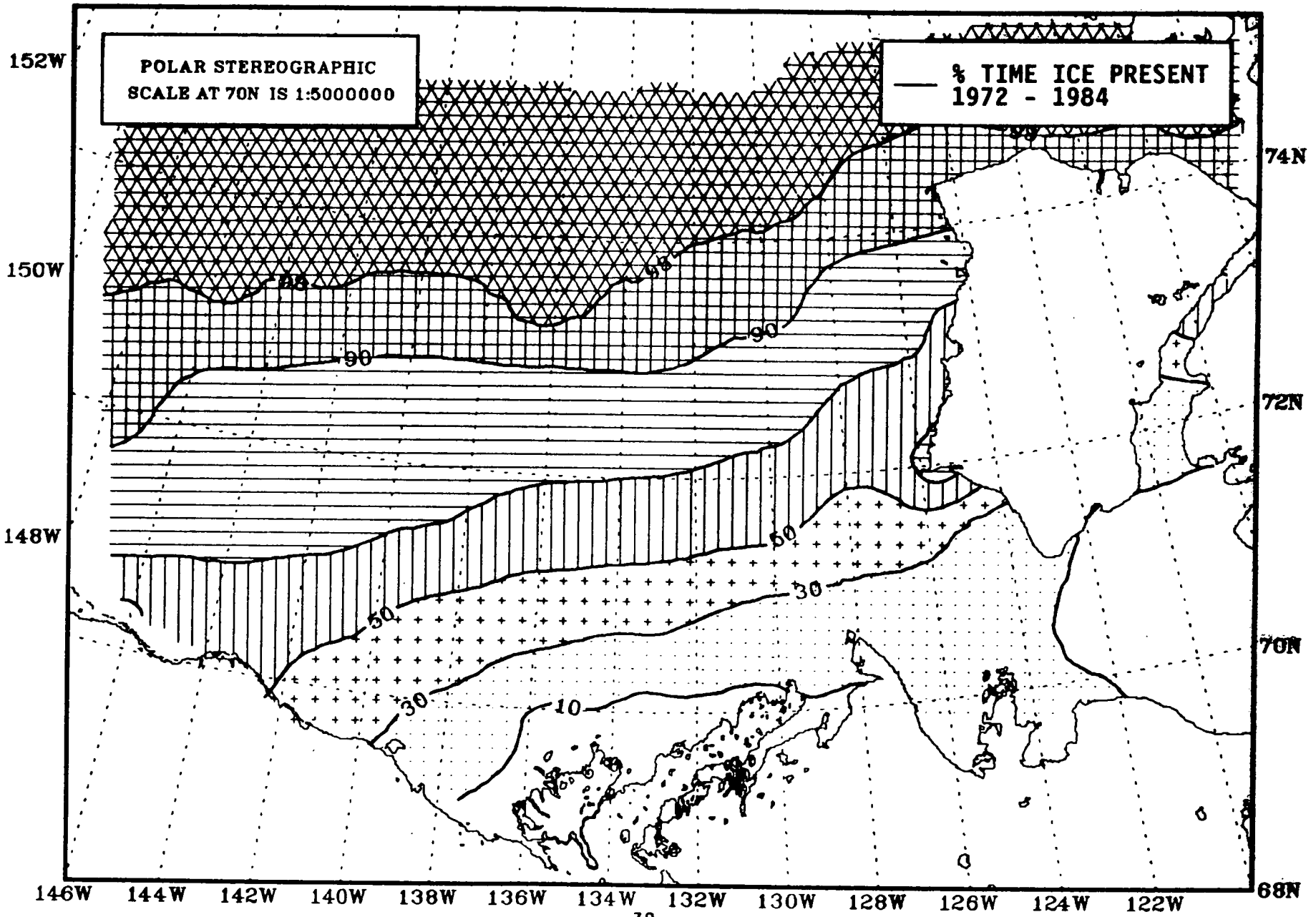

PERCENTAGE OCCURRENCE OF ANY ICE

SEP 1 – SEP 15

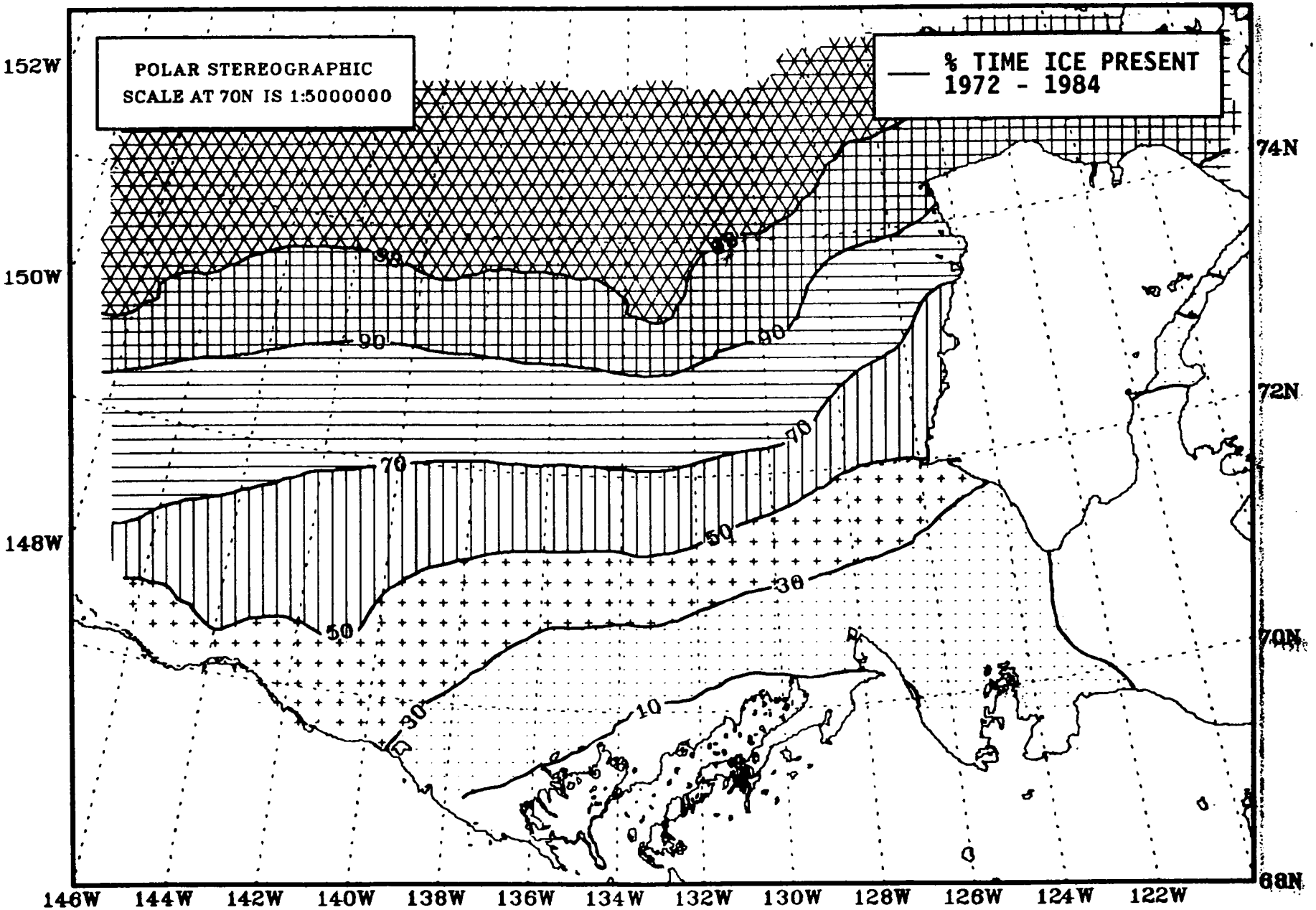

PERCENTAGE OCCURRENCE OF ANY ICE

SEP 16 – SEP 30

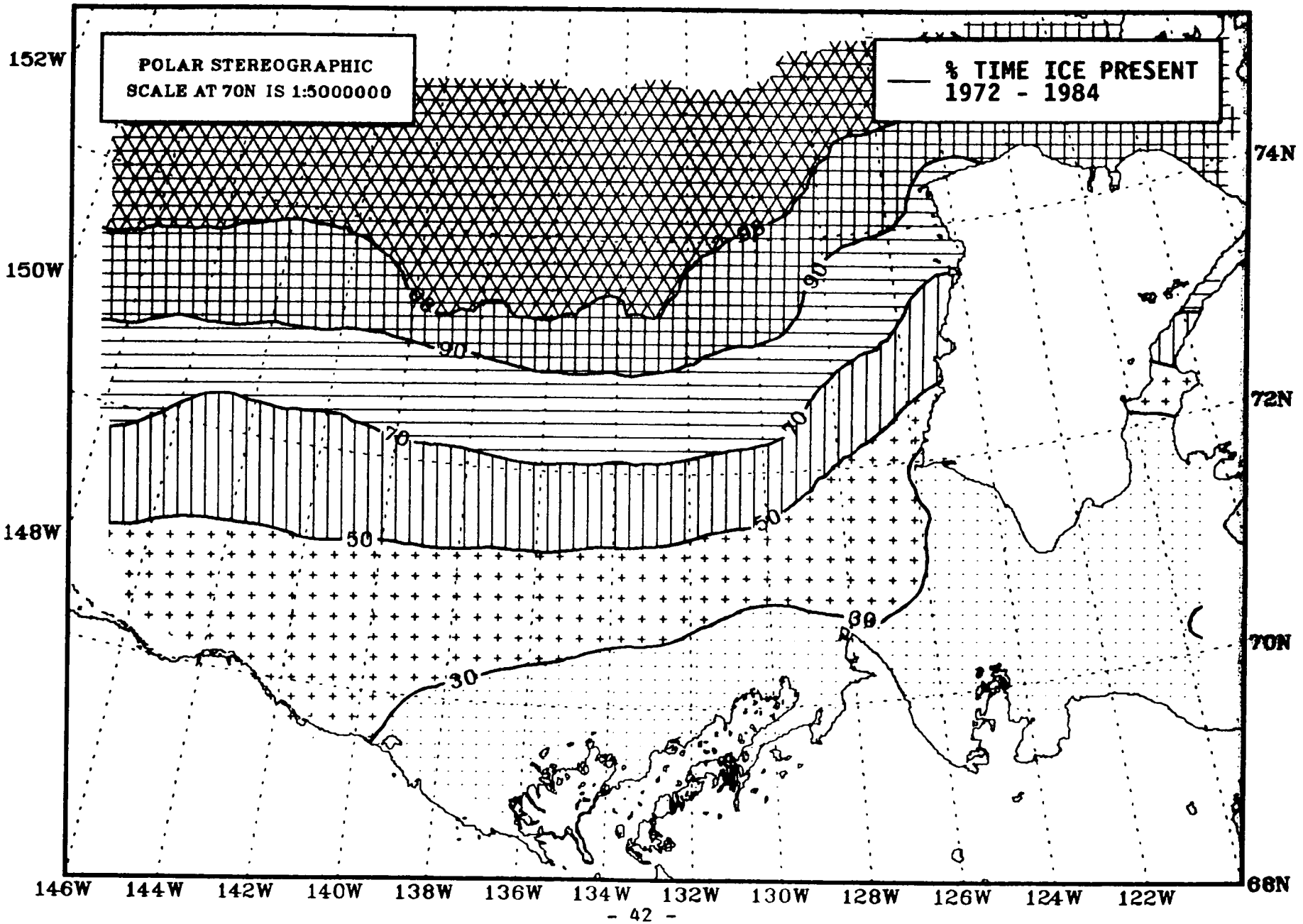

PERCENTAGE OCCURRENCE OF ANY ICE

OCT 1 – OCT 15

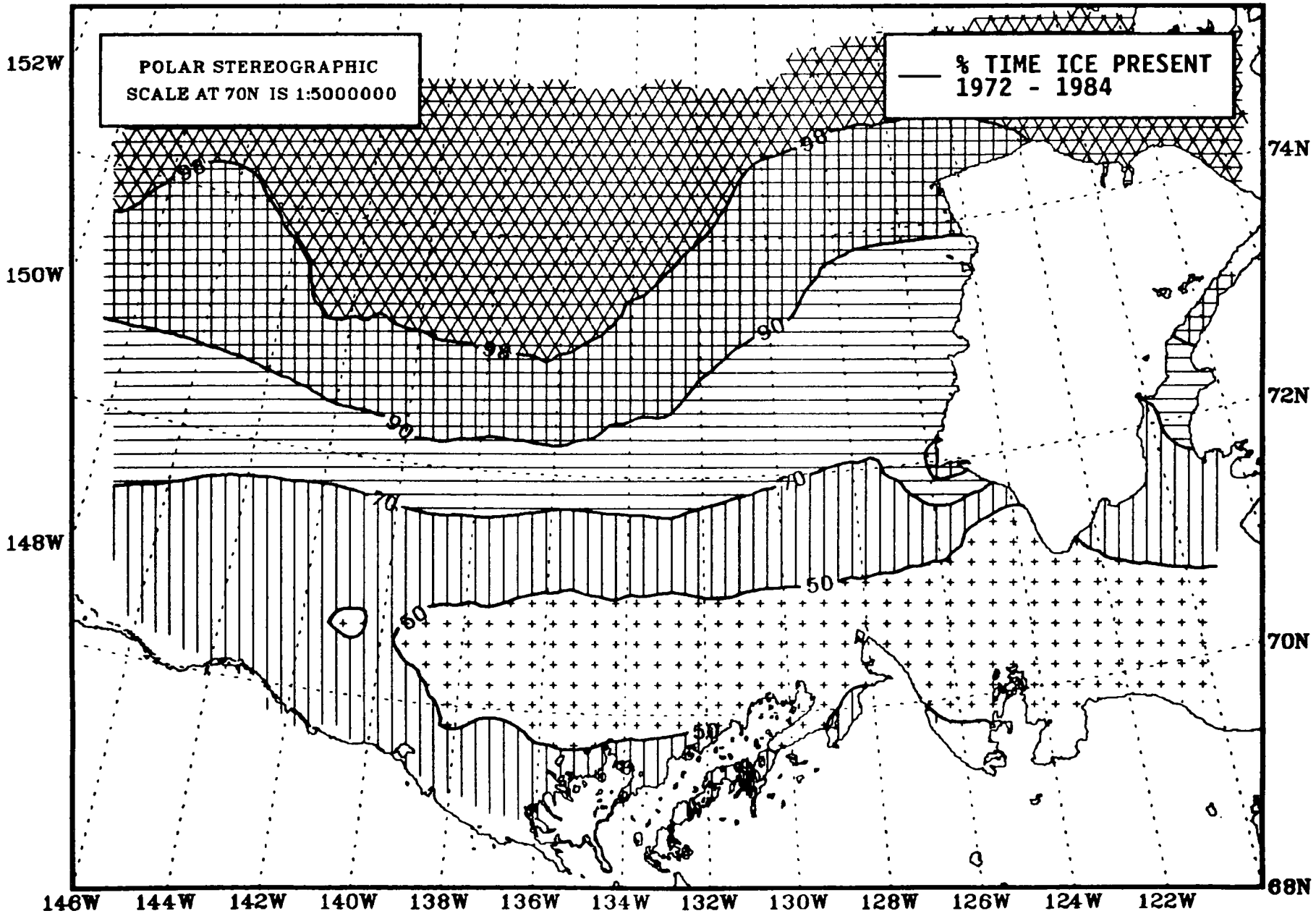

PERCENTAGE OCCURRENCE OF ANY ICE

OCT 16 – OCT 31

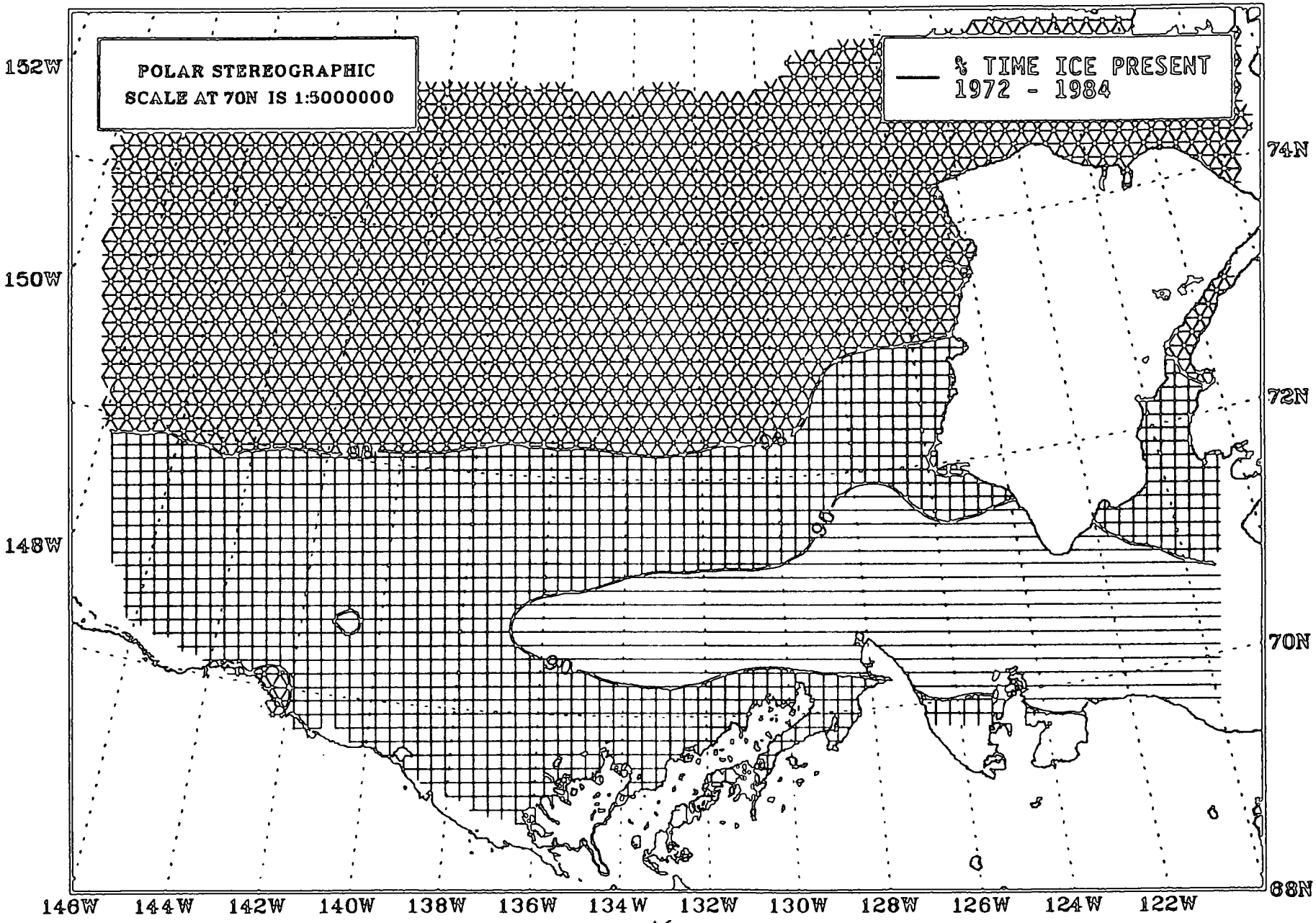

APPENDIX D
VERIFICATION RESULTS TIME SERIES PLOTS

BEAUFORT SEA HINDCAST

MANMAR, WAVERIDER AND MODEL GRID POINT LOCATIONS & DEPTHS

August 25, 1977 to August 28, 1977

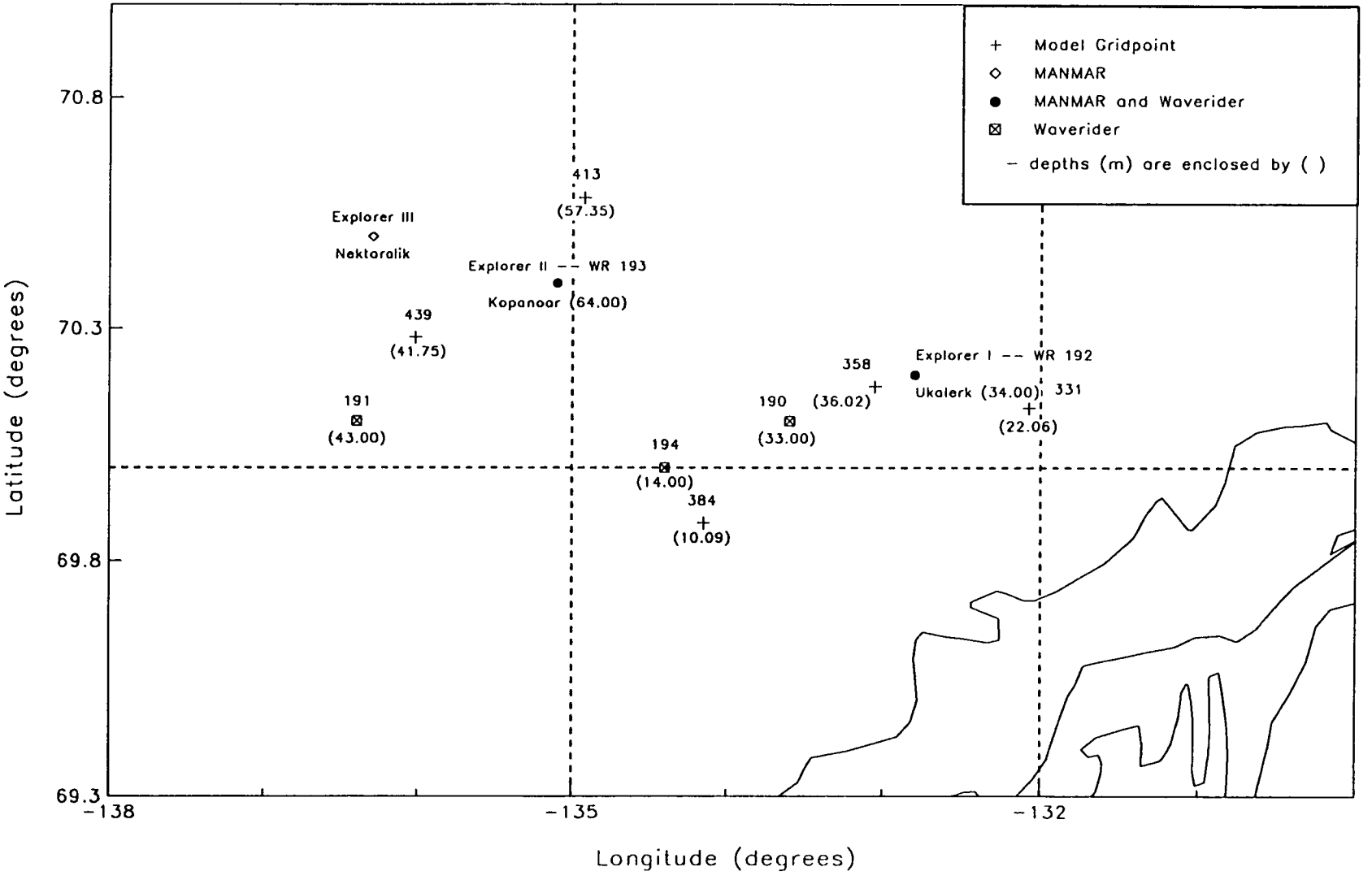

BEAUFORT SEA STORM VERIFICATION

GRID POINT 358 - WR 190

August 25, 1977 to August 28, 1977

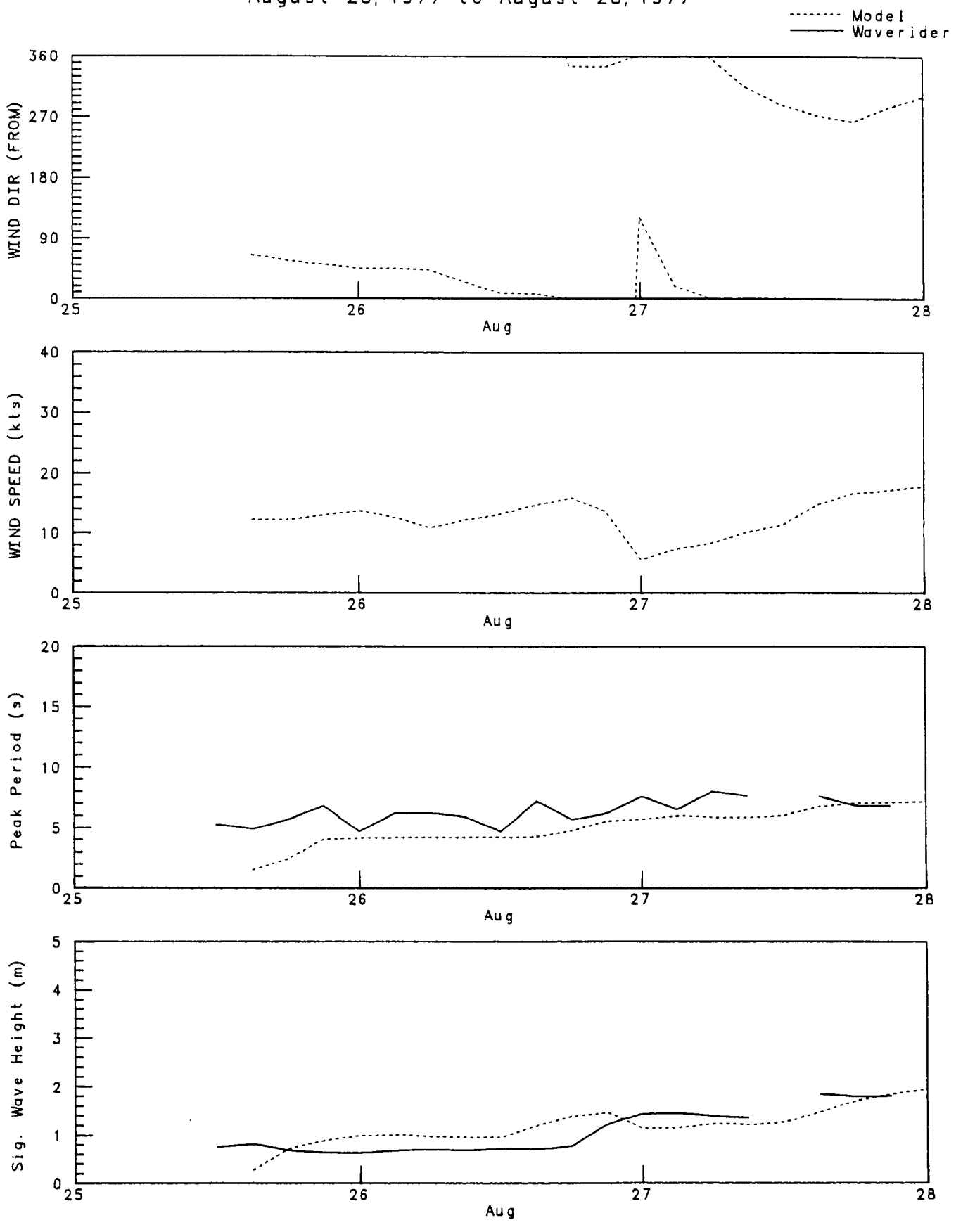

BEAUFORT SEA STORM VERIFICATION

GRID POINT 439 - WR 191

August 25, 1977 to August 28, 1977

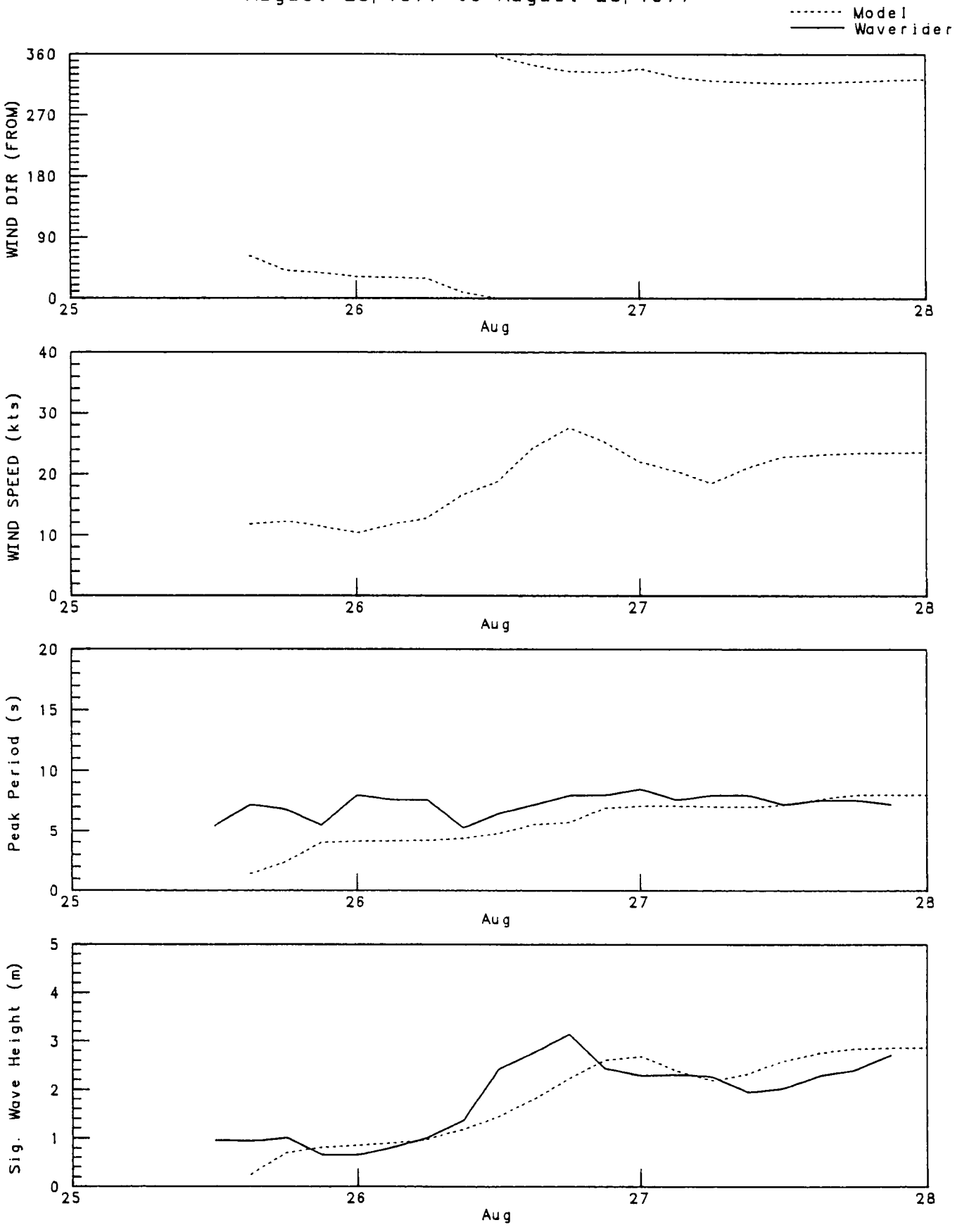

BEAUFORT SEA STORM VERIFICATION

GRID POINT 331 – EXPLORER I, UKALERK – WR 192

August 25, 1977 to August 28, 1977

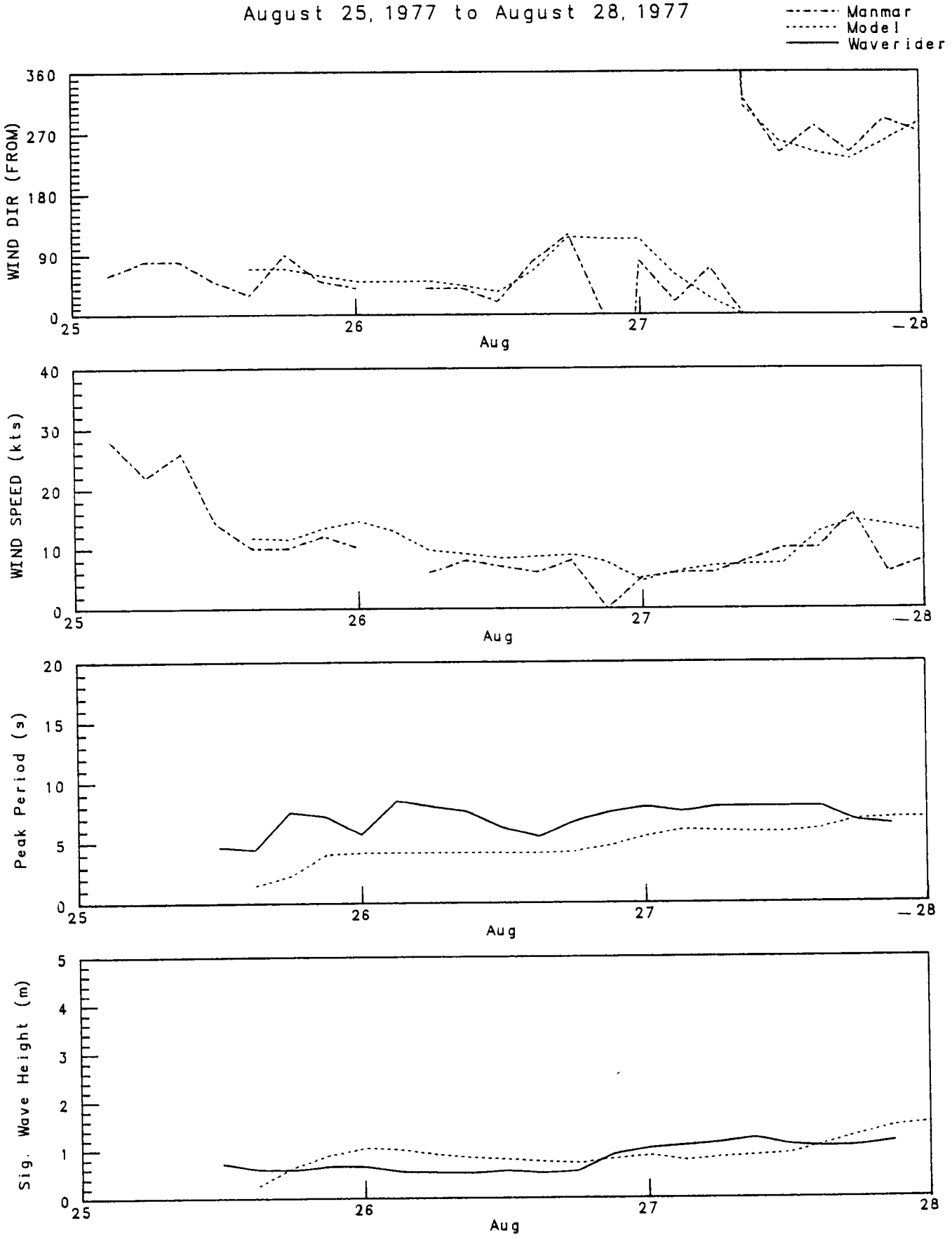

BEAUFORT SEA STORM VERIFICATION

GRID POINT 413 – EXPLORER II, KOPANOAR – WR 193

August 25, 1977 to August 28, 1977

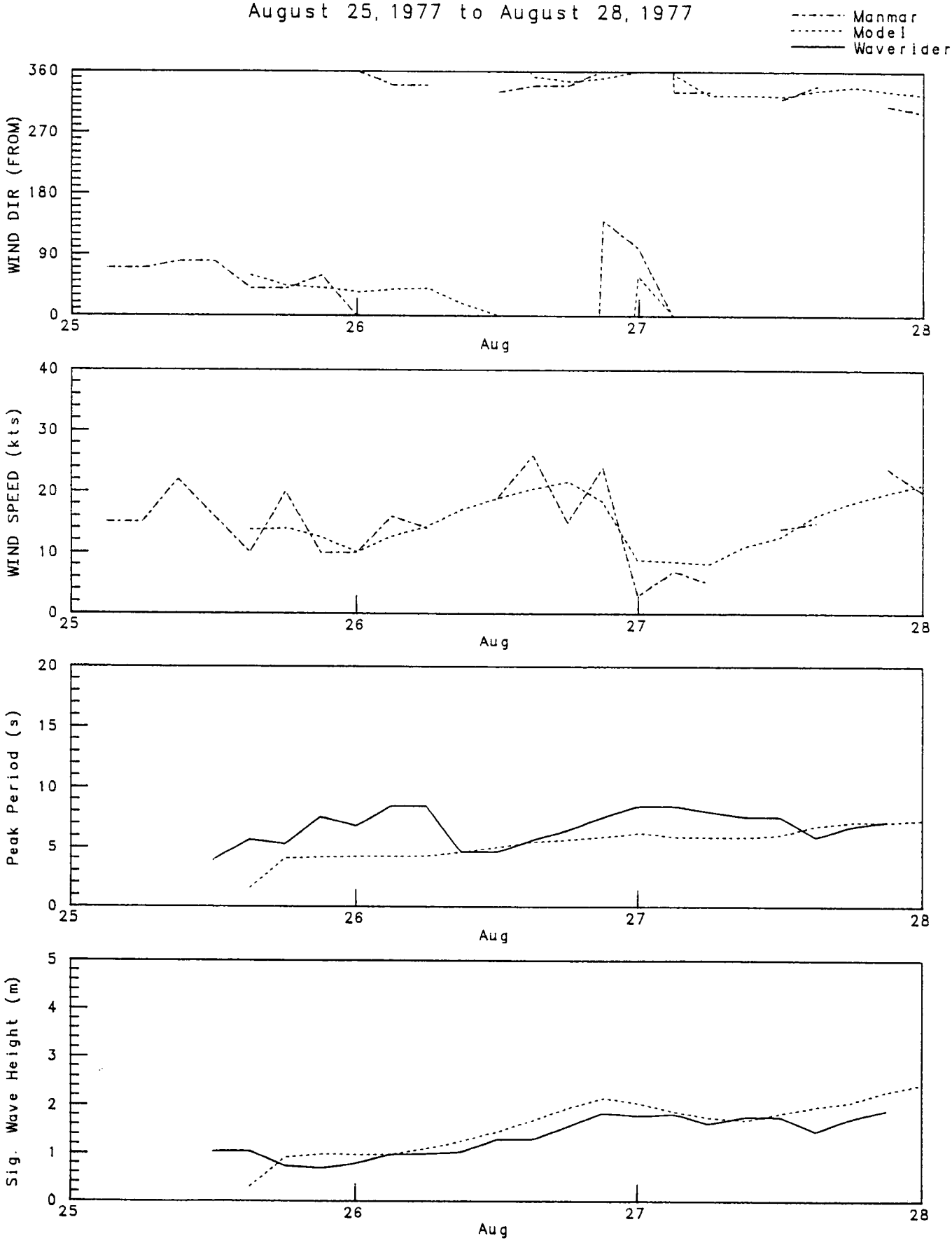

BEAUFORT SEA STORM VERIFICATION

GRID POINT 384 - WR 194

August 25, 1977 to August 28, 1977

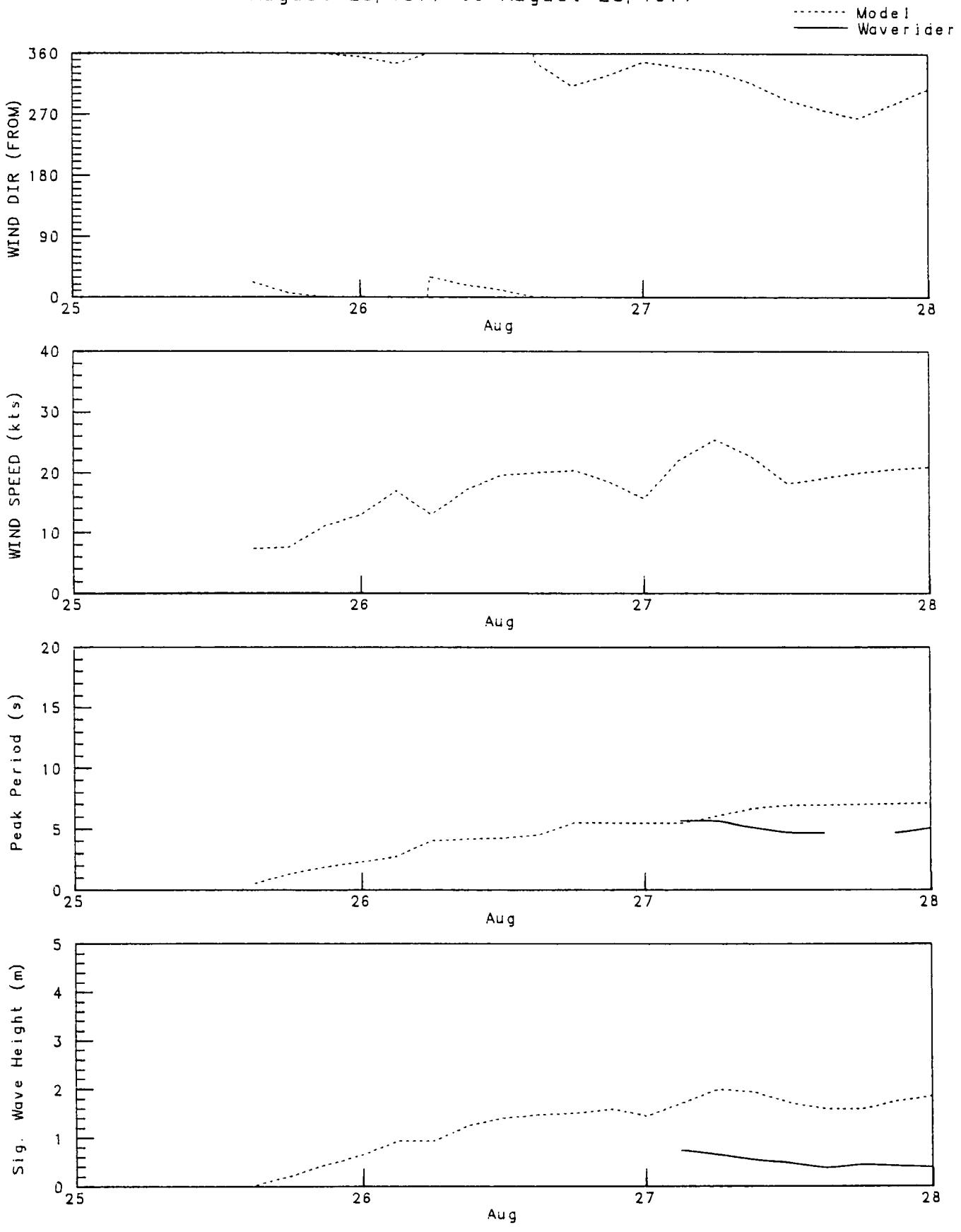

BEAUFORT SEA STORM VERIFICATION

GRID POINT 384 – EXPLORER III, NEKTORALIK

August 25, 1977 to August 28, 1977

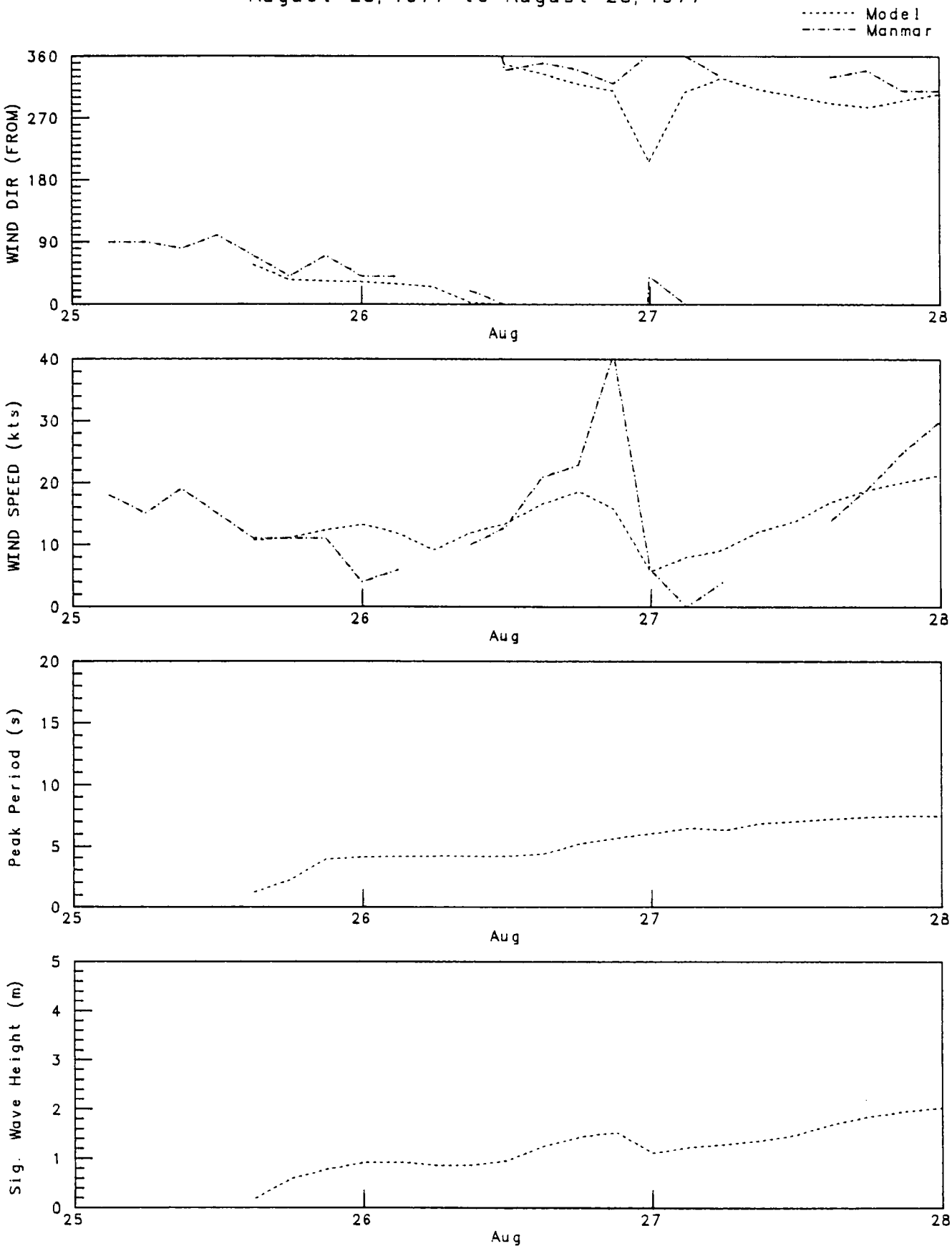

BEAUFORT SEA HINDCAST

MANMAR, WAVERIDER AND MODEL GRID POINT LOCATIONS & DEPTHS

September 28, 1978 to October 1, 1978

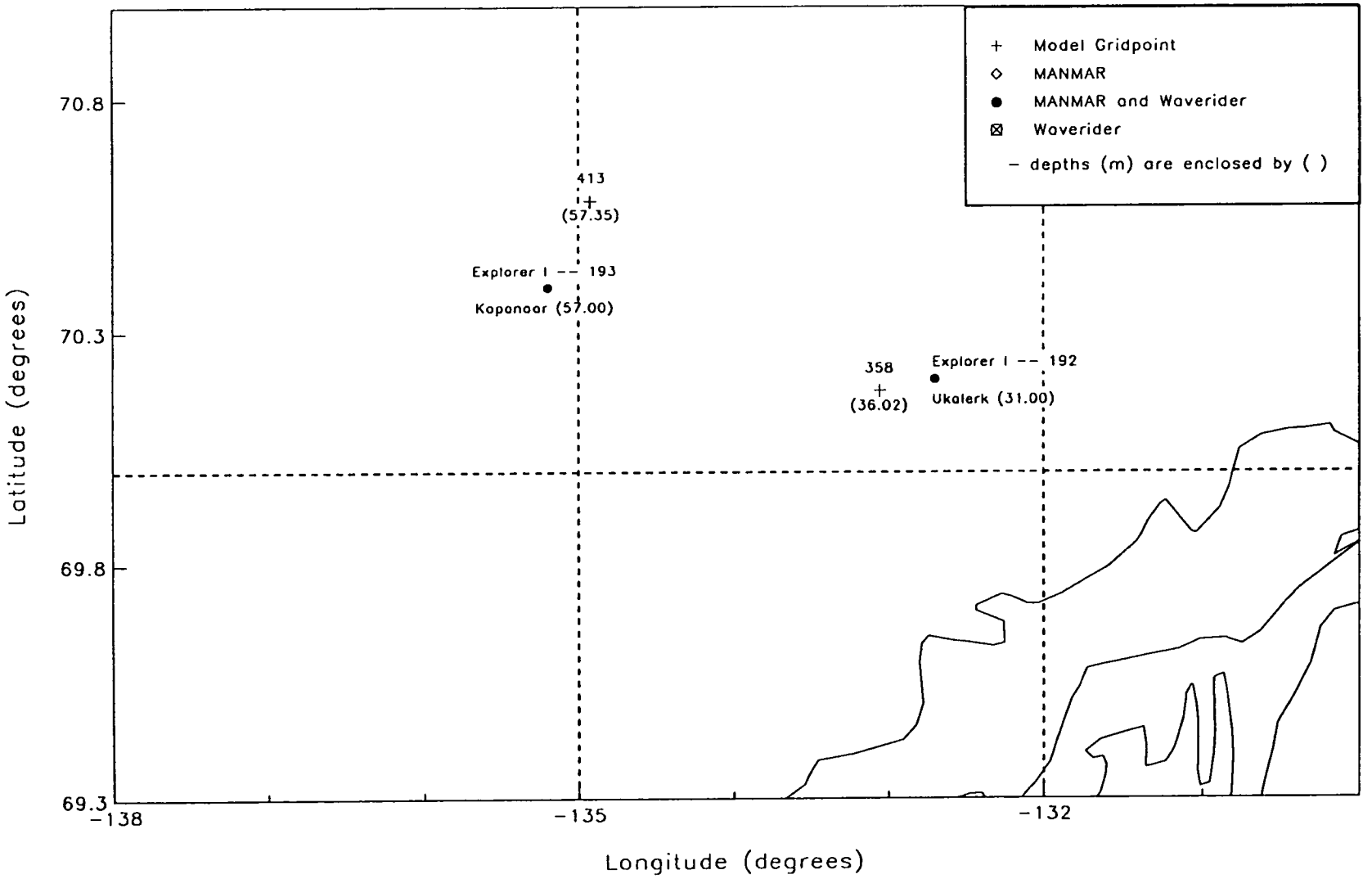

BEAUFORT SEA STORM VERIFICATION

GRID POINT 358 - EXPLORER I, UKALERK - WR 192

September 28, 1978 to October 1, 1978

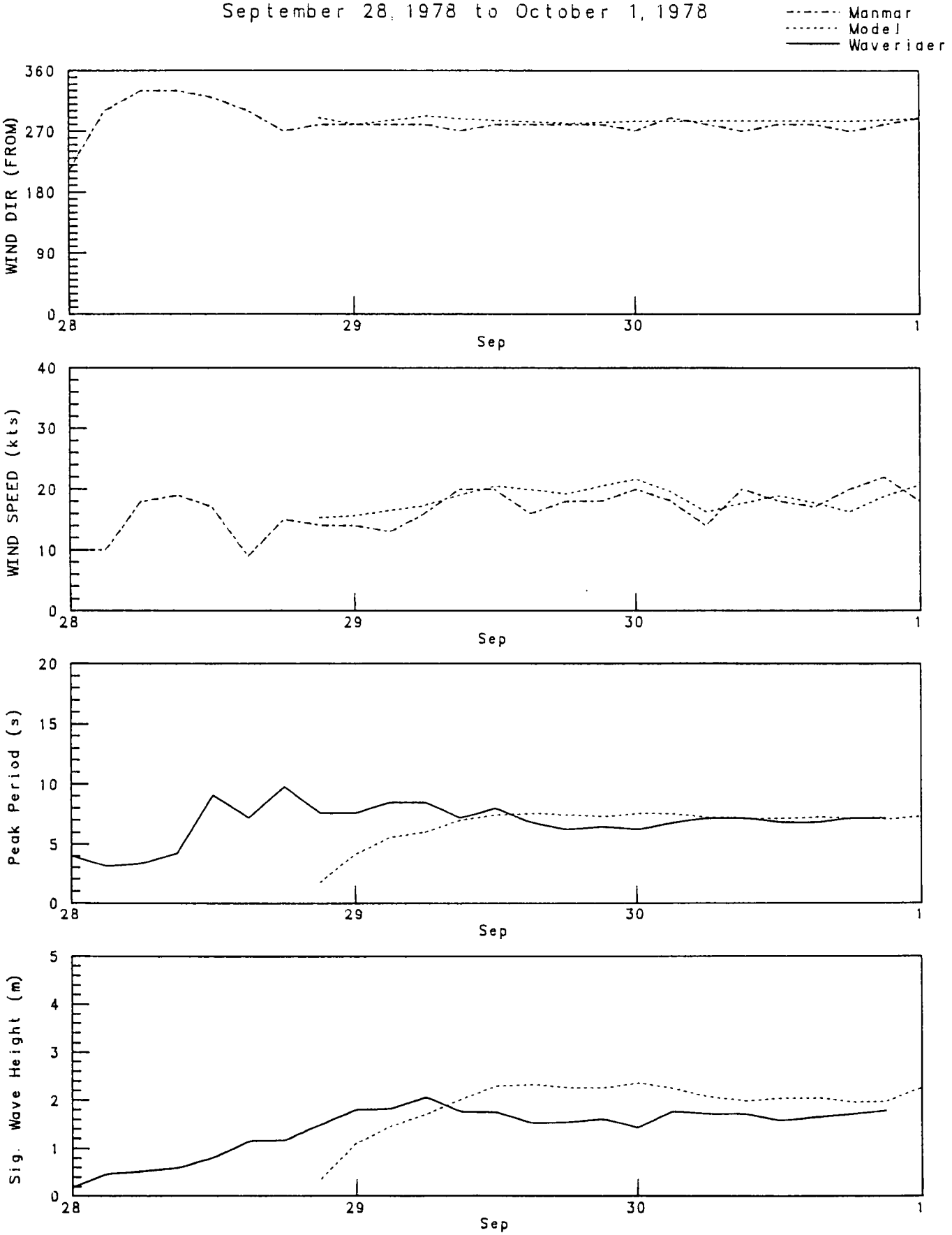

BEAUFORT SEA STORM VERIFICATION

GRID POINT 413 - EXPLORER I, KOPANOAR - WR 193

September 28, 1978 to October 1, 1978

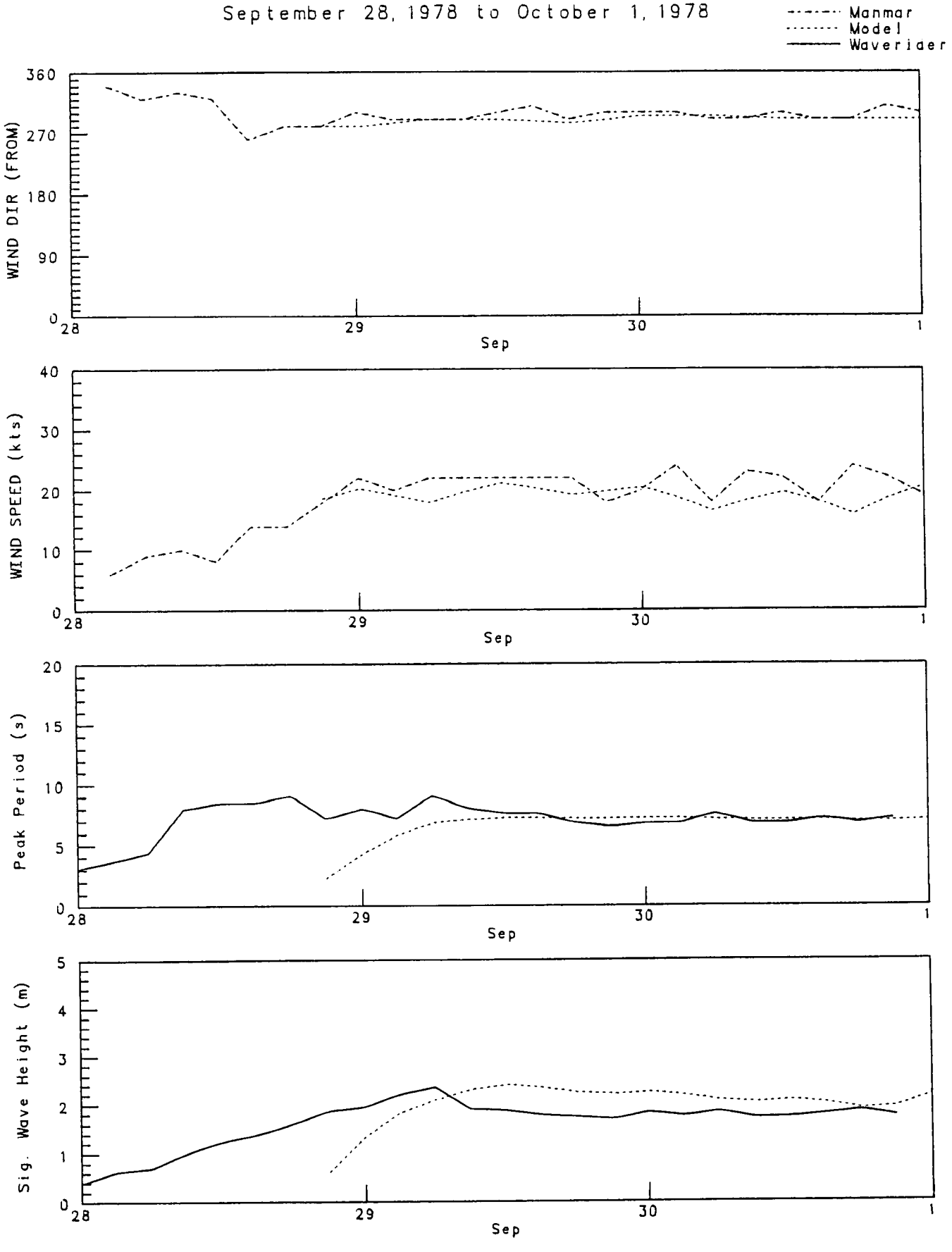

BEAUFORT SEA HINDCAST

MANMAR, WAVERIDER, AND MODEL GRID POINT LOCATIONS & DEPTHS

August 16, 1981 to August 19, 1981

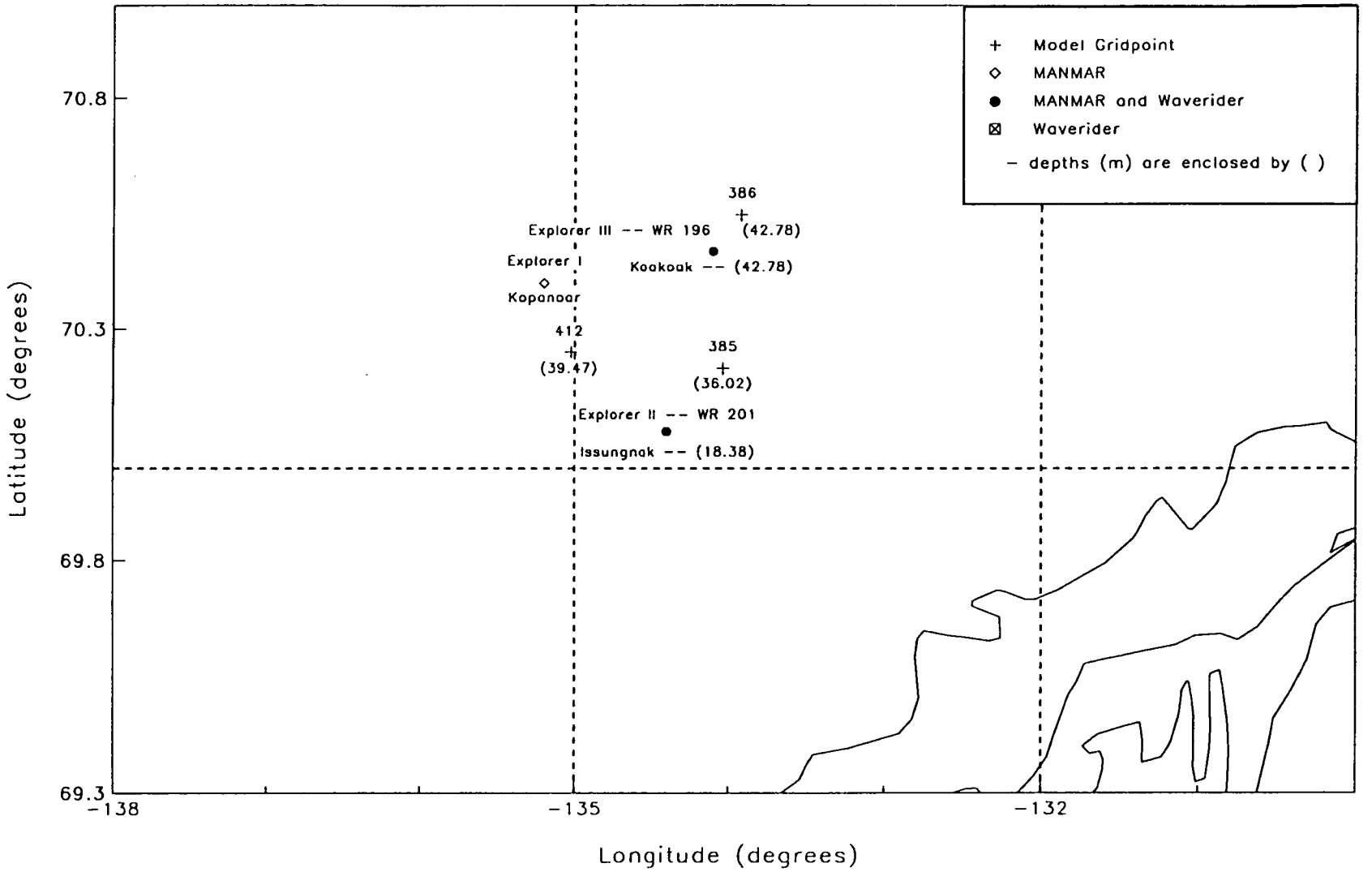

BEAUFORT SEA STORM VERIFICATION

GRID POINT 412 – EXPLORER I, KOPANOAR

August 16, 1981 to August 19, 1981

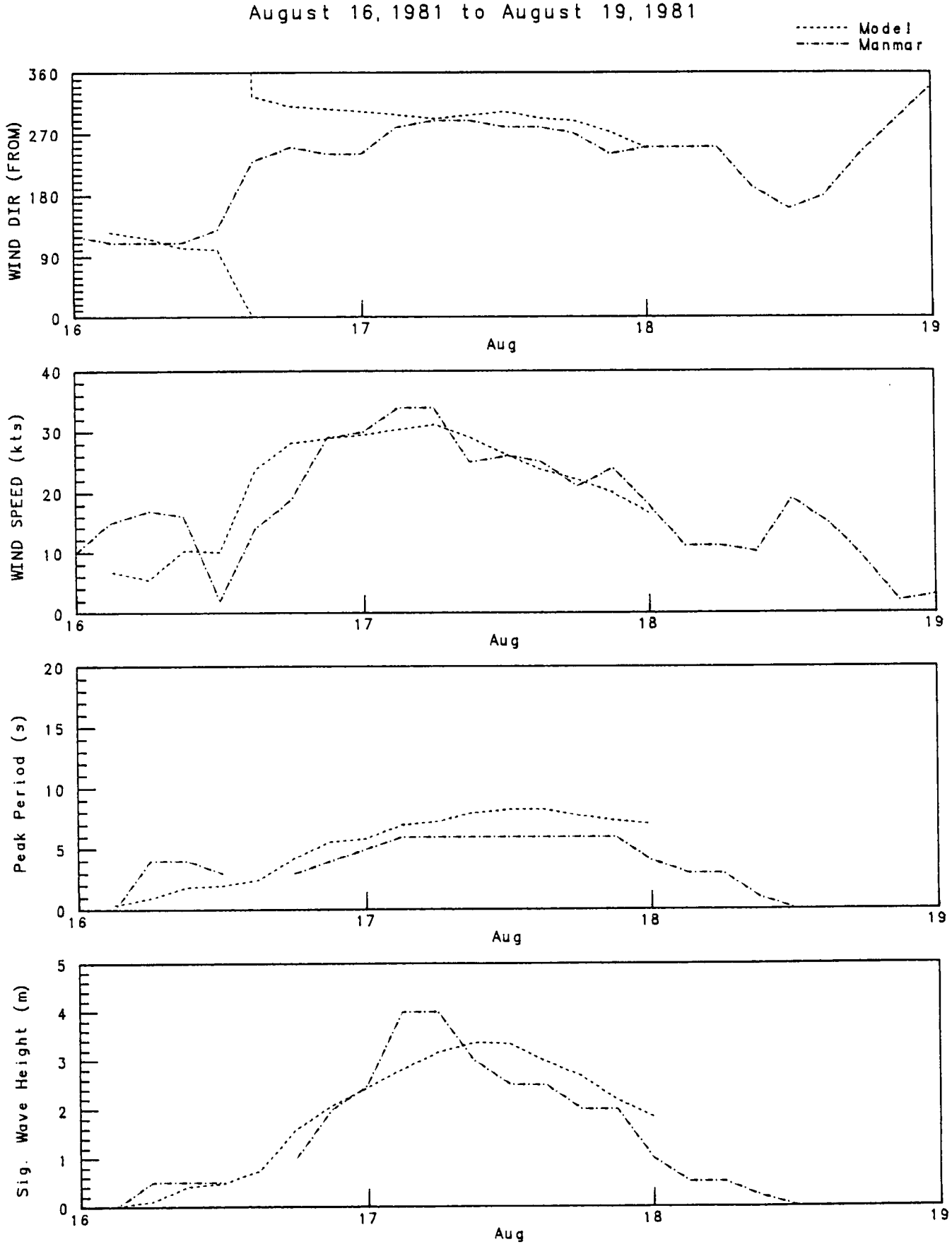

BEAUFORT SEA STORM VERIFICATION

GRID POINT 385 - EXPLORER II, ISSUNGNAK - WR 201

August 16, 1981 to August 19, 1981

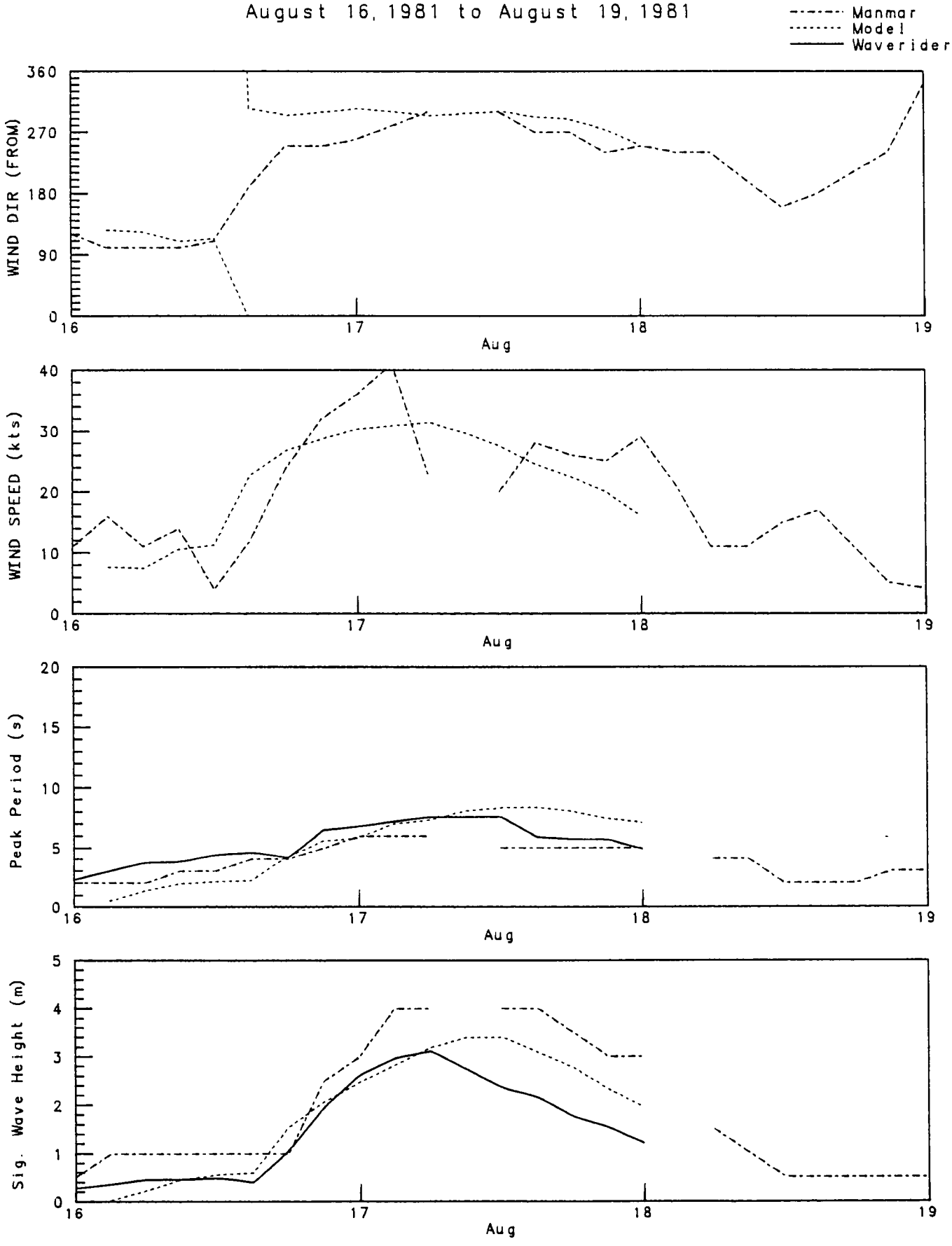

BEAUFORT SEA STORM VERIFICATION

GRID POINT 386 - EXPLORER III, KOAKOAK - WR 196

August 16, 1981 to August 19, 1981

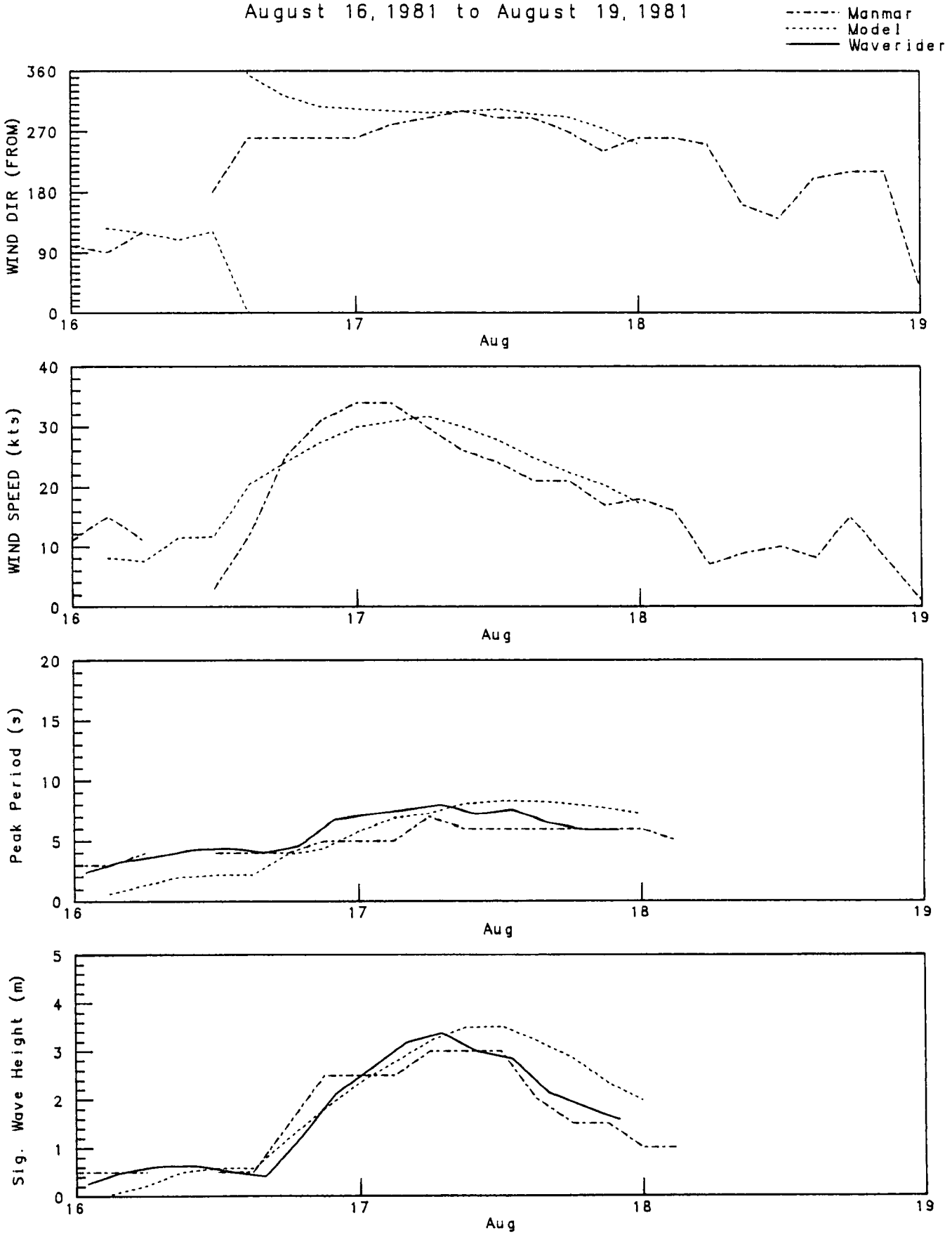

BEAUFORT SEA HINDCAST

MANMAR, WAVERIDER, AND MODEL GRID POINT LOCATIONS & DEPTHS

August 30, 1981 to September 2, 1981

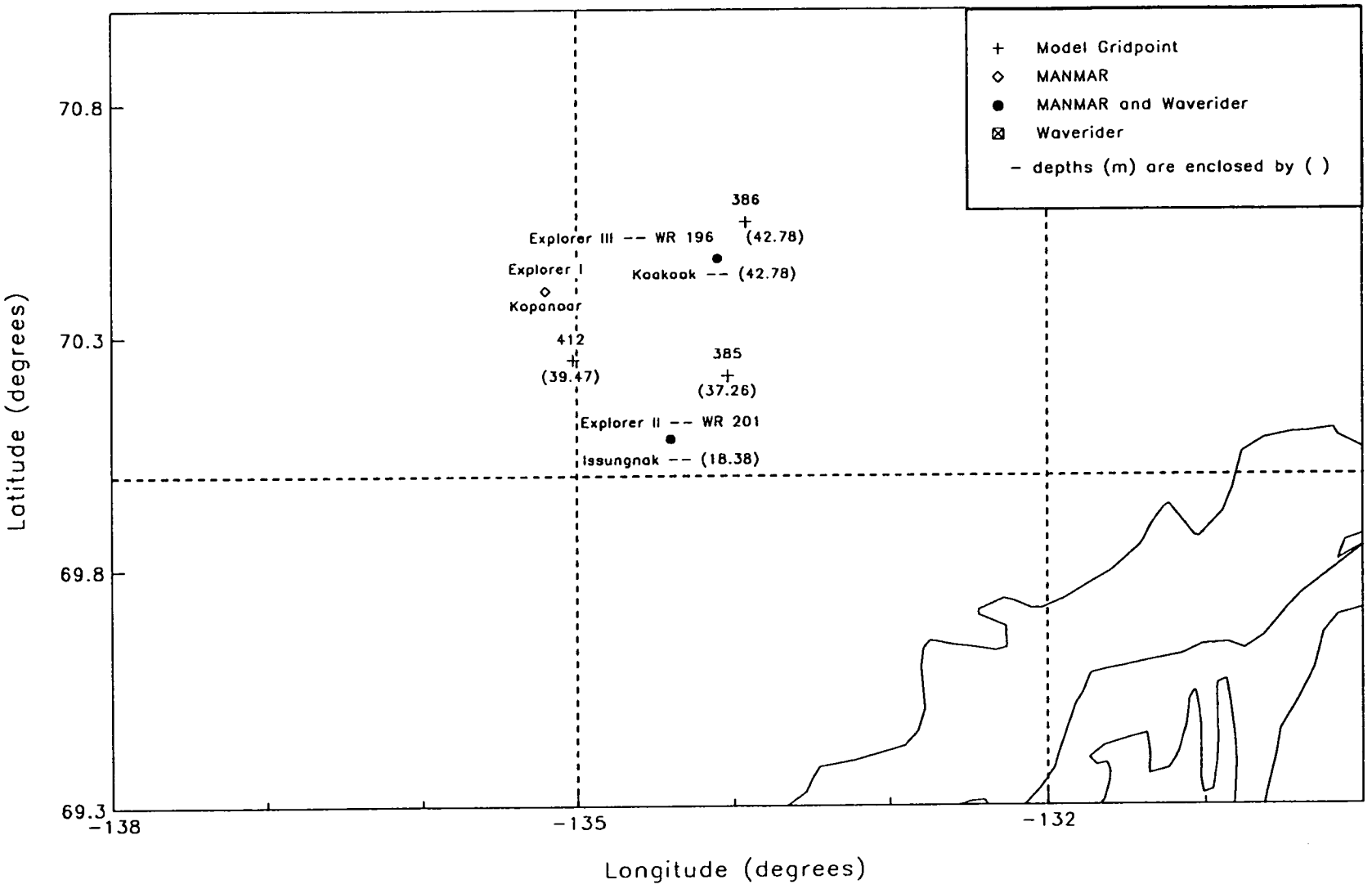

BEAUFORT SEA STORM VERIFICATION

GRID POINT 412 - EXPLORER I, KOPANOAR

August 30, 1981 to September 2, 1981

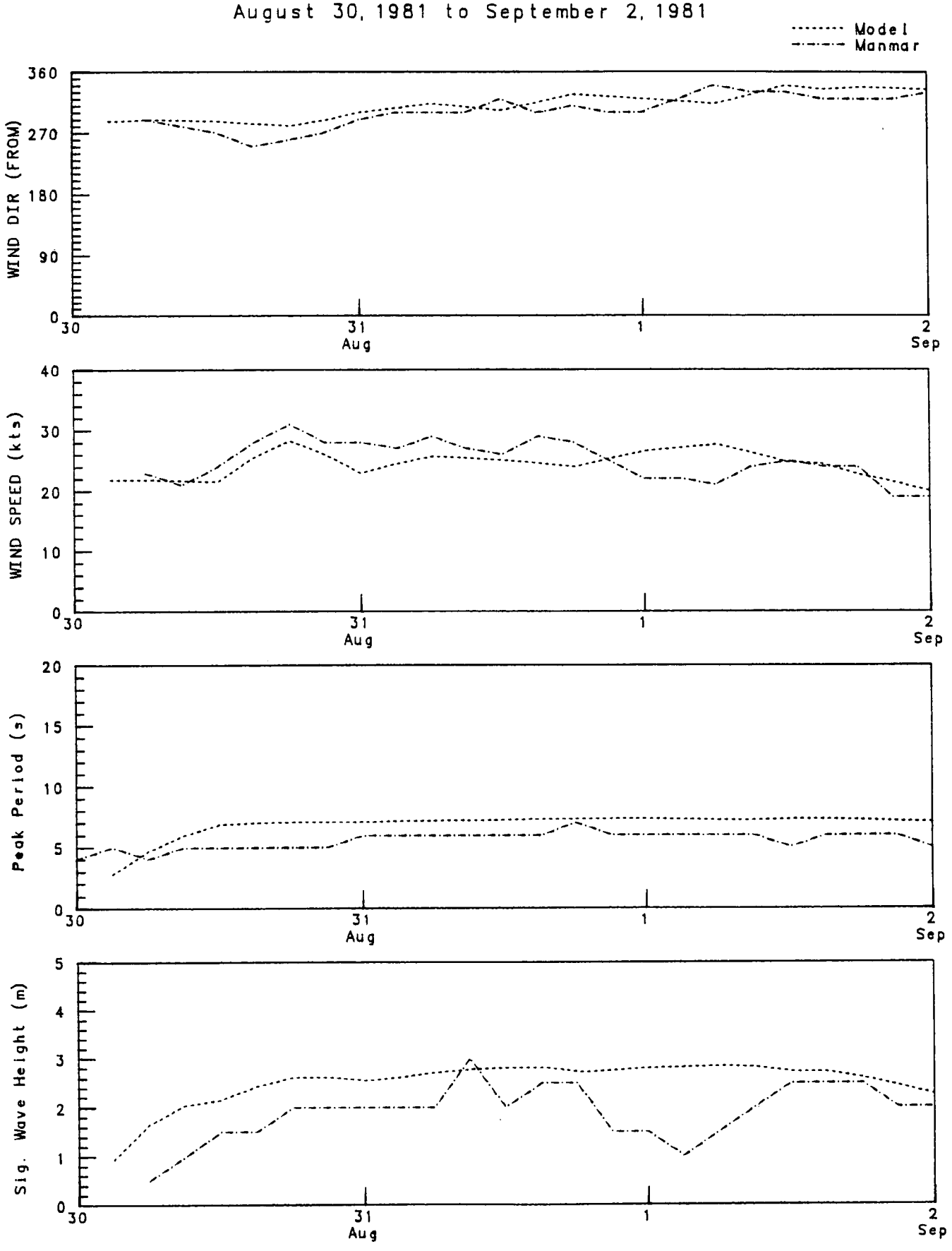

BEAUFORT SEA STORM VERIFICATION

GRID POINT 386 – EXPLORER III, KOAKOAK – WR 196

August 30, 1981 to September 2, 1981

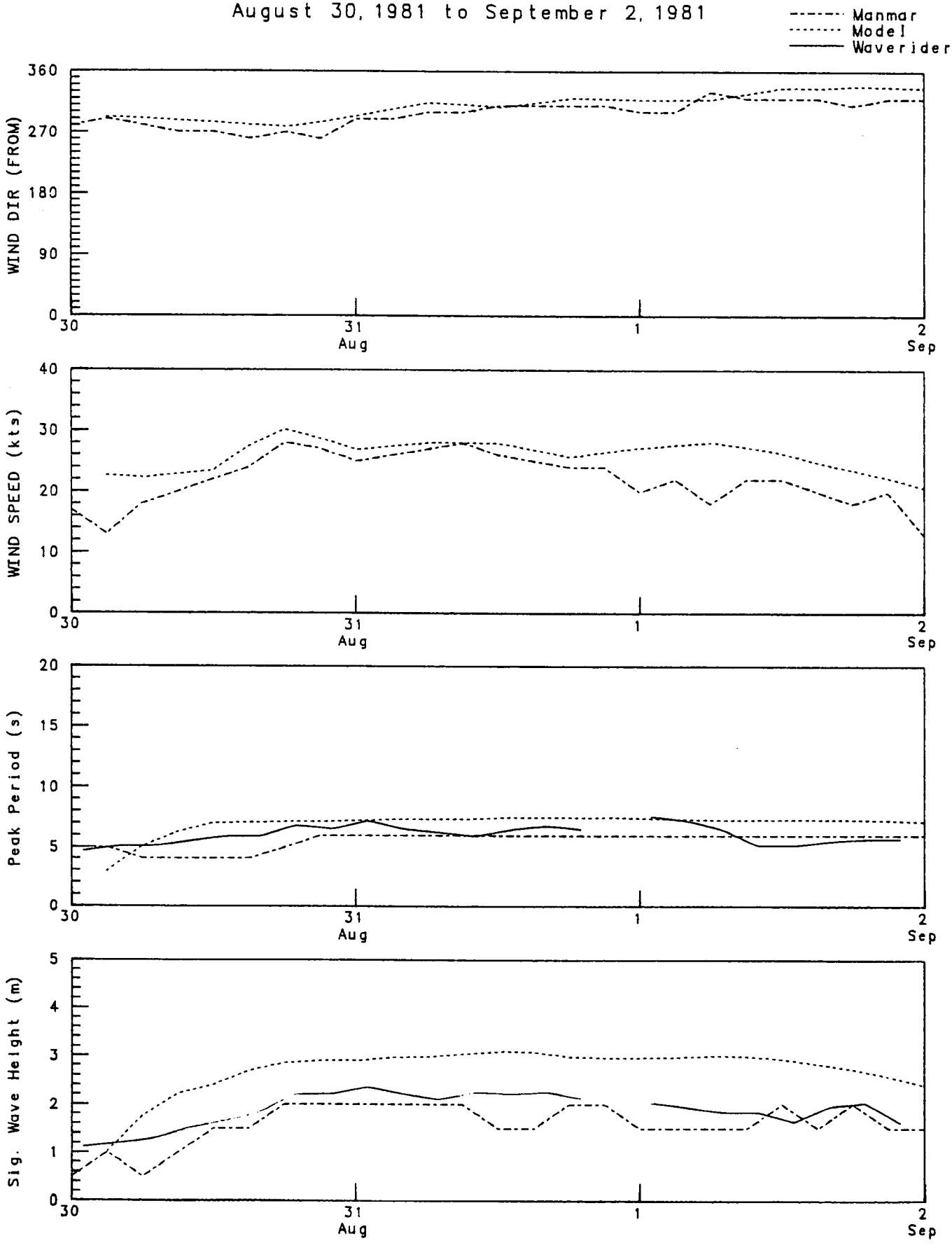

BEAUFORT SEA STORM VERIFICATION

GRID POINT 385 – EXPLORER II, ISSUNGNAK – WR 201

August 30, 1981 to September 2, 1981

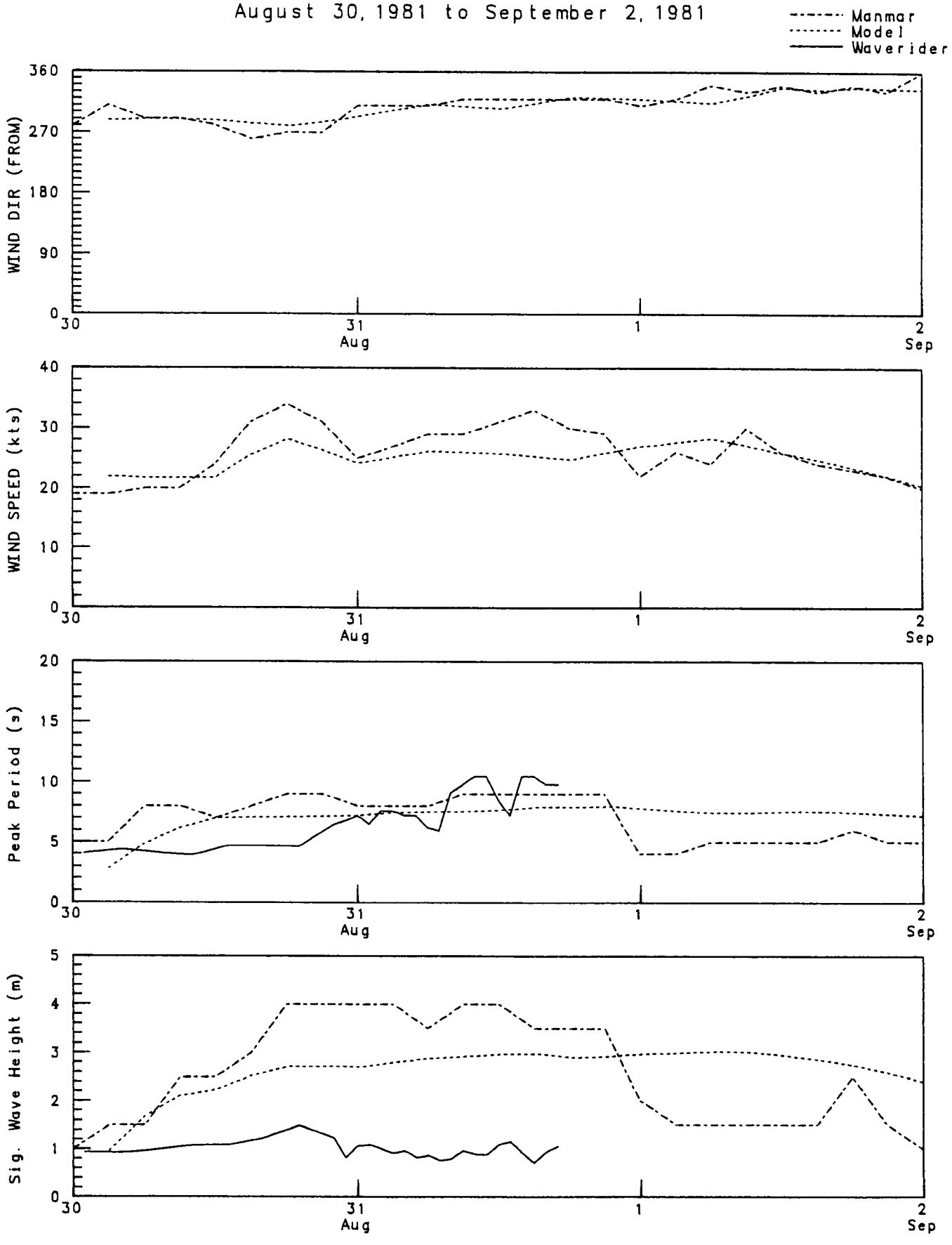

BEAUFORT SEA HINDCAST

MANMAR, WAVERIDER AND MODEL GRID POINT LOCATIONS & DEPTHS

September 20, 1982 to September 23, 1982

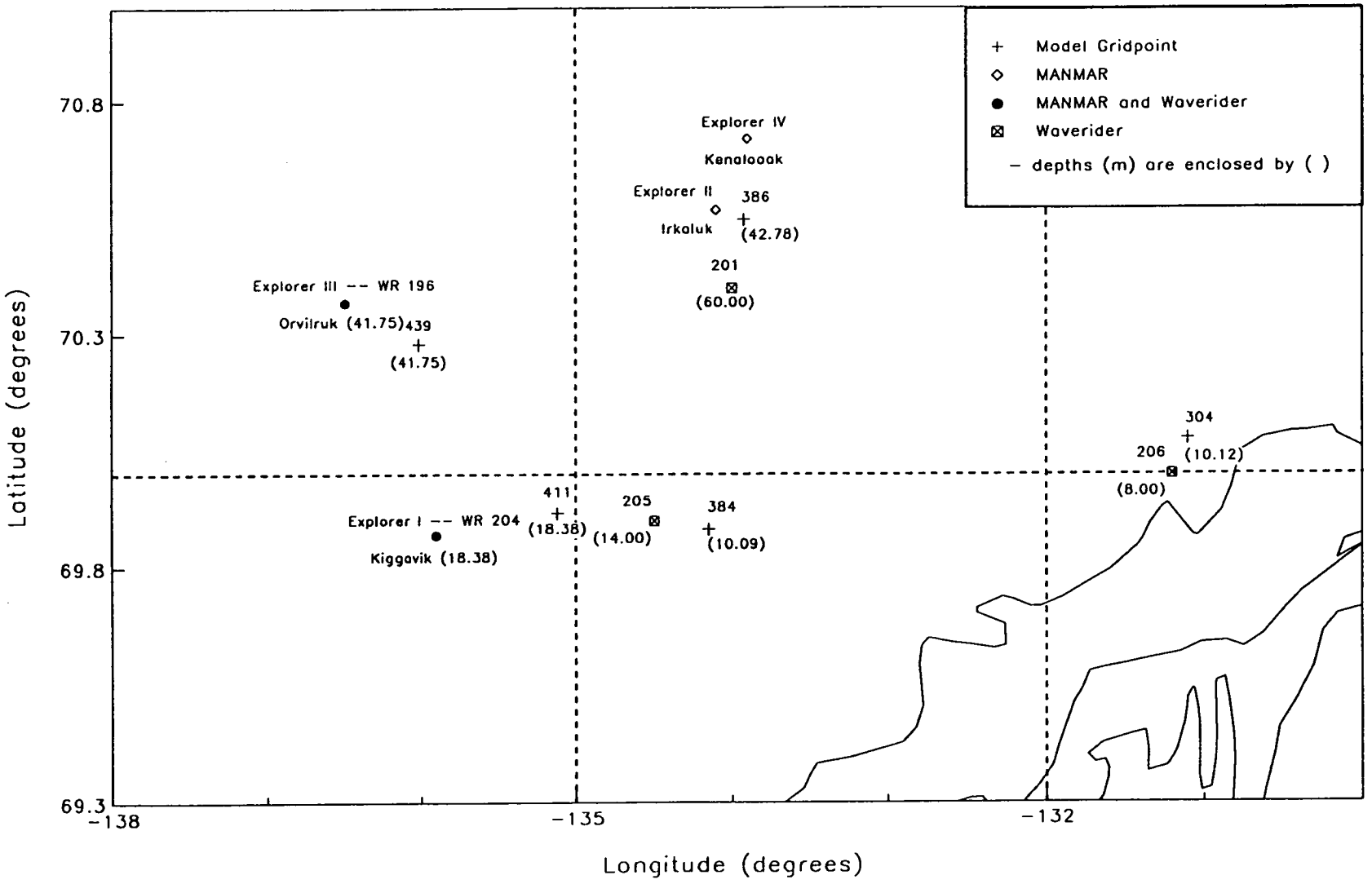

BEAUFORT SEA STORM VERIFICATION

GRID POINT 439 - EXPLORER III, ORVILRUK - WR 196

September 20, 1982 to September 23, 1982

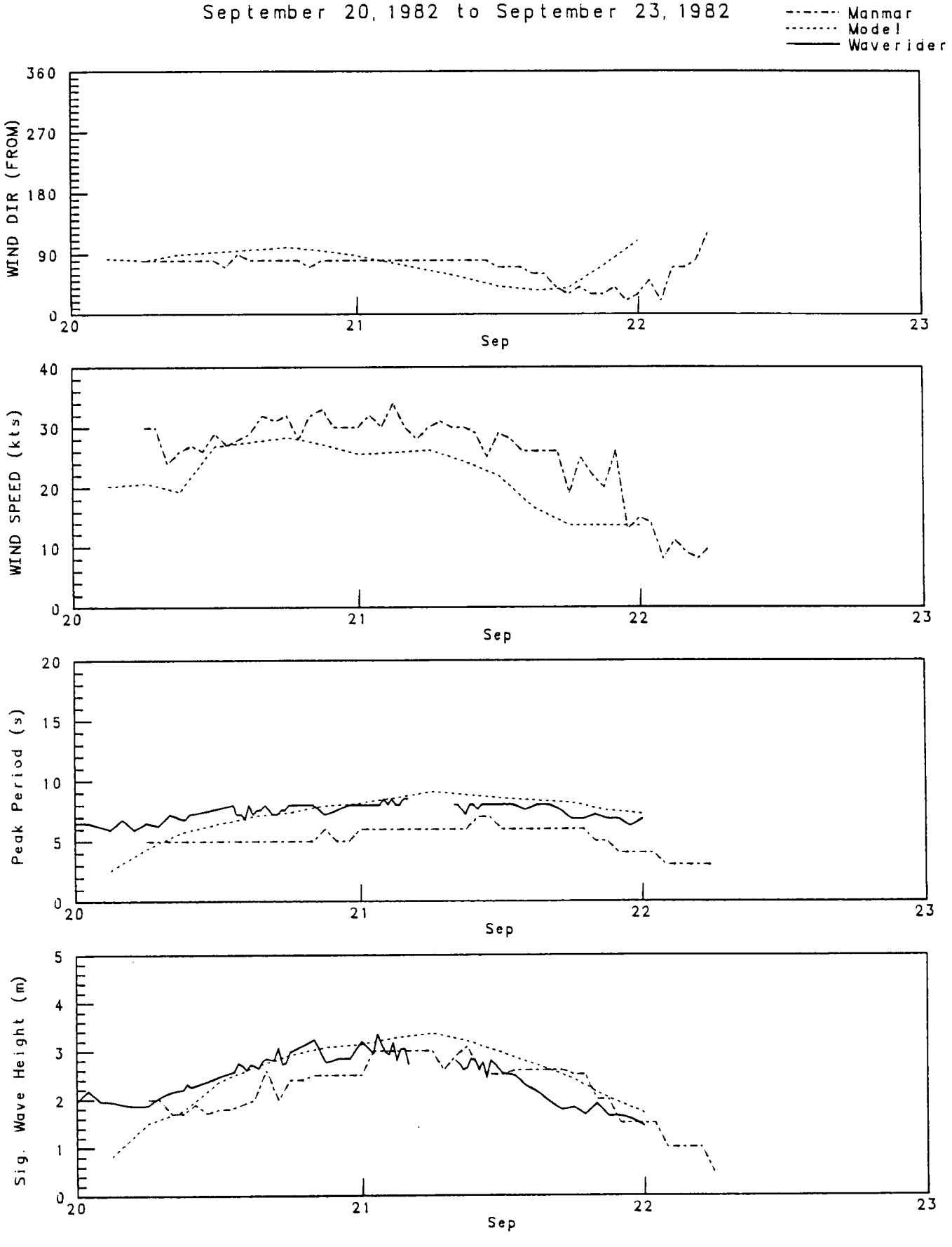

BEAUFORT SEA STORM VERIFICATION

GRID POINT 386 - WR 201

September 20, 1982 to September 23, 1982

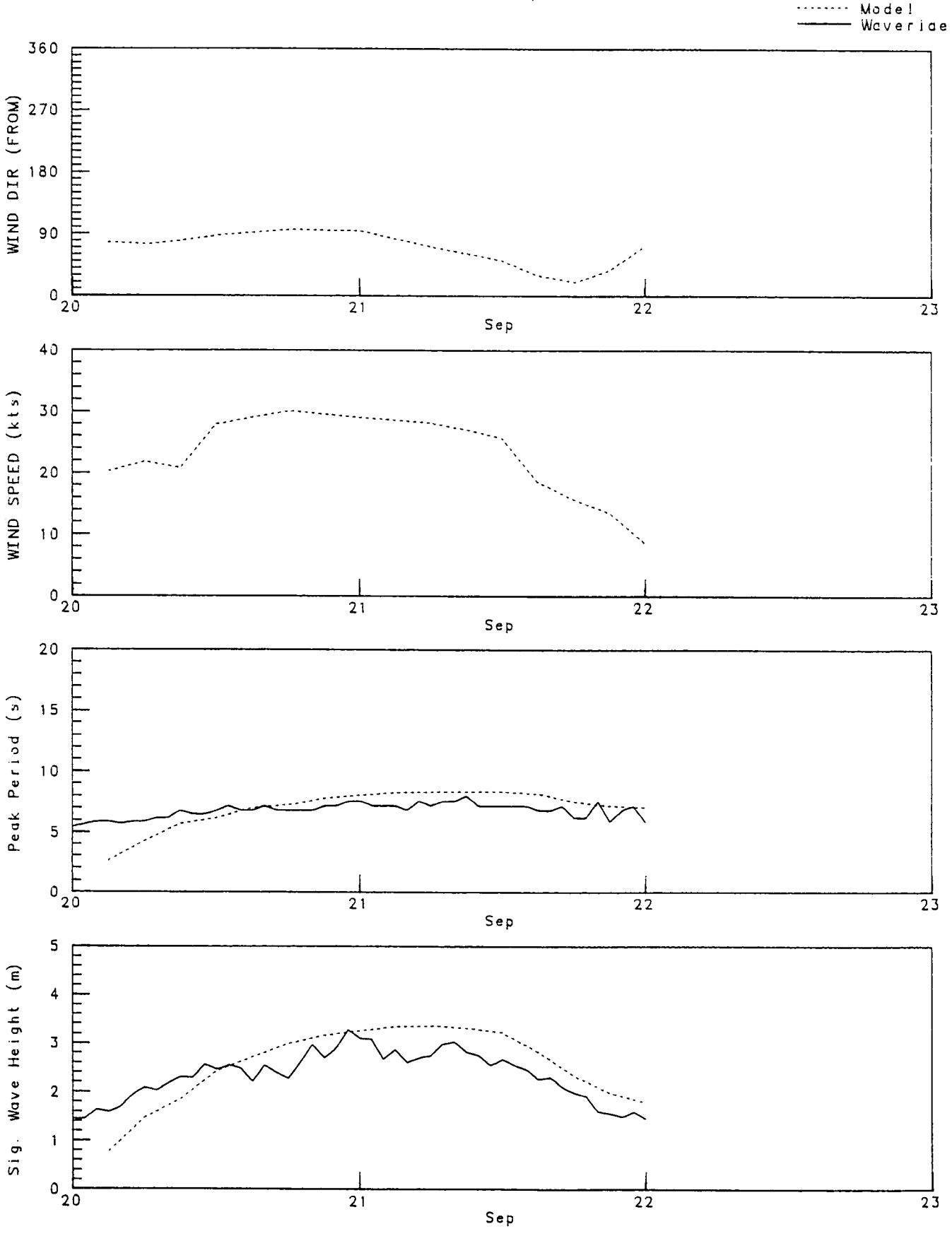

BEAUFORT SEA STORM VERIFICATION

GRID POINT 411 - EXPLORER I, KIGGAVIK - WR 204

September 20, 1982 to September 23, 1982

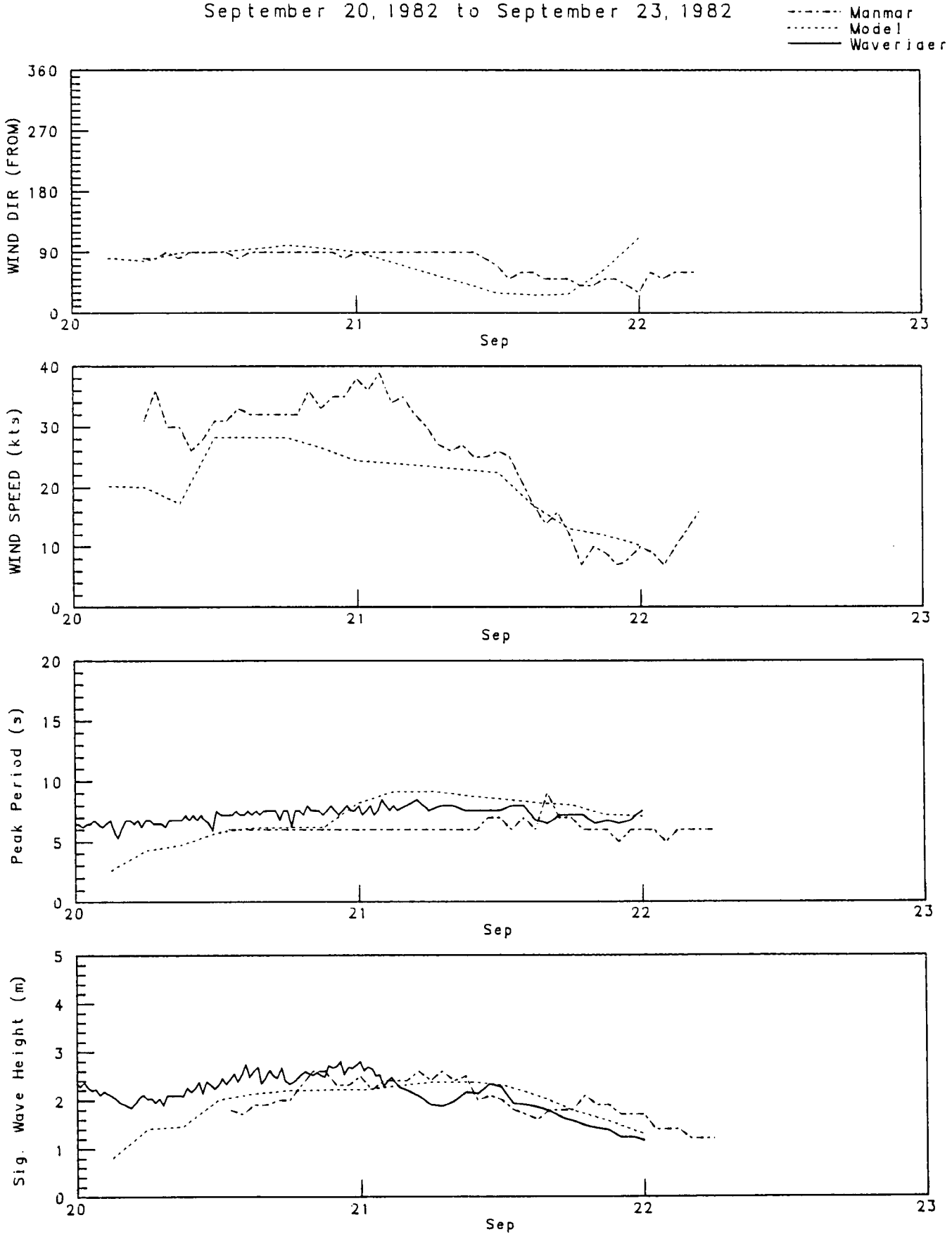

BEAUFORT SEA STORM VERIFICATION

GRID POINT 384 – WR 205

September 20, 1982 to September 23, 1982

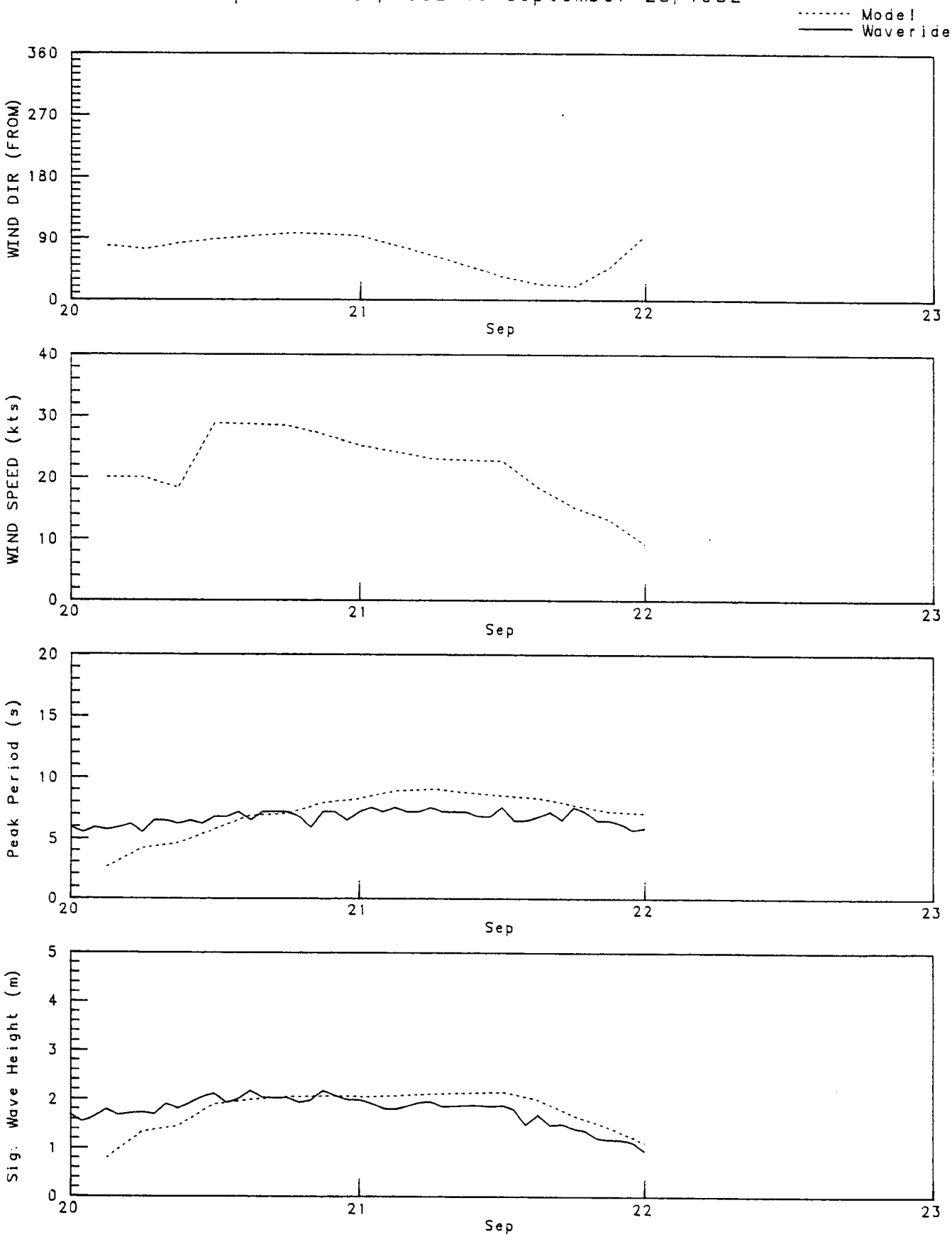

BEAUFORT SEA STORM VERIFICATION

GRID POINT 304 - WR 206

September 20, 1982 to September 23, 1982

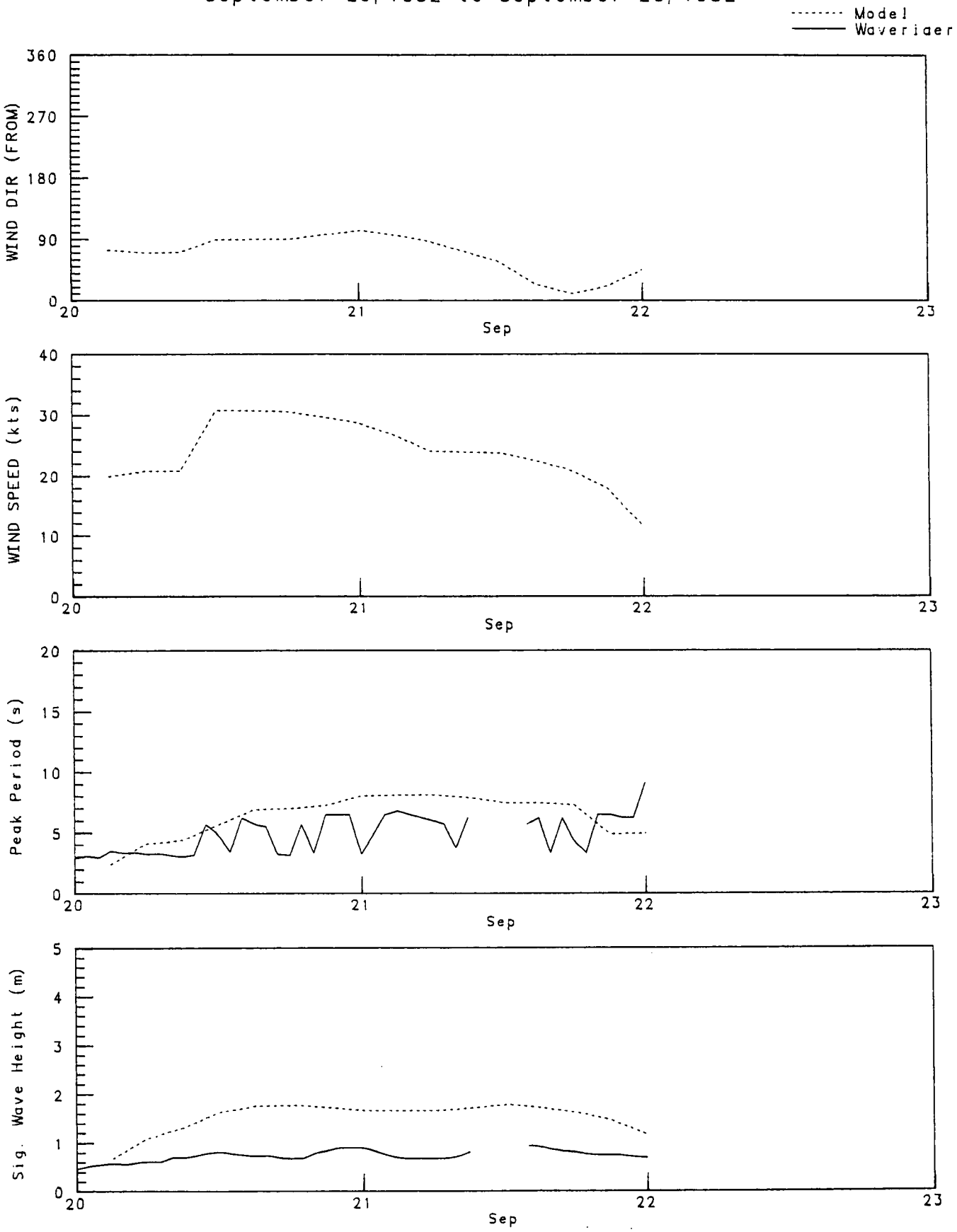

BEAUFORT SEA STORM VERIFICATION

GRID POINT 386 – EXPLORER II, IRKALUK

September 20, 1982 to September 23, 1982

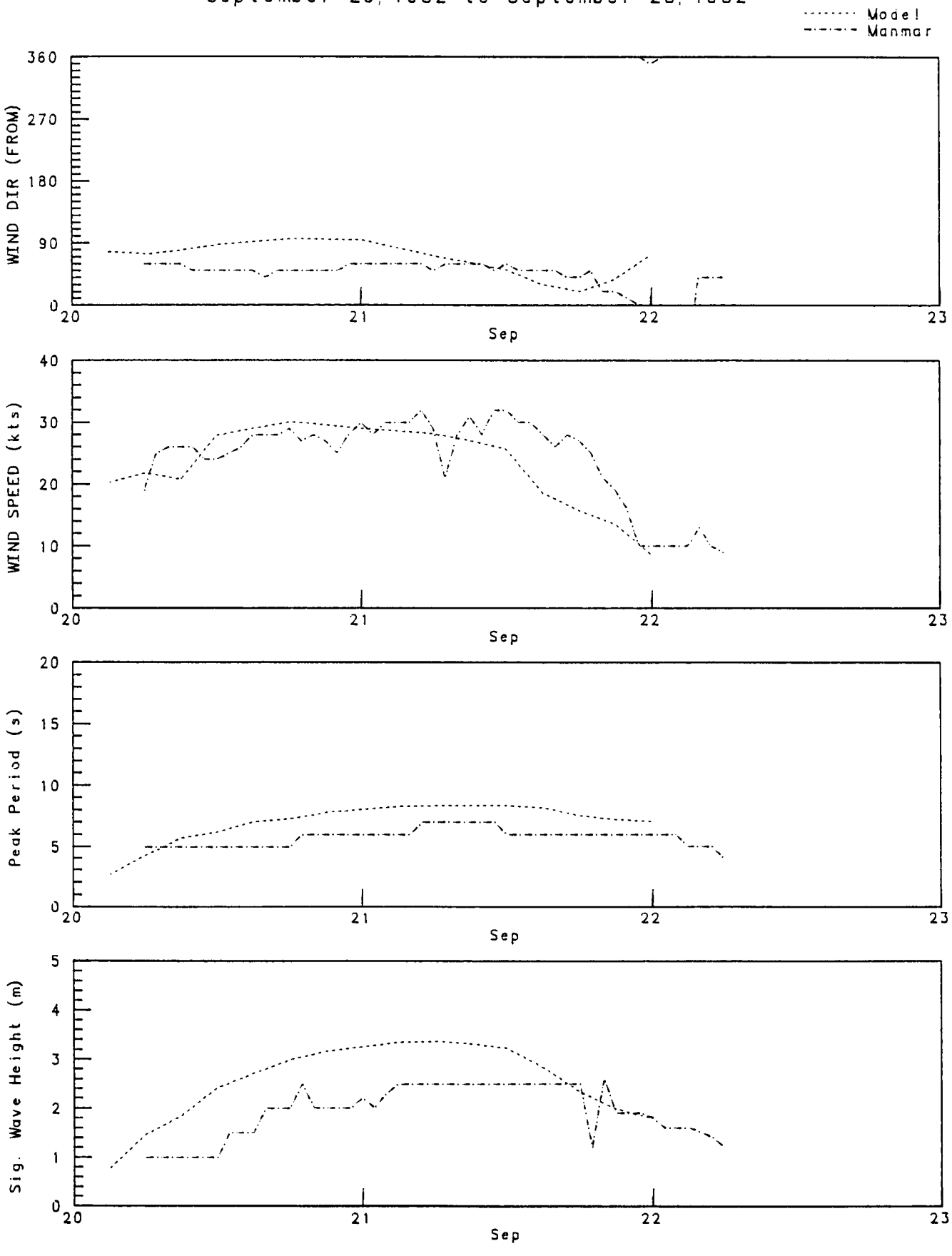

BEAUFORT SEA STORM VERIFICATION

GRID POINT 386 - EXPLORER IV, KENALOOAK

September 20, 1982 to September 23, 1982

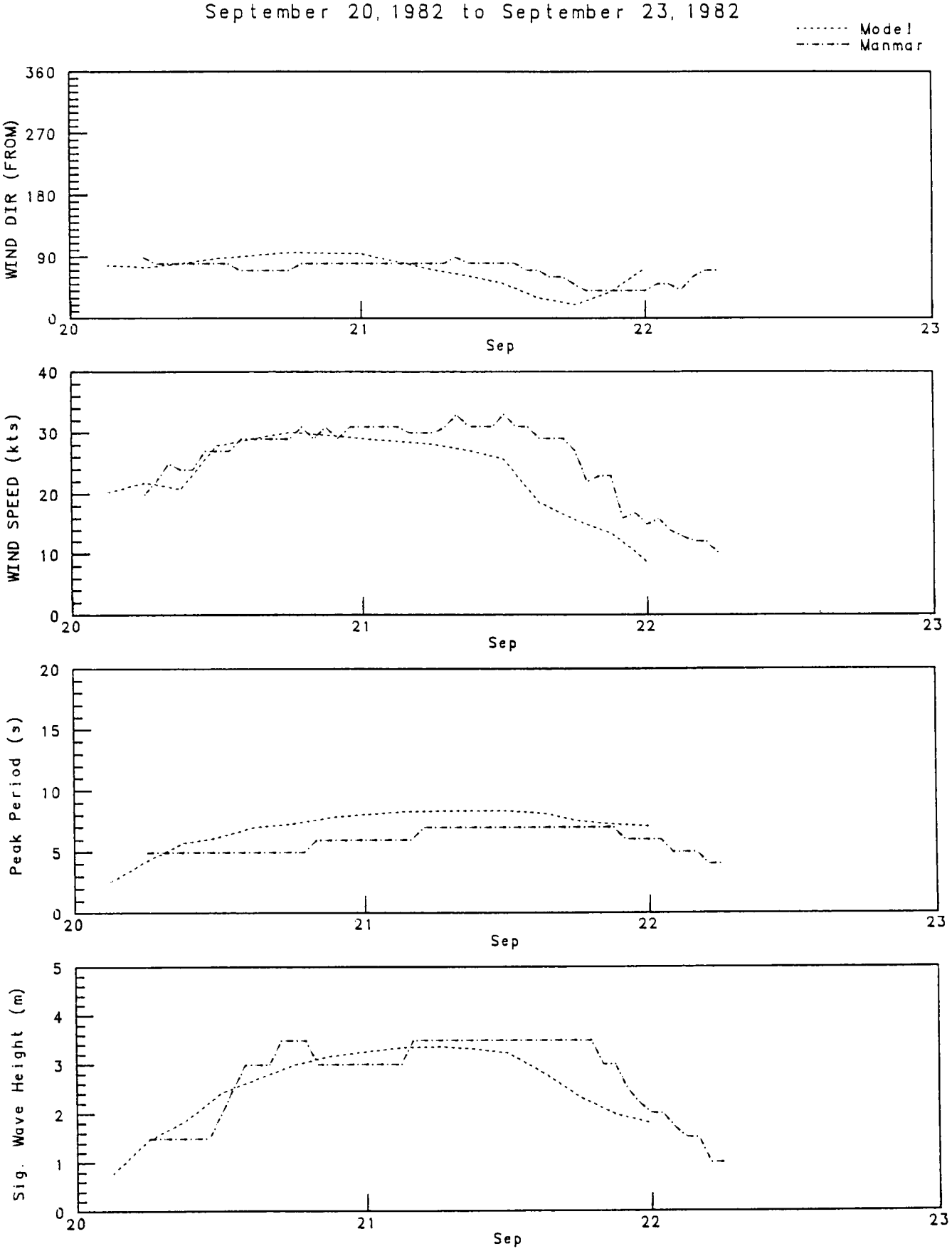

APPENDIX E
WAVE HINDCAST RESULTS
PEAK SIGNIFICANT WAVE HEIGHT FIELDS
FOR TOP 30 STORMS

BEAUFORT SEA STORM

7009

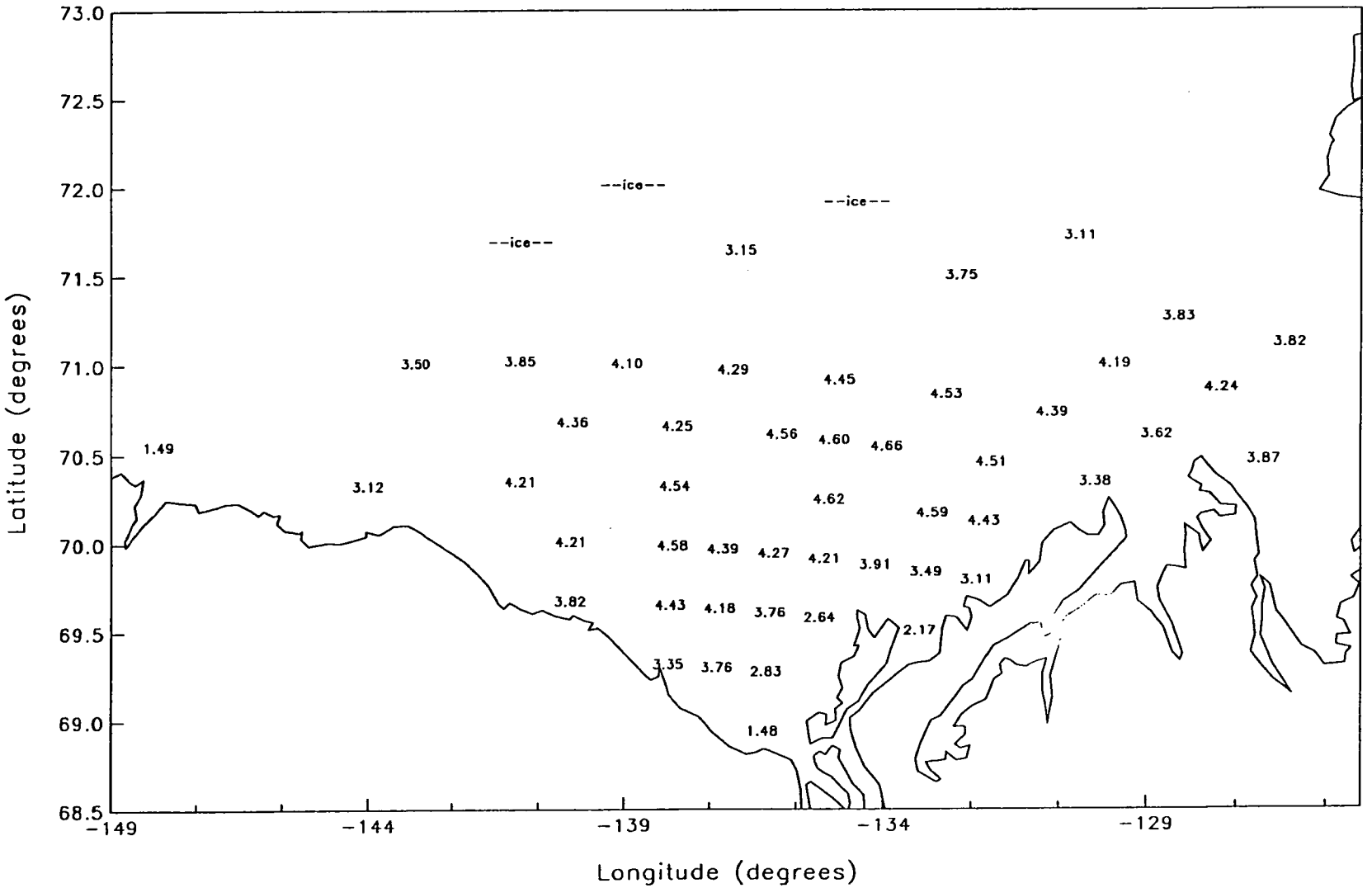

BEAUFORT SEA STORM

7508A

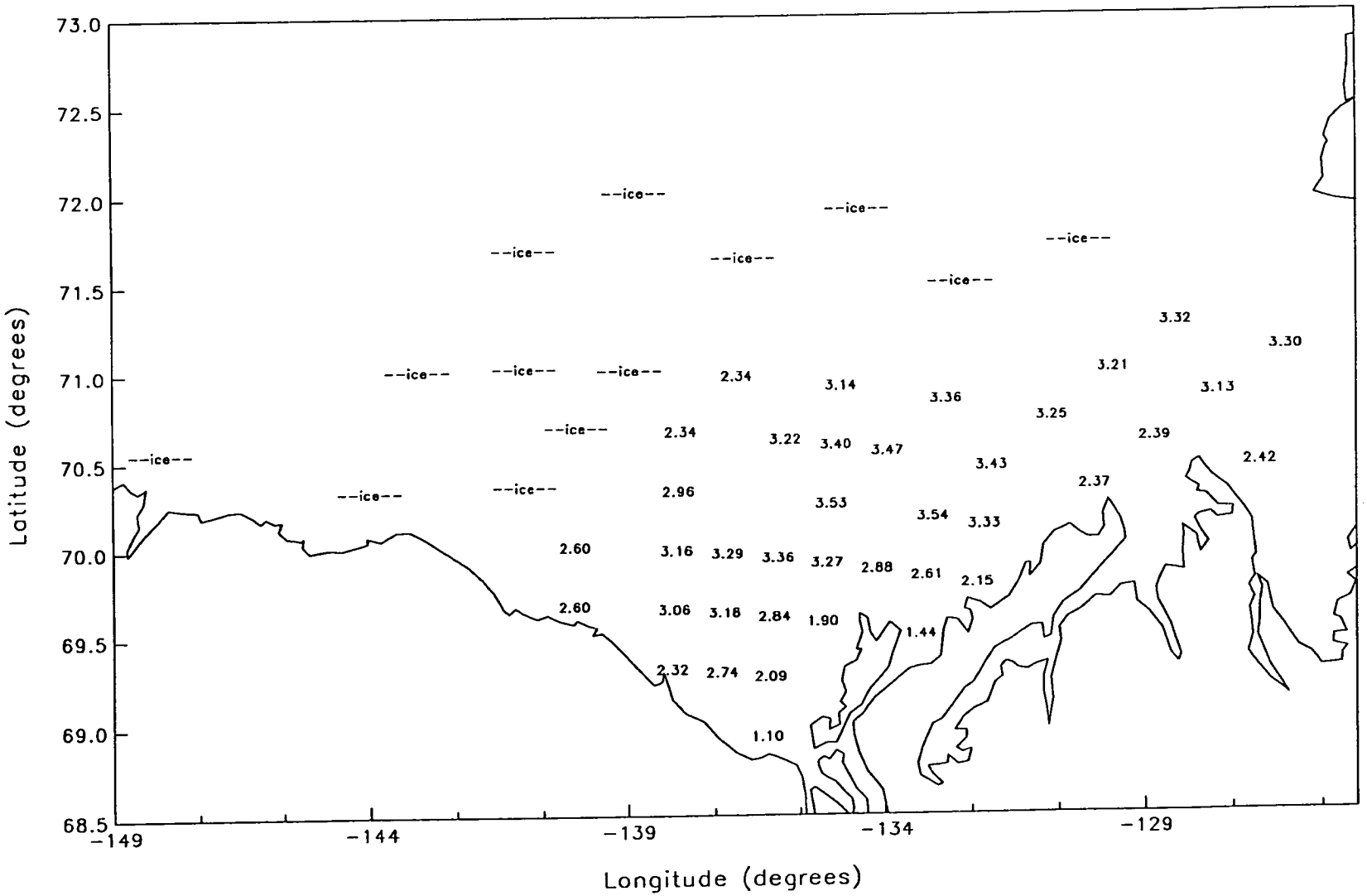

BEAUFORT SEA STORM

7508B

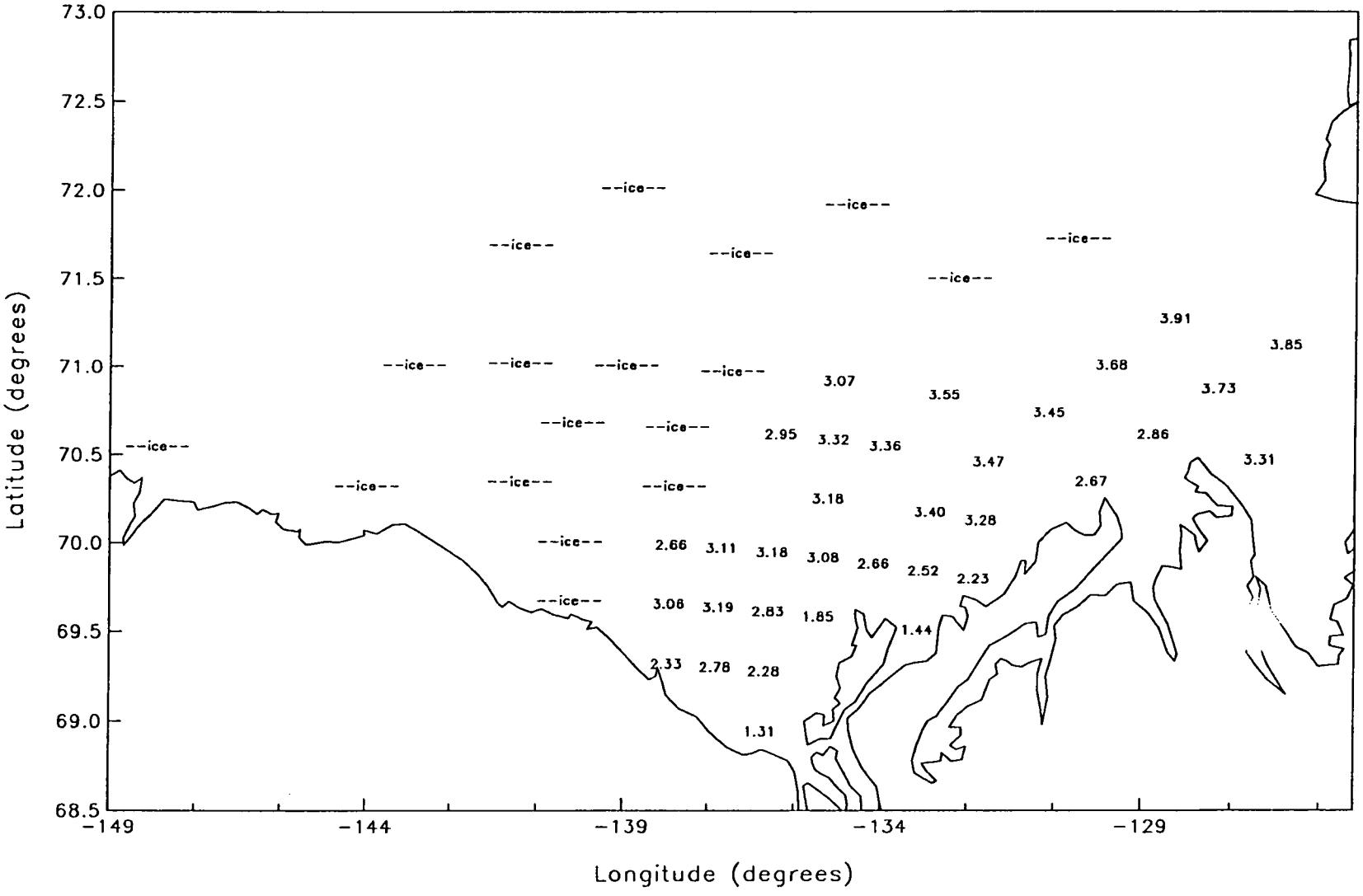

BEAUFORT SEA STORM

7608

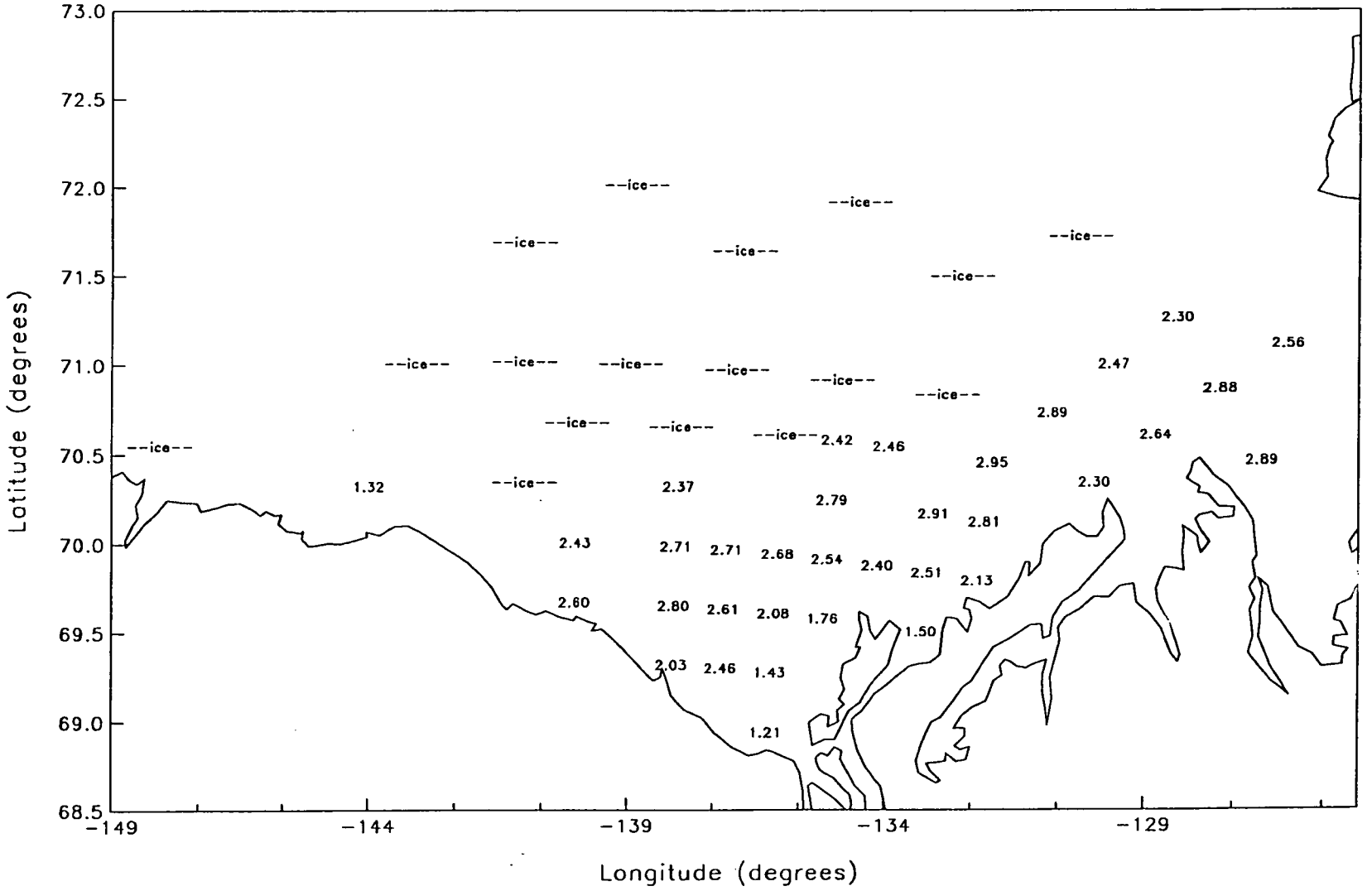

BEAUFORT SEA STORM

7609

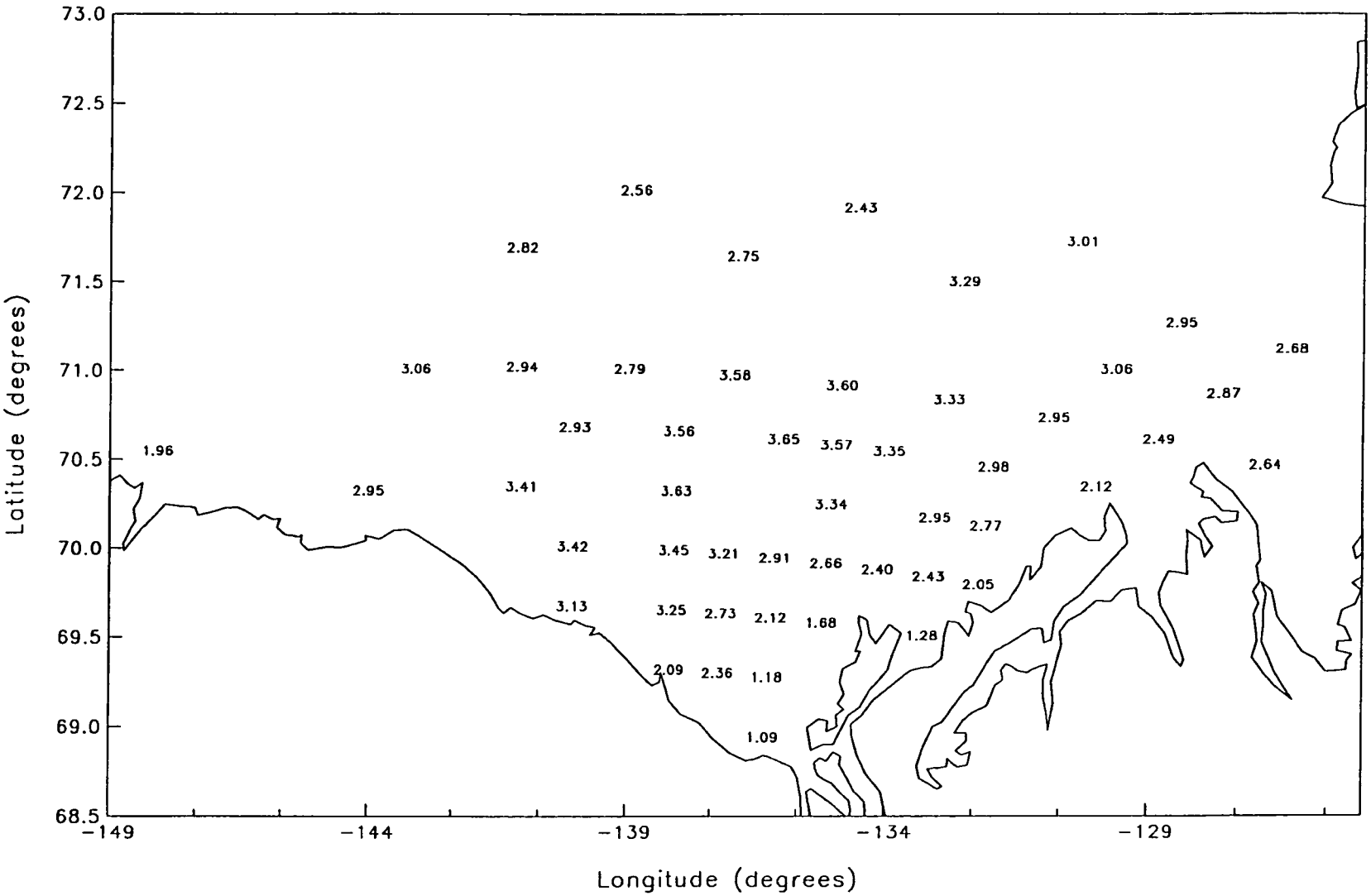

BEAUFORT SEA STORM

7708

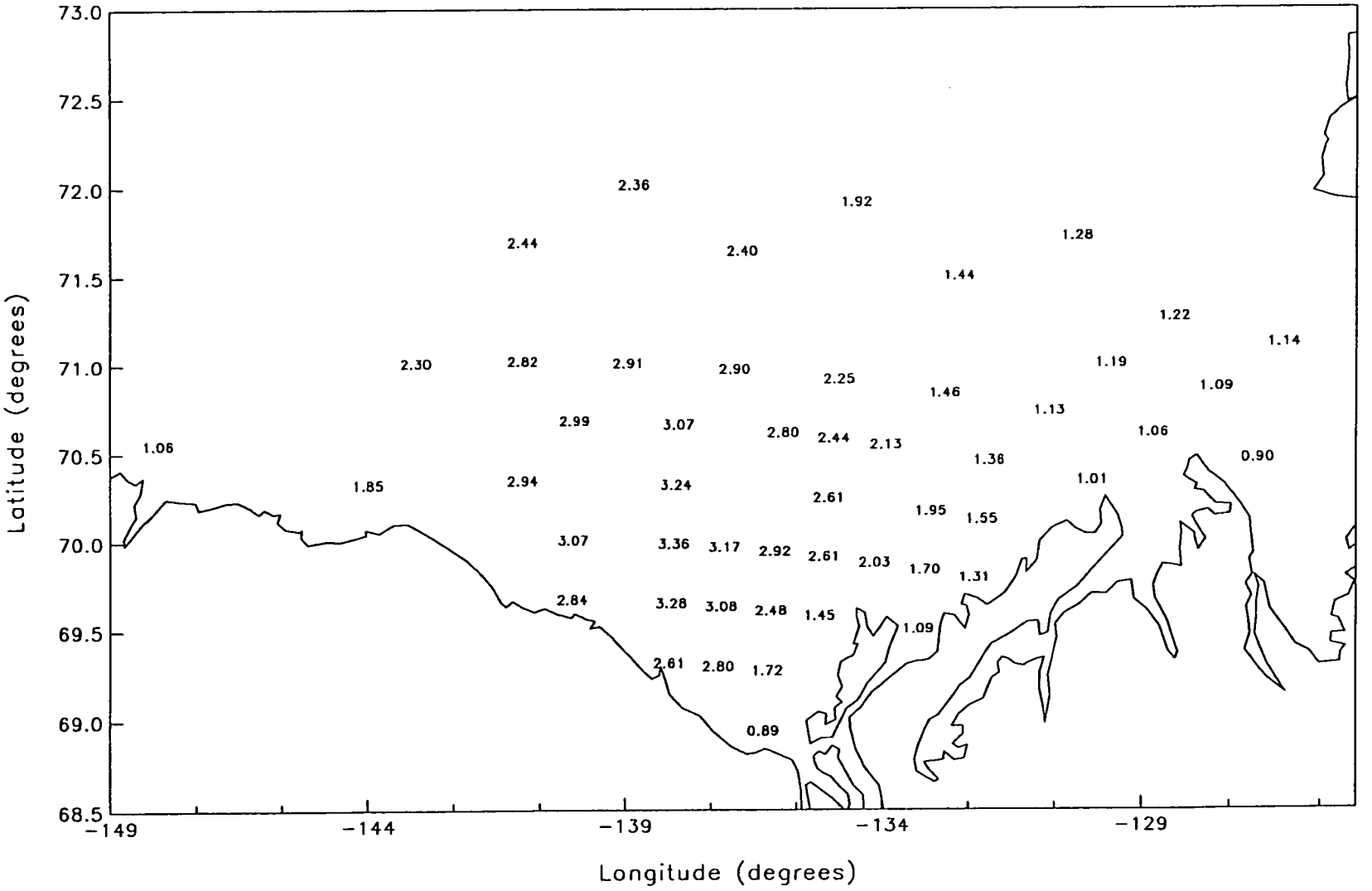

BEAUFORT SEA STORM

7709

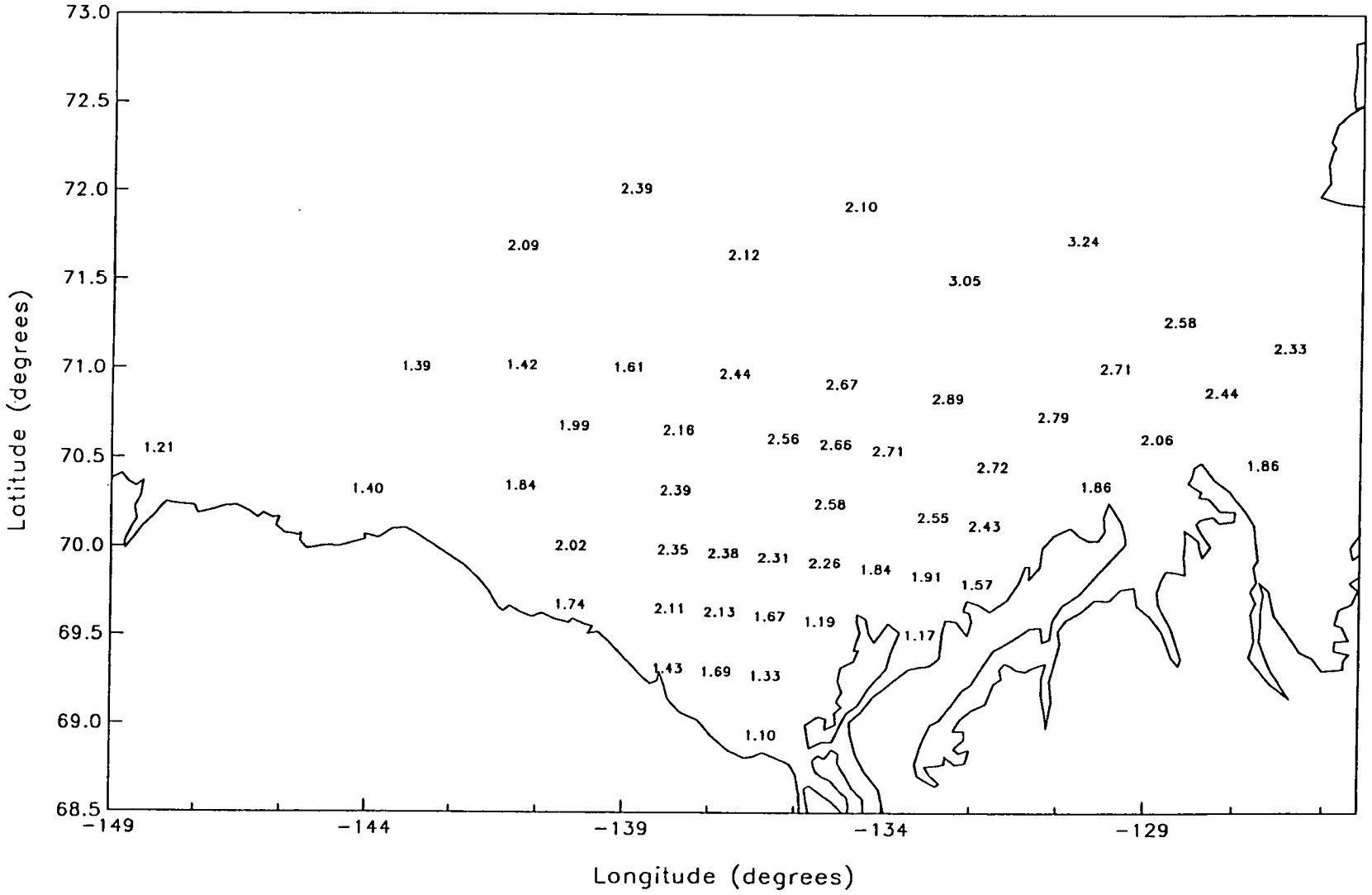

BEAUFORT SEA STORM

7809

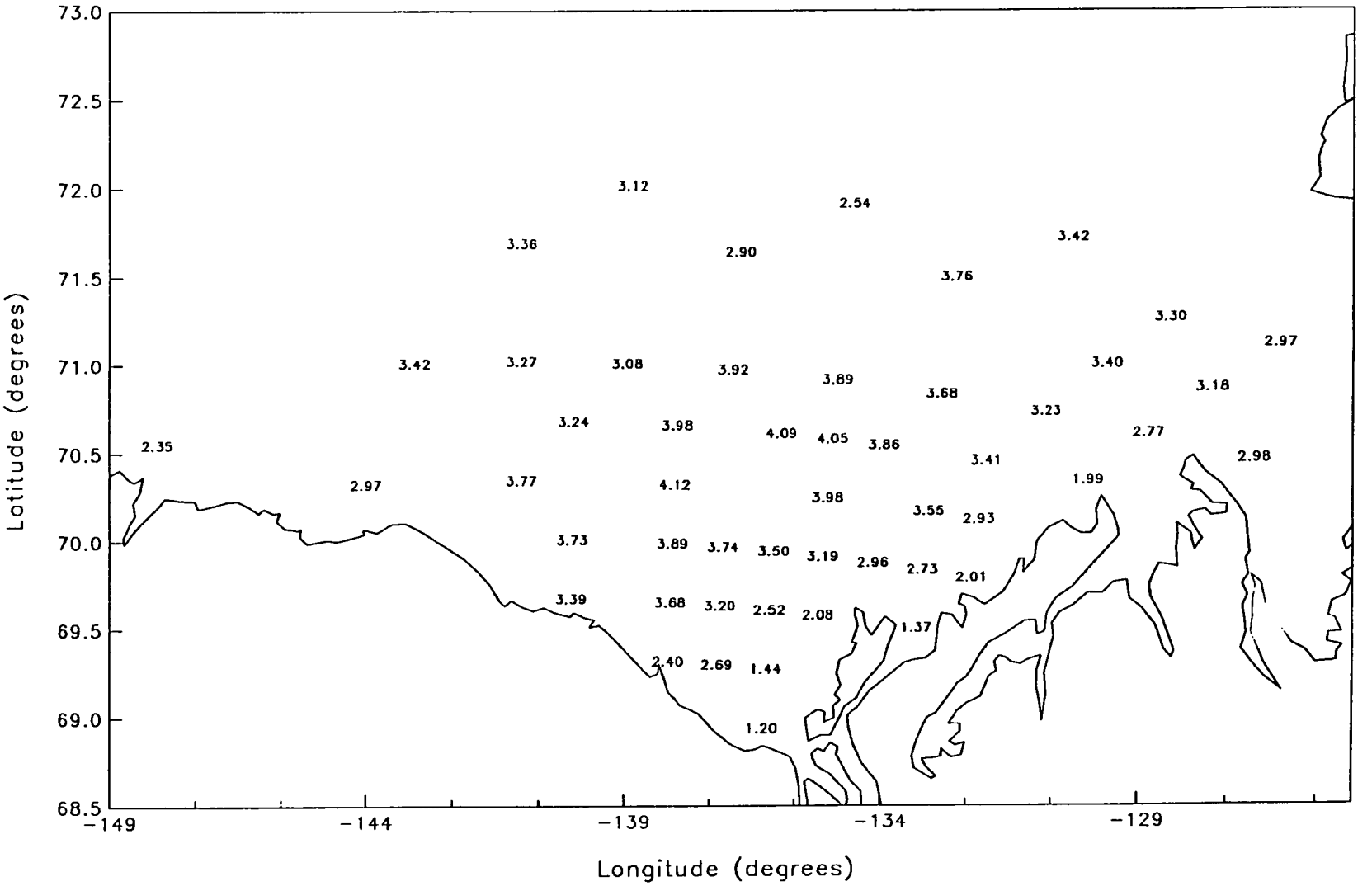

BEAUFORT SEA STORM

7810A

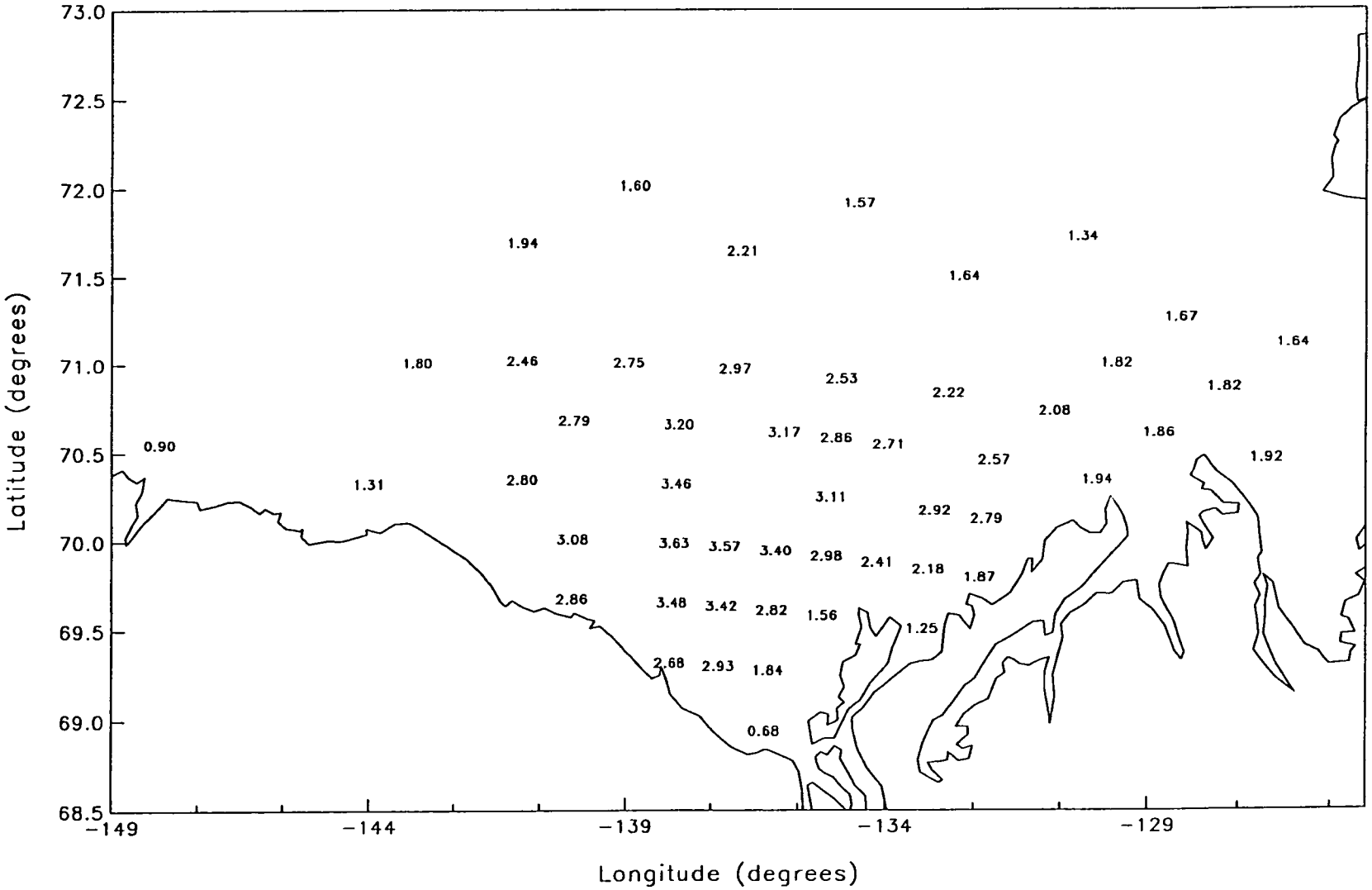

BEAUFORT SEA STORM

7810B

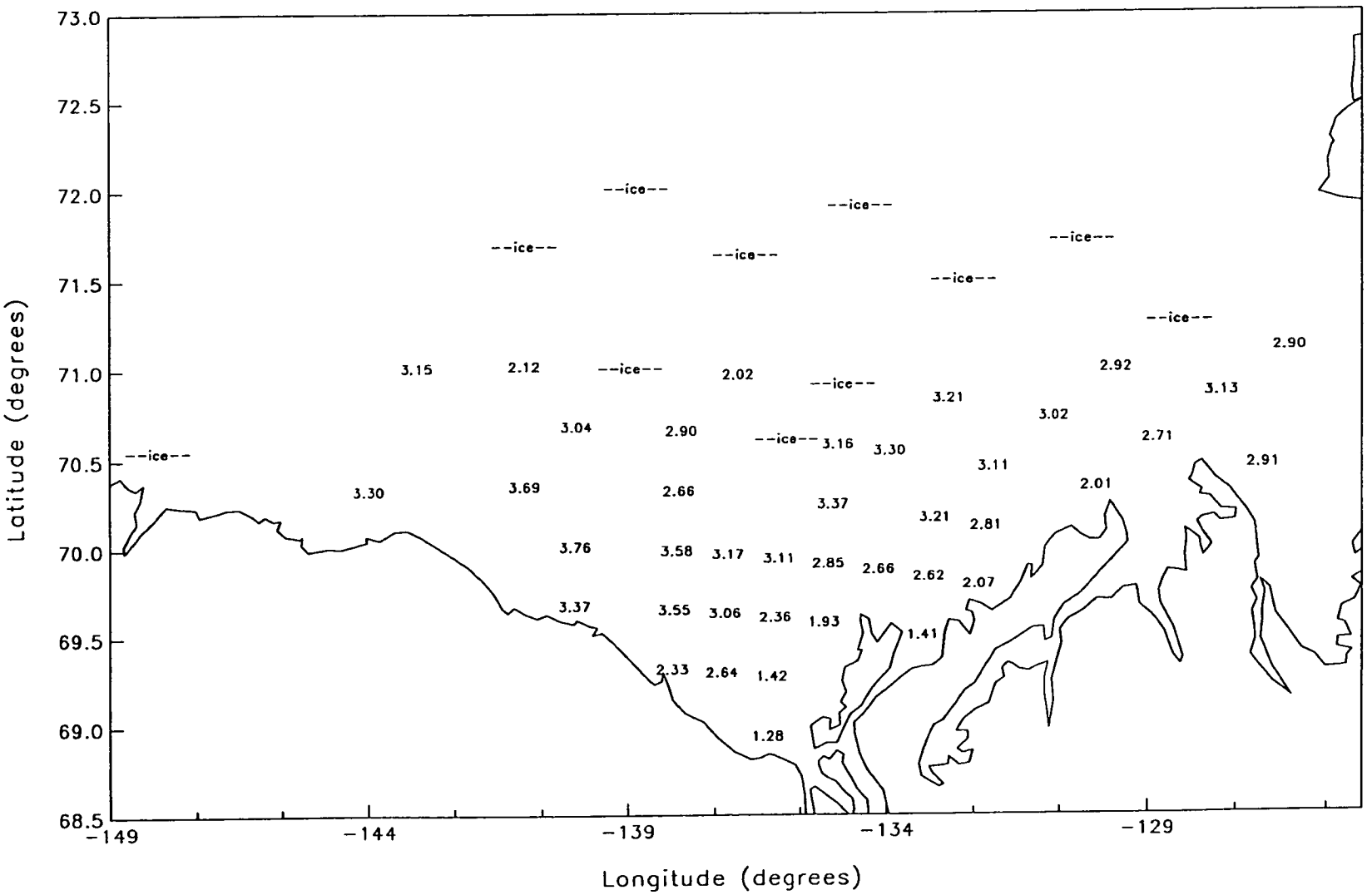

BEAUFORT SEA STORM

7909

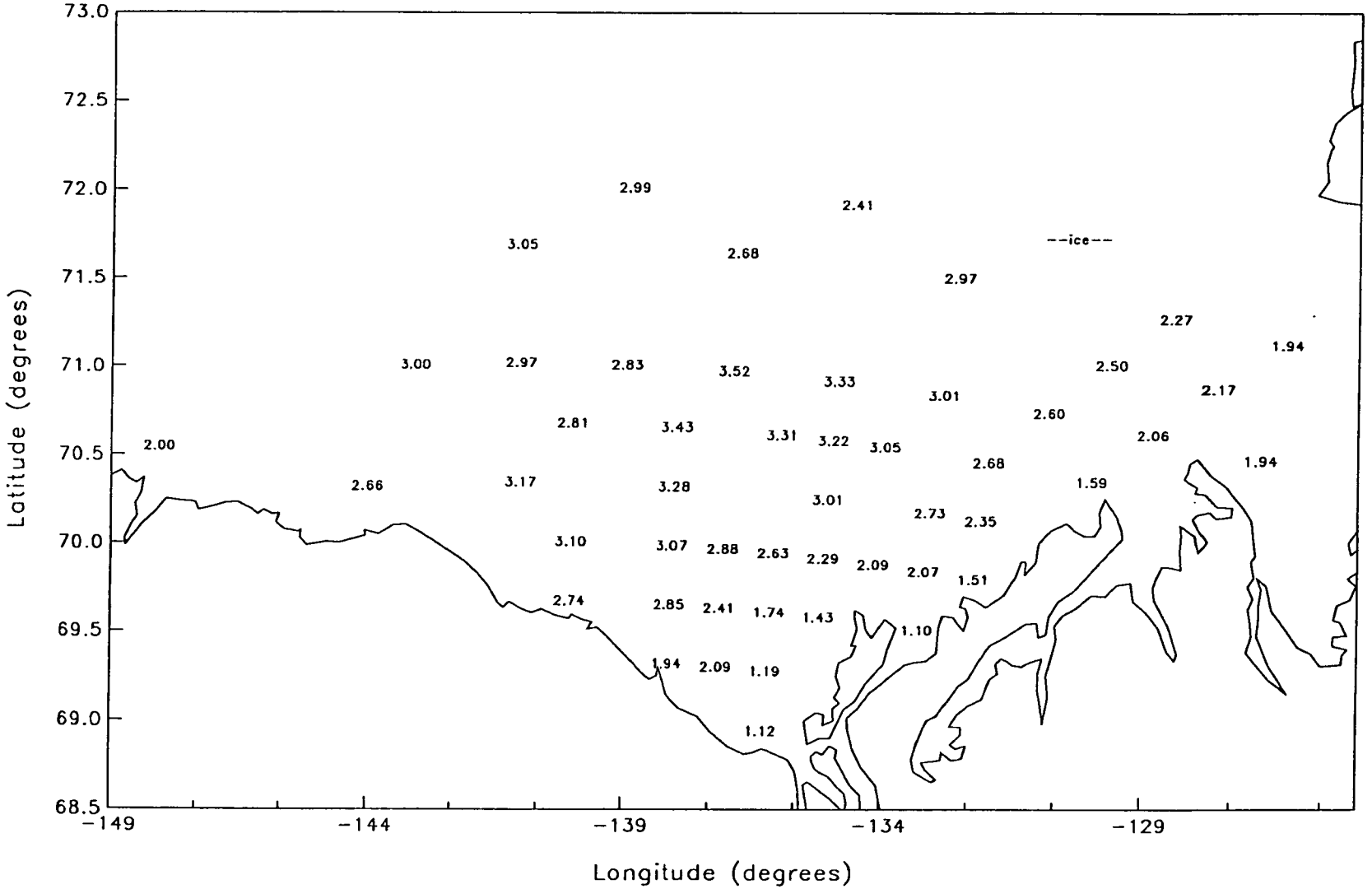

BEAUFORT SEA STORM

7910A

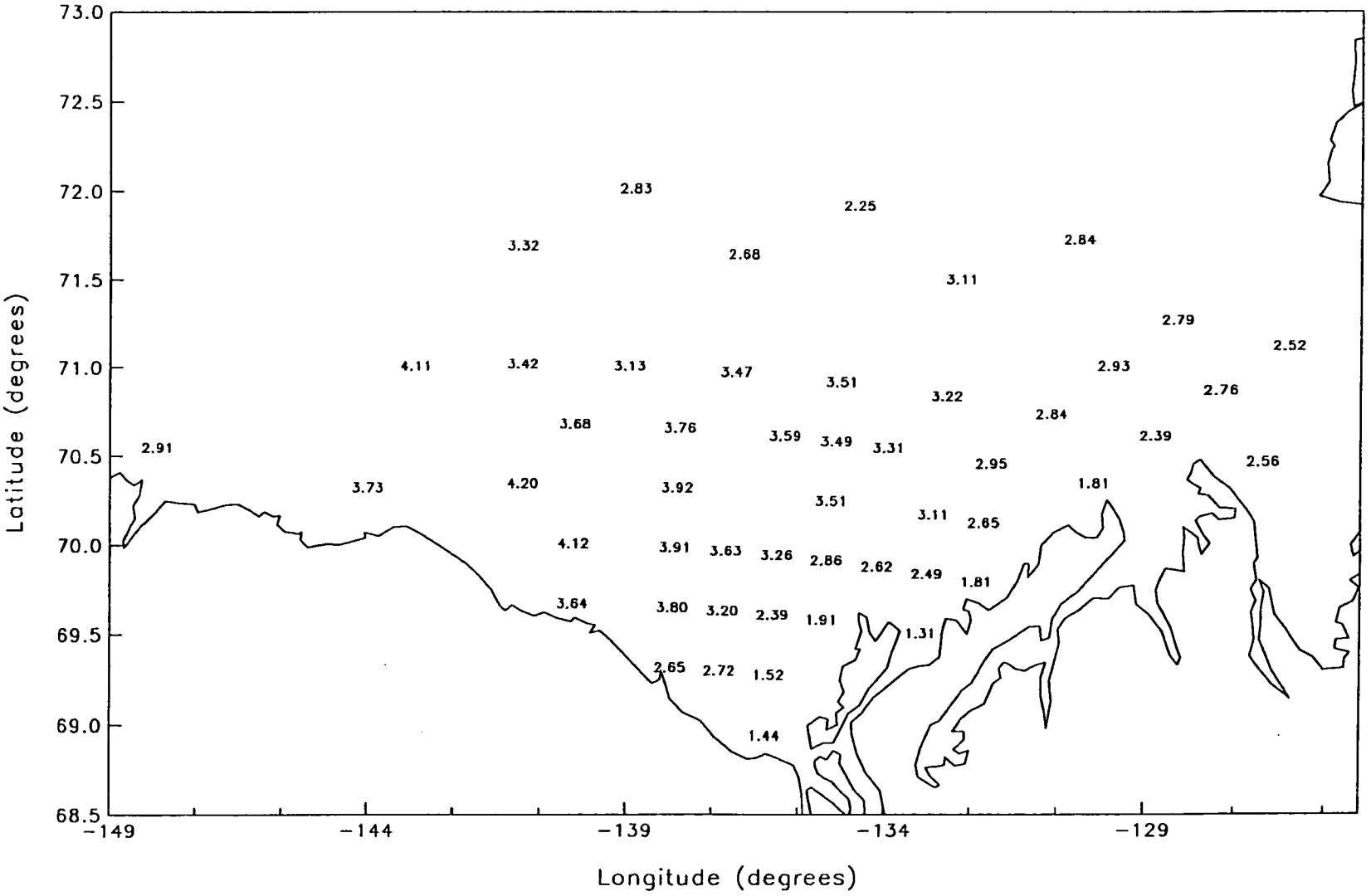

BEAUFORT SEA STORM

7910B

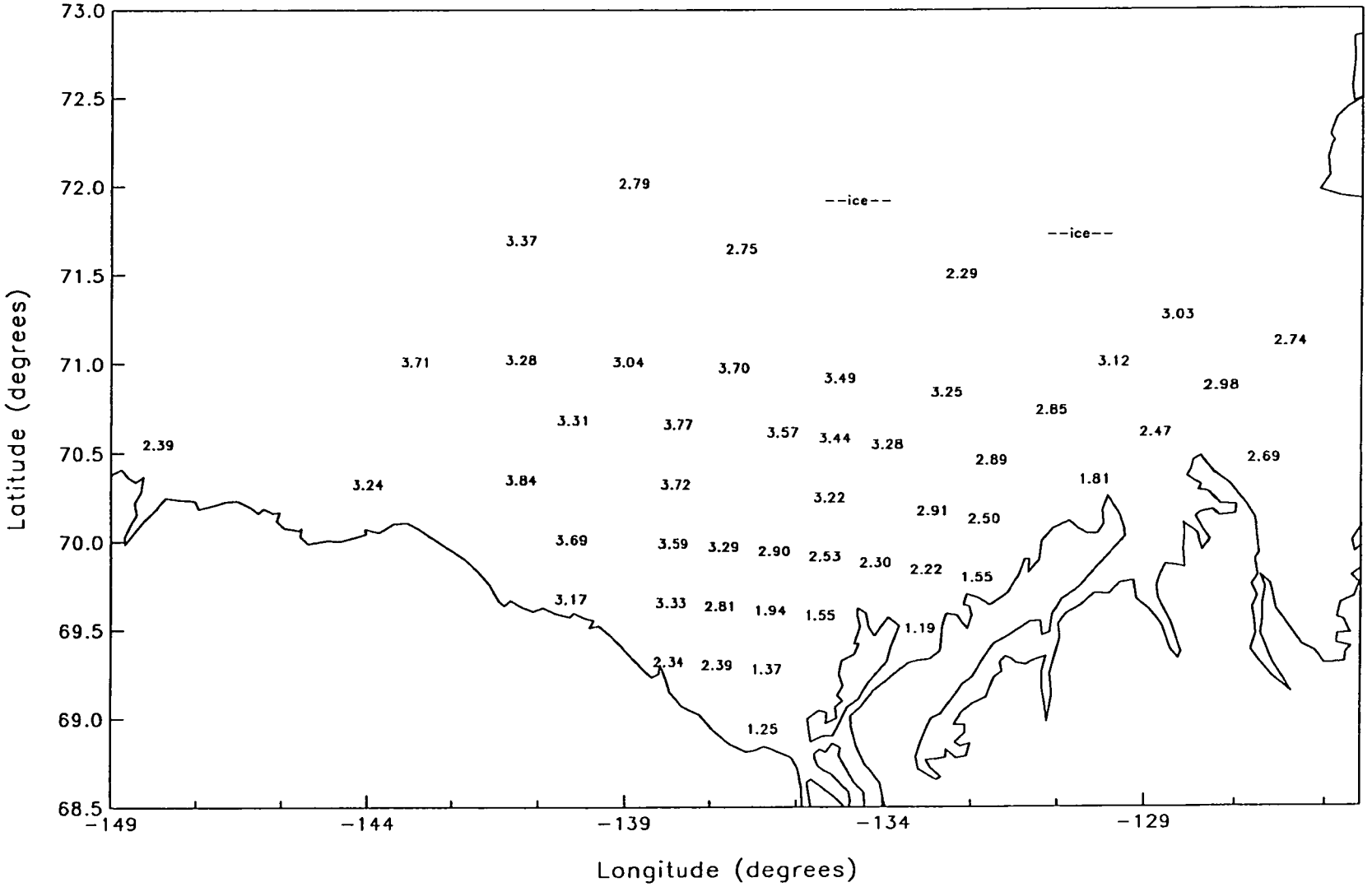

BEAUFORT SEA STORM

8008

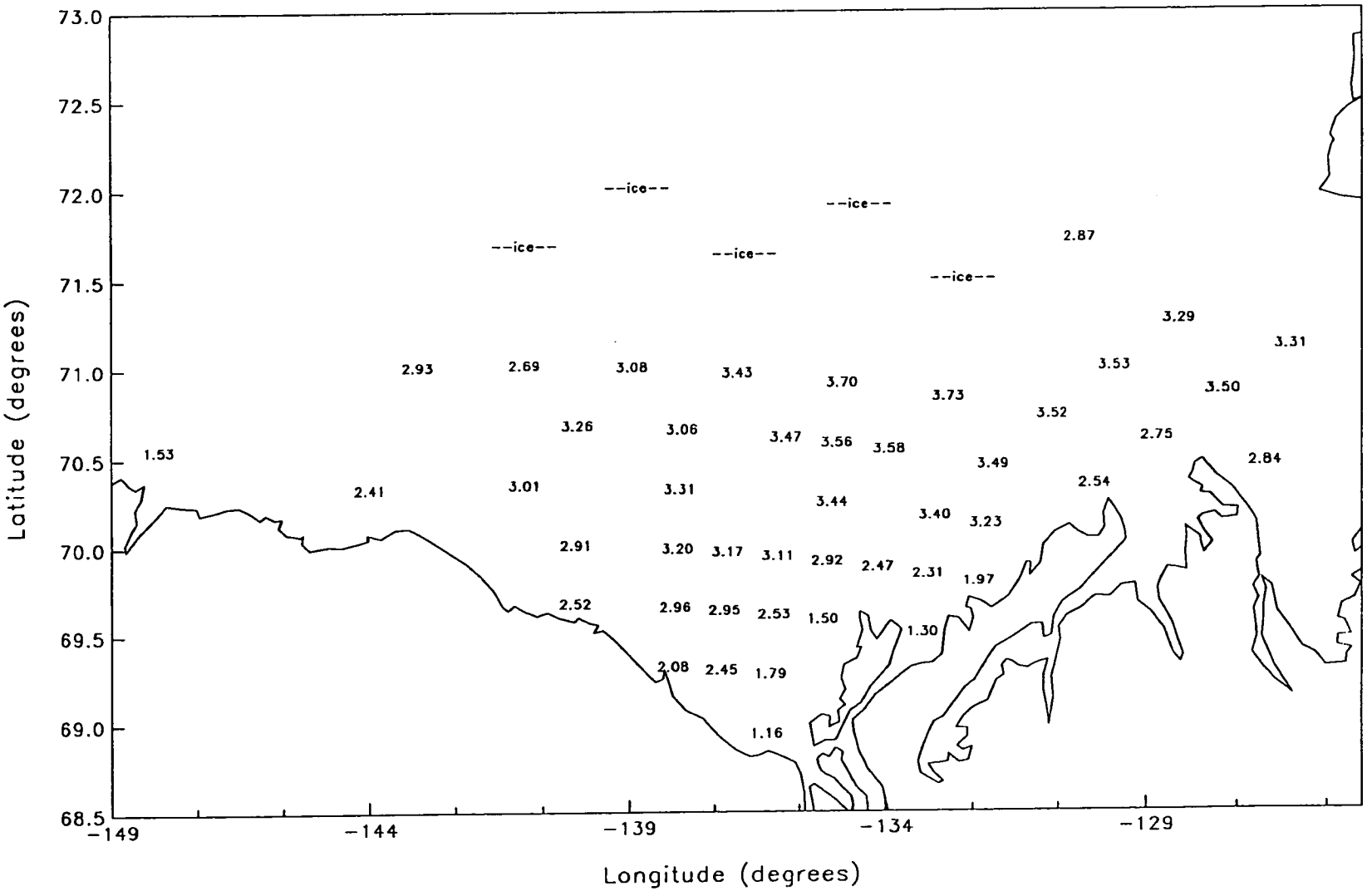

BEAUFORT SEA STORM

8108A

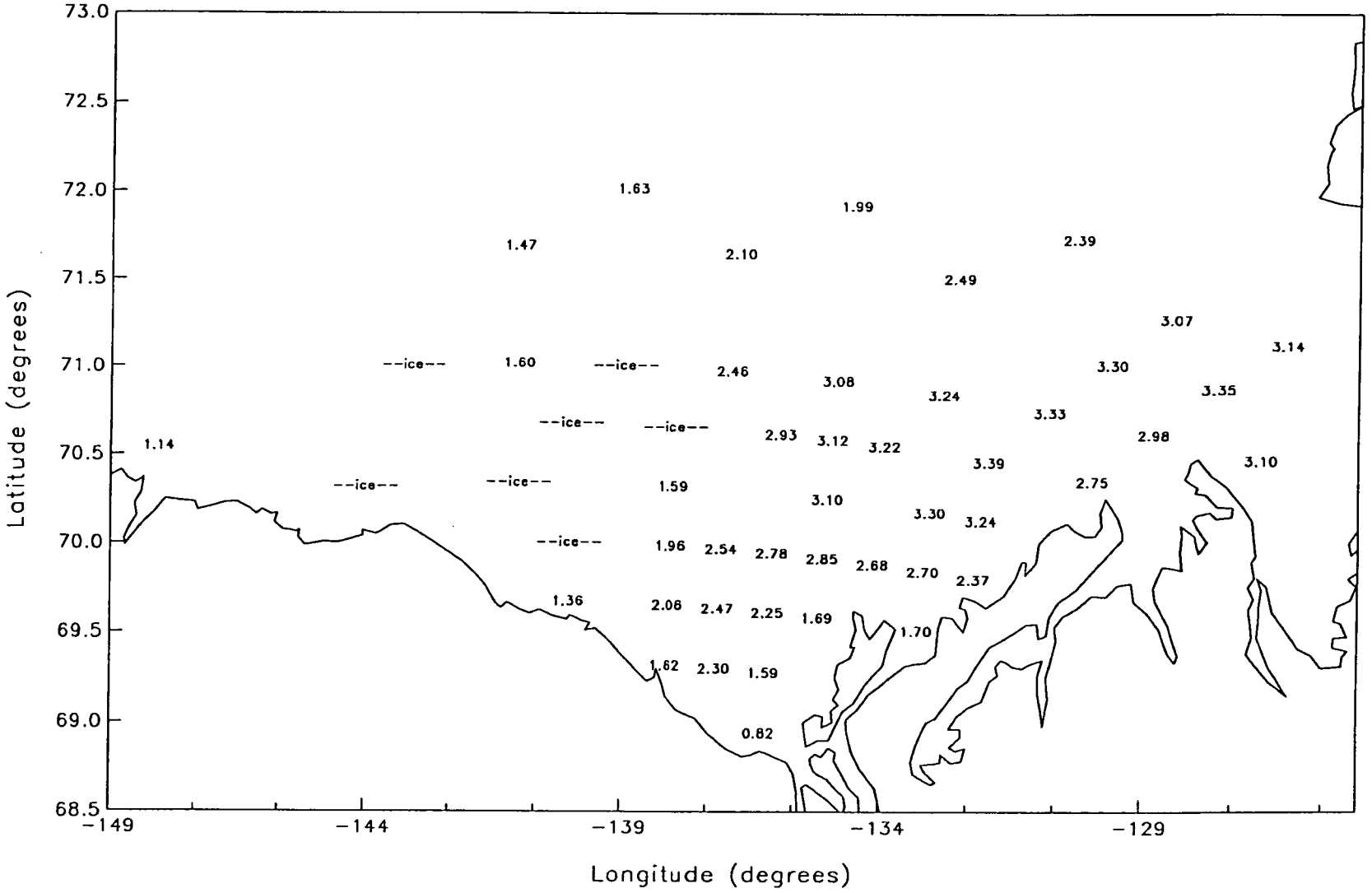

BEAUFORT SEA STORM

8108B

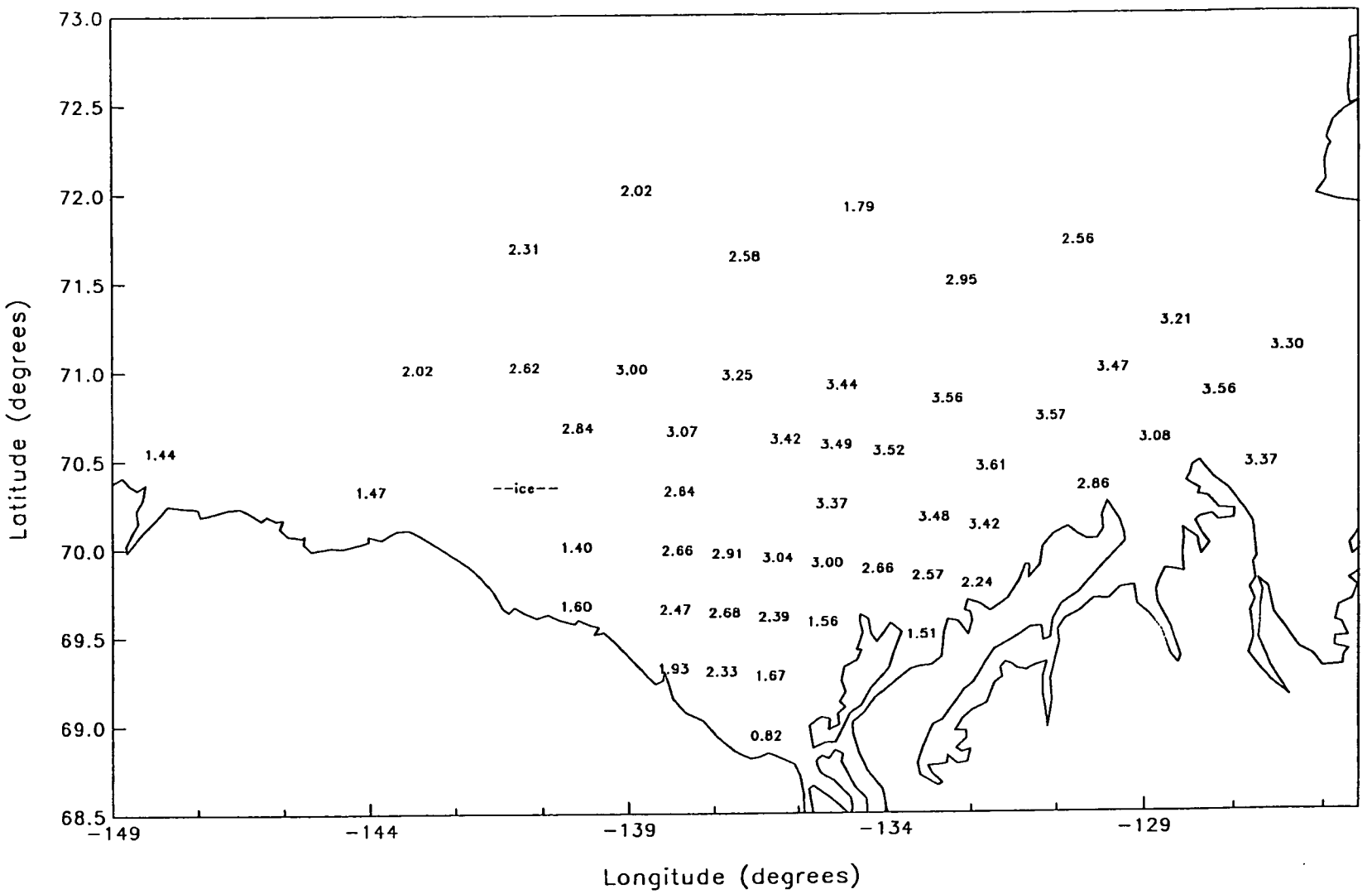

BEAUFORT SEA STORM

8108C

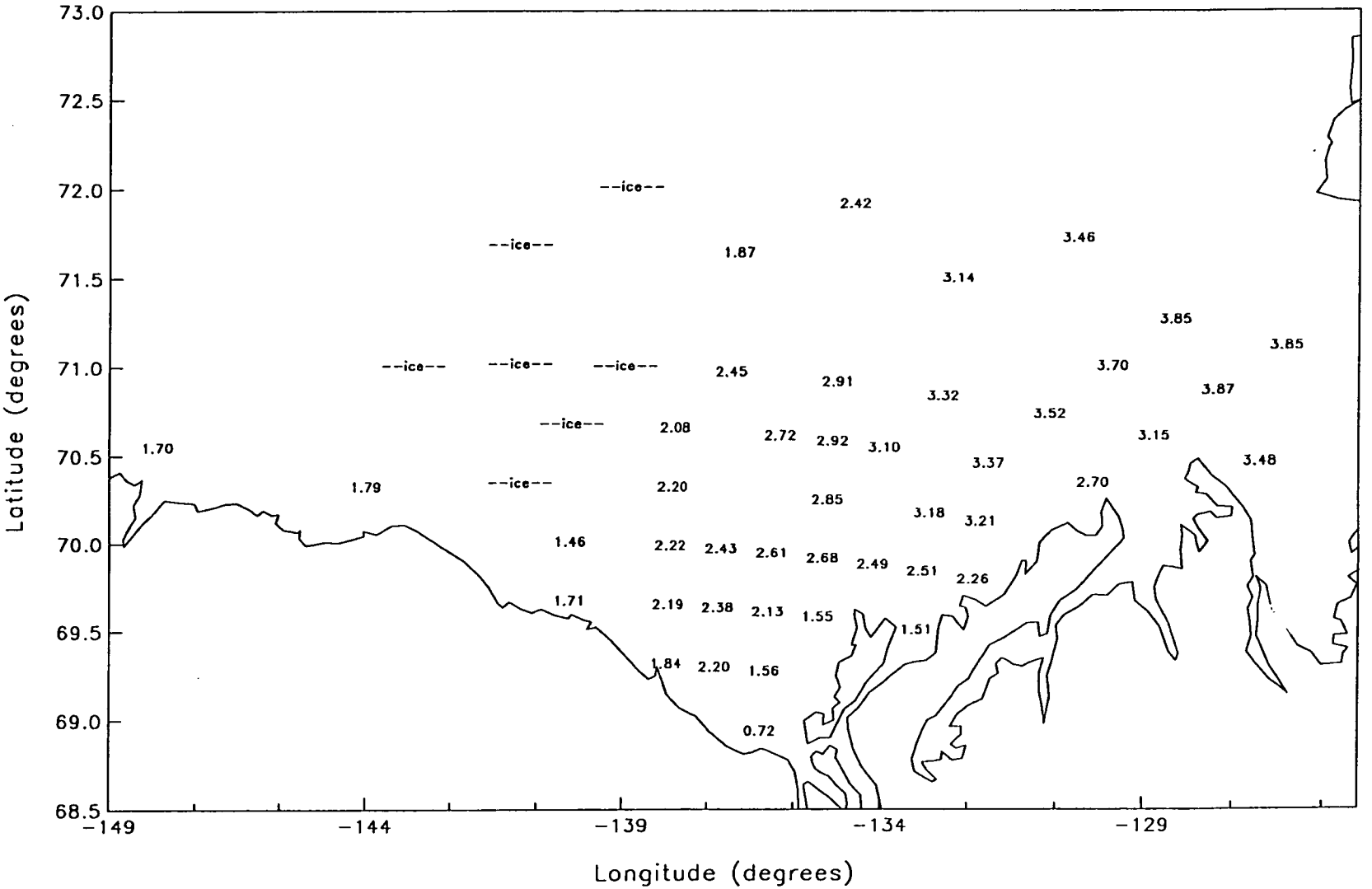

BEAUFORT SEA STORM

8109

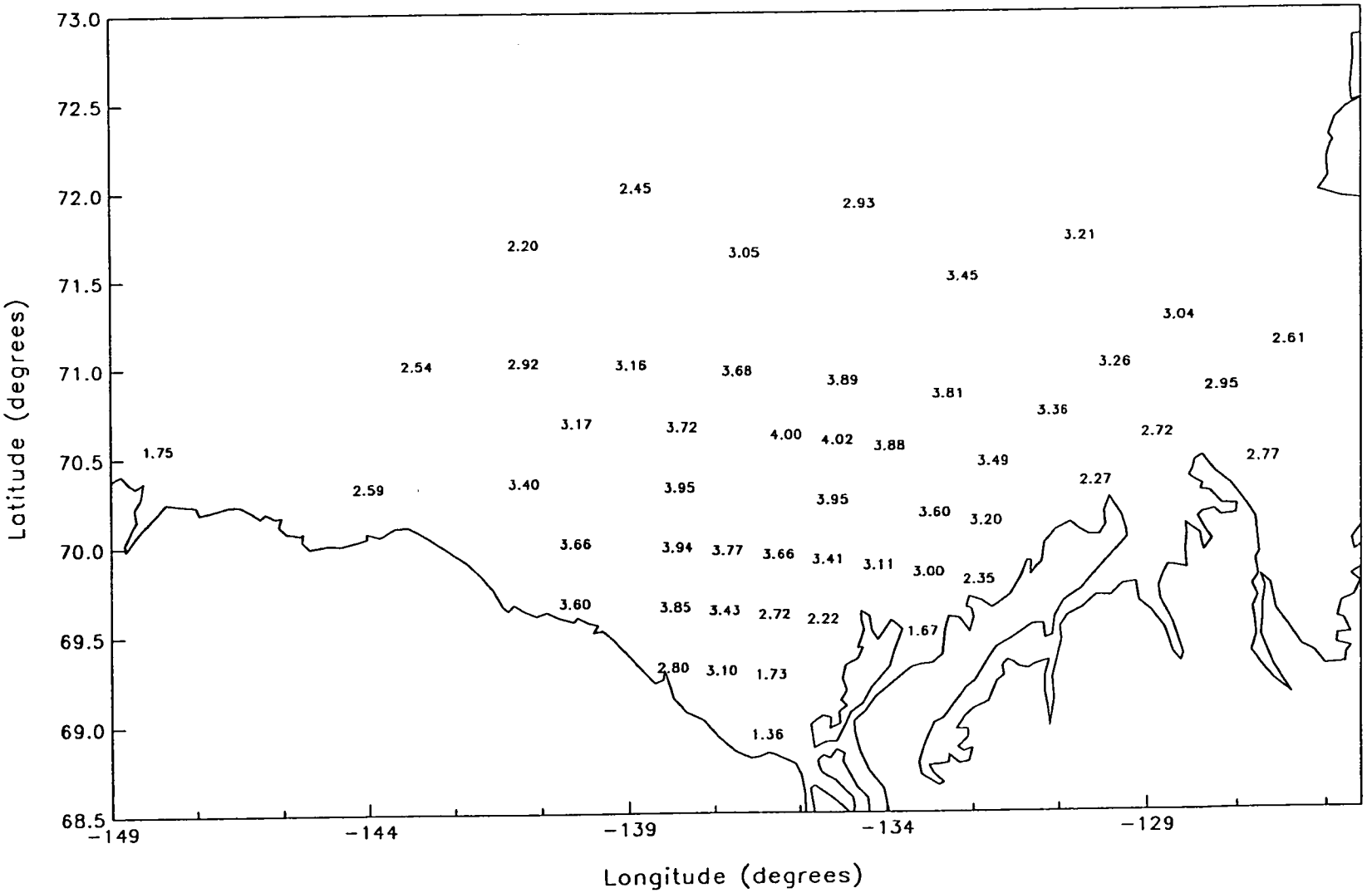

BEAUFORT SEA STORM

8207

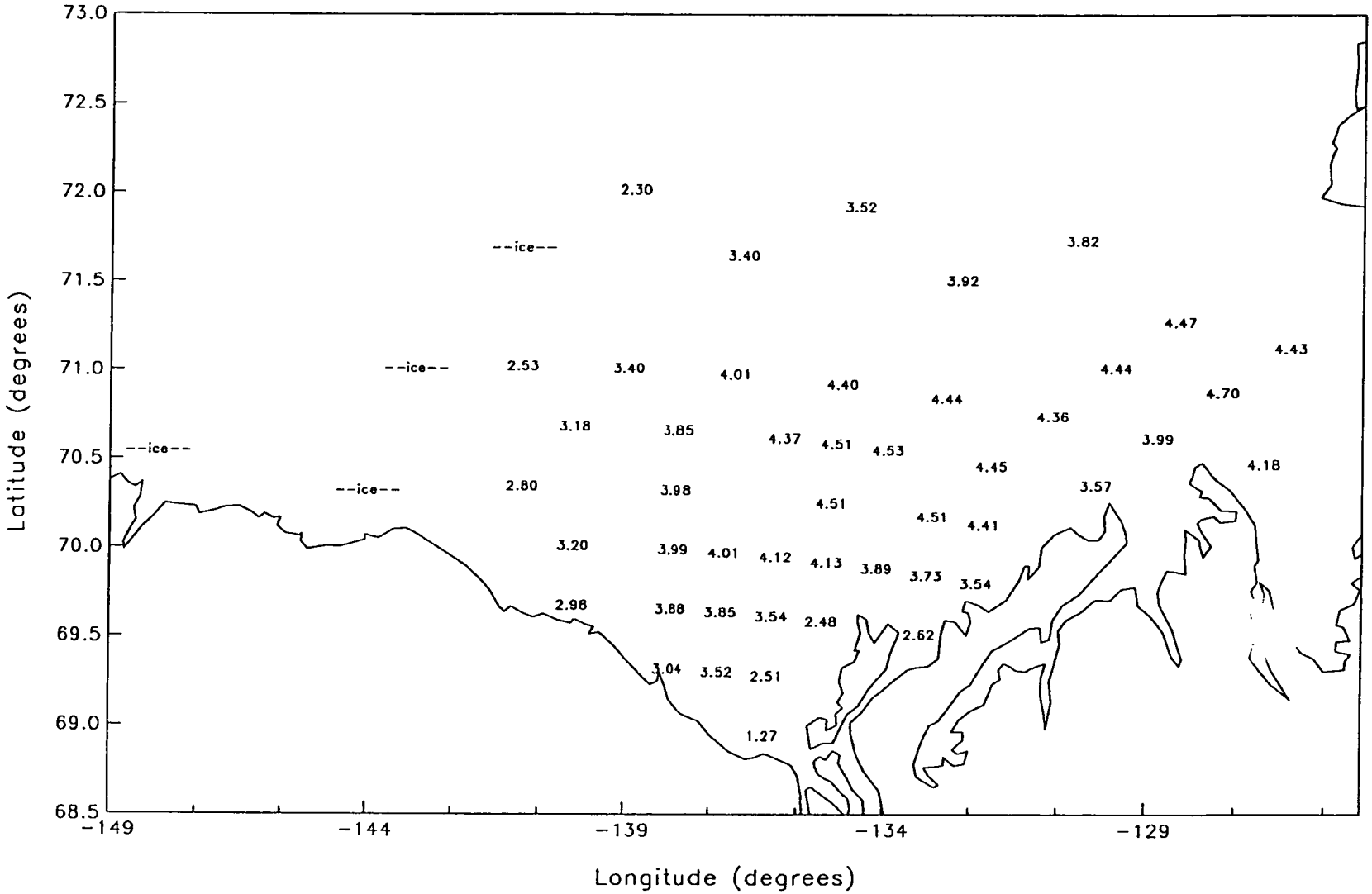

BEAUFORT SEA STORM

8208

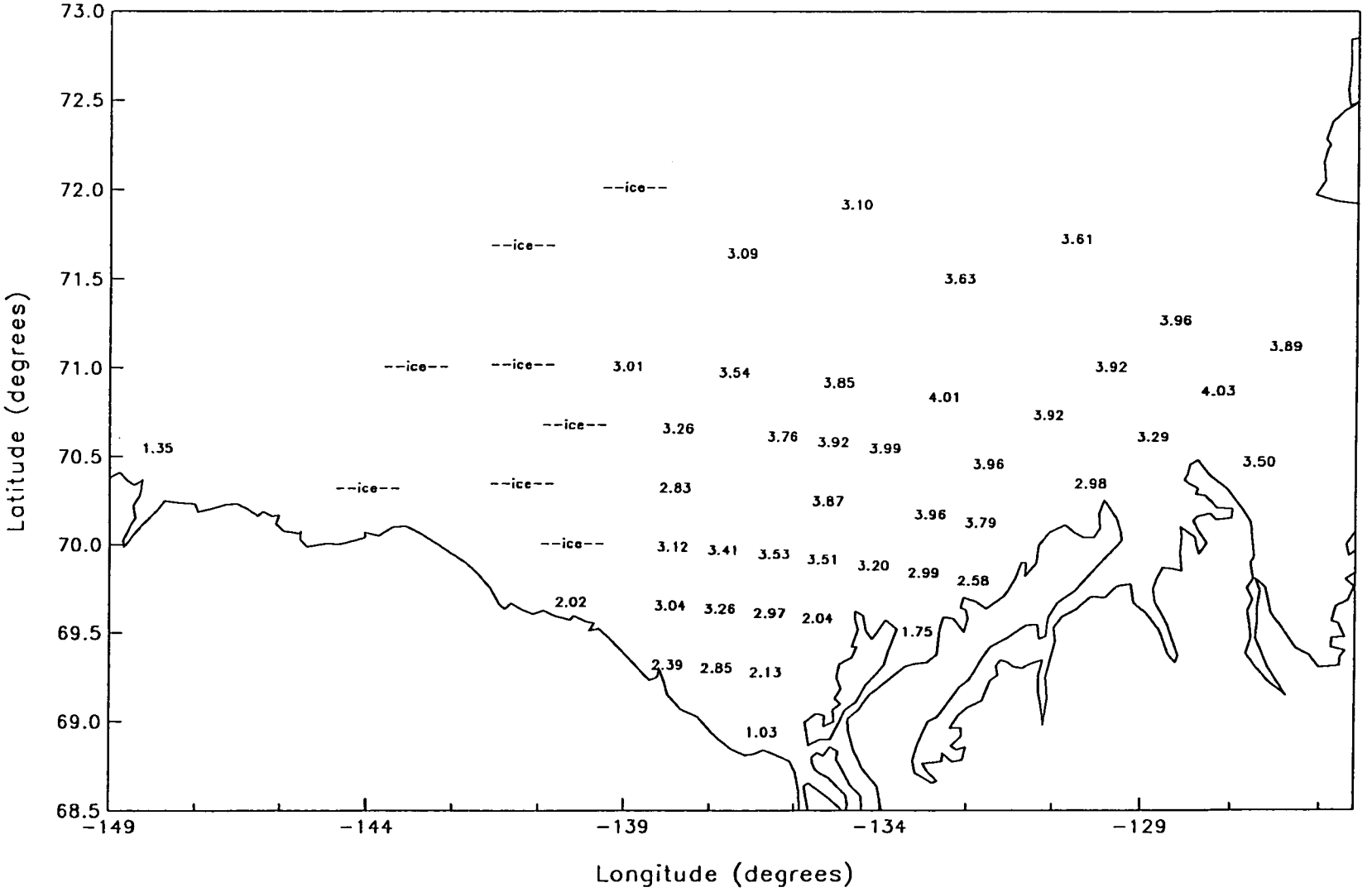

BEAUFORT SEA STORM

8209A

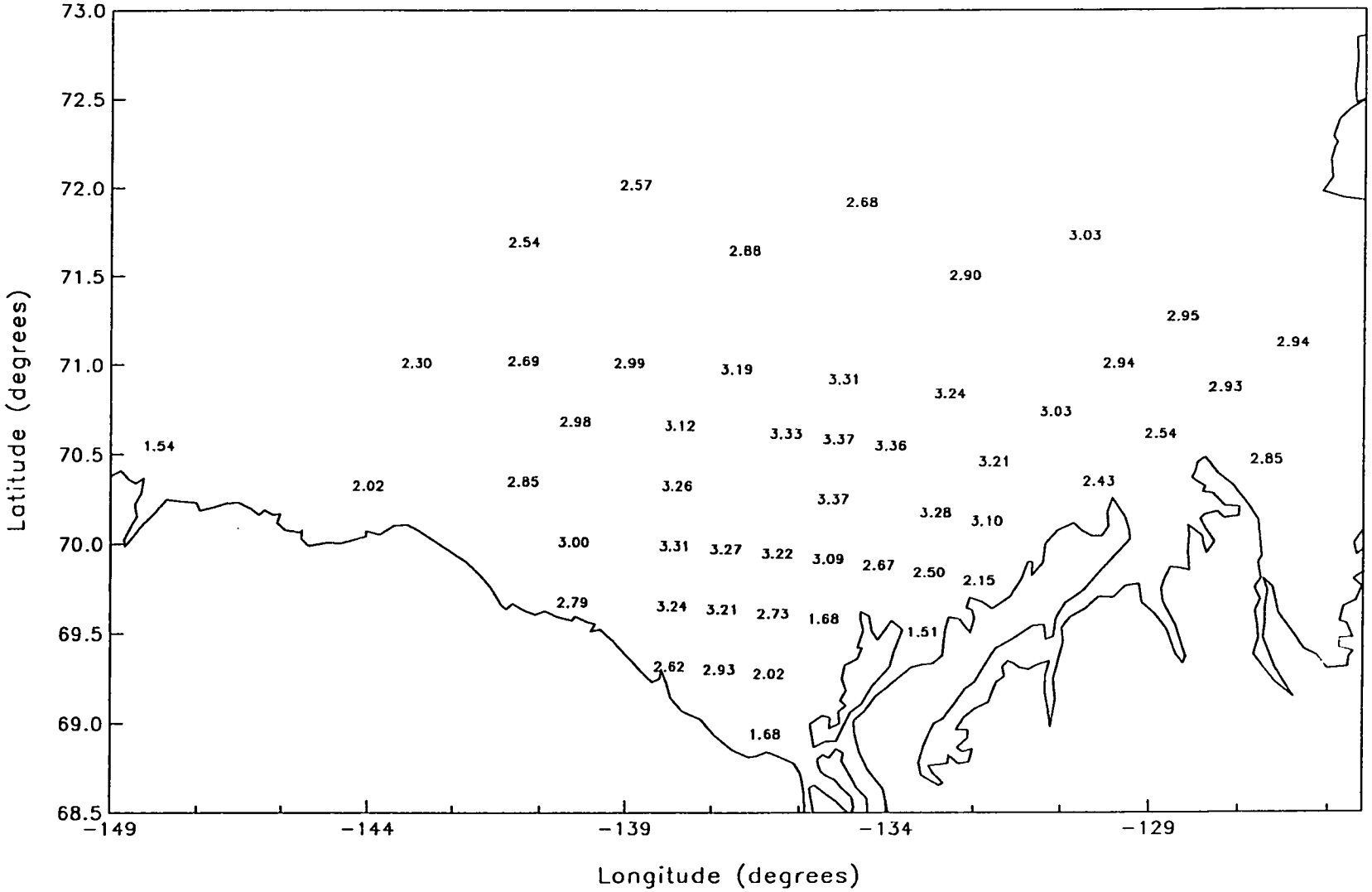

BEAUFORT SEA STORM

8209B

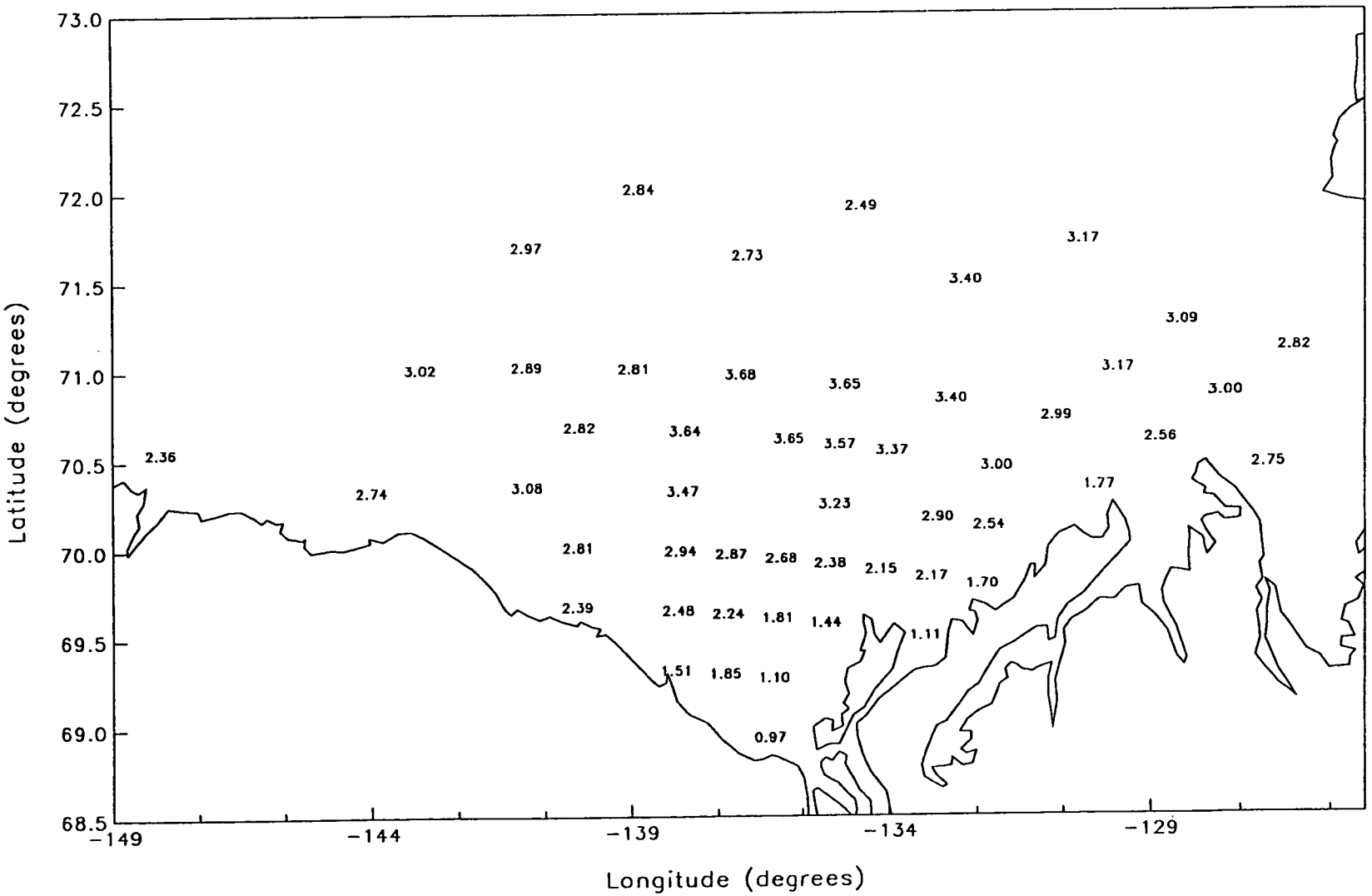

BEAUFORT SEA STORM

8210

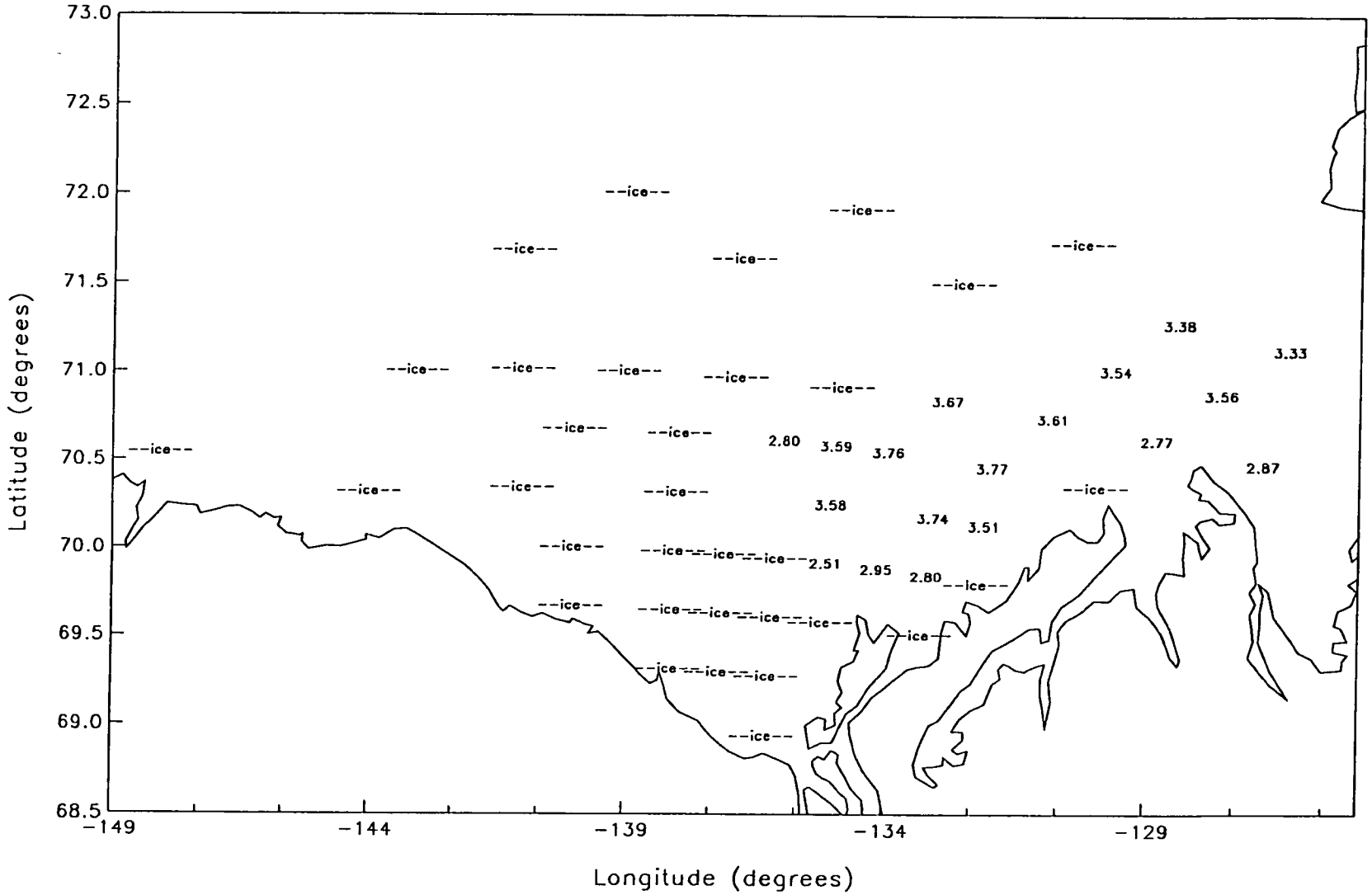

BEAUFORT SEA STORM

8408

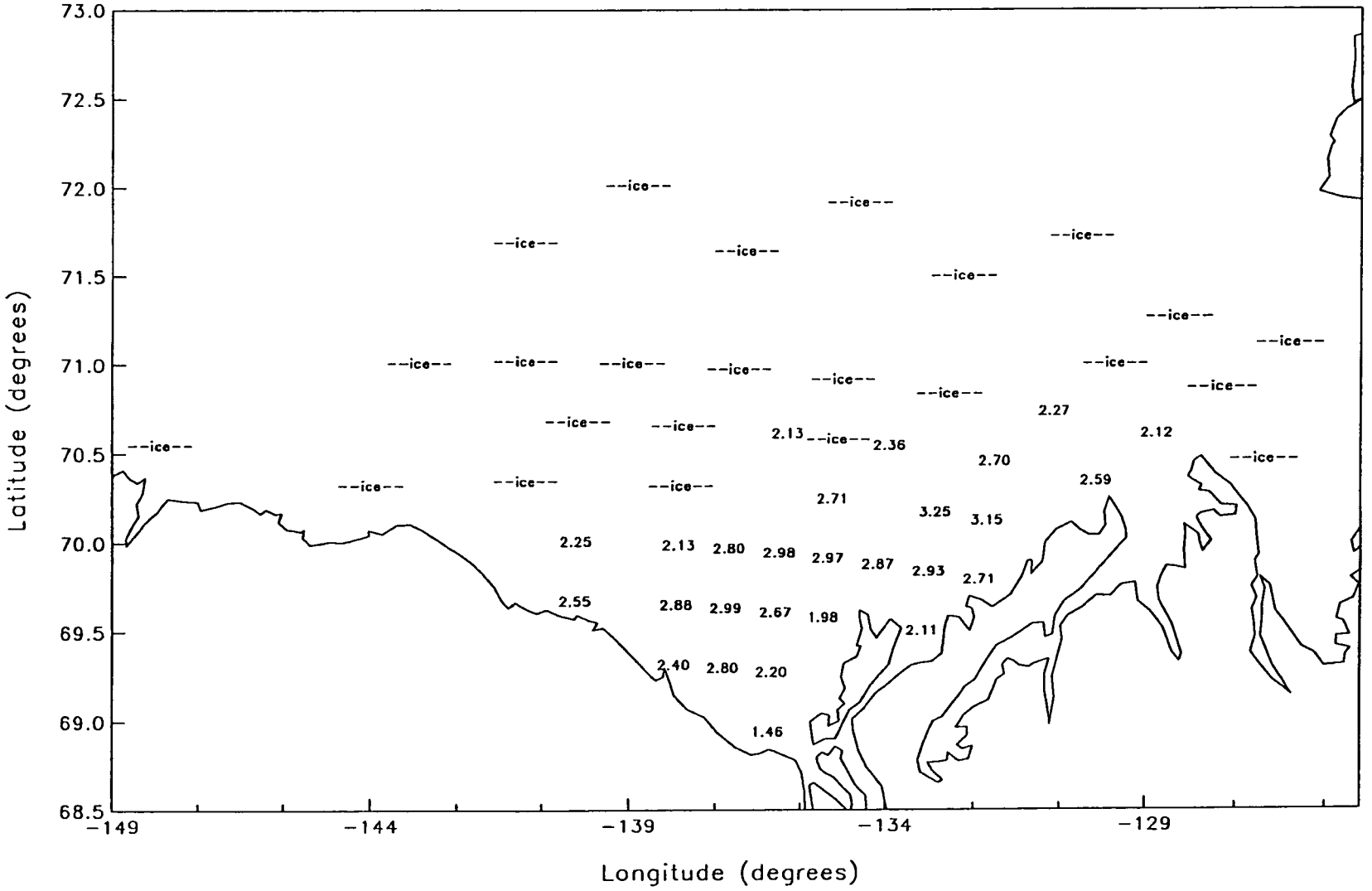

BEAUFORT SEA STORM

8410

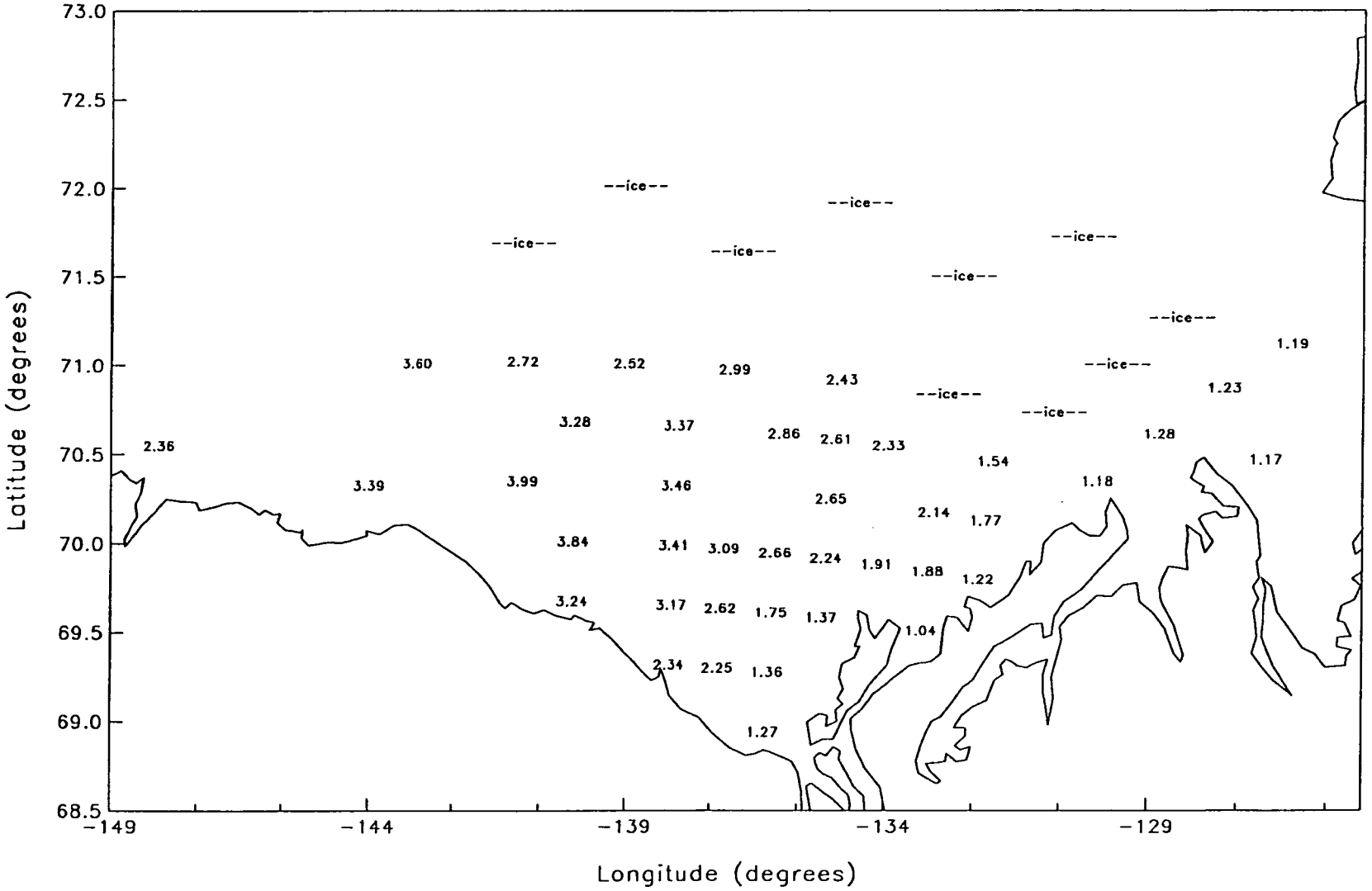

BEAUFORT SEA STORM

8509

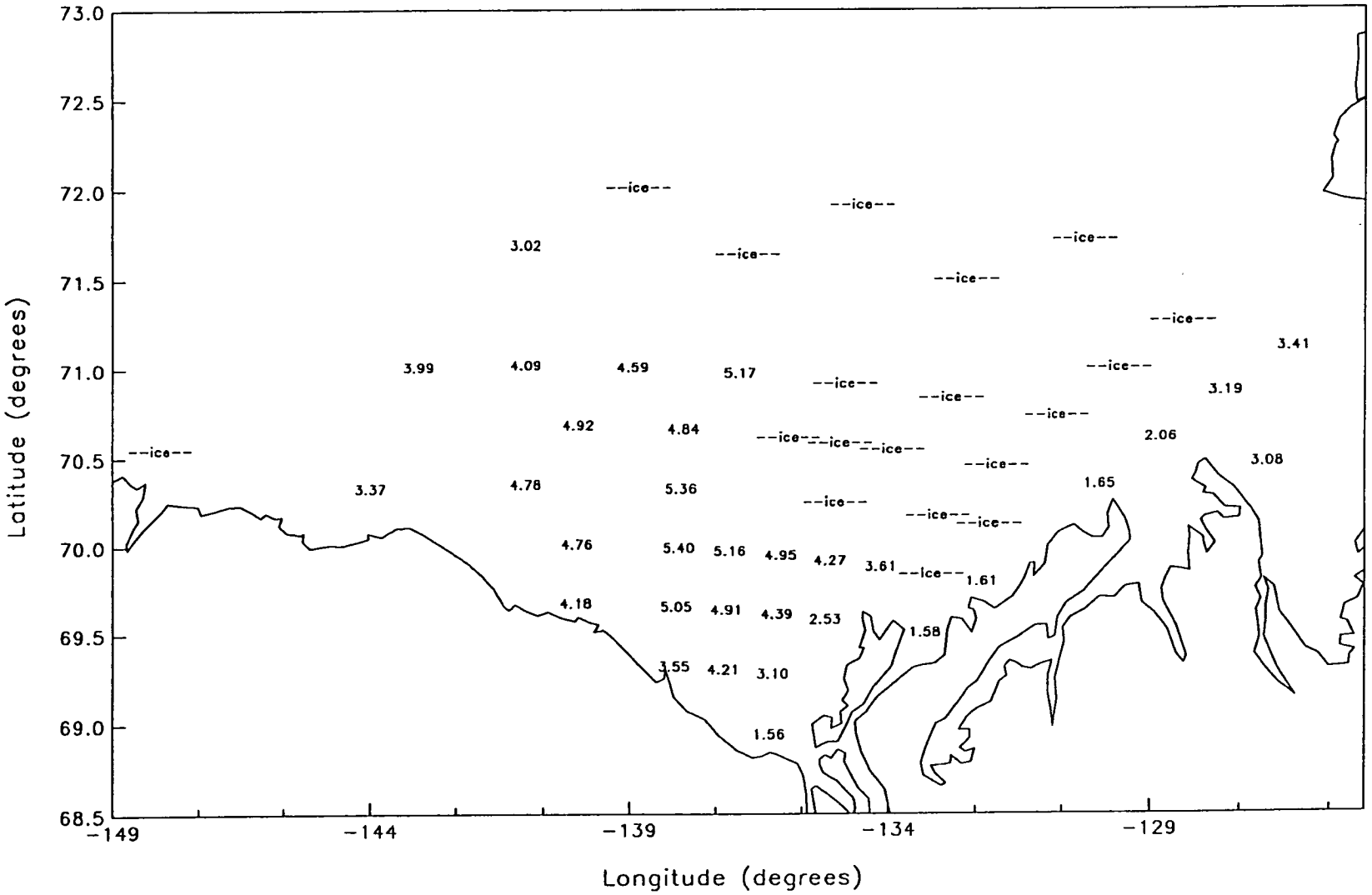

BEAUFORT SEA STORM

8608

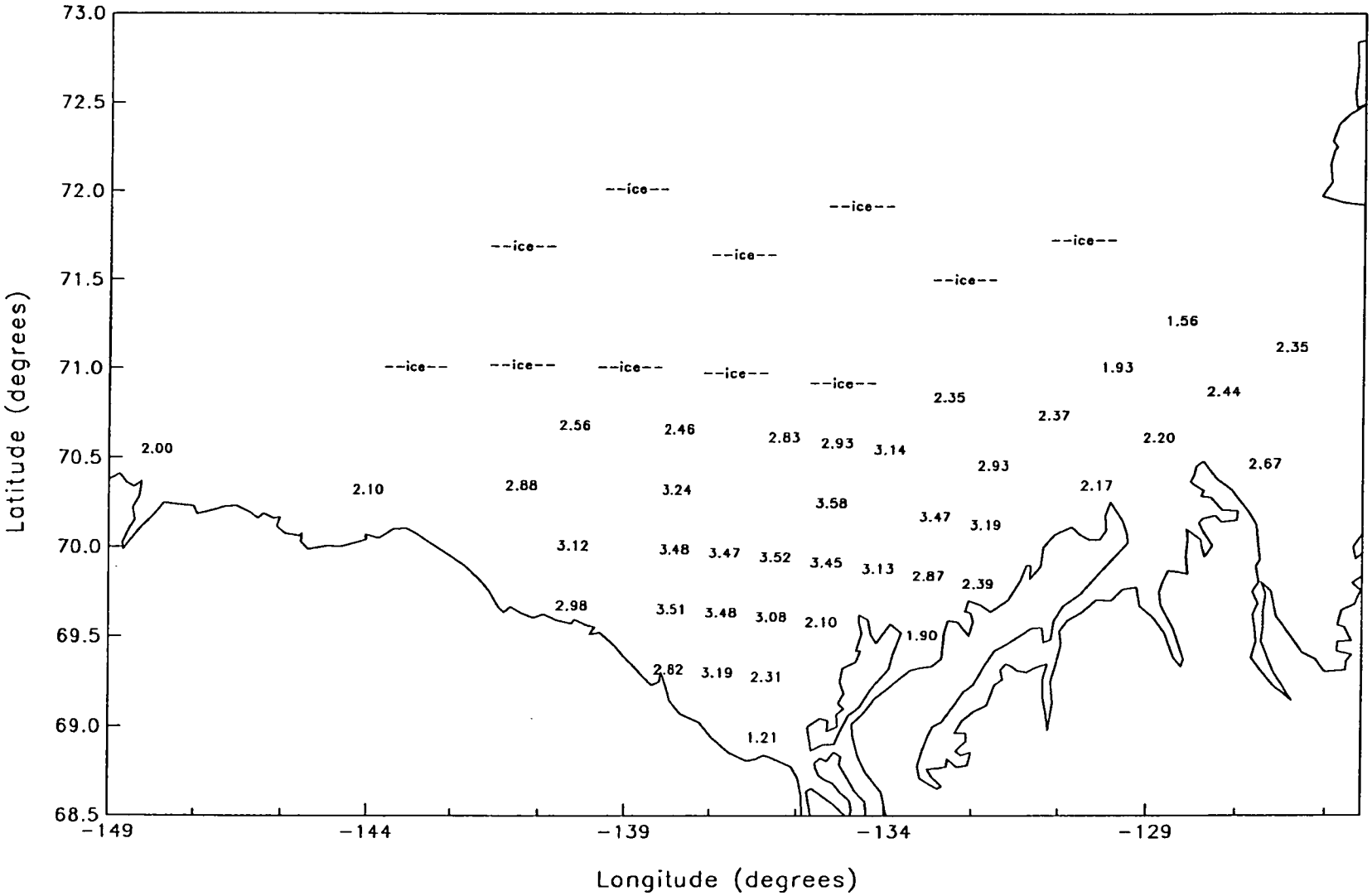

BEAUFORT SEA STORM

8609

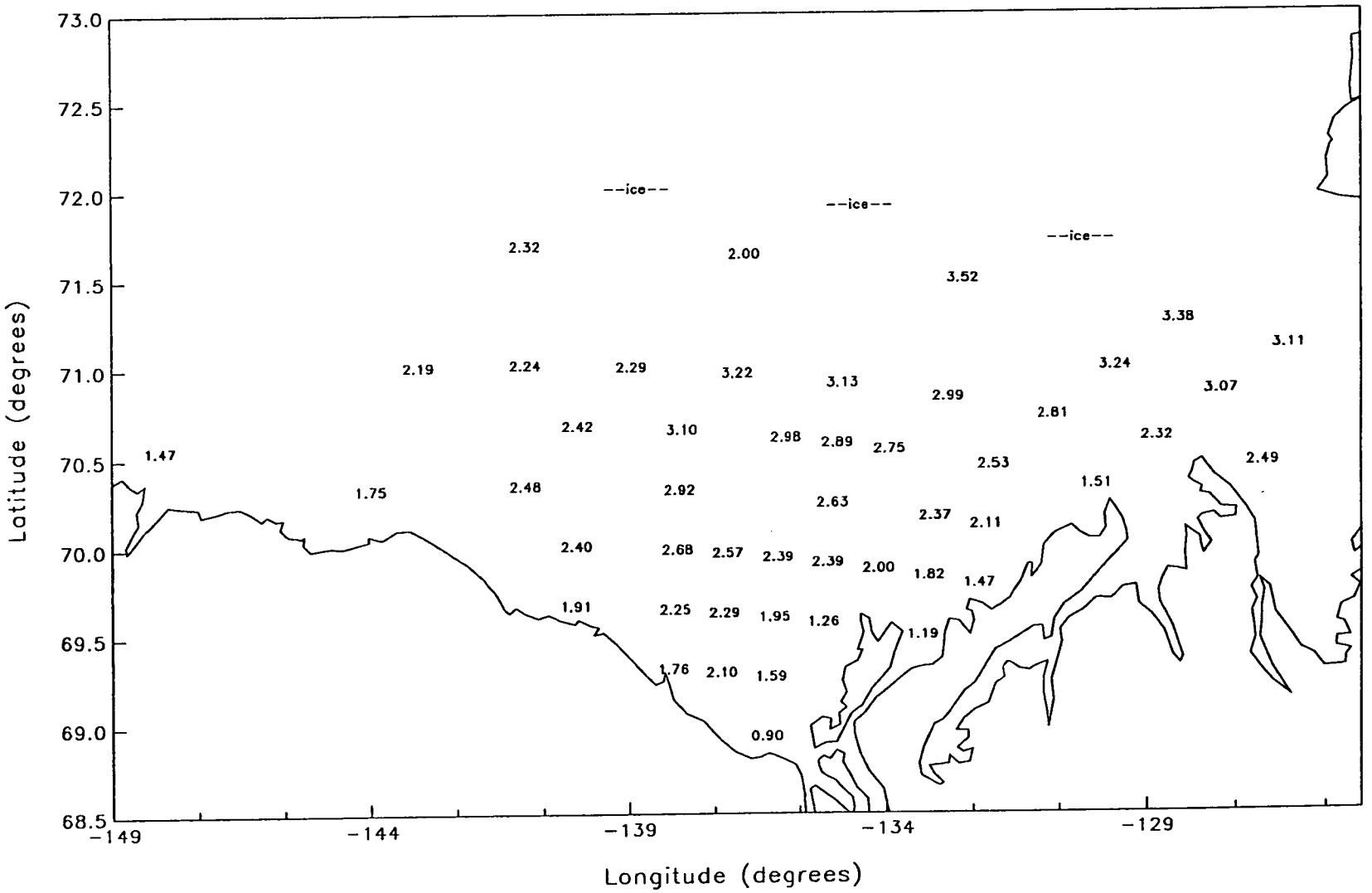

BEAUFORT SEA STORM

8708

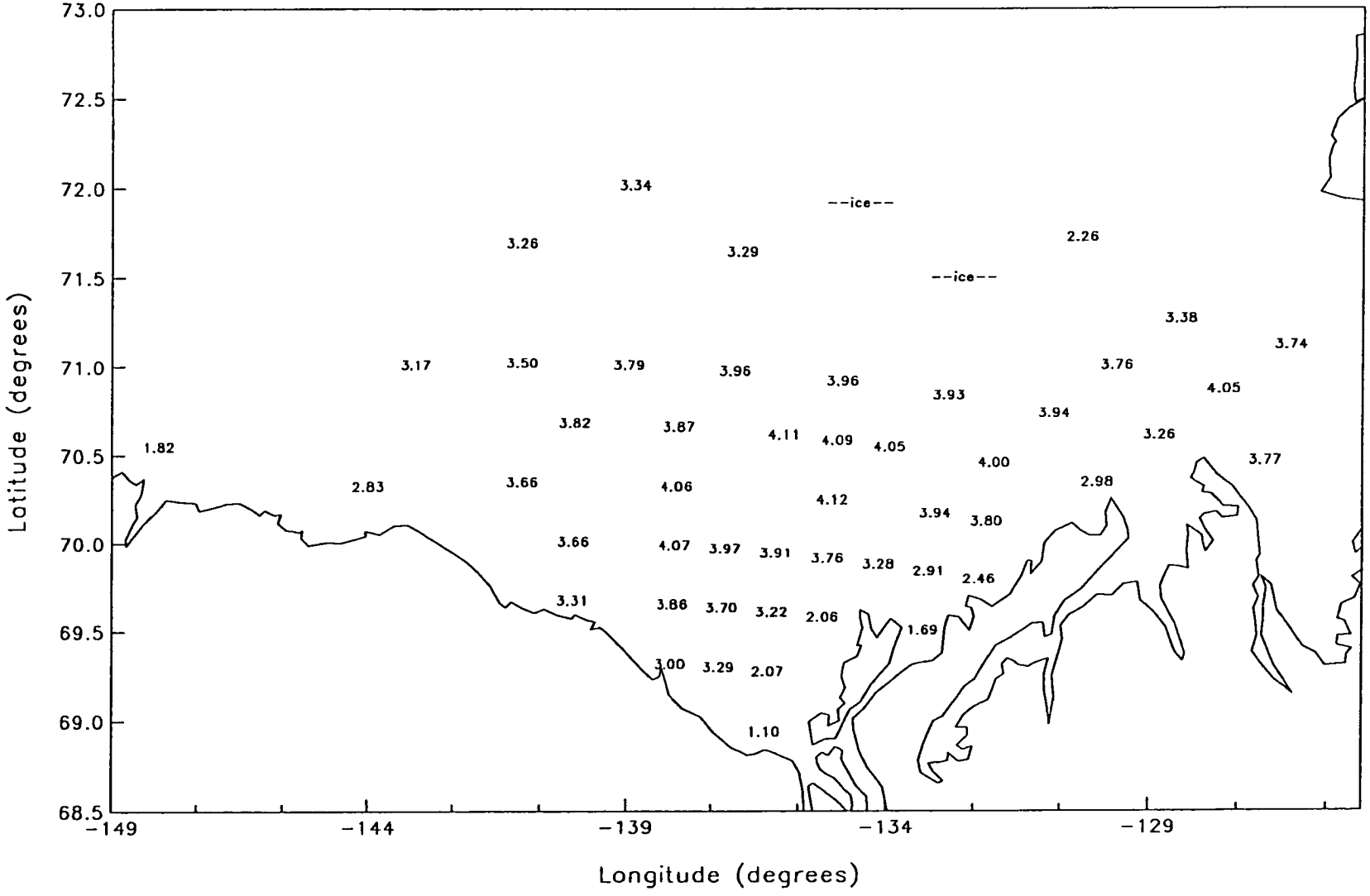

BEAUFORT SEA STORM

8808

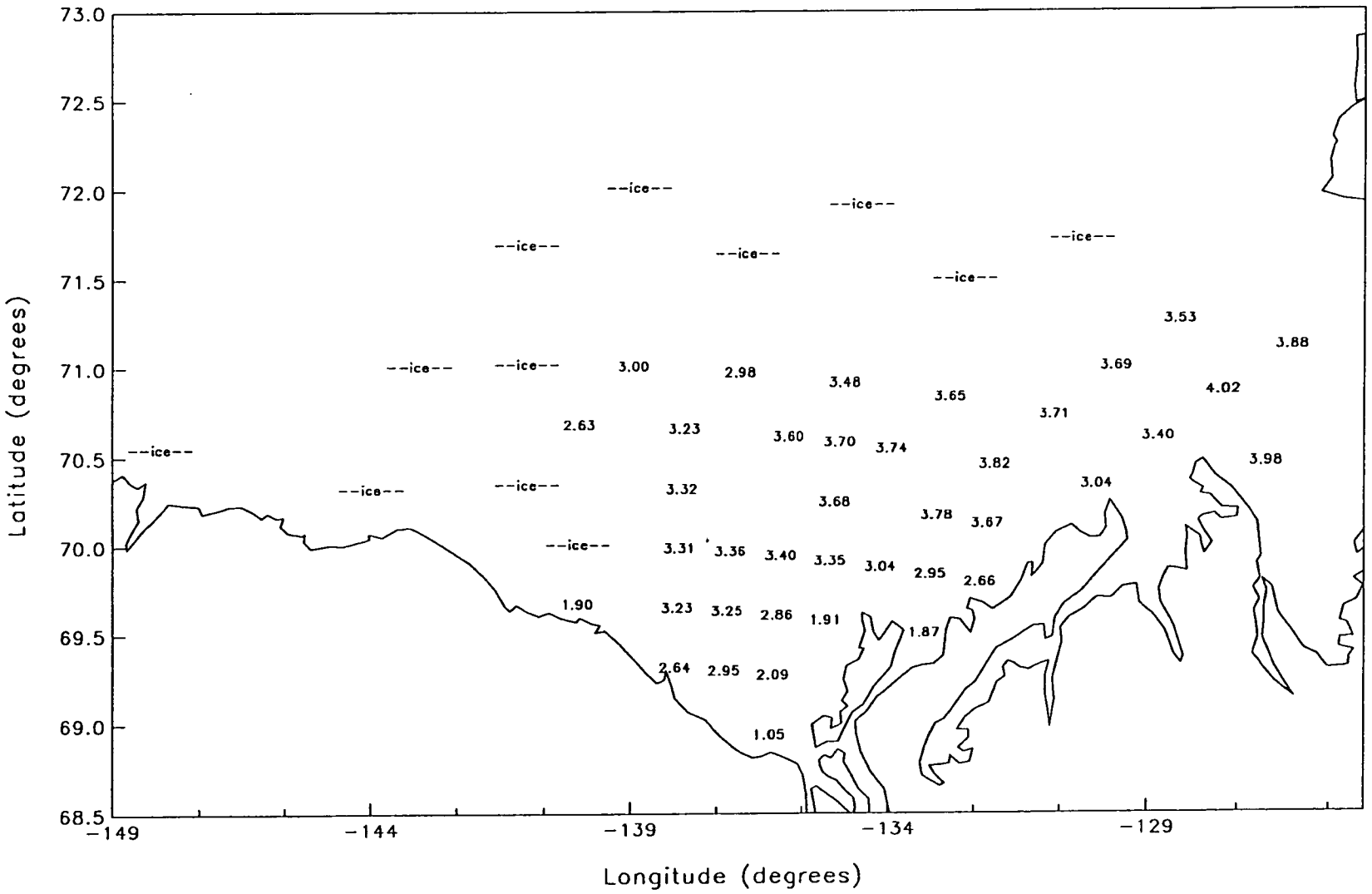

This publication is printed on paper containing recovered waste.